CELL BIOLOGY OF THE ARBUSCULAR MYCORRHIZAL SYMBIOSIS: LOCALIZATION AND FUNCTIONAL STUDIES OF MEDICAGO TRUNCATULA PHOSPHATE TRANSPORTERS AND VAPYRIN

by Nathan Stephen Pumplin

CELL BIOLOGY OF THE ARBUSCULAR MYCORRHIZAL SYMBIOSIS: LOCALIZATION AND FUNCTIONAL STUDIES OF *MEDICAGO TRUNCATULA* PHOSPHATE TRANSPORTERS AND VAPYRIN

A Dissertation

Presented to the Faculty of the Graduate School

of Cornell University

In Partial Fulfillment of the Requirements for the Degree of

Doctor of Philosophy

by

Nathan Stephen Pumplin

August 2010

CELL BIOLOGY OF THE AM SYMBIOSIS: LOCALIZATION AND FUNCTIONAL STUDIES OF *MEDICAGO TRUNCATULA* PHOSPHATE TRANSPORTERS AND VAPYRIN

Nathan Stephen Pumplin, Ph. D.

Cornell University 2010

The arbuscular mycorrhizal (AM) symbiosis is an ancient, widespread and ecologically important mutualism between plants and fungi. This symbiosis is characterized by highly-branched hyphae called arbuscules that form within plant cells to facilitate mutually beneficial nutrient exchange. These structures are surrounded by a specialized plant membrane termed the periarbuscular membrane. In the legume *Medicago truncatula*, phosphate is taken up across this membrane by the phosphate transporter MtPT4, which localizes around arbuscule branches. The experiments described in this dissertation employ molecular genetic approaches together with a system to study fluorescent fusion proteins in live cells hosting arbuscules. In the second chapter, the periarbuscular membrane is revealed to contain distinct, complementary protein domains. In the third chapter, the mechanism of polar targeting of MtPT4 to the periarbuscular membrane is dissected by studying the localization of fluorescent protein tagged-membrane proteins expressed during different stages of arbuscule development. These experiments revealed that asymmetric localization of MtPT4 is mediated by precise temporal expression, coupled with significant and temporary changes in the direction and cargo selection of the plant secretory pathway for newly synthesized proteins. Together, these data point towards a surprising but logical mechanism for polar protein localization during the AM symbiosis and highlight the extent to which cells can become specialized during

an intracellular biotic interaction. In addition, a mutant MtPT4 protein with a single amino acid change fails to localize in the periarbuscular membrane and instead is retained in the Trans-Golgi Network (TGN). This mutation causes a loss-of-function phenotype, confirming that localization of MtPT4 at the host-symbiont interface is required for its function. The fourth chapter describes additional *M. truncatula* phosphate transporters, one of which localizes specifically to the periarbuscular membrane. The fifth chapter reports discovery and characterization of a gene named *Vapyrin*. Knockdown of this gene impairs root penetration by AM fungi and abolishes arbuscule formation. *Vapyrin* is induced coincident with fungal infection, and encodes a novel protein containing a VAP (VAMP Associated Protein) domain and eight ankyrin repeats, both established protein-protein interaction domains. We hypothesize that Vapyrin functions in secretion during fungal infection through recruitment to an endosomal compartment.

BIOGRAPHICAL SKETCH

Nathan Pumplin was born in East Lansing, Michigan, near the banks of the red cedar. He graduated from East Lansing High School in 2000 and enrolled at Michigan State University to study Advertising. After changing majors, he received research training in the labs of Dr. Richard Lenski and Dr. Sheng Yang He, and studied for a year at the Albert-Ludwigs-Universität in Freiburg, Germany. In 2005, he graduated with a B.Sc. in Plant Biology and a B.A. in German. After a brief internship at The Institute for Genomic Research, he began graduate work in plant biology at Cornell and joined the lab of Maria Harrison at the Boyce Thompson Institute for Plant Research.

To my family, Veronica, and the many people with whom I've enjoyed this time

ACKNOWLEDGMENTS

I thank my parents for a unique and very effective education, and my entire family for their unconditional love and support. I'd like to thank all of my past advisors who invested their valuable time and taught me so many scientific lessons, in particular: Sheng Yang, Bill and Paula; Robin, Willem and Matt; Helene, Julien and Adam. Many teachers have prepared and inspired me over the years, and I thank in particular Ken Poff, who opened my eyes to biology and showed me how teaching means exciting, and connecting with, students. To all of the friends and colleagues at BTI, Cornell and beyond, the past five years here have been a wonderful experience on so many levels - it's been real a pleasure to work, debate, hike, skate, make music and revel with you all. Most importantly, I have to express my deepest gratitude to Maria Harrison, my advisor, for taking me in the lab, teaching me how to think about science on a higher level, providing the perfect mix of support and criticism, and encouraging me to pursue my own research interests.

TABLE OF CONTENTS

LIST OF FIGURES

LIST OF TABLES

CHAPTER 1

CELL BIOLOGY OF THE ARBUSCULAR MYCORRHIZAL SYMBIOSIS

The arbuscular mycorrhizal (AM) symbiosis is a fundamental evolutionary adaptation in the land plant lineage and plays a substantial role in nutrient cycling both in natural ecosystems and agriculture. It is characterized by the transfer of nutrients from fungus to plant and reciprocal exchange of carbon from plant to fungus. Nutrient exchange is facilitated by the establishment of fungal structures called arbuscules, which form within the confines of a cortical cell through a complex genetically-regulated reorganization of the plant cell. The research presented in this dissertation takes a molecular genetic approach, relying heavily on live-cell imaging techniques, to reveal aspects and mechanisms regulating this intriguing reorganization.

Evolution of the AM symbiosis

The transition from an aquatic habitat to terrestrial growth required plants to development resistance to desiccation and the ability to extract sufficient nutrients and water from arid soils. Pirozynski and Malloch (1975) proposed that the colonization of land by plants may have been facilitated by symbiotic association with fungi, and these were believed to be the ancient relatives of AM fungi. Subsequently, fossils characterized as ancient AM fungi were discovered from the Devonian (400 Million years ago (MYA) (Remy et al., 1994) and Ordovician (460 MYA) (Redecker et al., 2000) periods, and morphological and molecular phylogenetic analysis revealed that all AM fungal species are members of the phylum Glomeromycota, a monophyletic group within the fungal kingdom that diverged ~400 MYA (Simon et al., 1993; Schussler et al., 2001). Recently, Wang et al. (2010) reported phylogenetic analyses of three plant genes required for AM symbiosis across a wide range of families. The

study showed that orthologs are present in all lineages and genes from the most closely-related species share highest degree of sequence conservation, suggesting that they evolved in parallel with plant evolution. These data underscore the central role played by symbiosis in plant evolution and lend circumstantial support to the theory that this fungal association enabled terrestrial plant growth. The AM symbiosis is prevalent throughout the plant kingdom today, with an estimated 70% of vascular plants and 74-80% of angiosperms engaging in it (Wang and Qiu, 2006; Brundrett, 2009). An estimated 20% of carbon fixed globally by terrestrial plants may be delivered to AM fungi (Bago et al., 2000), illustrating the important role for this process in ecosystem dynamics.

While a majority of plants can participate in AM symbioses, the phylum Glomeromycota contains only 219 recognized species that all form obligate biotrophic interactions with plants (Schussler et al., 2001; Stockinger et al., 2010). These fungi are asexual, aseptate, coenocytic, and contain endobacteria, recognized as a monophyletic clade that diverged from the Mollicutes ~400 MYA (Naumann et al., 2010). In light of the fact that other fungal phyla include plant pathogens, it is interesting to note that despite the intimate growth of the AM fungi within plants, this group has not given rise to any true plant pathogens.

The nutrient exchange between symbionts of an arbuscular mycorrhiza requires growth of the fungus within the plant root, and this is facilitated by plant cellular reorganization. The benefit for the plant relies on the extraradical mycelium, which extends in the soil and accesses nutrients more efficiently than plant roots alone (Jakobsen et al., 1992; Javot et al., 2007a). In the case of phosphate, AM fungal hyphae not only greatly expand the area of soil exploited for uptake, but there is also evidence that they can solubilize phosphate fixed in organic complexes by secreting phosphatases (Joner et al., 2000; Koide and Kabir, 2000; Feng et al., 2003; Shibata

and Yano, 2003). In angiosperms, many experimental studies have established the beneficial role that AM fungi serve in allowing plants to take in nutrients such as phosphorus and nitrogen and improve resistance to disease (Smith et al., 2003; Govindarajulu et al., 2005; Liu et al., 2007; Smith and Read, 2008). Due to the increased phosphate taken up by most mycorrhizal plants, this interaction is of great interest as a possible strategy for improving the sustainability of crop production without increasing costs and environmental risks associated with increasing phosphate fertilization.

Morphological steps in AM symbiotic development

Development of the AM symbiosis in the roots of angiosperms has been well described at the morphological level, while knowledge of the genetic and chemical basis directing it has progressed rapidly in the past decade. Successful symbiosis with roots allows AM fungi to produce hardy spores that persist in the soil and can begin new infections (Smith and Read, 2008). Upon spore germination, hyphae grow through the soil, deriving energy primarily through breakdown of triacylglycerol stores by gluconeogenesis (Bago et al., 2000), and they must establish a successful nutrient exchange with plants before depleting their limited carbon reserves. Hyphal contact with a root initiates development of a hyphopodium, a similar structure to appressoria formed by biotrophic fungal pathogens, which facilitates penetration of the root epidermis (Bonfante and Perotto, 1995; Parniske, 2008). Hyphal growth proceeds intraradically through the root cortex, and can occur predominantly intra- or intercellularly, varying with the host species involved (Genre et al., 2008). The central developmental event of arbuscular mycorrhizas is formation of a branched hyphal structure within inner cortical cells, called an arbuscule, so named because it resembles a small tree. Two types of arbuscule morphology are recognized: *Arum*

type, characterized by a large hyphal trunk with many small proliferating dichotomous branches and exhibited in symbiosis between *M. truncatula* and *Glomus* species, and *Paris* type, characterized by prominent hyphal coils that give rise to small intercalary arbuscules (Cavagnaro et al., 2001; Smith and Read, 2008). Due to the predominant formation of *Arum*-type arbuscules in the interaction between roots of agronomically important plants and commonly-studied AM fungi, the majority of experimental data are derived from this type. Formation of arbuscules in cortical cells elicits synthesis of a new plant membrane, termed the periarbuscular membrane, which surrounds the fungus, separating it from the plant cytoplasm and facilitating nutrient exchange (discussed below). Arbuscules are transient organs that persist in cells for ~7-10 days, after which time they collapse and degenerate. Following collapse, cortical cells return to their previous un-colonized state with no apparent detrimental effects to the cell (Bonfante and Perotto, 1995; Gianinazzi-Pearson, 1996).

Studies on the timing of events in symbiotic development are complicated by the asynchronous nature of mycorrhizal colonization. Since root infection and arbuscule development is an ongoing process, the timing of events has been inferred by harvesting roots at measured time increments after inoculation. Developmental timing was initially described in a study by Brundrett et al (1985), in which leek roots were harvested in two-day increments following inoculation with the AM fungus *Glomus versiforme*. After the first two days, root penetration through epidermal cells and growth in the cortex was observed. After four days, arbuscules had formed in inner cortical cells and overall root colonization had increased. After six days, many fully mature arbuscules could be observed. A similar study reported by Alexander et al. (1989) assessed the developmental events in onion, bean and tomato colonized by *Glomus fasciculatum*, and found that timing was similar regardless of host, with arbuscule development lasting 2.5 days and a total lifespan from initiation to collapse

and degeneration lasting 7.5-8.5 days. While these results are based on light and electron microscopic analysis, access now to molecular markers should enable more detailed analysis of the lifespan of arbuscules at the level of individual cells, providing an important context for understanding development.

Plant genetic regulation of AM symbiosis

The past decade has seen a dramatic increase in our understanding of the genetic pathways that regulate AM symbiosis with the cloning of many genes underlying symbiosis-impaired plant mutants. All of the essential symbiotic genes reported to date were cloned from the legumes *Medicago truncatula* or *Lotus japonicus*, and most are also required for a functional symbiosis with nodule-forming rhizobia bacteria. This group of genes that regulate both symbioses is therefore referred to as "common symbiosis genes," and the fact that these pathways overlap has aided their identification as mycorrhiza-regulating factors, and also established that the root nodule symbiosis between legumes and rhizobia evolved by partially co-opting the genetic pathway that evolved for regulating AM symbiosis (Parniske, 2008). Mutants of the common *SYM* genes mostly impair epidermal penetration by AM fungi and lead to hyphopodial swelling and aborted infection on the root surface. These genes in *M. truncatula* (Mt) and *L. japonicus* (Lj), encode a receptor-like kinase, MtDMI2 (Endre et al., 2002)/LjSYMRK (Stracke et al., 2002), cation channels MtDMI1 (Ane et al., 2004)/LjPOLLUX (Imaizumi-Anraku et al., 2005) and LjCASTOR (Imaizumi-Anraku et al., 2005), nucleoporins LjNUP85 (Saito et al., 2007) and LjNUP133 (Kanamori et al., 2006), a calcium calmodulin-dependent kinase MtDMI3 (Levy et al., 2004; Mitra et al., 2004)/LjCCaMK (Tirichine et al., 2006) and its interaction partner MtIPD3/LjCYCLOPS (Yano et al., 2008). This knowledge, together with the observation of nuclear calcium spiking in epidermal cells responding

to AM fungi and rhizobia bacteria, has led to the current model of how the initial signaling between symbionts occurs: The receptor-like kinase DMI2 provides an essential signaling step, through an unknown mechanism, to initiate calcium spiking in the nucleus, which also requires the cation channels DMI1 and Castor (which does not have an ortholog in *M. truncatula*) and the nucleoporins. AM fungi and rhizobia elicit different calcium signatures in the plant nucleus (Kosuta et al., 2008), which is likely interpreted by the calcium calmodulin-dependent kinase DMI3, which in turn interacts with IPD3 to initiate the appropriate signaling pathway, eventually eliciting the cellular rearrangement necessary to allow for epidermal penetration of AM fungi and rhizobial infection (Parniske, 2008).

A model for genetic regulation of arbuscule development in cortical cells is less clear. For two of the common *sym* mutants, *ccamk* and *cyclops* of *L. japonicus,* arbuscule formation was impaired in rare cases where AM fungi successfully penetrate the root cortex. In contrast, arbuscule development is not impaired in *symrk* mutants (Demchenko et al., 2004; Kistner et al., 2005). This result suggests that the genetic pathway enabling arbuscule development may partially overlap with the program that allows epidermal penetration. Further genetic evidence for a shared program comes from analysis of *Vapyrin*, a gene shown to be required for arbuscule formation and efficient epidermal penetration in *M. truncatula* (Pumplin et al., 2010) and Chapter 5.

Only a few genes have been reported that are specifically required for arbuscule development. Two half-ABC transporters in *M. truncatula*, *STR* and *STR2*, are required for arbuscules to reach mature size, as *str* mutant plants or *STR2*-silened plants develop only stunted arbuscules (Zhang et al., 2010). Mutation of *MtPT4*, a phosphate transporter of *M. truncatula* specifically involved in phosphate acquisition from the arbuscule, permits full arbuscule development but causes rapid arbuscule death (Javot et al., 2007b). RNAi-mediated silencing of a phosphate transporter,

LjPT3 (Maeda et al., 2006) and two secreted subtilases, *SbtM1* and *SbtM3* (Takeda et al., 2009) from *L. japonicus,* and a calcium-dependent protein kinase from *M. truncatula* (Ivashuta et al., 2005) reduced the frequency of arbuscule formation in roots with no specific effect reported on development. Clearly, there are many gaps in our understanding of the genes, pathways and molecular mechanisms that regulate arbuscule development.

Chemical signaling between symbionts

In addition to genetic factors, a number of chemical signals that regulate the interaction have been recently described. Plants secrete a branching factor, which is recognized by hyphae growing in the soil and induces increased hyphal respiration, mitosis and a proliferation of hyphal branching, thus improving the likelihood of contacting a root (Akiyama et al., 2005; Besserer et al., 2006). This branching factor was recently identified as the sesquiterpene strigolactone, and the relative instability of this molecule in soil restricts its detection to the immediate vicinity of a root (Parniske, 2008). Interestingly, strigolactone also stimulates the germination of parasitic weeds such as *Striga* (Matusova et al., 2005), and was recently characterized as a previously-unrecognized hormone regulating shoot branching in rice and Arabidopsis (Gomez-Roldan et al., 2008; Umehara et al., 2008).

AM fungi also emit a chemical signal that elicits changes in the plant. The existence of this signaling molecule, or molecules, was predicted by experiments revealing induced transcriptome changes and calcium spiking in roots surrounded by a barrier that prevents physical contact between symbionts (Kosuta et al., 2003; Navazio et al., 2007; Kosuta et al., 2008). The nature of this chemical signal, termed "myc factor" is currently unknown. Its discovery, and the mechanism underlying its perception by plants may reveal additional parallels with the interaction between

legumes and rhizobia bacteria, which secrete nodulation (Nod) factors prior to root contact. Nod factors are modified chitin oligomers that determine the narrow host range of rhizobia species and are perceived by plant LysM domain-containing receptor-like kinases including *LjNFR1* and *LjNFR5* from *Lotus japonicus* (Madsen et al., 2003; Radutoiu et al., 2003) and *Medicago truncatula MtLYK3* and *MtNFP* (Limpens et al., 2003; Arrighi et al., 2006; Smit et al., 2007). To date, no 'myc' factor receptors have been reported.

Finally, a common membrane lipid molecule, lysophosphatidylcholine, was reported as an active signaling molecule that could induce transcription of mycorrhizal-specific genes including *LePT4* and *StPT4* from tomato and potato, respectively, in the absence of a fungal symbiont (Drissner et al., 2007). This molecule was isolated by activity-guided fractionation of mycorrhizal root extracts, and its origin and signaling function in a biological context remain unknown.

Cellular rearrangement during AM symbiosis

A major aspect of the AM symbiosis is a regulated reorganization of the plant cell to accommodate intracellular fungal growth, both for epidermal penetration and arbuscule formation in cortical cells. Many early descriptions of these cells were made by transmission electron microscopy (TEM), and recently the use of immunolocalization and live-cell imaging with fluorescently-tagged proteins has provided additional information about the cellular organization.

Arbuscule development is accompanied by drastic reorganization of the cortical cell components. Ultrastructure analyses of cells harboring developing arbuscules were made in dicot and monocot roots by a number of groups (Cox and Sanders, 1974; Kinden and Brown, 1975b, a; Cox and Tinker, 1976; Scannerini and Bonfante-Fasolo, 1982; Toth and Miller, 1984), revealing similar developmental

events across species, and the presence of a plant membrane surrounding the arbuscule at all stages of development. This membrane, termed periarbuscular membrane, is continuous with the plasma membrane and will be discussed in further detail below.

Arum-type arbuscules are composed of two hyphal types, trunk and branch (Cox and Tinker, 1976). The hypha that penetrates into a cortical cell becomes the trunk and is surrounded by a relatively thick plant cell wall (Figure 1-1). There is no evidence of papilla formation, as occurs surrounding the base of fungal haustoria (Cox and Sanders, 1974; Kinden and Brown, 1975a; Koh et al., 2005). As the hypha grows through the cell, it begins to bifurcate, forming much smaller branches, ~ 1µm in diameter, which are surrounded by a thin interfacial matrix composed of primary plant cell wall and fungal wall (Cox and Sanders, 1974; Kinden and Brown, 1975b; Toth and Miller, 1984). Whether arbuscule development is initiated at the point of hyphal entry into a cell or during intracellular growth is unknown. The data presented in Chapter 2 (Pumplin and Harrison, 2009) reveal that hyphal trunks and intracellular hyphae, which cross through cells without forming branches, are both surrounded by plasma membrane markers (Figure 1-1). Branches, in contrast, are surrounded by a periarbuscular membrane domain with specialized protein composition (Chapter 2 & 4) (Figure 1-1). This observation suggests the different fates of intracellular hyphae and arbuscules may result from a developmental event(s) initiated during growth within the cell. The final stage of arbuscule development, turnover, occurs ~ 7-10 days after formation. Rapid collapse of arbuscule branches is first observed, while the trunk, surrounded by a thicker cell wall, remains for longer in the cell (Toth and Miller, 1984).

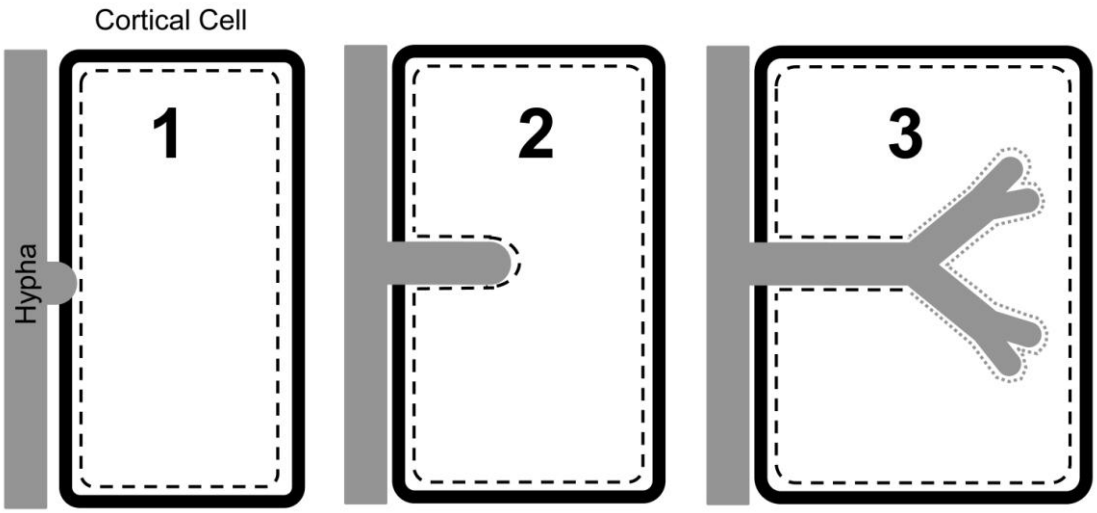

Figure 1-1 Diagram of arbuscule development.

Developmental events associated with a hypha (grey) growing into a cortical cell are depicted (cell wall shown in black, plasma membrane as black dashed line). Cell 1, hypha begins to penetrate. Cell 2, hypha, which will become the trunk, has grown into cell. Cell 3, arbuscule branching begins, and fungus is surrounded by periarbuscular membrane (grey dashed line).

Beyond the ultrastructure descriptions, these TEM studies were used for morphometric analyses that quantified changes in cell volume and surface area in cells harboring arbuscules. The volume of cell filled with an arbuscule ranges from 20-40%, plant cytoplasm increases 3-15 fold and the surface area of the plant protoplast relative to its volume increases up to 20-fold (Cox and Tinker, 1976; Toth and Miller, 1984; Alexander et al., 1989). This surface area increase is attributed to the synthesis of the periarbuscular membrane, which surrounds the bifurcating arbuscule branches and reaches an area estimated as 3-8 times the area of the plasma membrane. Fungal growth also leads to a reduction in protoplast volume, through a reduction in vacuolar space. As the large central vacuole reduces in volume to allow fungal growth, observations by TEM reveal individual small vacuoles surrounding fungal structures, either due to a single invaginated and convoluted vacuole, fragmentation of the central vacuole, or a combination of the two (Cox and Sanders, 1974; Scannerini and Bonfante-Fasolo, 1982; Bonfante-Fasolo, 1984; Toth and Miller, 1984; Gianinazzi-Pearson, 1996; Pumplin and Harrison, 2009) as discussed in Chapter 2. Electron microscopy studies also revealed a proliferation of cytoplasm and organelles, including endoplasmic reticulum (ER), Golgi, multivesicular bodies, plastids and mitochondria, which were located predominantly in the area of arbuscule branches (Cox and Sanders, 1974; Kinden and Brown, 1975b, a; Cox and Tinker, 1976; Toth and Miller, 1984; Brundrett et al., 1985; Gianinazzi-Pearson, 1996; Genre et al., 2008).

The concentration of organelles around arbuscule branches coincides with a reorganization of the plant cytoskeleton during arbuscule development, as determined by immunolocalization studies (Genre and Bonfante, 1997, 1998; Blancaflor et al., 2001). Actin microfilaments were reported to rearrange and surround branches of mature arbuscules and the plant nucleus, while being absent from the cell periphery

and the area surrounding trunks (Genre and Bonfante, 1998). Microtubules also reorganized to surround arbuscule branches and trunks, coincident with a loss of the typical cortical microtubule arrays normally present in root cortical cells (Genre and Bonfante, 1997, 1998; Blancaflor et al., 2001). Microtubules appeared to form connections between arbuscule branches, while actin filaments surrounded and were closely appressed to branches. Additionally microtubules in uninfected cells in the area of colonized cells became unorganized, and this is believed to reflect a cytoskeletal rearrangement prior to, and possibly in anticipation of, fungal invasion (Blancaflor et al., 2001).

Most recently, live-cell imaging techniques have exploited fluorophore-tagged proteins to observe the distribution of organelles in cells harboring arbuscules. These studies describe clustering of stromule-connected plastids (Fester et al., 2001; Hans et al., 2004), mitochondria (Lohse et al., 2005), ER (Genre et al., 2008; Pumplin and Harrison, 2009), Golgi and peroxisomes (Pumplin and Harrison, 2009) around arbuscule branches. These data are consistent with TEM data and illustrate that active metabolism in these cells is concentrated around arbuscule branches. This live-cell imaging approach also led to a new model for how fungi penetrate plant cells. Observing fluorescently-tagged microtubule-binding, actin-binding and ER-retained proteins in roots infected with AM fungi, Genre and colleagues (2005) observed cellular reorganization prior to fungal entry into cells. During epidermal penetration, the plant nucleus moved to an area opposite the hyphopodium, together with an accumulation of microtubules, actin and ER. The nucleus then moved away from the site of penetration, leaving behind a "tunnel" of microtubules, actin, cytoplasm and ER termed the prepenetration apparatus (PPA), through which the fungus grew. An interesting question regarding symbiotic development is which events are under control of the fungus and which are controlled by the plant. That is, does fungal

growth force plant cell membrane invagination or does the plant cell rearrange first and consequently direct fungal growth. The work of Genre *et al*. suggests that the plant establishes the fungal path of growth prior to entry.

A similar PPA-like response was observed in the cortex, where plant cells that are not yet infected displayed repositioning of nuclei and accumulation of ER, prior to arbuscule formation (Genre et al., 2008). If arbuscule development is regulated by PPA formation through a cellular program that partially overlaps with epidermal penetration, it is possible that the unique developmental program giving rise to arbuscules is initiated not at the point of cell penetration, but rather modulated at a later point, giving rise to a differentiated periarbuscular membrane surrounding the small branches. Consistent with this idea, live-cell imaging has led to the discovery that the periarbuscular membrane is separated into two domains that differ in protein composition, as introduced above. Chapter 2 (Pumplin and Harrison, 2009) presents evidence that a glycosylphosphatidylinositol-anchored blue copper-binding protein, MtBcp1, and a plasma membrane marker, AtPIP2a, are localized in the plasma membrane, the periarbuscular membrane region only around the trunk, and the membrane surrounding intracellular hyphae, while the phosphate transporter MtPT4 is localized only around arbuscule branches. A developmental switch initiated during the phase of branch formation could explain these membrane compositions. This theory is also supported by analysis of the STR/STR2 ABC transporter, which localizes in the branch domain of the periarbuscular membrane, but not the trunk domain. In *str* mutant plants, fungal penetration of cortical cells occurs normally but branch formation is retarded and arbuscules collapse after forming only a few branches, preventing symbiosis (Zhang et al., 2010). It is likely therefore that STR functions in developing the specialized nutrient-exchanging domain of the periarbuscular membrane during branch formation. Taken together, these results

suggest that arbuscule branches are crucial for AM symbiosis and their differentiation is initiated during hyphal growth within plant cells.

Phosphate transport at the periarbuscular membrane

The major purpose of these cellular rearrangements is to establish a plant-fungal interface capable of mediating nutrient transfer. It is well-accepted that nutrients, such as phosphate, are transported from the fungus to the plant across the periarbuscular membrane. This theory was debated for a time however, as some researchers believed that nutrients were taken up from collapsed arbuscules during degeneration, rather than through active transport from mature arbuscules (Kinden and Brown, 1975b). This theory might explain the transient nature of arbuscules, but is not consistent with Pi flux measurements and would not explain the investment in complex cellular reorganization to create the large arbuscule surface area (Cox and Tinker, 1976). Evidence for active transport of nutrients across the periarbuscular membrane comes from a series of experiments: First, the periarbuscular membrane displays strong H^+-ATPase activity, which often functions to facilitate secondary active transport (Marx et al., 1982; Gianinazzi-Pearson et al., 1991; Bonfante and Perotto, 1995). An antibody that recognizes two H^+-ATPase proteins from tobacco, PMA2 and PMA4, was localized on the periarbuscular membrane (Gianinazzi-Pearson et al., 2000) and H^+-ATPase genes are induced in mycorrhizal roots of tobacco and *M. truncatula* (Gianinazzi-Pearson et al., 2000; Krajinski et al., 2002). Furthermore, the *M. truncatula* phosphate transporters MtPT4 (Harrison et al., 2002; Pumplin and Harrison, 2009), MtPT8 (Chapter 4), and rice OsPT11 (Kobae and Hata, 2010), which are members of the PHT1 family of proteins that mediate $Pi:H^+$ symport, are localized specifically in the periarbuscular membrane. In addition, mutation of *MtPT4* results in a loss of phosphate uptake through the symbiosis and premature degeneration of

polyphosphate-containing arbuscules (Javot et al., 2007b). This provided solid evidence that Pi is taken up across the periarbuscular membrane rather than being scavenged from collapsed arbuscules. Additional nutrients known to be exchanged during the symbiosis, such as ammonium from fungus to plant and carbon molecules from plant to fungus, are also likely transported across this membrane; however, direct experimental evidence for the site and mechanism of their transport is lacking.

Mechanisms underlying cellular reorganization and polar protein targeting

The mechanism that leads to localization of phosphate transporters such as MtPT4 in the periarbuscular membrane is an interesting open question, and is addressed in Chapter 3. Based on the unique protein composition of the periarbuscular membrane, which also includes H^+-ATPases and the STR/STR2 ABC transporter, a polarized secretion and/or protein sorting process has been hypothesized. However, the molecular mechanisms that carry out formation of the periarbuscular membrane during arbuscule development are entirely unknown. As discussed above, the precise time it takes for formation of an arbuscule is not known. However, it is likely on the order of a single day, as two days is sufficient for AM fungi to penetrate plant roots, grow through the cortex and develop arbuscules (Brundrett et al., 1985; Javot et al., 2007b; Zhang et al., 2010). The large periarbuscular membrane, estimated to be as large as eight times the area of the plasma membrane, must form within this brief time window, and the investment in its rapid synthesis is likely reflected in the proliferation of organelles that cluster around growing arbuscule branches. This context may suggest a mechanism for protein localization through secretion coupled with periarbuscular membrane synthesis (Chapter 3).

In plants, polar localization of transporters is best understood for the PIN family of auxin efflux pumps in *Arabidopsis thaliana*, which mediate polar auxin

transport by localizing to apical or basal domains of the plasma membrane. The mechanism directing this localization involves an initial symmetric secretion to the plasma membrane, followed by endocytosis and polar recycling based on differential phosphorylation states of protein motifs (Dhonukshe et al., 2008; Geldner, 2009). A theory is proposed in Chapter 3 that polar localization of MtPT4 in the periarbuscular membrane occurs not by a sorting mechanism based on specific motifs, but rather by bulk flow secretion to the site of arbuscule development regulated by precise temporal induction of gene expression and protein synthesis. This conclusion is based on experimental findings that a plasma membrane-localized phosphate transporter expressed in the epidermis and outer cortex, MtPT1, localizes in the periarbuscular membrane if expressed during arbuscule branch formation, while expression of MtPT4 or MtPT1 prior to arbuscule branch formation is insufficient for localization in this membrane domain.

Additional localization studies revealed that an MtPT4 mutant with a single amino acid change (substitution of serine 115 for phenylalanine) was retained in the trans-Golgi network (TGN). Furthermore, introducing the equivalent mutation into MtPT1 also caused retention of the protein in the TGN. These data implicate the TGN as an intermediate secretory compartment for phosphate transporters, as recently detailed for a boron transporter (Viotti et al., 2010), and also suggest that the mechanism of TGN to periarbuscular and plasma membrane secretion may involve shared components. While the identity of secretory regulators during the AM symbiosis is not known, speculation on mechanisms can be drawn from parallels with other plant-microbe interactions.

The interaction between plant cells and pathogenic haustorium-forming fungi shares morphological, and possibly developmental, similarities with mycorrhizal symbiosis. A series of studies of Arabidopsis genes required for non-host resistance

against incompatible powdery mildew pathogens indicate the involvement of a SNARE (soluble N-ethyl-maleimide-sensitive factor attachment protein receptor) complex, which mediates vesicle fusion at target membranes. This complex includes the syntaxin Pen1/Syp121, SNAP33, and the vesicle-SNAREs VAMP 721 and 722, and is required for polarized secretion and formation of a callose-rich papilla to resist fungal penetration (Sanderfoot et al., 2001; Collins et al., 2003; Kwon et al., 2008). VAMP 721 and 722 are also required for basic plant development, illustrating overlapping functions in secretory mechanisms for host-microbe interactions (Kwon et al., 2008).

A similar implication for a ubiquitous SNARE protein in plant-microbe interactions comes from studies of the root nodule symbiosis in *M. truncatula*. During nodule development, rhizobia bacteria are engulfed in a plant-derived symbiosome membrane, analogous to the periarbuscular membrane. Infected nodule cells can contain thousands of symbiosome-surrounded bacteroids, which reduce atmospheric dinitrogen and transfer ammonium to the plant (Udvardi and Day, 1997). Symbiosomes contain the target-SNARE Syp132, which is normally localized in the plasma membrane (Catalano et al., 2007; Limpens et al., 2009). This protein relocates to the infection thread and symbiosome membranes, where it likely mediates vesicle fusion of symbiosis-specific membrane and cargo (Limpens et al., 2009; Ivanov et al., 2010). It is expected that similar molecules function to regulate periarbuscular membrane synthesis; however the identity and mode of action of such molecules remains to be determined.

Interestingly, symbiosome membrane development in *M. truncatula* also requires a member of the Rab family of small GTPases, Rab7A2 (Limpens et al., 2009). This family encodes well-studied regulators of secretion that mediate transport and docking of secretory vesicles at target membranes and also function to specify

identity of endosomal compartments (Rutherford and Moore, 2002). Rab7A2 is normally localized to the tonoplast and multivesicular bodies, which mediate membrane protein turnover following endocytosis. Following bacteroid development, this protein localizes to the symbiosome membrane, suggesting an overlap between symbiosome development and endocytic processes (Limpens et al., 2009; Ivanov et al., 2010). While the involvement of Rab proteins has not been explored during the AM symbiosis, an RNA interference-based mutant screen in *M. truncatula* did reveal a requirement for a protein that may function on endosomes. Chapter 5 presents the discovery and characterization of Vapyrin, a protein predicted to mediate protein-protein interactions, which is localized on mobile endosomal-like compartments within AM fungal-infected cells. Knockdown of this gene impairs epidermal penetration by hyphae and abolishes arbuscule development, suggesting that the molecule may mediate a required secretion or signaling process for symbiotic development.

Taken together, the data presented in this dissertation provide analysis of protein localization during arbuscule development at a level of detail not previously available in live cells. This has enabled the development of theories about fundamental aspects of membrane formation during the AM symbiosis. Moreover, characterization of *MtPT4* membrane targeting (Chapter 3), and functional characterization of *MtPT8* (Chapter 4) and *Vapyrin* (Chapter 5) contribute to our understanding of the genetic landscape involved in regulating the AM symbiosis in the model legume *M. truncatula*.

REFERENCES

Akiyama, K., Matsuzaki, K., and Hayashi, H. (2005). Plant sesquiterpenes induce hyphal branching in arbuscular mycorrhizal fungi. Nature **435,** 824-827.

Alexander, T., Toth, R., Meier, R., and Weber, H.C. (1989). Dynamics of arbuscule development and degeneration in onion, bean and tomato with reference to vesicular-arbuscular mycorrhizae in grasses. Canadian Journal of Botany **67,** 2505-2513.

Ane, J.M., Kiss, G.B., Riely, B.K., Penmetsa, R.V., Oldroyd, G.E., Ayax, C., Levy, J., Debelle, F., Baek, J.M., Kalo, P., Rosenberg, C., Roe, B.A., Long, S.R., Denarie, J., and Cook, D.R. (2004). *Medicago truncatula* DMI1 required for bacterial and fungal symbioses in legumes. Science **303,** 1364-1367.

Arrighi, J.F., Barre, A., Ben Amor, B., Bersoult, A., Soriano, L.C., Mirabella, R., de Carvalho-Niebel, F., Journet, E.P., Gherardi, M., Huguet, T., Geurts, R., Denarie, J., Rouge, P., and Gough, C. (2006). The *Medicago truncatula* lysine motif-receptor-like kinase gene family includes NFP and new nodule-expressed genes. Plant Physiol **142,** 265-279.

Bago, B., Pfeffer, P.E., and Shachar-Hill, Y. (2000). Carbon metabolism and transport in arbuscular mycorrhizas. Plant Physiology **124,** 949-957.

Besserer, A., Puech-Pages, V., Kiefer, P., Gomez-Roldan, V., Jauneau, A., Roy, S., Portais, J.C., Roux, C., Becard, G., and Sejalon-Delmas, N. (2006). Strigolactones stimulate arbuscular mycorrhizal fungi by activating mitochondria. PLoS Biol **4,** e226.

Blancaflor, E.B., Zhao, L.M., and Harrison, M.J. (2001). Microtubule organization in root cells of *Medicago truncatula* during development of an arbuscular mycorrhizal symbiosis with *Glomus versiforme*. Protoplasma **217,** 154-165.

Bonfante-Fasolo, P. (1984). Anatomy and morphology of VA mycorrhizae. In VA Mycorrhizae, C.L. Powell and D.J. Bagyaraj, eds (Boca Raton, Florida: CRC Press), pp. 5-33.

Bonfante, P., and Perotto, S. (1995). Strategies of arbuscular mycorrhizal fungi when infecting host plants. New Phytologist **130,** 3-21.

Brundrett, M.C. (2009). Mycorrhizal associations and other means of nutrition of vascular plants: understanding the global diversity of host plants by resolving conflicting information and developing reliable means of diagnosis. Plant and Soil **320,** 37-77.

Brundrett, M.C., Piché, Y., and Peterson, R.L. (1985). A developmental study of the early stages in vesicular–arbuscular mycorrhiza formation. Can. J. Bot. **63,** 184–194.

Catalano, C.M., Czymmek, K.J., Gann, J.G., and Sherrier, D.J. (2007). *Medicago truncatula* syntaxin SYP132 defines the symbiosome membrane and infection droplet membrane in root nodules. Planta **225,** 541-550.

Cavagnaro, T.R., Gao, L.-L., Smith, F.A., and Smith, S.E. (2001). Morphology of arbuscular mycorrhizas is influenced by fungal identity New Phytologist **151,** 469-475.

Collins, N.C., Thordal-Christensen, H., Lipka, V., Bau, S., Kombrink, E., Qiu, J.L., Huckelhoven, R., Stein, M., Freialdenhoven, A., Somerville, S.C., and Schulze-Lefert, P. (2003). SNARE-protein-mediated disease resistance at the plant cell wall. Nature **425,** 973-977.

Cox, G., and Sanders, F. (1974). Ultrastructure of the host-fungus interface in a vesicular-arbuscular mycorrhiza. New Phytologist **73,** 901-912.

Cox, G., and Tinker, P.B. (1976). Translocation and transfer of nutrients in vesicular-arbuscular mycorrhizas: I. The arbuscule and phosphorus transfer: A quantitative ultrastructural study. New Phytologist **77,** 371-378.

Demchenko, K., Winzer, T., Stougaard, J., Parniske, M., and Pawlowski, K. (2004). Distinct roles of *Lotus japonicus* SYMRK and SYM15 in root colonization and arbuscule formation. New Phytologist **163,** 381-392.

Dhonukshe, P., Tanaka, H., Goh, T., Ebine, K., Mahonen, A.P., Prasad, K., Blilou, I., Geldner, N., Xu, J., Uemura, T., Chory, J., Ueda, T., Nakano, A., Scheres, B., and Friml, J. (2008). Generation of cell polarity in plants links endocytosis, auxin distribution and cell fate decisions. Nature **456,** 962-966.

Drissner, D., Kunze, G., Callewaert, N., Gehrig, P., Tamasloukht, M., Boller, T., Felix, G., Amrhein, N., and Bucher, M. (2007). Lyso-phosphatidylcholine is a signal in the arbuscular mycorrhizal symbiosis. Science **318,** 265-268.

Endre, G., Kereszt, A., Kevei, Z., Mihacea, S., Kalo, P., and Kiss, G.B. (2002). A receptor kinase gene regulating symbiotic nodule development. Nature **417,** 962-966.

Feng, G., Song, Y.C., Li, X.L., and Christie, P. (2003). Contribution of arbuscular mycorrhizal fungi to utilization of organic sources of phosphorus by red clover in a calcareous soil. Applied Soil Ecology **22,** 139-148.

Fester, T., D., S., and Hause, B. (2001). Reorganization of tobacco root plastids during arbuscule development. Planta **213,** 864-868.

Geldner, N. (2009). Cell polarity in plants: a PARspective on PINs. Curr Opin Plant Biol **12,** 42-48.

Genre, A., and Bonfante, P. (1997). A mycorrhizal fungus changes microtubule orientation in tobacco root cells. Protoplasma **199,** 30-38.

Genre, A., and Bonfante, P. (1998). Actin versus tubulin configuration in arbuscule-containing cells from mycorrhizal tobacco roots. New Phytologist **140,** 745-752.

Genre, A., Chabaud, M., Timmers, T., Bonfante, P., and Barker, D.G. (2005). Arbuscular mycorrhizal fungi elicit a novel intracellular apparatus in *Medicago truncatula* root epidermal cells before infection. Plant Cell **17,** 3489-3499.

Genre, A., Chabaud, M., Faccio, A., Barker, D.G., and Bonfante, P. (2008). Prepenetration apparatus assembly precedes and predicts the colonization patterns of arbuscular mycorrhizal fungi within the root cortex of both *Medicago truncatula* and *Daucus carota*. Plant Cell **20,** 1407-1420.

Gianinazzi-Pearson, V. (1996). Plant cell responses to arbuscular myorrhiza fungi: Getting to the roots of the symbiosis. Plant Cell **8,** 1871-1883.

Gianinazzi-Pearson, V., Smith, S.E., Gianinazzi, S., and Smith, F.A. (1991). Enzymatic studies on the metabolism of vesicular-arbuscular mycorrhizas. New Phytologist **117,** 61-74.

Gianinazzi-Pearson, V., Arnould, C., Oufattole, M., Arango, M., and Gianinazzi, S. (2000). Differential activation of H+-ATPase genes by an arbuscular mycorrhizal fungus in root cells of transgenic tobacco. Planta **211,** 609-613.

Gomez-Roldan, V., Fermas, S., Brewer, P.B., Puech-Pages, V., Dun, E.A., Pillot, J.P., Letisse, F., Matusova, R., Danoun, S., Portais, J.C., Bouwmeester, H., Becard, G., Beveridge, C.A., Rameau, C., and Rochange, S.F. (2008). Strigolactone inhibition of shoot branching. Nature **455,** 189-194.

Govindarajulu, M., Pfeffer, P.E., Jin, H.R., Abubaker, J., Douds, D.D., Allen, J.W., Bucking, H., Lammers, P.J., and Shachar-Hill, Y. (2005). Nitrogen transfer in the arbuscular mycorrhizal symbiosis. Nature **435,** 819-823.

Hans, J., Hause, B., Strack, D., and Walter, M.H. (2004). Cloning, characterization, and immunolocalization of a mycorrhiza-inducible 1-deoxy-d-xylulose 5-phosphate reductoisomerase in arbuscule-containing cells of maize. Plant Physiol **134,** 614-624.

Harrison, M.J., Dewbre, G.R., and Liu, J. (2002). A phosphate transporter from *Medicago truncatula* involved in the acquisition of phosphate released by arbuscular mycorrhizal fungi. Plant Cell **14,** 2413-2429.

Imaizumi-Anraku, H., Takeda, N., Charpentier, M., Perry, J., Miwa, H., Umehara, Y., Kouchi, H., Murakami, Y., Mulder, L., Vickers, K., Pike, J., Downie, J.A., Wang, T., Sato, S., Asamizu, E., Tabata, S., Yoshikawa, M., Murooka, Y., Wu, G.J., Kawaguchi, M., Kawasaki, S., Parniske, M., and Hayashi, M. (2005). Plastid proteins crucial for symbiotic fungal and bacterial entry into plant roots. Nature **433,** 527-531.

Ivanov, S., Fedorova, E., and Bisseling, T. (2010). Intracellular plant microbe associations: secretory pathways and the formation of perimicrobial compartments. Curr Opin Plant Biol**,** *In press*.

Ivashuta, S., Liu, J., Lohar, D.P., Haridas, S., Bucciarelli, B., VandenBosch, K.A., Vance, C.P., Harrison, M.J., and Gantt, J.S. (2005). RNA interference identifies a calcium-dependent protein kinase involved in *Medicago truncatula* root development. Plant Cell **17,** 2911-2921.

Jakobsen, I., Abbott, L.K., and Robson, A.D. (1992). External hyphae of vesicular-arbuscular mycorrhizal fungi associated with *Trifolium subterraneum*L. 2. Hyphal transport of ^{32}P over defined distances. New Phytol. **120,** 509-516.

Javot, H., Pumplin, N., and Harrison, M.J. (2007a). Phosphate in the arbuscular mycorrhizal symbiosis: transport properties and regulatory roles. Plant Cell Environ **30,** 310-322.

Javot, H., Penmetsa, R.V., Terzaghi, N., Cook, D.R., and Harrison, M.J. (2007b). A *Medicago truncatula* phosphate transporter indispensable for the arbuscular mycorrhizal symbiosis. Proc Natl Acad Sci U S A **104,** 1720-1725.

Joner, E.J., Ravnskov, S., and Jakobsen, I. (2000). Arbuscular mycorrhizal phosphate transport under monoxenic conditions using radio-labelled inorganic and organic phosphate. Biotechnology Letters **22,** 1705-1708.

Kanamori, N., Madsen, L.H., Radutoiu, S., Frantescu, M., Quistgaard, E.M., Miwa, H., Downie, J.A., James, E.K., Felle, H.H., Haaning, L.L., Jensen, T.H., Sato, S., Nakamura, Y., Tabata, S., Sandal, N., and Stougaard, J. (2006). A nucleoporin is required for induction of Ca2+ spiking in legume nodule development and essential for rhizobial and fungal symbiosis. Proc Natl Acad Sci U S A **103,** 359-364.

Kinden, D.A., and Brown, M.F. (1975a). Electron microscopy of vesicular-arbuscular mycorrhizae of yellow poplar. III Host-endophyte interactions during arbuscular development. Can J Microbiol **21,** 1930-1939.

Kinden, D.A., and Brown, M.F. (1975b). Electron microscopy of vesicular-arbuscular mycorrhizae of yellow poplar. II. Intracellular hyphae and vesicles. Can J Microbiol **21,** 1768-1780.

Kistner, C., Winzer, T., Pitzschke, A., Mulder, L., Sato, S., Kaneko, T., Tabata, S., Sandal, N., Stougaard, J., Webb, K.J., Szczyglowski, K., and Parniske, M. (2005). Seven *Lotus japonicus* genes required for transcriptional reprogramming of the root during fungal and bacterial symbiosis. Plant Cell **17,** 2217-2229.

Kobae, Y., and Hata, S. (2010). Dynamics of periarbuscular membranes visualized with a fluorescent phosphate transporter in arbuscular mycorrhizal roots of rice. Plant Cell Physiol **51,** 341-353.

Koh, S., Andre, A., Edwards, H., Ehrhardt, D., and Somerville, S. (2005). *Arabidopsis thaliana* subcellular responses to compatible *Erysiphe cichoracearum* infections. Plant Journal **44,** 516-529.

Koide, R.T., and Kabir, Z. (2000). Extraradical hyphae of the mycorrhizal fungus *Glomus intraradices* can hydrolyse organic phosphate. New Phytologist **148,** 511-517.

Kosuta, S., Chabaud, M., Lougnon, G., Gough, C., Denarie, J., Barker, D.G., and Becard, G. (2003). A diffusible factor from arbuscular mycorrhizal fungi induces symbiosis-specific MtENOD11 expression in roots of *Medicago truncatula*. Plant Physiol **131,** 952-962.

Kosuta, S., Hazledine, S., Sun, J., Miwa, H., Morris, R.J., Downie, J.A., and Oldroyd, G.E. (2008). Differential and chaotic calcium signatures in the symbiosis signaling pathway of legumes. Proc Natl Acad Sci U S A **105,** 9823-9828.

Krajinski, F., Hause, B., Gianinazzi-Pearson, V., and Franken, P. (2002). *Mtha1*, a plasma membrane H+-ATPase gene from *Medicago truncatula*, shows arbuscule-specific induced expression in mycorrhizal tissue. Plant Biology **4,** 754-761.

Kwon, C., Neu, C., Pajonk, S., Yun, H.S., Lipka, U., Humphry, M., Bau, S., Straus, M., Kwaaitaal, M., Rampelt, H., El Kasmi, F., Jurgens, G., Parker, J., Panstruga, R., Lipka, V., and Schulze-Lefert, P. (2008). Co-option of a default secretory pathway for plant immune responses. Nature **451,** 835-840.

Levy, J., Bres, C., Geurts, R., Chalhoub, B., Kulikova, O., Duc, G., Journet, E.P., Ane, J.M., Lauber, E., Bisseling, T., Denarie, J., Rosenberg, C., and Debelle, F. (2004). A putative Ca2+ and calmodulin-dependent protein kinase required for bacterial and fungal symbioses. Science **303,** 1361-1364.

Limpens, E., Franken, C., Smit, P., Willemse, J., Bisseling, T., and Geurts, R. (2003). LysM domain receptor kinases regulating rhizobial Nod factor-induced infection. Science **302,** 630-633.

Limpens, E., Ivanov, S., van Esse, W., Voets, G., Fedorova, E., and Bisseling, T. (2009). *Medicago* N2-fixing symbiosomes acquire the endocytic identity marker Rab7 but delay the acquisition of vacuolar identity. Plant Cell **21,** 2811-2828.

Liu, J., Maldonado-Mendoza, I.E., Lopez-Meyer, M., Cheung, F., Town, C.D., and Harrison M, J. (2007). The arbuscular mycorrhizal symbiosis is accompanied by local and systemic alterations in gene expression and an increase in disease resistance in the shoots. The Plant Journal **50,** 529-544.

Lohse, S., Schliemann, W., Ammer, C., Kopka, J., Strack, D., and Fester, T. (2005). Organization and metabolism of plastids and mitochondria in arbuscular mycorrhizal roots of *Medicago truncatula*. Plant Physiology **139,** 329-340.

Madsen, E.B., Madsen, L.H., Radutoiu, S., Olbryt, M., Rakwalska, M., Szczyglowski, K., Sato, S., Kaneko, T., Tabata, S., Sandal, N., and Stougaard, J. (2003). A receptor kinase gene of the LysM type is involved in legume perception of rhizobial signals. Nature **425,** 637-640.

Maeda, D., Ashida, K., Iguchi, K., Chechetka, S.A., Hijikata, A., Okusako, Y., Deguchi, Y., Izui, K., and Hata, S. (2006). Knockdown of an Arbuscular Mycorrhiza-inducible Phosphate Transporter Gene of *Lotus japonicus* Suppresses Mutualistic Symbiosis. Plant Cell Physiol. **47,** 807-817.

Marx, C., Dexheimer, J., Gianinazzipearson, V., and Gianinazzi, S. (1982). Enzymatic Studies on the Metabolism of Vesicular-Arbuscular Mycorrhizas .4.

Ultracytoenzymological Evidence (Atpase) for Active Transfer Processes in the Host-Arbuscule Interface. New Phytologist **90,** 37-43.

Matusova, R., Rani, K., Verstappen, F.W., Franssen, M.C., Beale, M.H., and Bouwmeester, H.J. (2005). The strigolactone germination stimulants of the plant-parasitic *Striga* and *Orobanche* spp. are derived from the carotenoid pathway. Plant Physiol **139,** 920-934.

Mitra, R.M., Gleason, C.A., Edwards, A., Hadfield, J., Downie, J.A., Oldroyd, G.E., and Long, S.R. (2004). A Ca2+/calmodulin-dependent protein kinase required for symbiotic nodule development: Gene identification by transcript-based cloning. Proc Natl Acad Sci U S A **101,** 4701-4705.

Naumann, M., Schussler, A., and Bonfante, P. (2010). The obligate endobacteria of arbuscular mycorrhizal fungi are ancient heritable components related to the Mollicutes. ISME J **4,** 862-871.

Navazio, L., Moscatiello, R., Genre, A., Novero, M., Baldan, B., Bonfante, P., and Mariani, P. (2007). A diffusible signal from arbuscular mycorrhizal fungi elicits a transient cytosolic calcium elevation in host plant cells. Plant Physiol **144,** 673-681.

Parniske, M. (2008). Arbuscular mycorrhiza: the mother of plant root endosymbioses. Nature Reviews Microbiology **6,** 763-775.

Pirozynski, K.A., and Malloch, D.W. (1975). The origin of land plants: a matter of mycotrophism. Biosystems **6,** 153-164.

Pumplin, N., and Harrison, M.J. (2009). Live-cell imaging reveals periarbuscular membrane domains and organelle location in *Medicago truncatula* roots during arbuscular mycorrhizal symbiosis. Plant Physiol **151,** 809-819.

Pumplin, N., Mondo, S.J., Topp, S., Starker, C.G., Gantt, J.S., and Harrison, M.J. (2010). *Medicago truncatula* Vapyrin is a novel protein required for arbuscular mycorrhizal symbiosis. Plant J **61,** 482-494.

Radutoiu, S., Madsen, L.H., Madsen, E.B., Felle, H.H., Umehara, Y., Gronlund, M., Sato, S., Nakamura, Y., Tabata, S., Sandal, N., and Stougaard, J. (2003). Plant recognition of symbiotic bacteria requires two LysM receptor-like kinases. Nature **425,** 585-592.

Redecker, D., Kodner, R., and Graham, L.E. (2000). Glomalean fungi from the Ordovician. Science **289,** 1920-1921.

Remy, W., Taylor, T.N., Hass, H., and Kerp, H. (1994). Four hundred-million-year-old vesicular arbuscular mycorrhizae. Proc Natl Acad Sci U S A **91,** 11841-11843.

Rutherford, S., and Moore, I. (2002). The Arabidopsis Rab GTPase family: another enigma variation. Curr Opin Plant Biol **5,** 518-528.

Saito, K., Yoshikawa, M., Yano, K., Miwa, H., Uchida, H., Asamizu, E., Sato, S., Tabata, S., Imaizumi-Anraku, H., Umehara, Y., Kouchi, H., Murooka, Y., Szczyglowski, K., Downie, J.A., Parniske, M., Hayashi, M., and Kawaguchi, M. (2007). NUCLEOPORIN85 is required for calcium spiking, fungal and bacterial symbioses, and seed production in *Lotus japonicus*. Plant Cell **19,** 610-624.

Sanderfoot, A.A., Kovaleva, V., Bassham, D.C., and Raikhel, N.V. (2001). Interactions between syntaxins identify at least five SNARE complexes within the golgi/prevacuolar system of the *Arabidopsis* cell. Molecular Biology of the Cell **12,** 3733-3743.

Scannerini, S., and Bonfante-Fasolo, P. (1982). Comparative ultrastructural analysis of mycorrhizal associations. Canadian Journal of Botany **61,** 917-943.

Schussler, A., Schwarzott, D., and Walker, C. (2001). A new fungal phylum, the Glomeromycota: phylogeny and evolution. Mycological Research **105,** 1413-1421.

Shibata, R., and Yano, K. (2003). Phosphorus acquisition from non-labile sources in peanut and pigeonpea with mycorrhizal interaction. Applied Soil Ecology **24,** 133-141.

Simon, L., Bousquet, J., Levesque, R.C., and Lalonde, M. (1993). Origin and diversification of endomycorrhizal fungi and coincidence with vascular land plants. Nature **363,** 67-69.

Smit, P., Limpens, E., Geurts, R., Fedorova, E., Dolgikh, E., Gough, C., and Bisseling, T. (2007). *Medicago* LYK3, an entry receptor in rhizobial nodulation factor signaling. Plant Physiol **145,** 183-191.

Smith, S.E., and Read, D.J. (2008). Mycorrhizal Symbiosis. (San Diego, CA: Academic Press, Inc.).

Smith, S.E., Smith, F.A., and Jakobsen, I. (2003). Mycorrhizal fungi can dominate phosphate supply to plants irrespective of growth responses. Plant Physiol. **133,** 16-20.

Stockinger, H., Kruger, M., and Schussler, A. (2010). DNA barcoding of arbuscular mycorrhizal fungi. New Phytol**,** *In press*.

Stracke, S., Kistner, C., Yoshida, S., Mulder, L., Sato, S., Kaneko, T., Tabata, S., Sandal, N., Stougaard, J., Szczyglowski, K., and Parniske, M. (2002). A plant receptor-like kinase required for both bacterial and fungal symbiosis. Nature **417,** 959-962.

Takeda, N., Sato, S., Asamizu, E., Tabata, S., and Parniske, M. (2009). Apoplastic plant subtilases support arbuscular mycorrhiza development in *Lotus japonicus*. Plant J **58,** 766-777.

Tirichine, L., Imaizumi-Anraku, H., Yoshida, S., Murakami, Y., Madsen, L.H., Miwa, H., Nakagawa, T., Sandal, N., Albrektsen, A.S., Kawaguchi, M., Downie, A., Sato, S., Tabata, S., Kouchi, H., Parniske, M., Kawasaki, S., and Stougaard, J. (2006). Deregulation of a Ca2+/calmodulin-dependent kinase leads to spontaneous nodule development. Nature **441,** 1153-1156.

Toth, R., and Miller, R. (1984). Dynamics of arbuscule development and degeneration in a *Zea mays* mycorrhiza. Amer. J. Bot. **71,** 449-460

Udvardi, M.K., and Day, D.A. (1997). Metabolite Transport across Symbiotic Membranes of Legume Nodules. Annu Rev Plant Physiol Plant Mol Biol **48,** 493-523.

Umehara, M., Hanada, A., Yoshida, S., Akiyama, K., Arite, T., Takeda-Kamiya, N., Magome, H., Kamiya, Y., Shirasu, K., Yoneyama, K., Kyozuka, J., and Yamaguchi, S. (2008). Inhibition of shoot branching by new terpenoid plant hormones. Nature **455,** 195-200.

Viotti, C., Bubeck, J., Stierhof, Y.D., Krebs, M., Langhans, M., van den Berg, W., van Dongen, W., Richter, S., Geldner, N., Takano, J., Jurgens, G., de Vries, S.C., Robinson, D.G., and Schumacher, K. (2010). Endocytic and Secretory Traffic in *Arabidopsis* Merge in the Trans-Golgi Network/Early Endosome, an Independent and Highly Dynamic Organelle. Plant Cell **22,** 1344-1357.

Wang, B., and Qiu, Y.L. (2006). Phylogenetic distribution and evolution of mycorrhizas in land plants. Mycorrhiza **16,** 299-363.

Wang, B., Yeun, L.H., Xue, J.Y., Liu, Y., Ane, J.M., and Qiu, Y.L. (2010). Presence of three mycorrhizal genes in the common ancestor of land plants suggests a key role of mycorrhizas in the colonization of land by plants. New Phytol **186,** 514-525.

Yano, K., Yoshida, S., Muller, J., Singh, S., Banba, M., Vickers, K., Markmann, K., White, C., Schuller, B., Sato, S., Asamizu, E., Tabata, S., Murooka, Y., Perry, J., Wang, T.L., Kawaguchi, M., Imaizumi-Anraku, H., Hayashi, M., and Parniske, M. (2008). CYCLOPS, a mediator of symbiotic intracellular accommodation. Proc Natl Acad Sci U S A **105,** 20540-20545.

Zhang, Q., Blaylock, L.A., and Harrison, M.J. (2010). Two *Medicago truncatula* Half-ABC Transporters Are Essential for Arbuscule Development in Arbuscular Mycorrhizal Symbiosis. Plant Cell **22,** 1483-1497.

.

CHAPTER 2

LIVE-CELL IMAGING REVEALS PERIARBUSCULAR MEMBRANE DOMAINS AND ORGANELLE LOCATION IN *MEDICAGO TRUNCATULA* ROOTS DURING ARBUSCULAR MYCORRHIZAL SYMBIOSIS[1]

Abstract

In the arbuscular mycorrhizal symbiosis, the fungal symbiont colonizes root cortical cells, where it establishes differentiated hyphae called arbuscules. As each arbuscule develops, the cortical cell undergoes a transient reorganization and envelops the arbuscule in a novel symbiosis-specific membrane, called the periarbuscular membrane. The periarbuscular membrane, which is continuous with the plant plasma membrane of the cortical cell, is a key interface in the symbiosis, however, relatively little is known of its composition or the mechanisms of its development. Here, we used fluorescent protein fusions to obtain both spatial and temporal information about the protein composition of the periarbuscular membrane. The data indicate that the periarbuscular membrane is composed of at least two distinct domains, an 'arbuscule branch domain' that contains the symbiosis-specific phosphate transporter, MtPT4, and an 'arbuscule trunk domain', that contains MtBcp1. This suggests a developmental transition from plasma membrane to periarbuscular membrane, with biogenesis of a novel membrane domain associated with the repeated dichotomous branching of the hyphae. Additionally, we took advantage of available organelle-specific fluorescent marker proteins to further evaluate cells during arbuscule

[1] This paper was published as **Pumplin, N. and Harrison, M.J.** (2009) Live-cell imaging reveals periarbuscular membrane domains and organelle location in *Medicago truncatula* roots during arbuscular mycorrhizal symbiosis. *Plant Physiol*, **151**, 809-819. It is reprinted with permission.

development and degeneration. The three dimensional data provide new insights into relocation of Golgi and peroxisomes, and also illustrate that cells with arbuscules can retain a large continuous vacuolar system throughout development.

Introduction

In order to survive on land, plants have evolved many strategies to take up essential nutrients from the soil. One important mechanism for nutrient acquisition that is shared by a majority of plant phyla is the arbuscular mycorrhizal (AM) symbiosis (Bonfante and Genre, 2008; Parniske, 2008). At a functional level, the AM symbiosis is characterized by nutrient exchange, primarily phosphate and nitrogen, from obligate biotrophic fungi of the phylum Glomeromycota to the plant, and reciprocal carbon transfer from the plant to the fungus (Parniske, 2008; Smith and Read, 2008). The ecological importance of the AM symbiosis is illustrated by its ancient origin, estimated at 460 million years ago and coincident with plant colonization of land (Remy et al., 1994; Redeker et al., 2000; Bonfante and Genre, 2008), its evolutionary conservation in ~80% of land plant species, and experimental data showing the prominent role of the symbiosis in nutrient uptake and improvement in plant health (Smith et al., 2003; Javot et al., 2007; Liu et al., 2007; Smith and Read, 2008).

During AM symbiosis, the fungus grows within plant roots both intra- and intercellularly and subsequently colonizes the cortical cells where it forms highly branched hyphae called arbuscules (Bonfante-Fasolo, 1984). Arbuscules are the site of mineral nutrient transfer to the plant and potentially the site of carbon acquisition by the fungus. Although arbuscules form within the cortical cells, they remain separated from the plant cell cytoplasm by a plant-derived membrane, called the periarbuscular membrane. The resulting interface, delimited by the periarbuscular

membrane, establishes a large surface area within the relatively small volume of a cell, which appears optimal for nutrient transfer. Arbuscules are transient structures and following development, which is estimated to take 2-4 days, they collapse and degenerate. The complete arbuscule life cycle is estimated to take seven to ten days, although this varies depending on the symbionts involved (Alexander et al., 1989; Brown and King, 1991).

Arbuscule development is accompanied by drastic reorganization of the cortical cell. As the penetrating hypha enters the cortical cell, the plant plasma membrane is not breached but invaginates and is then extended to form the periarbuscular membrane (Cox and Sanders, 1974; Bonfante-Fasolo, 1984; Toth and Miller, 1984). Transmission electron microscopy (TEM) studies showed accumulation of cytoplasm and organelles, including endoplasmic reticulum (ER), Golgi bodies, plastids and mitochondria in the area around arbuscule branches (Cox and Sanders, 1974; Scannerini and Bonfante-Fasolo, 1982). In addition, the tonoplast invaginates and the TEM micrographs revealed the presence of multiple small vacuole compartments (Cox and Sanders, 1974; Toth and Miller, 1984), which led to the interpretation that arbuscule development is accompanied by fragmentation of the plant central vacuole (Scannerini and Bonfante-Fasolo, 1982; Bonfante and Perotto, 1995; Gianinazzi-Pearson, 1996; Harrison, 1999). Immunolocalization studies showed that arbuscule development is accompanied by reorganization of plant cytoskeletal components which surround the developing arbuscule and likely directs membrane deposition and organelle accumulation (Blancaflor *et al.* 2001, Genre and Bonfante 1997, Genre and Bonfante 1998). Recently, live-cell imaging with fluorescently-tagged proteins has been used to follow the rearrangement of plastids (Fester et al., 2001), mitochondria (Lohse et al., 2005) and ER (Genre et al., 2008) in cells with arbuscules. It has also been proposed that cellular reorganization in cortical

cells precedes and guides arbuscule development in a similar manner to the prepenetration apparatus (PPA) that facilitates AM fungal penetration into epidermal cells (Genre et al., 2005; Genre et al., 2008).

The periarbuscular membrane has been suggested to arise by *de novo* membrane synthesis (Bonfante and Perotto, 1995; Gianinazzi-Pearson, 1996); however, evidence for the origin of the membrane material and the secretion pathway is lacking. TEM studies have shown that the periarbuscular membrane is continuous with the plasma membrane but relatively little is known of its lipid or protein composition. Phosphate transporters that are expressed exclusively in AM roots in cells with arbuscules, have been cloned from monocots and dicots (Harrison et al., 2002; Paszkowski et al., 2002; Glassop et al., 2005; Nagy et al., 2005; Bucher, 2007) including *Medicago truncatula*, where the phosphate transporter, MtPT4, was shown to reside exclusively in the periarbuscular membrane (Harrison et al., 2002). In addition, H^+-ATPases, which create proton gradients necessary for secondary active transporters such as MtPT4, are induced in AM roots and have been localized to the periarbuscular membrane. In contrast, the H^+-ATPase activity of the plasma membrane of cortical cells is much lower than that of the periarbuscular membrane (Gianinazzi-Pearson et al., 1991; Bonfante and Perotto, 1995; Gianinazzi-Pearson et al., 2000; Krajinski et al., 2002). These examples provided the first evidence that the periarbuscular membrane differs from the plasma membrane.

In a comparison of membrane proteins from AM and non-AM *M. truncatula* roots (Valot et al., 2006) identified two candidates present exclusively in mycorrhizal roots: a H^+-ATPase, MtHA1 and a blue copper-binding protein, MtBcp1, which is predicted to be post-translationally modified with a glycosylphosphatidylinositol (GPI) moiety. GPI anchors, which are added to secreted proteins in the endoplasmic reticulum after cleavage of a C-terminal peptide signal, result in localization of

modified proteins to the extracellular leaflet of the plasma membrane (Eisenhaber et al., 2003). Consistent with detection of the protein in AM roots, *MtBcp1* transcripts levels are elevated in AM roots (Liu et al., 2003) and a transcriptional fusion of the promoter to the *UidA* reporter showed expression in cortical cells with arbuscules and in adjacent non-colonized cortical cells (Liu et al., 2003; Hohnjec et al., 2005). Development and maintenance of arbuscules and the periarbuscular membrane is crucial to the symbiosis and influences its longevity and function. To begin to determine the mechanisms by which a root cortical cell reorganizes its structure to develop the periarbuscular membrane, we prepared fluorescently-tagged *M. truncatula* protein markers that are expressed exclusively in the AM symbiosis and label the periarbuscular membrane. The markers are suitable for live cell imaging and provide the first evidence of distinct domains within the periarbuscular membrane. Additionally, we used available fluorescent marker protein fusions to monitor plant membranes and plant organelle distribution during arbuscule development and degeneration in *M. truncatula* cells. The data complement the earlier TEM studies and 3-dimensional reconstructions offer new insights into cellular reorganization during arbuscule development.

Results

MtPT4-GFP provides a live-cell marker of the periarbuscular membrane and defines an arbuscule branch domain of the periarbuscular membrane

The *M. truncatula* phosphate transporter MtPT4 is expressed specifically in cortical cells with arbuscules and was shown by immunolocalization to reside exclusively in the periarbuscular membrane (Harrison et al., 2002). In order to develop a fluorescent marker of the periarbuscular membrane suitable for live-cell imaging, we created an MtPT4-GFP fusion protein and determined whether this would localize to

the periarbuscular membrane. An expression vector, *pMtPT4:MtPT4-GFP*, was constructed by fusing the promoter region of *MtPT4* (Harrison et al., 2002) to the coding sequences of *MtPT4* and *GFP*, resulting in a chimeric protein with GFP fused to the carboxy terminus of MtPT4. This construct was introduced into *M. truncatula* roots by *Agrobacterium rhizogenes*-mediated root transformation (Boisson-Dernier et al., 2001). After colonization by the arbuscular mycorrhizal fungus *Glomus versiforme*, roots expressing GFP were excised, bisected longitudinally, and undisrupted cells in layers below the section plane were imaged by confocal microscopy. *pMtPT4:MtPT4-GFP* shows cell-specific expression in cortical cells with arbuscules and the fusion protein is localized to the periarbuscular membrane (Fig. 1). Specifically, MtPT4-GFP was observed on the periarbuscular membrane in the region surrounding the branches of midsize and mature arbuscules but there was no GFP signal on the membrane surrounding the trunk of arbuscules (Fig. 1 and Appendix 2-1). The fusion protein was first visible when the arbuscules reached a developmental stage with several branches. These results are consistent with previous immunolocalization data that indicated MtPT4 protein surrounded branches of arbuscules but not on arbuscule trunks or in very young arbuscules with a few branches (Harrison et al., 2002). As reported previously, MtPT4 is not located in the plasma membrane and the MtPT4-GFP marker is consistent with this and did not label the plasma membrane. In the previous immunolocalization studies, MtPT4 protein was not detected around arbuscules undergoing collapse. In *pMtPT4:MtPT4-GFP* roots with collapsing arbuscules, a "haze" of GFP signal was observed throughout the cell but excluded from the region of the arbuscule in a pattern which indicates GFP in the vacuole (Tamura et al., 2003; Kleine-Vehn et al., 2008) (Appendix 2-1). Together with the previous immunolocalization results, these data suggest that MtPT4 is degraded during arbuscule collapse.

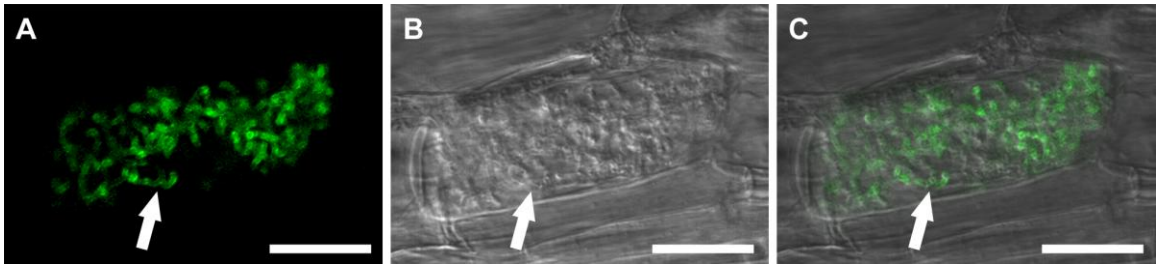

Figure 2-1 Localization of MtPT4-GFP to the periarbuscular membrane.
M. truncatula roots transformed with *pMtPT4:MtPT4-GFP* and colonized with *G. versiforme*. A, GFP signal; B, differential interference contrast (DIC) bright field image; C, overlay. The images show the fusion protein localizes to the periarbuscular membrane around the branches of a mature arbuscule (arrow). A and C are projections of eight optical sections on the z axis taken at 0.22 μm intervals. B is a single DIC section to best define structural outlines. Zoom = 2.0, Scale bar = 20 μm.

MtBcp1 is localized in the plasma membrane and the periarbuscular membrane around the arbuscule trunk

To further evaluate the protein composition of the periarbuscular membrane, we set out to find additional proteins that would localize to this membrane. Based on previous array data and promoter analyses (Liu et al., 2003; Hohnjec et al., 2005), *MtBcp1* is induced specifically in the root cortex in colonized regions of AM roots. While the specific function of MtBcp1 is unknown, the protein is predicted to be post-translationally modified with a glycosylphosphatidylinositol (GPI) anchor (Eisenhaber et al., 2003). GPI modifications are known to confer polar localization to proteins in animals (Brown et al., 1989; Lisanti et al., 1989), and plants (Schindelman et al., 2001; Roudier et al., 2005) and loss of plant genes involved in GPI biosynthesis results in defects in polar developmental processes (Lalanne et al., 2004; Gillmor et al., 2005). As development of the periarbuscular membrane likely involves polarized growth, we selected MtBcp1 as a potential candidate for a periarbuscular membrane resident protein.

To determine the subcellular localization of MtBcp1, GFP was translationally fused to the coding sequence of *MtBcp1* and expressed under its endogenous promoter (Hohnjec et al., 2005). Because MtBcp1 has a predicted cleaved secretion signal, *pMtBcp1:GFP-MtBcp1* was created by fusing GFP within the *MtBcp1* open reading frame downstream of the cleavage site resulting in an N-terminal fusion of GFP to the mature form of the MtBcp1 protein. This approach has been used successfully for tagging a GPI-anchored protein in tomato (Sun et al., 2004).

Following transformation into *M. truncatula* roots and colonization with *G. versiforme*, expression of *pMtBcp1:GFP-MtBcp1* was observed in cortical cells with arbuscules and also in cortical cells adjacent to fungal hyphae (Fig. 2 A-C). This is consistent with previous studies of transcriptional *MtBcp1* promoter:UidA fusions

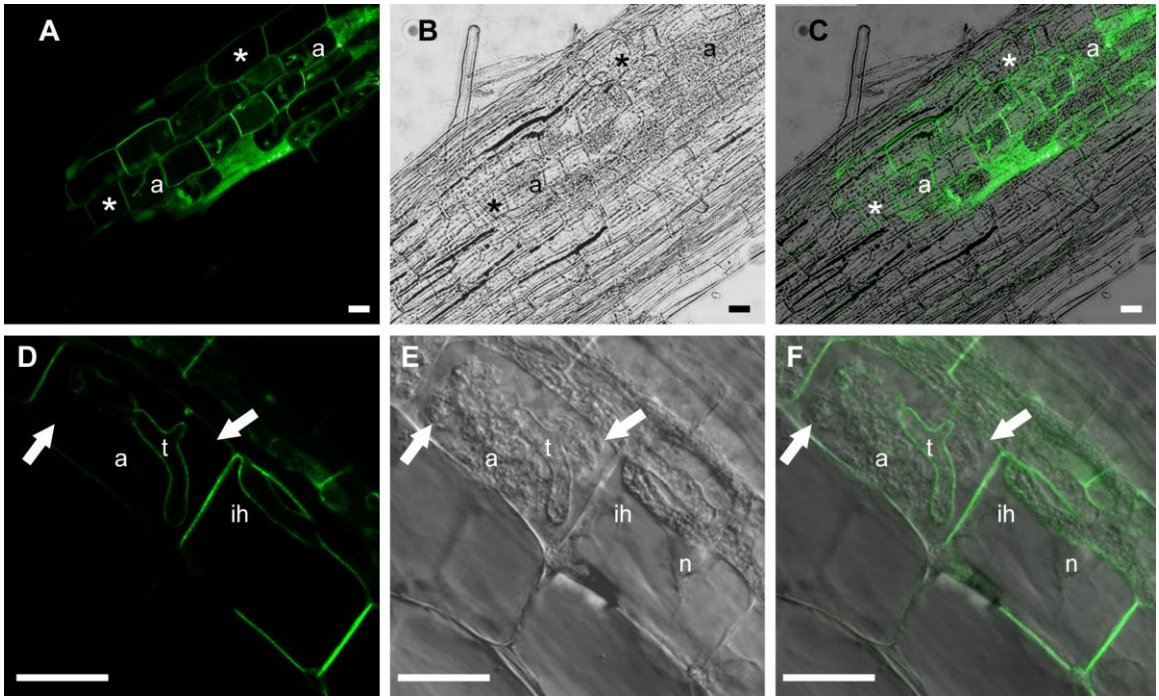

Figure 2-2 Localization of GFP-MtBcp1 to the plasma membrane, perihyphal membrane and periarbuscular membrane.
M. truncatula roots transformed with *pMtBcp1:GFP-MtBcp1* and colonized with *G. versiforme*. A and D, GFP signal; B and E, bright field image; C and F, overlays. A-C, GFP-MtBcp1 is present in the plasma membrane of root cortical cells with arbuscules (a) and cells without arbuscules (*), zoom = 2.2. D-F, GFP-MtBcp1 labels plasma membrane and periarbuscular membrane around an arbuscule trunk (t) in a cell with an arbuscule (a), but the signal is absent from the arbuscule branches (arrows). GFP-MtBcp1 signal also surrounds intracellular hyphae (IH), zoom = 2.9. A-C, E and F are single optical sections. D is a projection of four optical sections on the z axis taken at 0.4 μm intervals. Scale bar = 20 μm.

(Hohnjec et al., 2005). In cortical cells without arbuscules, GFP signal was seen around the periphery of the cell consistent with location in the plasma membrane which is expected for a GPI anchored protein (Fig. 2 A-C). During colonization of *M. truncatula* roots, *G. versiforme* shows linear, inter- and intracellular hyphal growth within the cortex; in cortical cells harboring an intracellular hypha, we observed GFP signal on the plasma membrane and also around the hypha (Fig. 2 D-F, Appendix 2-2). This suggests that the membrane that surrounds the hypha, termed the perihyphal membrane, shares characteristics of the plasma membrane. The perihyphal membrane is continuous with the plasma membrane and the GFP signal is likewise continuous (Appendix 2- 2). In cells with arbuscules, the GFP signal was again visible on the plasma membrane and in addition, there was a clear signal on the periarbuscular membrane around the arbuscule trunks. Occasionally the initial thick, dichotomous branches of a very young arbuscule showed some staining (data not shown), but there was no GFP signal around the branches of the midsize or mature arbuscules (Fig. 2 D-F). Thus, the location of MtBcp1 is opposite to that of MtPT4. These results suggests that the periarbuscular membrane, defined previously as the membrane the surrounds the arbuscule, is in fact be composed of distinct membrane domains; a domain surrounding the arbuscule trunk, that contains MtBcp1 and shares features with the plasma membrane, and a domain surrounding arbuscule branches that contains MtPT4, and is likely active in nutrient exchange.

A plasma membrane marker displays partial overlap with MtBcp1-GFP

To determine whether a typical plasma membrane protein would also localize to the perihyphal membrane and trunk domain of the periarbuscular membrane, we evaluated expression of a plasma membrane aquaporin. An *Arabidopsis* aquaporin, *AtPIP2a*, with a carboxy-terminal fusion to the red fluorescent protein mCherry,

driven by the constitutive 35s promoter (*p35s:PIP2a-mCherry*) (Nelson et al., 2007) was transformed into *M. truncatula* roots. In order to mark regions of fungal colonization, the transformation was performed in a transgenic *M. truncatula* line expressing GFP under the *MtSCP1* promoter, which is specifically induced in cortical cells surrounding fungal colonization (Liu et al., 2003; Gomez et al., 2009). The free GFP signal enabled visualization of cytoplasm and nuclei in cells with arbuscules and neighboring cortical cells (Appendix 2-3).

In non-colonized cortical cells, the AtPIP2a-mCherry marker labeled the plasma membrane as expected (Fig. 3 A-C). In cells with intracellular hyphae, AtPIP2a-mCherry labeled the plasma membrane and showed a strong perihyphal signal similar to that of GFP-MtBcp1 (Fig. 3 D-F and Appendix 2-4). In cells with arbuscules, AtPIP2a-mCherry labeled the plasma membrane and in most, but not all cells, displayed signal on the periarbuscular membrane at the base of the arbuscule trunks (Fig. 3 A-F). AtPIP2a-mCherry did not label the periarbuscular membrane around the arbuscule branches. This labeling pattern is essentially the same as that of GFP-MtBcp1 but the relative signal intensities differed slightly. GFP-MtBcp1 showed a stronger relative signal around in the trunk domain of the arbuscules that than that of the AtPIP2a-mCherry. Taken together, the protein markers suggest that the perihyphal membrane and the periarbuscular trunk domains resemble the plasma membrane, while the branch domain of the periarbuscular membrane is clearly distinct. The data are consistent with a developmental transition in the periarbuscular membrane and suggests that biogenesis of a unique domain of the periarbuscular membrane maybe be coordinated with the repeated dichotomous branching of the fungal hyphae that creates the arbuscule.

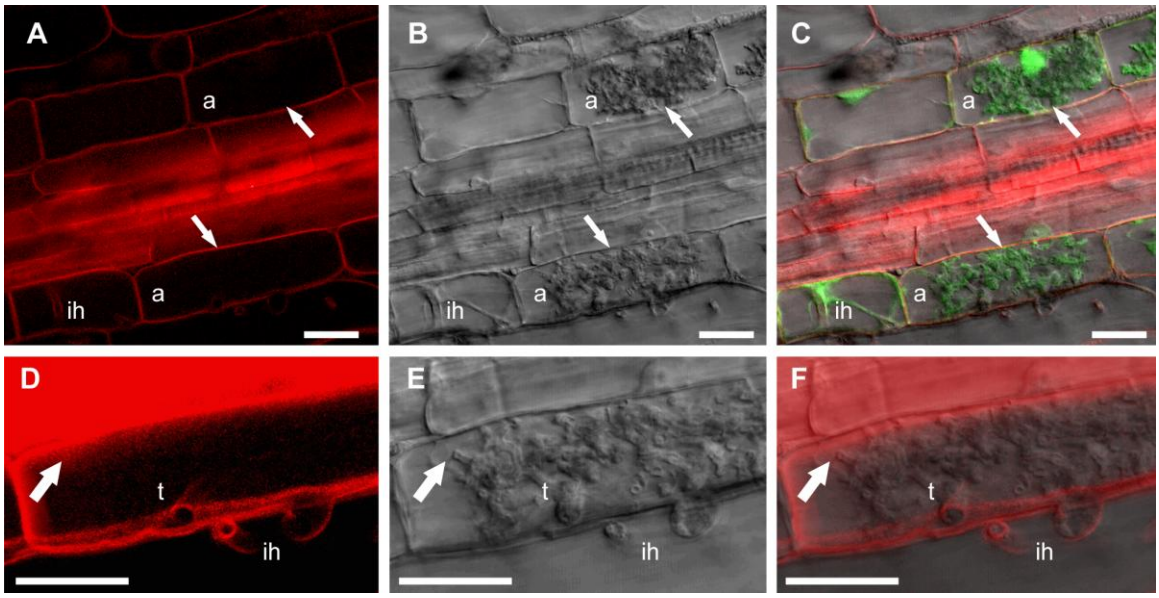

Figure 2-3 Localization of a plasma membrane marker to the plasma membrane and to the periarbuscular membrane around arbuscule trunks.
Roots of a stable transgenic *M. truncatula* MtSCP1-GFP plants transformed with a plasma membrane marker construct *35S:AtPIP2a-mCherry*. The green signal in C is free GFP expressed from the MtSCP1 promoter. A, AtPIP2a-mCherry, B, DIC, and C, overlay, zoom = 1.7. A-C, AtPIP2a signal is visible on the plasma membrane of cells with and without arbuscules (a), and also on the perihyphal membrane surrounding intracellular hyphae (ih). D-F, enlarged images of the lower arbuscule (a) from panels A-C. The enlarged image shows AtPIP2a signal on the periarbuscular membrane surrounding the trunk (t) and surrounding an intracellular hypha in the neighboring cell (ih), but signal is absent from arbuscule branches (arrow), zoom = 2.6. Signal is continuous from the plasma membrane to the arbuscule trunk. A-C and E are single optical sections. D is a projection of 11 optical sections taken at 0.71 µm intervals along the z axis assembled and modified using VOLOCITY software. F is an overlay of D and E created using Photoshop. Scale bar = 20 µm.

Organelle markers uncover cellular dynamics in live cells

To gain insights into cellular processes that may contribute to periarbuscular membrane formation we utilized this experimental platform to study the distribution of organelles in cells containing arbuscules at different stages of development. Previously, TEM studies have provided high resolution images of organelles in colonized cortical cells. Live imaging offers an opportunity to extend these analyses and in particular, enables additional 3- dimensional information to be obtained. mCherry fluorescent protein fusions that act as markers of the plasma membrane (see above) endoplasmic reticulum (ER), golgi, peroxisome and vacuole have been developed and well-characterized in Arabidopsis (Nelson et al., 2007). Some have also been used in other species where the fidelity has been confirmed, including *M. truncatula* for analysis of the rhizobium-legume symbiosis (Fournier et al., 2008) and tobacco BY-2 cells (Nebenfuhr et al., 1999). These fusion proteins, expressed under the 35s promoter, were transformed into roots of the transgenic MtSCP1:GFP *M. truncatula* line.

In plants expressing the ER marker, mCherry signal was observed in a characteristic reticulate pattern at the periphery of root cells as well as a perinuclear ring (Appendix 2-5). In a cell containing a hypha with a single dichotomous branch, the hypha was surrounded by a layer of ER and cytoplasm and the nucleus was located close to the young arbuscule as previously described (Fig. 4 A-C) (Balestrini et al., 1992; Genre et al., 2008). While in some cells, the ER marker indicated significant accumulation of ER surrounding young arbuscules, in others the ER appeared appressed to arbuscules (compare Fig. 4 A-C and Appendix 2-5 E-H).. In cells with mature arbuscules, ER was distributed throughout the space surrounding the arbuscule, and perinuclear ER was also prominent (Fig. 4 D-F). In

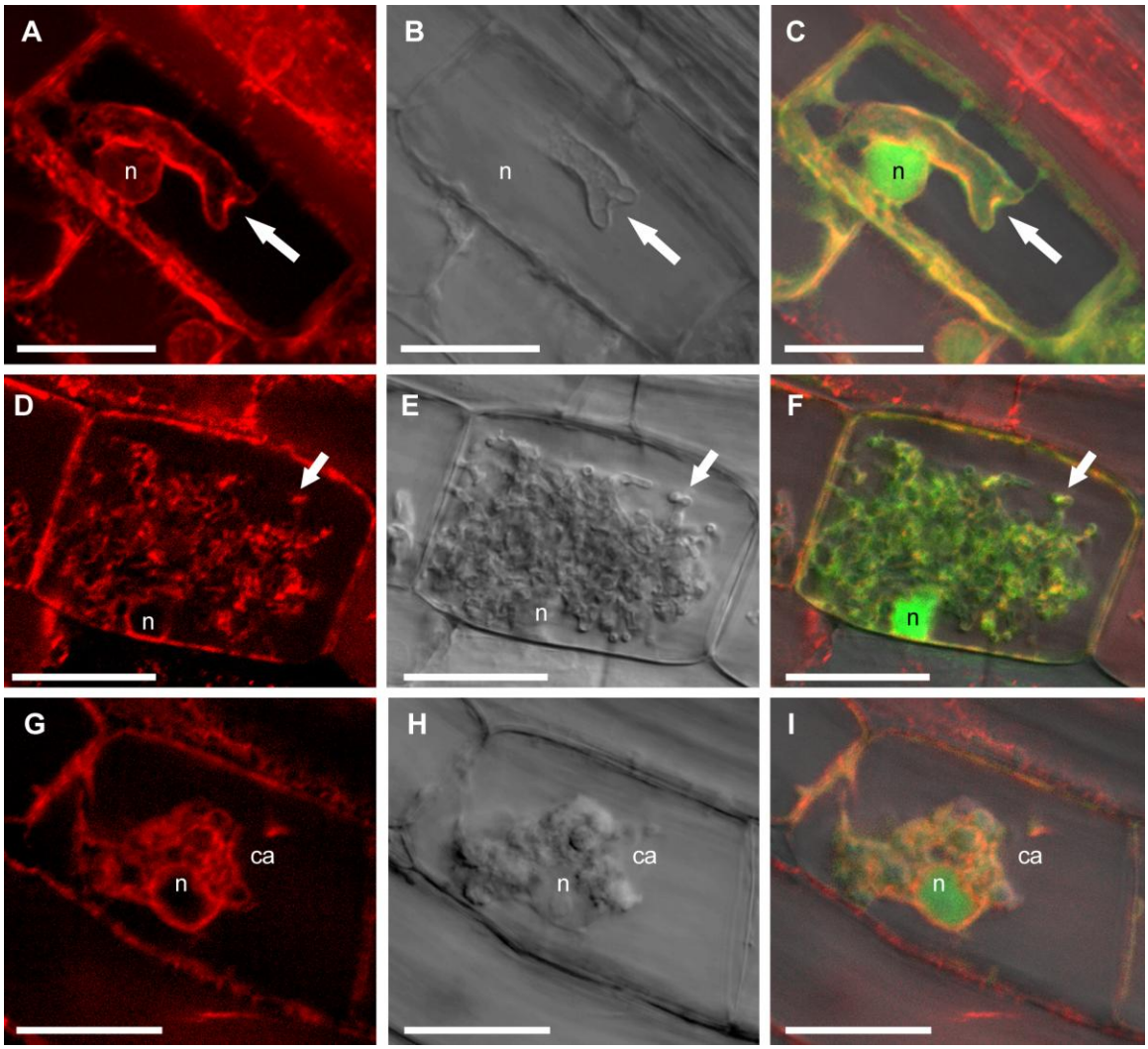

Figure 2-4 Localization of ER in root cortical cells containing arbuscules at different stages of development.

Roots of a stable transgenic *M. truncatula* MtSCP1-GFP plant transformed with 35S:mCherry-HDEL. A, D, G, mCherry-HDEL labeling the ER in cells with arbuscules; B, E, H, DIC of single z sections; C, F, I, overlay including free GFP (green signal) expressed from the MtSCP1 promoter. A-C shows a hypha (arrow) making the first dichotomous branch of arbuscule development, surrounded by a thin layer of cytoplasm and ER. A and C are projections of 32 optical sections taken at 0.3 µm intervals along the z-axis, zoom = 4.3. Perinuclear ER surrounds the nucleus (n). D-F, single confocal sections of a mature arbuscule surrounded by ER and cytoplasm, an arbuscule branch is highlighted with an arrow, nucleus (n), zoom = 4.6. G-I, ER and cytoplasm surrounds a collapsing arbuscule (ca) with closely associated plant nucleus (n). G and I are projections of four optical sections taken at 0.4 µm intervals on the z-axis, zoom = 4.7. Scale bar = 20 µm.

cells with degenerating arbuscules, the association of arbuscule, ER and plant nucleus was maintained (Fig. 4 G-I). These patterns are consistent with the active secretion directed towards the periarbuscular membrane throughout arbuscule development and degeneration, and may indicate a requirement for secreted proteins not only to build the periarbuscular membrane and the interfacial matrix, but also to deconstruct it during the degeneration phase.

In non-colonized root cells, the Golgi marker labeled small, endosomal bodies located at the cell periphery, as described in Arabidopsis cells (Appendix 2-6). A diffuse signal, potentially throughout the vacuole, was also observed which suggests that this marker may be somewhat unstable in *M. truncatula* roots (Fig. 5 A-C). In cells with young and mature arbuscules, almost all the Golgi relocated to the area surrounding arbuscule branches and were rarely present at the cell periphery (Fig. 5 A-C). Golgi bodies did not appear to associate with the extreme tips of arbuscule branches but rather along the sides of hyphae behind branching nodes (Fig. 5 A-C, Appendix 2-6). In cells with degenerating arbuscules, some Golgi bodies clustered around the arbuscule (Fig. 5 D-F) but a significant proportion of the population relocated to the periphery of the cell.

A peroxisome marker labeled bodies slightly larger than Golgi in cortical cells (Appendix 2-7) as previously described for Arabidopsis epidermal cells (Nelson et al., 2007; Genre et al., 2008). In colonized cortical cells, peroxisomes localized predominantly adjacent to the arbuscules, in a pattern similar to the Golgi marker (Fig. 5 G-H, Appendix 2-7). In contrast with the Golgi, in cells with degenerating arbuscules, the majority of the peroxisomes remained close to the degenerating arbuscule and almost entirely surrounded the degenerating mass (Fig. 5 G-H).
In non-mycorrhizal roots, the tonoplast marker revealed a large central vacuole appressed to the cell periphery with space representing nuclear invaginations

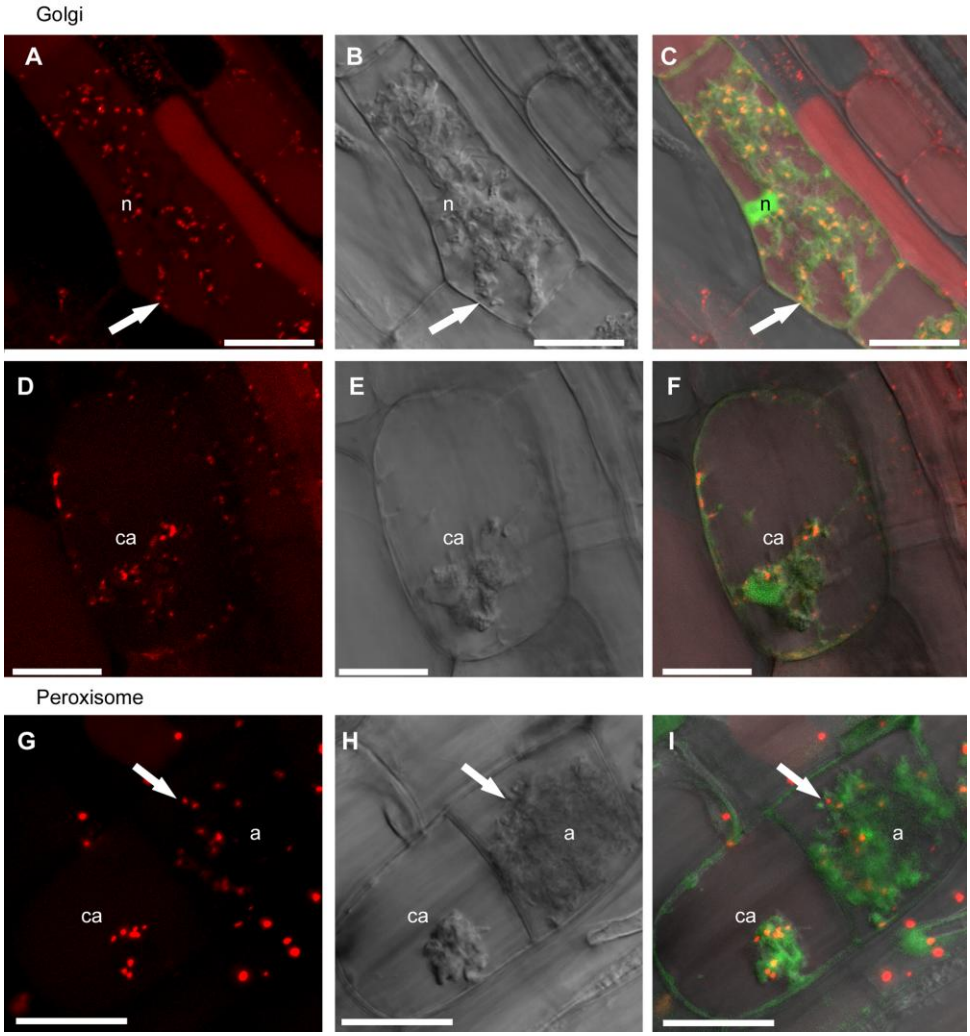

Figure 2-5 Golgi and Peroxisome distribution in cells containing arbuscules at different stages of development. Roots of stable transgenic line *M. truncatula* MtSCP1-GFP transformed with 35S: GmMan1-mCherry (A-G) and 35S:mCherry-PTS1 (G-I). A, C, D, F, GmMan1-mCherry Golgi marker; G, I, mCherry-PTS1 peroxisome marker; B, E, H, DIC of single z sections. C, F, I are overlays including free GFP expressed from the MtSCP1 promoter (green). A-C, Golgi cluster around the branches of a mature arbuscule and are generally absent from the cell periphery. Single arbuscule branch (arrow) and nucleus (n) are indicated. A and C are projections of 11 optical sections taken at 0.27 µm intervals on the z-axis, zoom = 3.5. D-F, Golgi surround a collapsing arbuscule (ca) and cell periphery, single optical sections, zoom = 3.5. G-I, Peroxisomes are closely associated with mature arbuscules (a, arrow) and cluster around a collapsing arbuscule (ca). G and I are projection of five optical sections taken at 0.25 µm intervals on the z-axis, zoom = 4.2. Scale bar = 20 µm.

(Appendix 2-8). In mycorrhizal roots, cortical cells anticipating fungal penetration had repositioned nuclei and cytoplasmic accumulations consistent with previous reports (Balestrini et al., 1992; Genre et al., 2008). During this response, cytoplasmic strands formed through the cell and were surrounded by tonoplast membrane (Appendix 2-8). In cells with young arbuscules, the tonoplast surrounded the cytoplasm and nucleus, which are directly appressed to the arbuscule (Fig. 6 A-C), suggesting the large vacuole is maintained but invaginated to allow for arbuscule development. In cells harboring fully-developed arbuscules, the tonoplast marker labeled discrete spots which may represent fragmented tonoplast; however, there also appeared to be a continuous tonoplast surrounding arbuscule structures (Fig. 6 A-F), suggesting the vacuole does not entirely fragment. Upon arbuscule turnover, the tonoplast continued to surround the collapsing fungus until the vacuole regained its original large central conformation (Fig. 6 G-I).

To illustrate that the root cells selected for imaging remain viable beyond the typical 30 minute time period used for our experiments, we prepared roots samples expressing free GFP driven from the MtSCP1 promoter and imaged a single cell harboring a young arbuscule for over three hours (Appendix 2-9). Throughout the experiment, the cell showed a strong GFP signal and active cytoplasmic streaming even three hours after sample preparation.

-

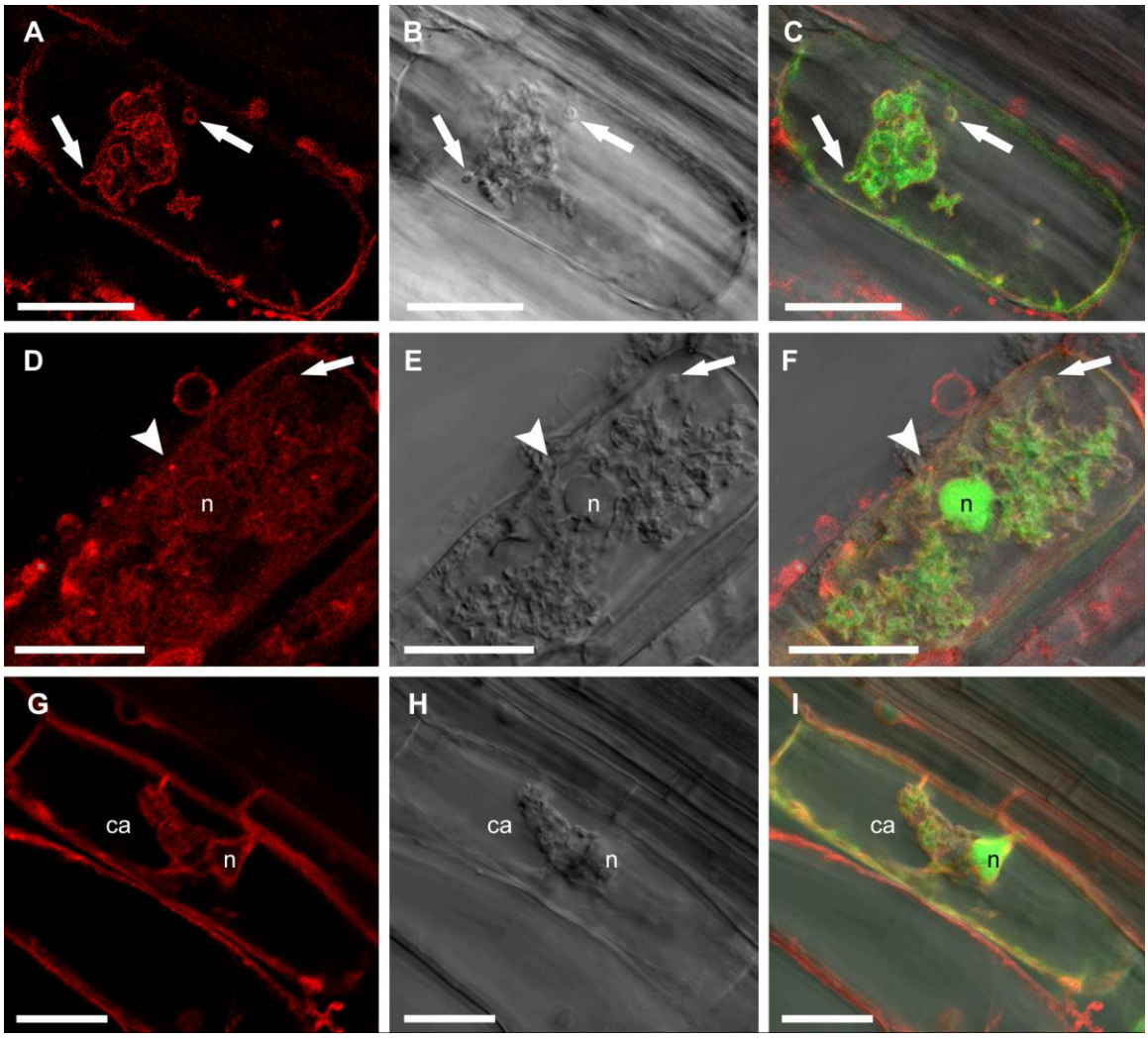

Figure 2-6 The tonoplast membrane envelops arbuscules
Roots of stable transgenic line *M. truncatula* MtSCP1-GFP transformed with 35S: γ TIP-mCherry. A, D and F, γ TIP-mCherry tonoplast marker; B, E and H, DIC of single z sections; C, F and I overlays including free GFP expressed under the SCP1 promoter (green). A-C, Tonoplast membrane surrounds the thin layer of plant cytoplasm appressed to an arbuscule (arrows), single confocal section, zoom = 3.3 D-F, a mature arbuscule, some distinct points of fluorescence were observed, possibly representing fragmented vacuoles (arrowhead). However, it appeared that a continuous tonoplast surrounded the mature arbuscule (arrow) and plant nucleus (n). D and F projection of 3 optical sections taken at 0.55 µm intervals on the z-axis, zoom = 2.6. G-I, Collapsing arbuscule (ca), nucleus (n) and cytoplasmic strands surrounded by tonoplast membrane. Scale bar = 20 µm.

Discussion

The periarbuscular membrane separates the arbuscule and the root cortical cell and plays a central role in nutrient exchange between the symbionts (Harrison, 2005; Parniske, 2008). As this membrane forms transiently in the inner cortical cells of the root it is not readily accessible. Consequently, many of membrane analysis techniques cannot be applied and the composition of the membrane and its mode of development are not well understood. Fluorescent protein markers provide a way to visualize the periarbuscular membrane and also to evaluate its protein composition. Here, we developed two AM specific marker protein fusions, MtPT4-GFP and GFP-MtBcp1. Both are driven by their native promoters so that protein location is observed in its correct spatial and temporal context. Consistent with previous immunolocalization studies (Harrison et al., 2002), the MtPT4-GFP marker is localized exclusively in the periarbuscular membrane in the region around the hyphal branches and there is no signal arising from the membrane around the arbuscule trunk or from the plasma membrane of the cell. In contrast, GFP-tagged MtBcp1 shows the opposite location and labels the plasma membrane of cortical cells before and during the growth of arbuscules, and the periarbuscular membrane surrounding arbuscule trunks, but not arbuscule branches (Fig. 7). The periarbuscular membrane is defined as a membrane that surrounds an arbuscule and is continuous with the plasma membrane. The finding that MtBcp1 and the plasma membrane marker AtPIP2a both label plasma membranes, perihyphal membranes and trunk domains of the periarbuscular membrane suggests that transition to a periarbuscular membrane that is functionally distinct from the plasma membrane may not occur until an arbuscule develops branches. Whether the MtBcp1 and AtPIP2a proteins that label the trunk domain are newly synthesized and secreted or redistribute from the plasma membrane is not

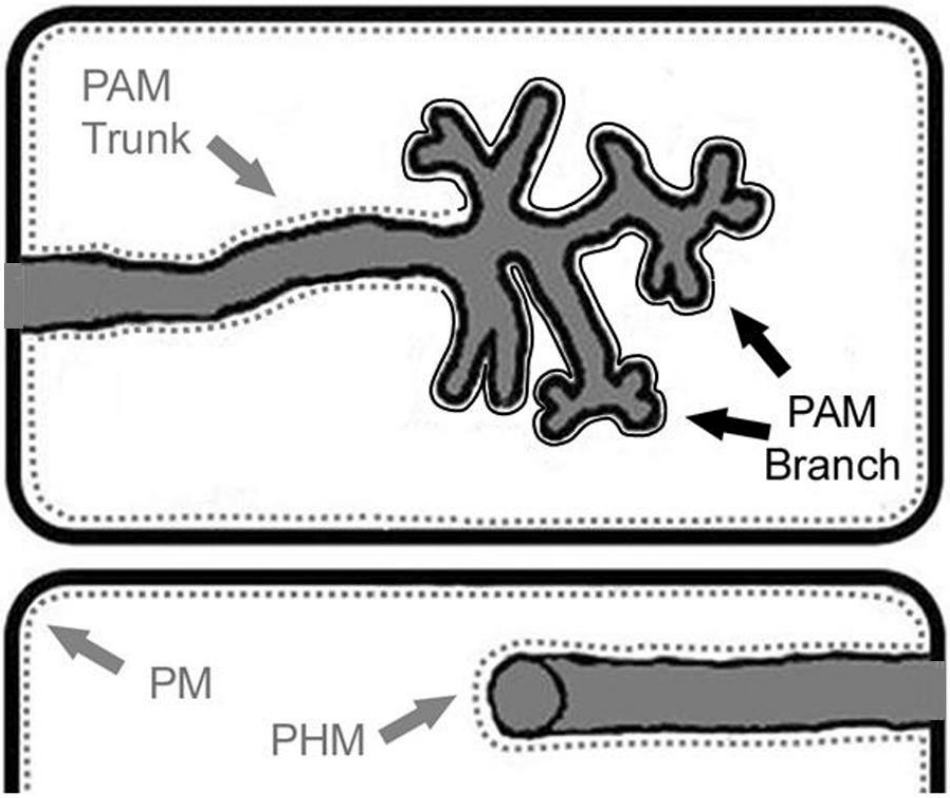

Figure 2-7 Illustration of proposed periarbuscular membrane domains
Two cortical cells are depicted, with an arbuscule (upper) and with an intracellular hypha (lower) shown in gray. Fluorescently-tagged MtBcp1 and AtPIP2a mark the plasma membrane (PM), perihyphal membrane (PHM) and the trunk region of the periarbuscular membrane (PAM), represented by the gray dashed line. MtPT4 localizes on the branch region of the periarbuscular membrane, complementary to the trunk domain and represented by the unbroken black line.

known, but our data do show continuous localization of these markers from plasma membrane to arbuscule trunk domain. The strong presence of MtBcp1 on trunks and weaker relative signal of AtPIP2a also suggests that additional mechanisms may regulate protein composition in this membrane. Interestingly, Fournier and colleagues (2008) showed that AtPIP2a labels the infection thread membrane that develops to allow entry of Rhizobia bacteria into the root for nodule formation. In legumes, the genetic pathways that regulate symbioses with AM fungi and Rhizobia bacteria overlap and it is possible that aspects of membrane synthesis and deposition that lead to microbial accommodation are also shared.

Arbuscules share similar functions to the haustoria formed by biotrophic pathogens and the interface of each with their respective host cells are morphologically analogous. Haustoria are surrounded by a plant extrahaustorial membrane (EHM) that is believed to mediate transport of nutrients to the pathogen (O'Connell and Panstruga, 2006). Studies of the interaction between Arabidopsis and a powdery mildew pathogen found that plasma membrane markers, including AtPIP2a, did not localize to the EHM but did localize to the haustorial neck (Koh et al., 2005). In addition, a monoclonal antibody has been reported that recognizes a protein on the EHM surrounding a mature haustorium and not the plasma membrane (Roberts et al., 1993). The haustorial neck region might be considered equivalent to the arbuscule trunk and while there are important structural differences between these two types of biotrophic interfaces, there are also some intriguing similarities. The fact that the protein domains of the EHM transitions from the plasma membrane protein-containing neck region to plasma membrane protein-excluding EHM region, which also contains a specific epitope, essentially parallels our description of trunk and branch domains of the periarbuscular membrane. It is tempting to speculate that the mechanism that guides localization of plasma membrane proteins to the haustorial

neck might be similar to that which guides the localization of AtPIP2a and MtBcp1 to the trunk domain of the periarbuscular membrane. Conversely, parallels may exist between mechanisms that control MtPT4 localization to the periarbuscular membranes and localization of proteins on the EHM; however, proteins that localize to the EHM have not yet been identified.

Our study has focused on membrane domains as defined by protein composition, however the lipid composition of the periarbuscular membrane may also differ from that of the plasma membrane or in fact differ between domains of the periarbuscular membrane. While isolation of periarbuscular membranes has not been reported, in the symbiosis between *M. truncatula* and *Rhizobia* bacteria, peribacteroid membranes surrounding symbiotic bacteria can be purified and their lipid and protein composition have been analyzed. Such studies have shown the peribacteroid membrane has a higher concentration of galactolipids than the plasma membrane (Gaude et al., 2004) and also a number of proteins involved in transport and secretion, including a syntaxin, MtSyp132, and also a putative GPI-anchored protein, MtEnod16 (Catalano et al., 2004; Catalano et al., 2007).

It is likely that the secretory system plays an important role in arbuscule development, as synthesis of the periarbuscular membrane requires significant deposition of membrane and newly-synthesized proteins (Alexander et al., 1989; Bonfante and Perotto, 1995; Gianinazzi-Pearson, 1996; Harrison et al., 2002). This hypothesis is supported by the presence of organelles involved in synthesizing and secreting proteins, namely the nucleus, ER, and Golgi, residing in close proximity to the developing periarbuscular membrane in addition to cytoskeletal components, actin and microtubules, necessary to direct secretion (Bonfante and Perotto, 1995; Gianinazzi-Pearson, 1996; Genre and Bonfante, 1997, 1998; Blancaflor et al., 2001).

Here, these organelles were observed by live-cell imaging and are consistent with, but extend, the data available from earlier EM studies.

Accumulation of cytoplasm and repositioning of the nucleus prior to fungal penetration into cortical cells was observed, consistent with the recent proposal from Genre *et al.* (2008) that hyphae are directed into cortical cells by a preformed apparatus marked by a large accumulation of ER and cytoplasm. We sometimes observed the ER marker comprising a large accumulation surrounding young arbuscules, but other times ER appeared appressed to arbuscules and an accumulation of ER in advance of fungal growth was not apparent. The slight differences between our results and those of Genre *et al*., may be due to differences in experimental conditions, or different fungal symbionts: our study used the AM fungus *Glomus versiforme* while Genre *et al.* used *Gigaspora gigantea*. Because each cell was only imaged at one time, it is also possible that an ER aggregation formed and was subsequently filled by the fungus before imaging.

Golgi bodies may be one of the last steps in the secretion pathway before fusion of membrane vesicles to the periarbuscular membrane (Jurgens, 2004). With this in mind, we observed carefully the distribution of Golgi and noted that they reside adjacent to arbuscule branch nodes and are not associated with branch tips. This finding supports the idea that secretion is active around growing arbuscules.
In cells with degenerating arbuscules, some Golgi remain associated with the fungus but a proportion of the population relocate to the periphery of the cell. However, there is a striking accumulation of peroxisomes around the collapsing structures. While the nature of arbuscule degradation has received little research attention, it is an interesting question. It would seem appropriate for the plant to metabolize the carbon resources invested in the arbuscule interface, and secretion of a new set of proteins may support degradation. The localization of peroxisomes surrounding collapsed

arbuscules may even signal an active lipid breakdown process through beta-oxidation, alternatively, they may ensure the sequestration of active oxygen species generated during membrane breakdown (Nyathi and Baker, 2006). Although the arbuscule dies, the plant cell remains alive and regains its former cellular structure. Protection against damaging radicals may be important to maintain cellular integrity. Overall, the distribution of organelles supports the idea that arbuscule degradation as an active cellular process.

By monitoring the localization of a tonoplast marker in cortical cells, we observed that a continuous tonoplast envelops the arbuscules at all stages of their development. While we did observe some bright spots of tonoplast fluorescence that may correspond to small vacuoles, these cells also appeared to have an intact, albeit highly convoluted, central vacuole. This interpretation is in contrast with the majority of the recent literature, which suggests that the large central vacuole fragments, creating multiple small vacuoles. Although the latter interpretation has become established in the literature, the authors of the early TEM micrographs (Toth and Miller, 1984), noted that the multiple small vacuole compartments visible in the single plane images, might represent individual vacuoles but alternatively, could represent a single vacuolar system that followed the elaborate contours of the arbuscule. Our confocal microscopy data contributes a third dimension to the discussion and provides support for the existence of both vacuole fragments and a large continuous vacuole system in cells with arbuscules.

In summary, the fluorescent markers provided insights into membrane dynamics and membrane domains within the periarbuscular membrane, and provide tools and a foundation for further studies of biogenesis of this essential symbiotic interface.

Materials and Methods

Plant material, transformation and growth conditions

Experiments were performed using *M. truncatula* cv. Jemalong, line A17. Organelle markers fused to mCherry were expressed in a stable transgenic A17 line, MtSCP1-GFP described in (Gomez et al., 2009). *A. rhizogenes*-mediated root transformation was performed according to (Boisson-Dernier et al., 2001). Briefly, *M. truncatula* seeds were surface-sterilized and germinated 24 hours in the dark to promote hypocotyl growth. Root tips were excised and inoculated with *A. rhizogenes* strain ARquaI carrying appropriate plasmids. Inoculated seedlings were grown on modified Fahraeus media supplemented with 25 mg/L kanamycin to select for transgenic roots for 20 days. Seedlings were then transplanted to sterile turface, four to six seedlings per 11-inch pot for 10 days, followed by inoculation with 250-350 surface-sterilized *G. versiforme* spores per plant as described in (Liu et al., 2007)). Plants were grown in growth rooms under a 16-h light (25 °C)/8-h (22 °C) dark regime and fertilized once a week with ½-strength Hoagland's solution with full-strength nitrogen and 20 uM potassium phosphate. Plants were evaluated 3-5 weeks post inoculation with *G. versiforme*.

Plasmid construction

pMtPT4:MtPT4-GFP was constructed by fusing the 3' end of the *MtPT4* cDNA in frame to the 5' end of the S65T variant of green fluorescent protein (GFP) (Chiu et al., 1996). The complete MtPT4 coding sequence was amplified with 5'AAGCTTGTCGACATGGGATTAGAAGTCCTTGAG 3' and 5'AAGCTTCCATGGCCTCAGTTCTTGAG 3', digested with Sal1 and Nco1 and ligated into the CaMV35S-sGFP(S65T)-Nos vector (Chiu et al., 1996). The vector was subsequently digested with Xba1 and Kpn1 to remove the 35S promoter and an

Xba1-Kpn1 MtPT4 promoter-MtPT4 gene fragment was ligated between the same sites. The Xba1-Kpn1 MtPT4 promoter-MtPT4 gene fragment was obtained by amplification with forward 5'GTCGGATCCTCTAGACTCGATCCACAACAAAG3' and reverse 5'AAGCTTCCATGGCCTCAGTTCTTGAG3' primers, followed by digestion with Xba1 and Kpn1. Finally, the complete MtPT4 promoter MtPT4 coding sequence:GFP gene fusion was released by digestion with HindII and EcoRI and this fragment was ligated between the same sites of the binary vector pCAMBIA 3300. *pMtBcp1:GFP-MtBcp1* was constructed to produce an N-terminal GFP fusion to the mature MtBcp1 protein similar to Sun et al. (2004). This arrangement enables visualization of the full length protein which is anchored in the membrane through a GPI anchor located at the C-terminal end of the protein. A genomic DNA sequence corresponding to the previously described *MtBcp1* promoter region (Hohnjec et al., 2005) and open reading frame of the cleavable secretion signal was amplified with the primers
5'-CACATCTAGAGAGAGGGAGATGTGTT-3' and 5'
TCTCGGATCCTGCAATTGCAACTGATGAAAG-3' which add 5' XbaI and 3' BamHI restriction sites, digested and ligated to the 5' end of GFP in the vector CaMV35S-sGFP(S65T)-Nos (Chiu et al., 1996). The remainder of the *MtBcp1* coding sequence including the TGA stop codon was amplified from genomic DNA with the primers 5'- GAGATGTACACTGATCACATTGTTGGTGATG-3' and
5'- TCTCGCGGCCGCTCATGCAAAGATGACTGCA-3' which add 5' BsrGI and 3' NotI restriction sites and ligated in frame to the 3' end of GFP in the same vector. This fusion including promoter, coding sequence with GFP and NOS terminator was subcloned into the expression vector pCAMBIA 2301 (http://www.cambia.org) with the restriction enzymes XbaI and EcoRI.

Organelle vectors are described in (Nelson et al., 2007) and are available from ABRC. Markers used in this study were expressed in pBIN vectors behind double 35s promoters with the coding sequence for mCherry fluorescent protein fused to: AtPIP2a (plasma membrane), HDEL retention signal (ER), GmMAN1 (Golgi), PTS1 targeting signal (peroxisome), and γ-TIP (tonoplast).

Confocal Microscopy

Root segments showing fluorescence associated with fungal colonization (from MtPT4, MtBcp1 or MtSCP1 promoters) were excised and cut longitudinally along the vascular tissue. Samples were sealed between slide and coverslip using VALAP (1:1:1 vaseline:lanolin:paraffin) to avoid desiccation (McGee-Russell and Allen, 1971). Cells below the section plane that had not been disrupted by cutting were imaged within 30 minutes of preparation, and cell viability in this system was observed over three hours after sample preparation. Roots were imaged using a Leica TCS-SP5 confocal microscope (Leica Microsystems, Exton, PA USA) with a X 63, numerical aperture 1.2, water immersion objective. GFP was excited with the blue argon ion laser (488 nm), and emitted fluorescence was collected from 505 nm to 545 nm; mCherry was excited with the Diode-Pumped Solid State (DPSS) laser at 561 nm and emitted fluorescence was collected from 590 to 640 nm. Controls were performed to assure no cross over between channels. DIC (differential interference contrast) images were collected simultaneously with the fluorescence using the transmitted light detector. Images were processed using Leica LAS-AF software (version 1.6.3 and 1.7.0), Adobe Photoshop CS2 version 7 (Adobe systems) and VOLOCITY (Improvision, UK). For MtBcp1-GFP, MtPT4-GFP and PIP2a-mCherry, data were collected from a minimum of 20 independently transformed root systems for each construct. For the organelle markers, data were obtained from a minimum of five

independently transformed root systems for each construct. In all cases, the interpretations are drawn from considering the whole data sets. The figures included in this manuscript are representative images.

APPENDIX

Appendix 2-1 Localization of MtPT4-GFP

Transgenic roots of *M. truncatula* expressing *pMtPT4:MtPT4-GFP* after colonization by *Glomus versiforme*. A and D, GFP signal; B and E, differential interference contrast (DIC) bright field image; C and F, overlay. A-C illustrate localization of MtPT4 surrounding arbuscule branches (arrowhead) but absent from arbuscule trunk (t). A-C are single confocal sections, zoom 4.1. D-F show MtPT4 localizing around arbuscule branches (arrowhead) in a cell with an arbuscule (a) and diffuse "haze" signal in a cell with a collapsed arbuscule (ca) suggesting localization in the vacuole. D and F are projections of three serial 0.5 µm z-axis sections, zoom 1.5. Scale bar = 10 µm in A-C, 20 µm in D-F.

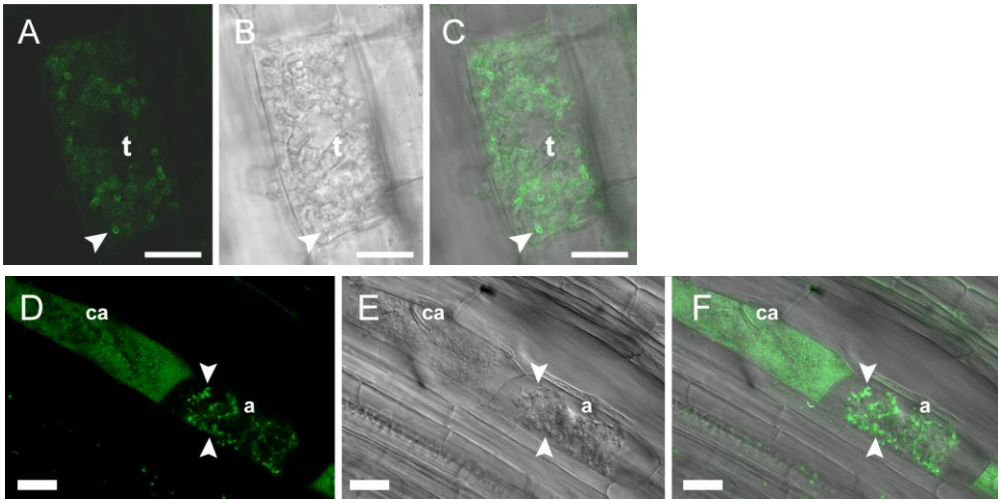

Appendix 2-2 Localization of GFP-MtBcp1 around an intracellular hypha

Roots expressing *pMtBcp1:GFP-MtBcp1* after colonization by *Glomus versiforme*. A, GFP signal; B, bright field image, and C, overlay. GFP-MtBcp1 is present in the plasma membrane and perihyphal membrane of root cortical cells with intracellular hyphae (ih). A and C are projections of seven 0.5 µm serial z-axis sections, B is a single section, zoom 3.7. Scale bar = 10 µm.

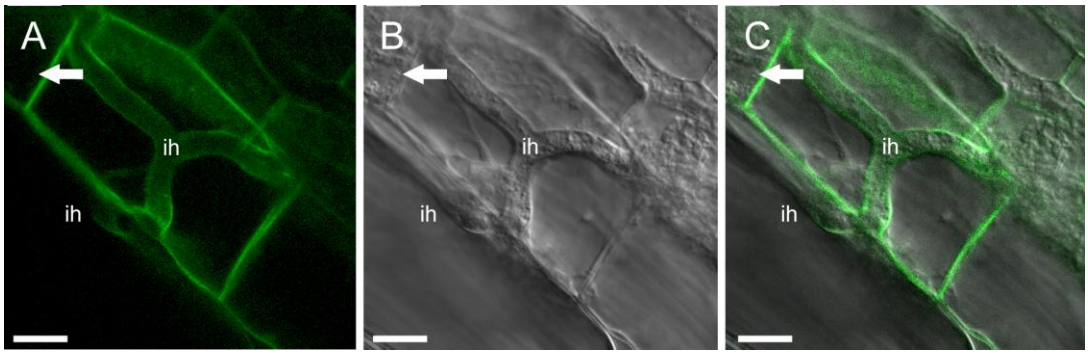

Appendix 2-3 Roots of transgenic M. truncatula plant expressing GFP under the MtSCP1 promoter (MtSCP1:GFP) colonized by G. versiforme

A, GFP fluorescence and B, bright field (DIC) of *M. truncatula* roots expressing free GFP under the MtSCP1 promoter. Image shows three cells harboring arbuscules (a) and an adjacent non-colonized cell (nc). Free GFP marks the cytoplasm and nuclei (n). Images are single confocal sections, zoom 1.7. Scale bar = 20 µm.

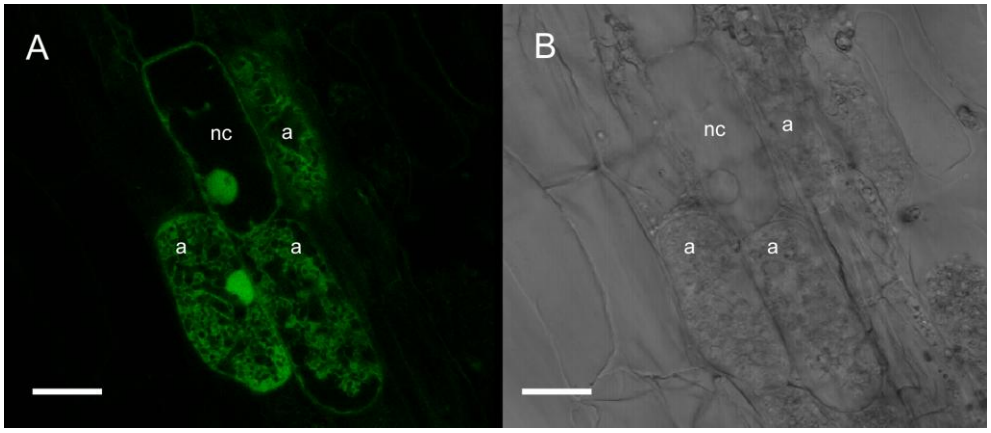

Appendix 2-4 Localization of a plasma membrane marker on the plasma membrane, perihyphal membrane and periarbuscular membrane trunk region.

Roots of a stable transgenic *M. truncatula MtSCP1:GFP* plants transformed with a plasma membrane marker construct *35s:AtPIP2a-mCherry*. Roots are colonized by *G. versiforme.* A and E, free GFP expressed under the MtSCP1 promoter; B and F, AtPIP2a-mCherry; C and G, single optical sections of brightfield (DIC); D and H, overlay. A-D show localization of AtPIP2a on the perihyphal membrane surrounding an intracellular hypha (ih). A, B, and D are projections of six 0.53 µm serial z-axis sections, zoom = 3.5.

E-H show localization of AtPIP2a on the trunk of an arbuscule (t) in addition to plasma membrane localization but no signal on arbuscule branches (arrow). E, F and H are projections of five 1 µm serial z-axis sections, zoom 4.4. Scale bar = 20 µm.

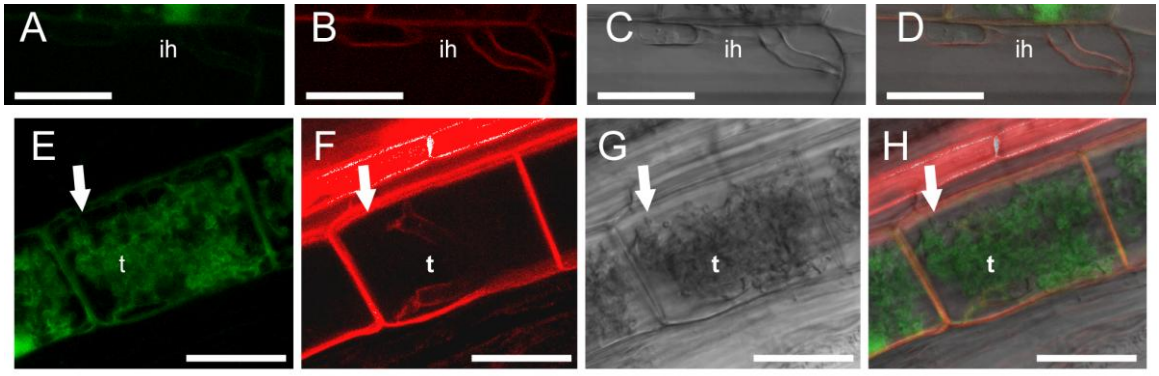

Appendix 2-5 Localization of ER in root cortex during AM symbiosis.
Roots of a stable transgenic *M. truncatula MtSCP1:GFP* plant transformed with *35S:mCherry-HDEL*. Roots are colonized by *G. versiforme.* A and E, free GFP expressed from the *MtSCP1* promoter; B and F mCherry-HDEL labeling ER; C and G single sections of brightfield (DIC); D and H, overlays. A-D, overview of root cortex showing ER surrounding arbuscules (a) and an intracellular hypha (ih). A, B and D, projections of eight 0.4 µm serial z-axis projections, zoom 1.7. E-H, ER and cytoplasmic aggregation surround a young arbuscule, with trunk marked (t). E, F and H are projections of nine 0.3 µm serial z sections, zoom 3.1. Scale bar = 20 µm.

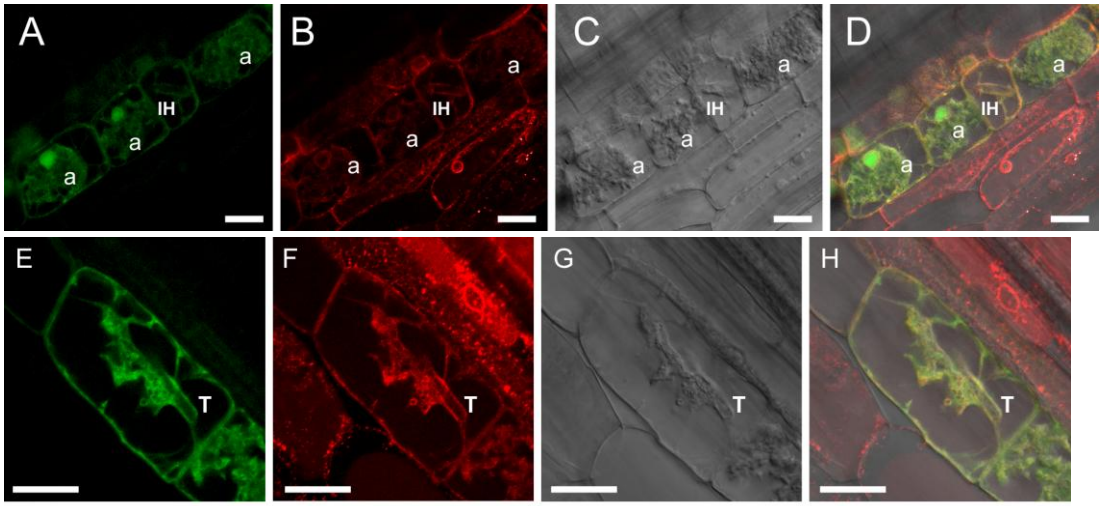

Appendix 2-6 Localization of Golgi in an M. truncatula root and in a cortical cell containing an arbuscule.

Roots of stable transgenic line *M. truncatula MtSCP1:GFP* transformed with 35S:GmMan1-mCherry. A and E, GmMan1-mCherry Golgi marker; B and F, DIC; C and G, overlay and D, free GFP from SCP1 promoter. A-C, Golgi are localized to the periphery of cortical cells in non-colonized roots. A-C are single confocal sections, zoom = 2.1. D-G, Golgi surround branches of a young arbuscule but do not associate with branch tips (arrows), single sections, zoom = 7.2. Scale bar = 20 µm.

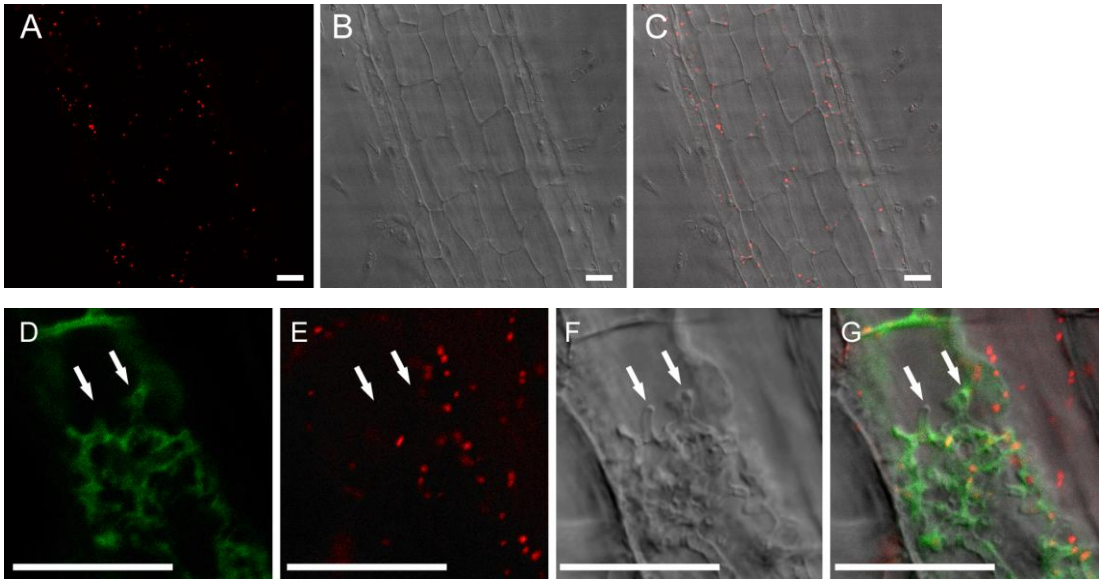

Appendix 2-7 Localization of peroxisomes in a M. truncatula root.

A, mCherry-PTS1 peroxisome marker, B, DIC and C, overlay show peroxisome localization in the cortex of a *M. truncatula* root. A-C are single confocal sections, zoom = 1.0. Scale bar = 20 µm.

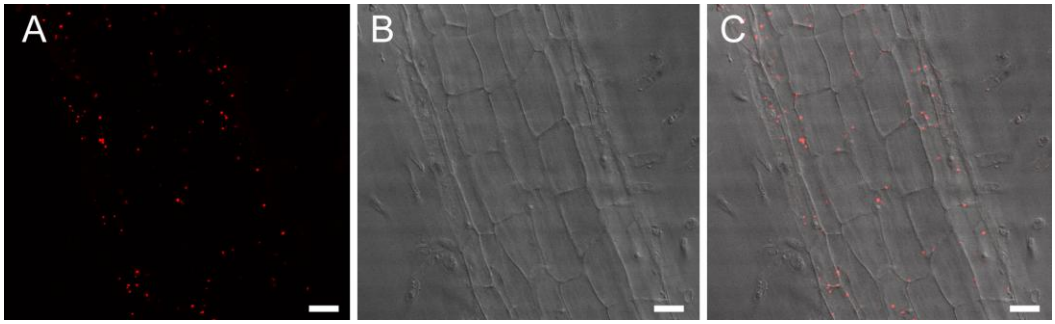

Appendix 2-8 Overview of a tonoplast membrane marker in mycorrhizal roots
A, free GFP under the SCP1 promoter, B, γ-TIP-mCherry tonoplast marker, C, DIC of single z section, D, overlay. Tonoplast membrane surrounds cell peripheries, nuclei (n), cytoplasmic strands (arrow) and a young arbuscule (a). A, B and D are projections of 19 serial 0.5 µm z-axis sections, zoom = 1.7. Scale bar = 20 µm. Roots are colonized with *G. ver*siforme.

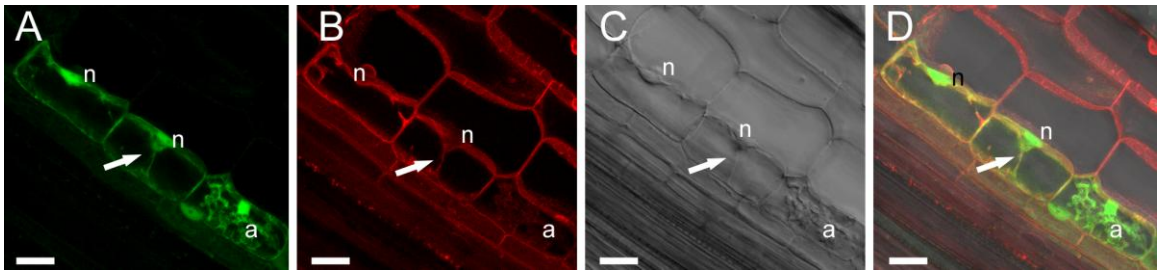

Appendix 2-9 M. truncatula root colonized with G. versiforme following imaging for three hours
A, free GFP driven by *MtSCP1* promoter, B, DIC and C, overlay, showing hyphal trunk (t) and branch (arrowhead) surrounded by plant cytoplasm. This single confocal section was taken more than three hours after sample preparation and following continuous imaging. Zoom = 2.2. Scale bar = 20 µm.

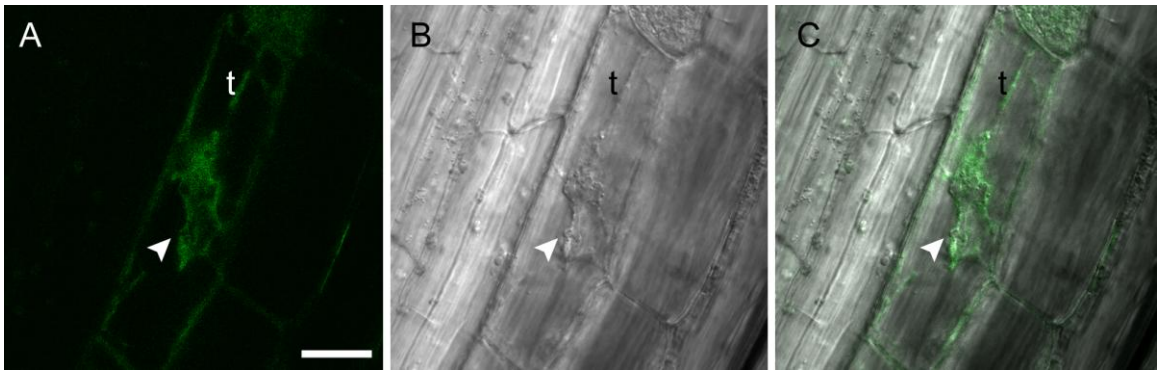

REFERENCES

Alexander, T., Toth, R., Meier, R., and Weber, H.C. (1989). Dynamics of arbuscule development and degeneration in onion, bean and tomato with reference to vesicular-arbuscular mycorrhizae in grasses. Canadian Journal of Botany **67,** 2505-2513.

Balestrini, R., Berta, G., and Bonfante, P. (1992). The plant nucleus in mycorrhizal roots: positional and structural modifications. Biology of the Cell **75,** 235-243.

Blancaflor, E.B., Zhao, L.M., and Harrison, M.J. (2001). Microtubule organization in root cells of Medicago truncatula during development of an arbuscular mycorrhizal symbiosis with Glomus versiforme. Protoplasma **217,** 154-165.

Boisson-Dernier, A., Chabaud, M., Garcia, F., Becard, G., Rosenberg, C., and Barker, D.G. (2001). *Agrobacterium* rhizogenes-transformed roots of *Medicago truncatula* for the study of nitrogen-fixing and endomycorrhizal symbiotic associations. Molecular Plant-Microbe Interactions **14,** 695-700.

Bonfante-Fasolo, P. (1984). Anatomy and morphology of VA mycorrhizae. In VA Mycorrhizae, C.L. Powell and D.J. Bagyaraj, eds (Boca Raton, Florida: CRC Press), pp. 5-33.

Bonfante, P., and Perotto, S. (1995). Strategies of arbuscular mycorrhizal fungi when infecting host plants. New Phytologist **130,** 3-21.

Bonfante, P., and Genre, A. (2008). Plants and arbuscular mycorrhizal fungi: an evolutionary-developmental perspective. Trends in Plant Science **13,** 492-498.

Brown, D.A., Crise, B., and Rose, J.K. (1989). Mechanism of Membrane Anchoring Affects Polarized Expression of 2 Proteins in Mdck Cells. Science **245,** 1499-1501.

Brown, M.F., and King, E.J. (1991). Morphology and Histology of Vesicular Arbuscular Mycorrhizae. In Methods and Principles of Mycorrhizal Research, N.C. Schenk, ed (St Paul, MN: APS press), pp. 15-21.

Bucher, M. (2007). Functional biology of plant phosphate uptake at root and mycorrhiza interfaces. New Phytologist **173,** 11-26.

Catalano, C.M., Lane, W.S., and Sherrier, D.J. (2004). Biochemical characterization of symbiosome membrane proteins from *Medicago truncatula* root nodules. Electrophoresis **25,** 519-531.

Catalano, C.M., Czymmek, K.J., Gann, J.G., and Sherrier, D.J. (2007). *Medicago truncatula* syntaxin SYP132 defines the symbiosome membrane and infection droplet membrane in root nodules. Planta **225,** 541-550.

Chiu, W.-l., Niwa, Y., Zeng, W., Hirano, T., Kobayashi, H., and Sheen, J. (1996). Engineered GFP as a vital reporter in plants. Current Biology **6,** 325-330.

Cox, G., and Sanders, F. (1974). Ultrastructure of the host-fungus interface in a vesicular-arbuscular mycorrhiza. New Phytologist **73,** 901-912.

Eisenhaber, B., Wildpaner, M., Schultz, C.J., Borner, G.H.H., Dupree, P., and Eisenhaber, F. (2003). Glycosylphosphatidylinositol lipid anchoring of plant proteins. Sensitive prediction from sequence- and genome-wide studies for *Arabidopsis* and rice. Plant Physiology **133,** 1691-1701.

Fester, T., D., S., and Hause, B. (2001). Reorganization of tobacco root plastids during arbuscule development. Planta **213,** 864-868.

Fournier, J., Timmers, A.C., Sieberer, B.J., Jauneau, A., Chabaud, M., and Barker, D.G. (2008). Mechanism of infection thread elongation in root hairs of *Medicago truncatula* and dynamic interplay with associated rhizobial colonization. Plant Physiol **148,** 1985-1995.

Gaude, N., Tippmann, H., Flemetakis, E., Katinakis, P., Udvardi, M., and Dormann, P. (2004). The galactolipid digalactosyldiacylglycerol accumulates in the peribacteroid membrane of nitrogen-fixing nodules of soybean and *Lotus*. Journal of Biological Chemistry **279,** 34624-34630.

Genre, A., and Bonfante, P. (1997). A mycorrhizal fungus changes microtubule orientation in tobacco root cells. Protoplasma **199,** 30-38.

Genre, A., and Bonfante, P. (1998). Actin versus tubulin configuration in arbuscule-containing cells from mycorrhizal tobacco roots. New Phytologist **140,** 745-752.

Genre, A., Chabaud, M., Timmers, T., Bonfante, P., and Barker, D.G. (2005). Arbuscular mycorrhizal fungi elicit a novel intracellular apparatus in *Medicago truncatula* root epidermal cells before infection. Plant Cell **17,** 3489-3499.

Genre, A., Chabaud, M., Faccio, A., Barker, D.G., and Bonfante, P. (2008). Prepenetration apparatus assembly precedes and predicts the colonization patterns of arbuscular mycorrhizal fungi within the root cortex of both *Medicago truncatula* and *Daucus carota*. Plant Cell **20,** 1407-1420.

Gianinazzi-Pearson, V. (1996). Plant cell responses to arbuscular myorrhiza fungi: Getting to the roots of the symbiosis. Plant Cell **8,** 1871-1883.

Gianinazzi-Pearson, V., Smith, S.E., Gianinazzi, S., and Smith, F.A. (1991). Enzymatic studies on the metabolism of vesicular-arbuscular mycorrhizas. New Phytologist **117,** 61-74.

Gianinazzi-Pearson, V., Arnould, C., Oufattole, M., Arango, M., and Gianinazzi, S. (2000). Differential activation of H+-ATPase genes by an arbuscular mycorrhizal fungus in root cells of transgenic tobacco. Planta **211,** 609-613.

Gillmor, C.S., Lukowitz, W., Brininstool, G., Sedbrook, J.C., Hamann, T., Poindexter, P., and Somerville, C. (2005). Glycosylphosphatidylinositol-

Anchored Proteins Are Required for Cell Wall Synthesis and Morphogenesis in *Arabidopsis*. Plant Cell **17,** 1128-1140.

Glassop, D., Smith, S.E., and Smith, F.W. (2005). Cereal phosphate transporters associated with the mycorrhizal pathway of phosphate uptake into roots. Planta **222,** 688-698.

Gomez, S.K., Javot, H., Deewatthanawong, P., Torres-Jerez, I., Tang, Y.H., Blancaflor, E.B., Udvardi, M.K., and Harrison, M.J. (2009). *Medicago truncatula* and *Glomus intraradices* gene expression in cortical cells harboring arbuscules in the arbuscular mycorrhizal symbiosis. Bmc Plant Biology **9,** 1-19.

Harrison, M.J. (1999). Molecular and cellular aspects of the arbuscular mycorrhizal symbiosis. Annual Review of Plant Physiology and Plant Molecular Biology **50,** 361-389.

Harrison, M.J. (2005). Signaling in the arbuscular mycorrhizal symbiosis. Annual reviews of Microbiology **59,** 19-42.

Harrison, M.J., Dewbre, G.R., and Liu, J. (2002). A phosphate transporter from *Medicago truncatula* involved in the acquisition of phosphate released by arbuscular mycorrhizal fungi. Plant Cell **14,** 2413-2429.

Hohnjec, N., Vieweg, M.F., Pühler, A., Becker, A., and Küster, H. (2005). Overlaps in the transcriptional profiles of *Medicago truncatula* roots inoculated with two different *Glomus* fungi provide insights into the genetic program activated during arbuscular mycorrhiza. Plant Physiology **137,** 1283-1301.

Javot, H., Penmetsa, R.V., Terzaghi, N., Cook, D.R., and Harrison, M.J. (2007). A *Medicago truncatula* phosphate transporter indispensable for the arbuscular

mycorrhizal symbiosis. Proceedings of the National Academy of Sciences of the United States of America **104,** 1720-1725.

Jurgens, G. (2004). Membrane trafficking in plants. Annu Rev Cell Dev Biol **20,** 481-504.

Kleine-Vehn, J., Leitner, J., Zwiewka, M., Sauer, M., Abas, L., Luschnig, C., and Friml, J. (2008). Differential degradation of PIN2 auxin efflux carrier by retromer-dependent vacuolar targeting. Proceedings of the National Academy of Sciences of the United States of America **105,** 17812-17817.

Koh, S., Andre, A., Edwards, H., Ehrhardt, D., and Somerville, S. (2005). *Arabidopsis thaliana* subcellular responses to compatible *Erysiphe cichoracearum* infections. Plant Journal **44,** 516-529.

Krajinski, F., Hause, B., Gianinazzi-Pearson, V., and Franken, P. (2002). *Mtha1*, a plasma membrane H+-ATPase gene from *Medicago truncatula*, shows arbuscule-specific induced expression in mycorrhizal tissue. Plant Biology **4,** 754-761.

Lalanne, E., Honys, D., Johnson, A., Borner, G.H.H., Lilley, K.S., Dupree, P., Grossniklaus, U., and Twell, D. (2004). SETH1 and SETH2, Two Components of the Glycosylphosphatidylinositol Anchor Biosynthetic Pathway, Are Required for Pollen Germination and Tube Growth in *Arabidopsis*. Plant Cell **16,** 229-240.

Lisanti, M.P., Caras, I.W., Davitz, M.A., and Rodriguezboulan, E. (1989). A Glycophospholipid Membrane Anchor Acts as an Apical Targeting Signal in Polarized Epithelial-Cells. Journal of Cell Biology **109,** 2145-2156.

Liu, J., Maldonado-Mendoza, I.E., Lopez-Meyer, M., Cheung, F., Town, C.D., and Harrison M, J. (2007). The arbuscular mycorrhizal symbiosis is

accompanied by local and systemic alterations in gene expression and an increase in disease resistance in the shoots. The Plant Journal **50,** 529-544.

Liu, J., Blaylock, L., Endre, G., Cho, J., Town, C.D., VandenBosch, K., and Harrison, M.J. (2003). Transcript profiling coupled with spatial expression analyses reveals genes involved in distinct developmental stages of the arbuscular mycorrhizal symbiosis. Plant Cell **15,** 2106-2123.

Lohse, S., Schliemann, W., Ammer, C., Kopka, J., Strack, D., and Fester, T. (2005). Organization and metabolism of plastids and mitochondria in arbuscular mycorrhizal roots of *Medicago truncatula*. Plant Physiology **139,** 329-340.

McGee-Russell, S., and Allen, R. (1971). Reversible stabilization of labile microtubules in the reticulopodial network of Allogromia. Advances in Cell and Molecular Biology **1,** 153-184.

Nagy, R., Karandashov, V., Chague, W., Kalinkevich, K., Tamasloukht, M., Xu, G.H., Jakobsen, I., Levy, A.A., Amrhein, N., and Bucher, M. (2005). The characterization of novel mycorrhiza-specific phosphate transporters from *Lycopersicon esculentum* and *Solanum tuberosum* uncovers functional redundancy in symbiotic phosphate transport in solanaceous species. Plant Journal **42,** 236-250.

Nebenfuhr, A., Gallagher, L.A., Dunahay, T.G., Frohlick, J.A., Mazurkiewicz, A.M., Meehl, J.B., and Staehelin, L.A. (1999). Stop-and-go movements of plant Golgi stacks are mediated by the acto-myosin system. Plant Physiol **121,** 1127-1142.

Nelson, B.K., Cai, X., and Nebenfuhr, A. (2007). A multicolored set of in vivo organelle markers for co-localization studies in Arabidopsis and other plants. Plant Journal **51,** 1126-1136.

Nyathi, Y., and Baker, A. (2006). Plant peroxisomes as a source of signalling molecules. Biochim Biophys Acta **1763,** 1478-1495.

O'Connell, R.J., and Panstruga, R. (2006). Tete a tete inside a plant cell: establishing compatibility between plants and biotrophic fungi and oomycetes. New Phytologist **171,** 699-718.

Parniske, M. (2008). Arbuscular mycorrhiza: the mother of plant root endosymbioses. Nature Reviews Microbiology **6,** 763-775.

Paszkowski, U., Kroken, S., Roux, C., and Briggs, S.P. (2002). Rice phosphate transporters include an evolutionarily divergent gene specifically activated in arbuscular mycorrhizal symbiosis. Proceedings of the National Academy of Sciences, USA **99,** 13324-13329.

Redeker, D., Kodner, R., and Graham, L. (2000). Glomalean fungi from the Ordovician. Science **289,** 1920-1921.

Remy, W., Taylor, T., Hass, H., and Kerp, H. (1994). Four Hundred-Million-Year-Old Vesicular Arbuscular Mycorrhizae. PNAS **91,** 11841-11843.

Roberts, A.M., Mackie, A.J., Hathaway, V., Callow, J.A., and Green, J.R. (1993). Molecular Differentiation in the Extrahaustorial Membrane of Pea Powdery Mildew Haustoria at Early and Late Stages of Development. Physiological and Molecular Plant Pathology **43,** 147-160.

Roudier, F., Fernandez, A.G., Fujita, M., Himmelspach, R., Borner, G.H.H., Schindelman, G., Song, S., Baskin, T.I., Dupree, P., Wasteneys, G.O., and Benfey, P.N. (2005). COBRA, an Arabidopsis extracellular glycosyl-phosphatidyl inositol-anchored protein, specifically controls highly anisotropic expansion through its involvement in cellulose microfibril orientation. Plant Cell **17,** 1749-1763.

Scannerini, S., and Bonfante-Fasolo, P. (1982). Comparative ultrastructural analysis of mycorrhizal associations. Canadian Journal of Botany **61,** 917-943.

Schindelman, G., Morikami, A., Jung, J., Baskin, T.I., Carpita, N.C., Derbyshire, P., McCann, M.C., and Benfey, P.N. (2001). COBRA encodes a putative GPI-anchored protein, which is polarly localized and necessary for oriented cell expansion in *Arabidopsis*. Genes Dev. **15,** 1115-1127.

Smith, S.E., and Read, D.J. (2008). Mycorrhizal Symbiosis. (San Diego, CA: Academic Press, Inc.).

Smith, S.E., Smith, F.A., and Jakobsen, I. (2003). Mycorrhizal fungi can dominate phosphate supply to plants irrespective of growth responses. Plant Physiology **133,** 16-20.

Sun, W.X., Zhao, Z.D., Hare, M.C., Kieliszewski, M.J., and Showalter, A.M. (2004). Tomato LeAGP-1 is a plasma membrane-bound, glycosylphosphatidylinositol-anchored arabinogalactan-protein. Physiologia Plantarum **120,** 319-327.

Tamura, K., Shimada, T., Ono, E., Tanaka, Y., Nagatani, A., Higashi, S., Watanabe, M., Nishimura, M., and Hara-Nishimura, I. (2003). Why green fluorescent fusion proteins have not been observed in the vacuoles of higher plants. Plant Journal **35,** 545-555.

Toth, R., and Miller, R.M. (1984). Dynamics of arbuscule development and degeneration in a *Zea mays* mycorrhiza. American Journal of Botany **71,** 449-460.

Valot, B., Negroni, L., Zivy, M., Gianinazzi, S., and Dumas-Gaudot, E. (2006). A mass spetrometric approach to identify arbuscular mycorrhiza-related proteins in root plasma membrane fractions. Proteomics **6,** 145-155.

CHAPTER 3

ASYMMETRIC LOCALIZATION OF THE PHOSPHATE TRANSPORTER MTPT4 DURING ARBUSCULAR MYCORRHIZAL SYMBIOSIS IS MEDIATED BY TRANSIENT POLARIZED SECRETION TO THE PERIARBUSCULAR MEMBRANE[2]

Abstract

Establishing asymmetric membrane domains with distinct protein compositions is a basic requirement for eukaryotic cellular function, and for the generation of specialized interfaces in plant-microbe interactions. In the arbuscular mycorrhizal (AM) symbiosis, formed between the majority of land plants and obligate biotrophic soil fungi, highly-branched hyphae called arbuscules form within plant cells to facilitate nutrient exchange. These structures are surrounded by a specialized plant membrane termed the periarbuscular membrane, which contains a unique suite of proteins including the phosphate transporter MtPT4 from *Medicago truncatula* (Harrison et al., 2002). MtPT4 is required for phosphate uptake through the symbiosis and maintenance of arbuscules (Javot et al., 2007b), but the mechanism regulating its polar localization is unknown. Studying the localization of fluorescently-tagged membrane proteins expressed under different promoters, we show that MtPT4 polar targeting is mediated by precise temporal expression, coupled with significant and temporary changes in the direction and cargo selection of the plant secretory pathway for newly synthesized proteins. In addition, a single amino acid change in MtPT4 caused it to accumulate in the Trans-Golgi Network and resulted in a loss-of-function phenotype.

[2] $MtPT4^{S115F}$-GFP plasmid construction and initial analysis of *mtpt4-3* was performed by Roslyn Noar.

Introduction

Like all organisms, plants must take in essential nutrients; their source, however, is limited to the soil in direct contact with roots, and this presents challenges for acquiring phosphate, which is immobile and often available in concentrations limiting for plant growth (Vance et al., 2003). The arbuscular mycorrhizal symbiosis evolved between plants and fungi of the phylum Glomeromycota approximately 400 million years ago and persists in 80% of angiosperms as a strategy for enhancing nutrient acquisition, particularly phosphate (Smith and Read, 2008). AM symbiosis is established by fungal penetration through root epidermal cells and subsequent growth within the root cortex, where hyphae penetrate cortical cells and branch profusely to form arbuscules. Arbuscule development is accompanied by deposition of the plant-derived periarbuscular membrane, which surrounds the arbuscule and is continuous with the plant plasma membrane (Bonfante and Perotto, 1995). The highly-branched interface between the two organisms creates a large area in a single cell to mediate nutrient exchange. Through the symbiosis, the plant roots are connected to large hyphal networks which extend into the soil. In legumes, the periarbuscular membrane grows to an estimated eight times the area of a cortical cell plasma membrane and is thought to be synthesized *de novo* during the course of arbuscule development (Alexander et al., 1989). While the precise time it takes for an arbuscule to develop is not known, mature arbuscules are observed within two days post inoculation, suggesting rapid development (Alexander et al., 1989; Javot et al., 2007b; Zhang et al., 2010). Despite this large resource investment, arbuscules are transient structures that collapse approximately one week after forming (Brundrett et al., 1985; Alexander et al., 1989; Kobae and Hata, 2010).

The periarbuscular membrane contains H^+-ATPase activity, necessary for secondary active transport, and the phosphate transporters MtPT4 from *Medicago*

truncatula and OsPT11 from rice (Marx et al., 1982; Gianinazzi-Pearson et al., 2000; Harrison et al., 2002; Kobae and Hata, 2010). *MtPT4* and *OsPT11* are members of the PHT1 family of phosphate transporters, a large gene family whose members are involved in Pi transport at many locations throughout the plant (Javot et al., 2007a). *MtPT4* and *OsPT11* are expressed only in cortical cells harboring arbuscules. Other members of the PHT1 family, including *M. truncatula* MtPT1, localize in the plasma membrane and mediate phosphate uptake from the soil into epidermal and cortical cells (Chiou et al., 2001; Misson et al., 2004). Because MtPT4 localizes in the periarbuscular membrane, but not the plasma membrane, the protein is considered to be polarized. In *mtpt4* mutant plants, arbuscules collapse more rapidly than in wild type plants, as early as two days after inoculation; inoculated mutant plants also do not accumulate increased shoot mass or phosphate, showing that MtPT4 function is required for functional symbiosis (Javot et al., 2007b). Despite the central role of MtPT4 in regulating the AM symbiosis, the mechanism directing polar localization of this phosphate transporter into the periarbuscular membrane has not been addressed.

In plants, polar localization of membrane proteins has been studied extensively for the PIN family of auxin efflux transporters. Auxin is the major growth regulating hormone and must be transported in a polar manner through the plant. PINs localize to the basal or apical membrane of cells to direct polar auxin transport, but are initially secreted in a non-polar manner to the plasma membrane (Dhonukshe et al., 2008; Geldner, 2009). Polarity is generated by subsequent endocytosis and recycling, and in the case of PIN1, the apical or basal localization is determined by differential phosphorylation of serine residues in the large cytoplasmic loop generated by the antagonistic action in Arabidopsis of the PINOID kinase and PP2A phosphatase (Michniewicz et al., 2007; Huang et al., 2010). While a similar endocytosis/recycling mechanism was recently described to confer polar localization of the boron transporter

BOR1 in the endodermis (Takano et al., 2010), this paradigm may not explain how all proteins become polarized in plants. The nature of polarity-generating mechanisms is thus an important question, particularly in cells developing new membranes during interactions with intracellular symbionts and pathogens. This study aimed to uncover mechanisms that enable asymmetric protein localization of the MtPT4 phosphate transporter in the periarbuscular membrane.

Results

We have reported previously that GFP-tagged MtPT4 protein expressed under its native promoter accumulates only in cortical cells with developing arbuscules and localizes in the periarbuscular membrane surrounding arbuscule branches, but not the plasma membrane (Fig. 3-1a) (Pumplin and Harrison, 2009). This same result was observed in immunolocalization experiments, which detected native MtPT4 protein exclusively surrounding branches of arbuscules (Harrison et al., 2002) (Fig. 3-6a). MtPT1 is a closely-related phosphate transporter that shares 61% sequence identity with MtPT4. MtPT1 is expressed in the root epidermis and cortex (Chiou et al., 2001; Xiao et al., 2006). Immunolocalization of the native MtPT1 protein and analysis of a translational GFP fusion expressed in a heterologous system revealed protein localization in the plasma membrane (Chiou et al., 2001), a result confirmed in transgenic roots expressing an MtPT1-GFP fusion construct under control of the native promoter (*pMtPT1:MtPT1-GFP*) (Fig. 3-1b). In an effort to establish a suitable system for dissecting the mechanism that mediates MtPT4 polar localization, we constructed a vector to express MtPT1-GFP under the MtPT4 promoter (*pMtPT4:MtPT1-GFP)* as a negative control that was anticipated to localize in the plasma membrane. After colonization of transgenic roots by the AM fungus *Glomus versiforme,* GFP signal was only detected in cortical cells harboring arbuscules as

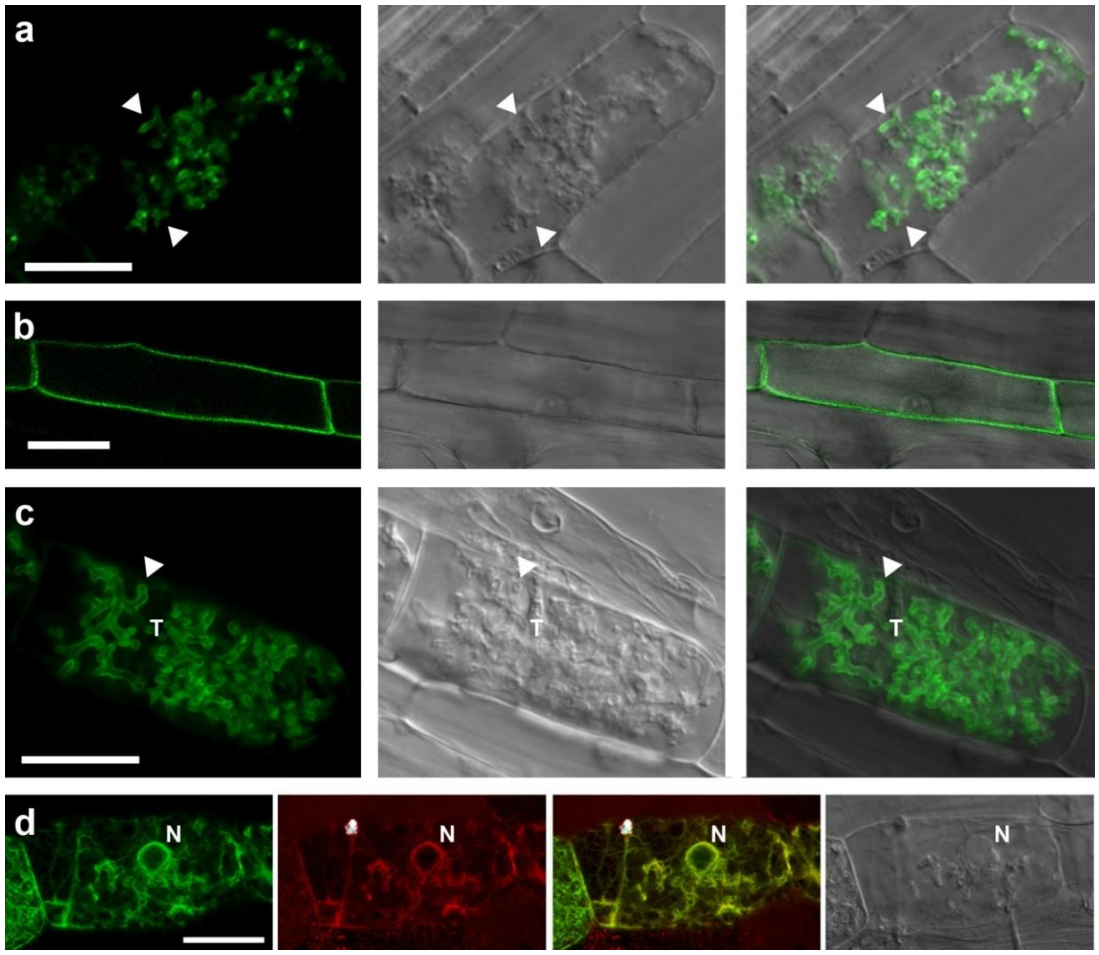

Figure 3-1: Localization of fluorescent protein fusions expressed under the pMtPT4 promoter.

Cortical cells of *M. truncatula* roots colonized by *G. versiforme* and expressing *pMtPT4:MtPT4-GFP* (a), *pMtPT4:MtPT1-GFP* (c) and *pMtPT4:AtPIP2a-GFP* coexpressed with *p35S:HDEL-mCherry* (d). b, root epidermal cell expressing *pMtPT1:MtPT1-GFP*. a-c, left panel shows GFP fluorescence, middle panel differential interference contrast bright-field (DIC), right panel overlay. d, left panel, GFP fluorescence; middle left, HDEL-mCherry fluorescence; middle right overlay of both channels; right, DIC. Arrowheads, arbuscule branches; T, arbuscule trunk; N, plant nucleus surrounded by perinuclear ER. Bars = 20 µm.

anticipated. Surprisingly however, MtPT1-GFP localized predominantly in the branch domain of the periarbuscular membrane, and not in the plasma membrane or the trunk domain, when expressed under the MtPT4 promoter (Fig. 3-1c). While some cells displayed weak peripheral signal, based on the uneven pattern and occasional perinuclear signal, this was more likely peripheral ER than plasma membrane; weak ER signal was also evident in some epidermal cells expressing *pMtPT1:MtPT1-GFP*. To determine whether another plasma membrane protein is targeted to the periarbuscular membrane if expressed in cells with developing arbuscules, the Arabidopsis aquaporin *AtPIP2a*, encoding a six-transmembrane domain protein commonly used as a plasma membrane marker (Nelson et al., 2007), was fused to GFP and expressed under the MtPT4 promoter. Previous experiments showed this protein localized to the plasma membrane of *M. truncatula* cortical cells and membranes surrounding intracellular hyphae and the trunk domain of the periarbuscular membrane when expressed under the 35S promoter (Pumplin and Harrison, 2009). Under the MtPT4 promoter, this protein did not localize to the periarbuscular membrane or the plasma membrane, but rather was retained in the ER as indicated by a reticulate pattern, perinuclear signal and colocalization with an HDEL ER marker (Fig. 3-1d).

Because AtPIP2a displayed different localizations when expressed from the 35S or MtPT4 promoters, we asked if localization of MtPT4 and MtPT1 would be different is expressed from the 35S promoter. In roots expressing *p35S:MtPT4-GFP*, GFP signal was faint and primarily observed in the vacuole, while occasional signal was also evident in the cell periphery and in a perinuclear pattern, suggesting ER retention (Fig 2-2a). Similar ER retention in a heterologous system was reported for the rice ortholog of MtPT4, OsPT11 (Kobae and Hata, 2010). In *p35S:MtPT4-GFP-*

expressing roots, GFP signal was observed predominantly in pericycle cells, where 35S promoter activity is strongest in *M. truncatula* roots. This suggests the MtPT4 protein is unstable and quickly degraded in cells without a periarbuscular membrane. Interestingly, when these roots were colonized by *G. versiforme*, MtPT4 protein localization was not observed in the periarbuscular membrane (Fig. 3-2a). Roots expressing *p35S:MtPT1-GFP* displayed the anticipated plasma membrane signal in root cells; upon AM fungal colonization, GFP signal was observed in the plasma membrane in cells harboring arbuscules, and also in the membrane surrounding intracellular hyphae (Fig. 3-2b), a pattern similar to the plasma membrane marker *p35S:AtPIP2a-mcherry* (Pumplin and Harrison, 2009). As with *p35S:MtPT4-GFP*, no MtPT1-GFP signal was observed in the periarbuscular membrane surrounding arbuscule branches (Fig. 3-2b). In addition, signal was weaker in cells harboring arbuscules relative to other cortical cells (Fig. 3-2d).

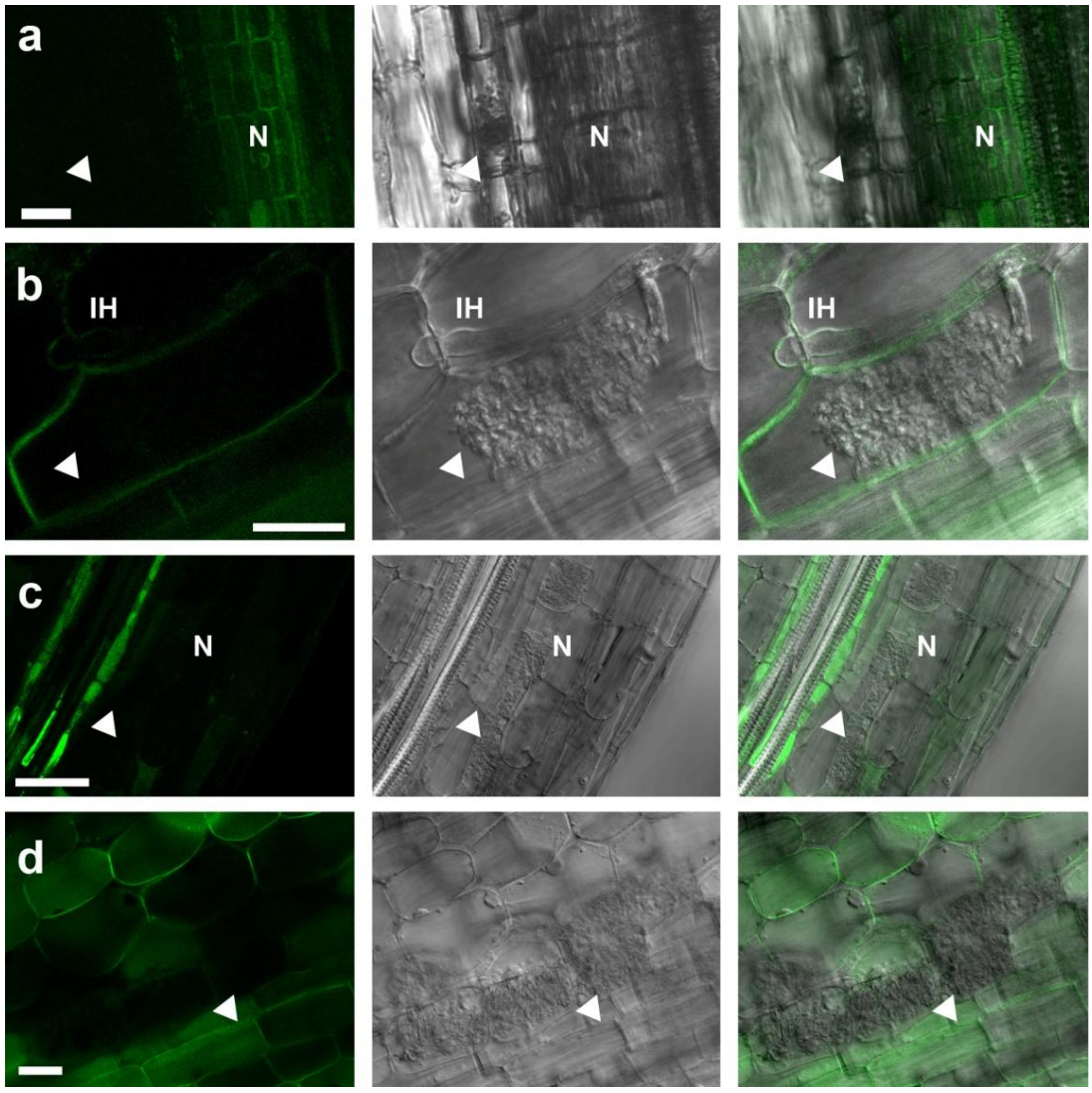

Figure 3-2: Localization of fluorescent protein fusions expressed under the p35S promoter.

M. truncatula roots colonized by *G. versiforme* and expressing *p35S:MtPT4-GFP* (a), *p35S:MtPT1-GFP* (b), *p35S:MtPT4 5'UTR-MtPT4-GFP* (c) and *p35S:MtPT4 5'UTR:MtPT1-GFP* (d). Left panel shows GFP fluorescence, middle panel differential interference contrast bright-field (DIC), right panel overlay. Arrowheads point to arbuscules, N, nucleus, IH, intracellular hypha. Bars = 20 µm, a,b,d; 50 µm, c.

These results suggest that the MtPT4 5' regulatory region may influence protein localization. Because the *pMtPT4:MtPT1-GFP* construct was created by replacing the *MtPT4* sequence with the *MtPT1* open reading frame at the ATG, this construct retained the *MtPT4* 5' untranslated region (UTR). To determine whether the 5' UTR or the promoter influenced periarbuscular membrane localization, a set of replacements were created by fusing the 5' UTR region of the 35S promoter to the MtPT4 promoter at the putative TATA boxes, and *vice versa*. The pattern of localization observed from these constructs followed the promoter and not the 5' UTR: roots expressing *pMtPT4:35S 5'UTR-MtPT4-GFP* or *pMtPT4:35S 5'UTR-MtPT1-GFP* displayed GFP signal in the periarbuscular membrane (Fig. 3-3), while roots expressing *p35S:MtPT4 5'UTR-MtPT4-GFP* (Fig 2-2c) or *p35S:MtPT4 5'UTR-MtPT1-GFP* (Fig 2-2d) did not display any periarbuscular membrane signal. The localization patterns of the UTR replacement constructs did not differ from the original constructs. This indicates that the periarbuscular membrane localization of MtPT4

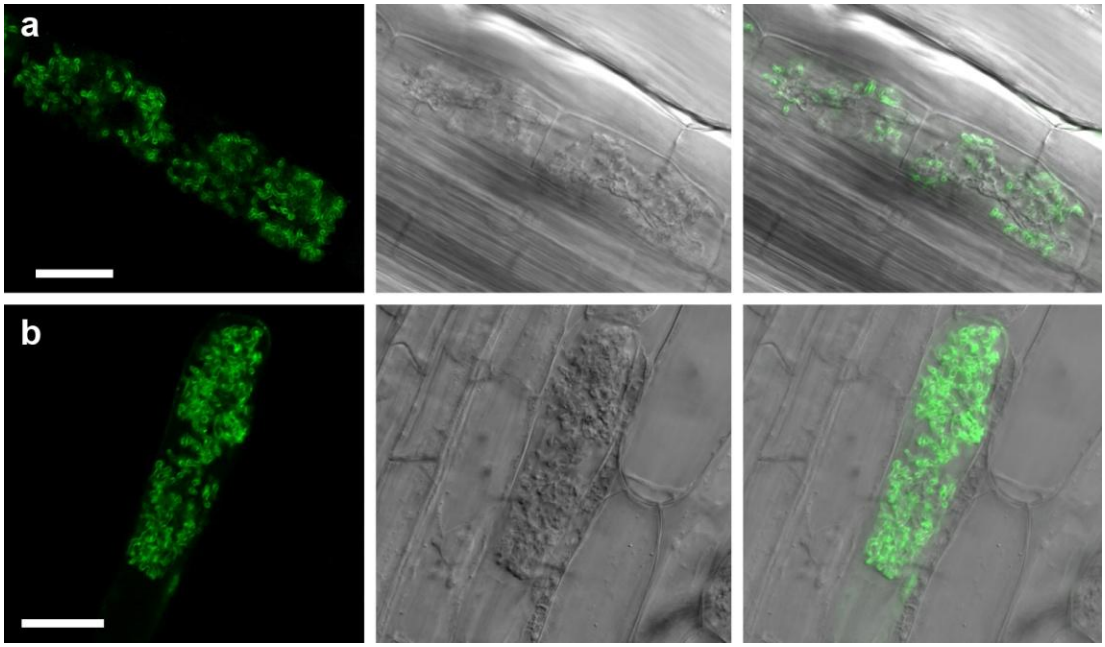

Figure 3-3: Localization of MtPT4 and MtPT1 fluorescent protein fusions expressed under pMtPT4 with the 35S 5' UTR.
M. truncatula roots colonized by *G. versiforme* and expressing *pMtPT4:35s 5'UTR-MtPT4-GFP* (a), and *pMtPT4:35s 5'UTR-MtPT1-GFP* (b). Left panel shows GFP fluorescence, middle panel differential interference contrast bright-field (DIC), right panel overlay. Localization pattern is similar to that observed from constructs that contain the native MtPT4 5' UTR. Bars = 20 μm.

and pMtPT4:MtPT1 occurs when the constructs are expressed from the MtPT4 promoter, and therefore the temporal expression pattern conferred by this promoter is critical for localization.

These findings, together with the observation that native MtPT4 is only detected after arbuscules reach a size with multiple branches, and that expression of MtPT4 and MtPT1 under 35S promoter does not result in periarbuscular membrane localization imply the following: 1) The MtPT4 promoter is only active in cells with developing and branching arbuscules, as inferred by previous immunolocalization and GFP fusion results (Harrison et al., 2002; Pumplin and Harrison, 2009); 2) Secretion of newly synthesized proteins during this period of arbuscule development is predominantly directed towards the developing periarbuscular membrane and not towards the plasma membrane; and 3) 35S promoter activity is reduced in cells with developing arbuscules expressing MtPT4. To further test these hypotheses and monitor protein localization prior to and during the initial stages of arbuscule development, we expressed fluorescently-tagged MtPT1, MtPT4 and AtPIP2a under the MtBcp1 promoter. *MtBcp1* is specifically expressed in the root cortex before and during cortical cell penetration by AM fungi (Hohnjec et al., 2005; Pumplin and Harrison, 2009), making it an ideal promoter to monitor protein localization in cells with developing arbuscules before and during the phase of MtPT4 promoter activity. Roots expressing *pMtBcp1:MtPT4-GFP* displayed relatively weak ER-localized signal in cells with very young arbuscules, reminiscent of the previous ectopic expression results (Fig. 3-4a). However in cells harboring arbuscules with multiple branches, GFP signal was observed in the branch domain of the periarbuscular membrane, similar to expression under the native promoter (Fig 2-4a). Roots expressing *pMtBcp1:MtPT1-GFP* revealed GFP signal on the plasma membrane of cortical cells

adjacent to infected cells, and in both the trunk and branch domains of the periarbuscular membrane (Fig. 3-4b). *pMtBcp1:AtPIP2a-mCherry* displayed the opposite pattern to *pMtBcp1:MtPT4-GFP*, with signal observed in the plasma membrane and periarbuscular membrane trunk domain, and in the ER of cells containing branched arbuscules (Fig. 3-4c and d). Cotransformation of *pMtBcp1:MtPT1-GFP* and *pMtBcp1:AtPIP2a-mCherry* revealed overlapping localization in the plasma membrane and arbuscule trunk domain in cells with young arbuscules, but contrasting ER retention of AtPIP2a-mCherry and branch domain localization of MtPT1-GFP (Fig. 3-4c). Similarly, coexpression of *pMtBcp1:AtPIP2a-mCherry* and *pMtPT4:AtPIP2a-GFP* highlighted the difference of cargo secretion during the phase of arbuscule branch formation, as plasma membrane-localized signal was observed when expressed from the MtBcp1 promoter, but not from the MtPT4 promoter (Fig. 3-4d). Localization results are summarized in Fig. 3-4e and support the hypothesis that timing of expression, conferred by a tightly-regulated promoter, is essential for localization of MtPT4 in the periarbuscular membrane. In addition, these results suggest that not only is the destination of secretion during arbuscule development altered from plasma membrane to periarbuscular membrane, but that the protein cargo enabled to pass through the secretion pathway is altered. In cells with no, or very young, arbuscules, MtPT4 is retained in the ER while AtPIP2a is secreted to the plasma membrane and trunk domain of the periarbuscular membrane. After an arbuscule begins to branch, MtPT4 is able to traffic to the periarbuscular membrane and AtPIP2a is retained in the ER (Fig. 3-10).

Figure 3-4: Localization of fluorescent protein fusions expressed under the pMtBcp1 promoter.

M. truncatula roots colonized by *G. versiforme* and expressing *pMtBcp1:MtPT4-GFP* (a), *pMtBcp1:MtPT1-GFP* (b), *pMtBcp1:MtPT1-GFP* coexpressed with *pMtBcp1:AtPIP2a-mCherry* (c) and *pMtPT4:AtPIP2a-GFP* coexpressed with *pMtBcp1:AtPIP2a-mCherry* (d). a, b, left panel shows GFP fluorescence, middle panel DIC, right panel overlay. c, d, left panel, GFP fluorescence; middle left, mCherry fluorescence; middle right overlay of both channels; right, DIC. Arrowheads, arbuscule branches; T, arbuscule trunk; IH, intracellular hypha; N, plant nucleus. bars = 20 µm.

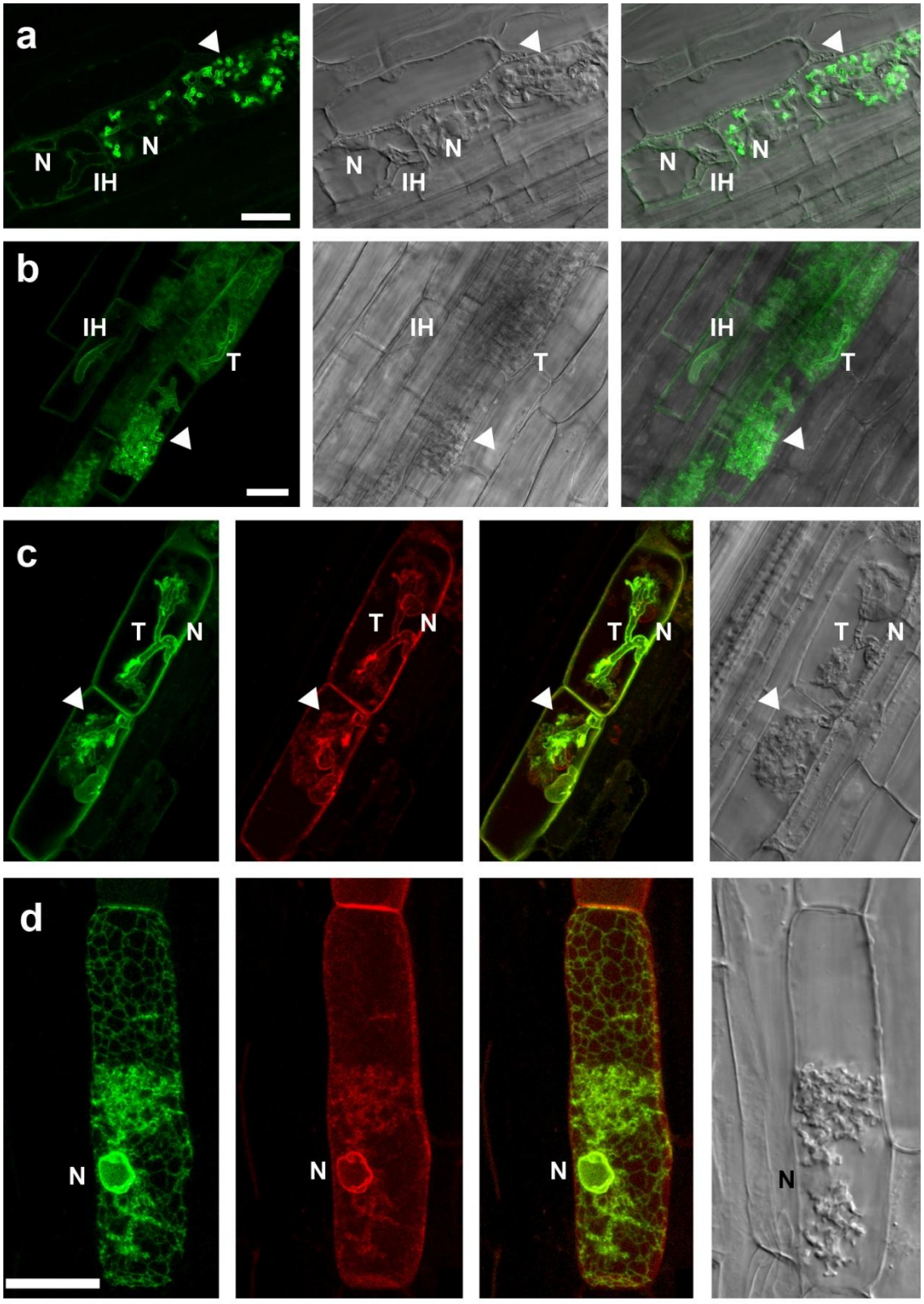
a
N
N
IH
N
N
IH
N
N
IH
b
IH
T
IH
T
IH
T
c
T
N
T
N
T
N
T
N
d
N
N
N
N

Table 3-1: Summary of protein localizations

Summary of protein localizations

Protein Marker:	Promoter: pMtPT4	p35S	pMtBcp1
MtPT4	Periarbuscular Membrane	ER	ER and Periarbuscular Membrane
MtPT1	Periarbuscular Membrane	Plasma Membrane	Plasma Membrane and Periarbuscular Membrane
AtPIP2a	ER	Plasma Membrane	Plasma Membrane and ER

To determine features of the MtPT4 protein that are required for its secretion to the periarbuscular membrane, we constructed a series of MtPT4 deletion and substitution variants fused to GFP. These were expressed from the native MtPT4 promoter. Previous reports have established a requirement for the soluble carboxy-terminal tail in subcellular targeting of the mammalian Glut4 hexose transporter (Verhey et al., 1993; Shewan et al., 2000). MtPT4 deletions included two truncations of the soluble carboxy-terminal tail at amino acid positions 492 and 506, and one of the soluble amino-terminus. These constructs all localized in the periarbuscular membrane in a similar manner as the full length protein (Fig. 3-5a and data not shown). MtPT4 localization also was not compromised by Y to A mutagenesis of two putative tyrosine-based sorting/endocytic motifs (YXXΦ) in the large central loop (Fig. 3-5b), while a YXXΦ motif was shown to mediate polar localization of the Arabidopsis boron transporter BOR1 (Dhonukshe et al., 2007; Takano et al., 2010). Finally, insertion of a sequence present in MtPT1 but not in MtPT4, TDKGYPTGIG, between the last two transmembrane domains did not affect periarbuscular membrane localization of MtPT4 (Fig. 3-5c).

A TILLING screen for *mtpt4* mutants revealed previously that plants harboring a loss-of-function *mtpt4* allele displayed an early arbuscule death phenotype and loss of phosphate uptake through the symbiosis (Javot et al., 2007b). Localization of these *mtpt4* mutant proteins was assessed by immunolocalization in mutant plants and expression of GFP fusions in wild type plants. One allele containing a single transition mutation of C-to-T causes an amino acid substitution of serine 115 to phenylalanine (S115F) and was named *mtpt4-3*. This serine residue is highly conserved in the PHT1 family of phosphate transporters and resides at the end of the third transmembrane domain facing the lumenal/extracellular face based on topology prediction (TMHMM).

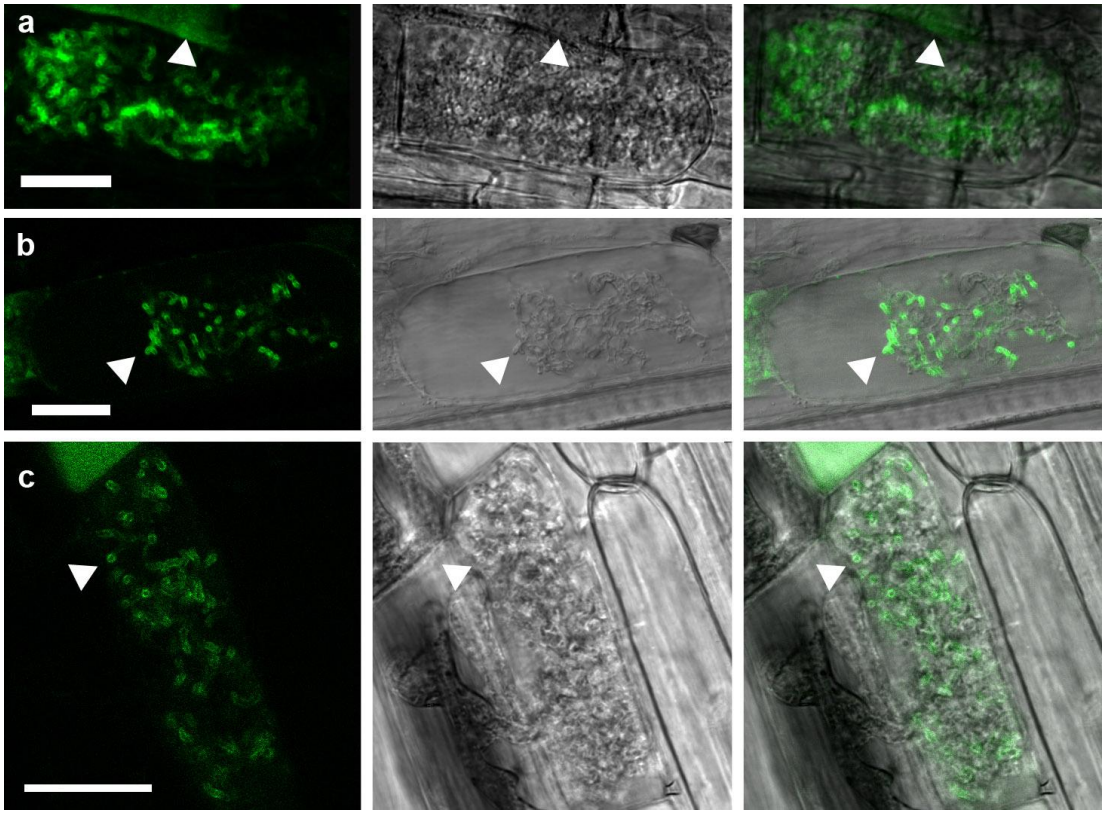

Figure 3-5: Mutation of known sorting motifs present in MtPT4 does not affect localization.

Expression of MtPT4 derivatives under the native promoter harboring: a, a deletion of the soluble carboxy-terminus, MtPT4$^{\Delta 506}$-GFP; b, insertion of TDKGYPTGIG motif from MtPT1 into MtPT4^{TDKGYPTGIG} -GFP; c, mutation of two tyrosines to alanine from putative YXXΦ endocytosis motifs, MtPT4$^{Y228/239A}$-GFP. Left panel shows GFP fluorescence, middle panel differential interference contrast bright-field (DIC), right panel overlay. Localization in the branch domain is observed for all proteins (arrowheads). Bars = 20 µm.

When *mtpt4*^{S115F} was expressed as a GFP fusion under the MtPT4 promoter, it did not traffic to the periarbuscular membrane, but rather was retained in the endomembrane system (Fig. 3-6 c-e). *mtpt4-3* mutant plants displayed the early arbuscule death phenotype that also leads to lack of symbiotic phosphate uptake (Fig. 3-6 a and b) (Javot et al., 2007b), confirming that localization of MtPT4 in the periarbuscular membrane is required for a functional AM symbiosis.

To determine the nature of the endosomal localization of mtpt4^{S115F}, the GFP fusion was cotransformed into *M. truncatula* roots together with a *p35S:HDEL-mCherry* ER marker (Fig. 3-6c), *p35S:GmMan1-mCherry* Golgi marker (Fig. 3-6d) and *p35S:AtSyp61-mRFP* Trans-Golgi Network (TGN) marker (Fig. 3-6e). While our results suggest that 35S promoter activity is reduced during the span of arbuscule development, sufficient protein remains in these cells for imaging purposes, and the localization pattern of endosomal markers is unaffected. Colocalization was observed between mtpt4^{S115F}-GFP and the ER marker, showing this protein is partially retained in the ER (Fig. 3-6c). The endosomal bodies illuminated by mtpt4^{S115F}-GFP colocalized with the Syp61-mRFP TGN marker, while the Man1-mCherry Golgi marker showed adjacent or independent localization to mtpt4^{S115F}-GFP (Fig. 3-6d and e). This pattern of coexpression with TGN and Golgi markers was reported in previous studies of TGN-resident proteins (Viotti et al., 2010). Some vacuolar signal was also observed in *p35S:AtSyp61-mRFP*-expressing roots, suggesting partial instability of the marker (Fig. 3-6e). Time-lapse confocal imaging of cells expressing mtpt4^{S115F}-GFP and Syp61-mRFP showed co-labeled endosomal bodies moving in the cell , confirming the colocalization result. The ER accumulation of mtpt4^{S115F} could be the result of direct retention due to inefficient ER exit, or possibly a result of overaccumulation of mutant protein in the TGN that leads subsequently to accumulation in the ER. Additionally, immunolocalization with a polyclonal

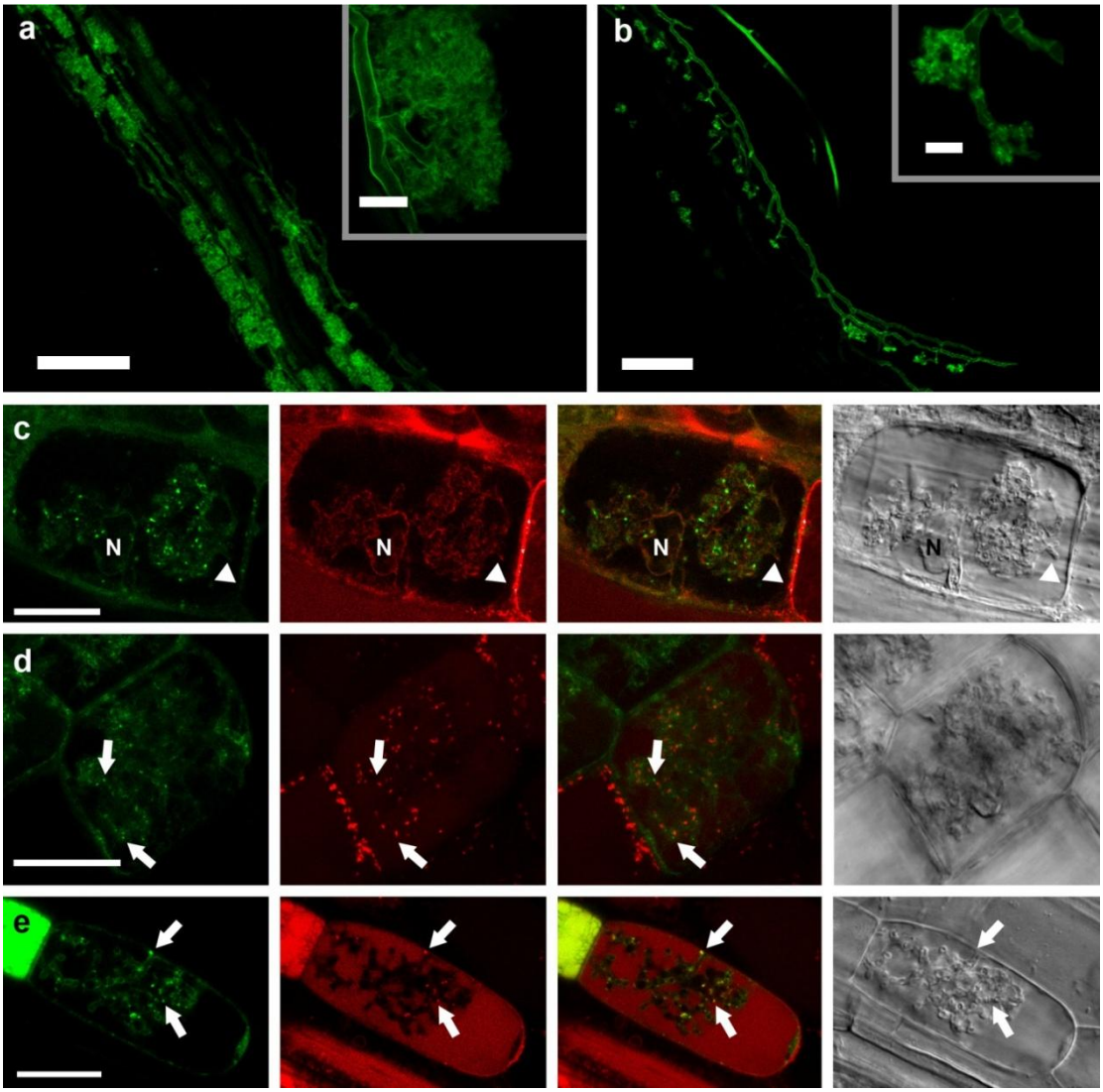

Figure 3-6: Phenotype of *mtpt4-3* and localization of mtpt4^{S115F}.
Mature arbuscule morphology in roots of wild type (a) and prematurely collapsed arbuscules in *mtpt4-3* mutant roots (b), visualized by the chitin stain WGA-AlexaFluor 488 (green). Bars = 100 µm, inset 10 µm. Localization of mtpt4^{S115F}-GFP expressed under pMtPT4 and coexpressed with HDEL-mCherry ER marker (c), GmMAN1-mCherry Golgi marker (d) and AtSyp61-mRFP TGN marker (e). Left panel, GFP fluorescence; middle left, mCherry/mRFP fluorescence; middle right overlay of both channels; right, DIC. N, nucleus; arrowhead, arbuscule branch; arrow, endosomal localization of mtpt4^{S115F}-GFP. mtpt4^{S115F}-GFP is colocalized with the ER and TGN markers but not with the Golgi marker. Bars in c-e = 20 µm.

antibody raised against MtPT4 (Harrison et al., 2002) in *mtpt4-3* roots detected the native mtpt4^{S115F} protein localized in endosomal structures, while immunolocalization in wild type roots reveals periarbuscular membrane localization (Fig. 3-7a and b).

Phosphorylation of serine residues can affect subcellular localization of transporters in plant cells (Huang et al., 2010). To test genetically if the S115 residue could be phosphorylated, a site-directed mutagenesis constructs were made with S115 mutations to alanine and the phosphoserine mimic glutamate. MtPT4^{S115A} mutant proteins localized in the periarbuscular membrane similar to WT MtPT4, while and MtPT4^{S115E} was retained in the ER with no evidence of TGN localization (Fig. 3-8a and b). Retention in the ER of MtPT4^{S115E} suggests these mutations compromised ER export to a greater degree than mtpt4^{S115F}. As the S115A mutant protein localizes correctly, these results do not support the hypothesis that phosphorylation of S115 enables TGN exit, but instead point to mtpt4^{S115F} accumulation in the TGN resulting from phenylalanine addition at position 115 rather than a loss of serine.

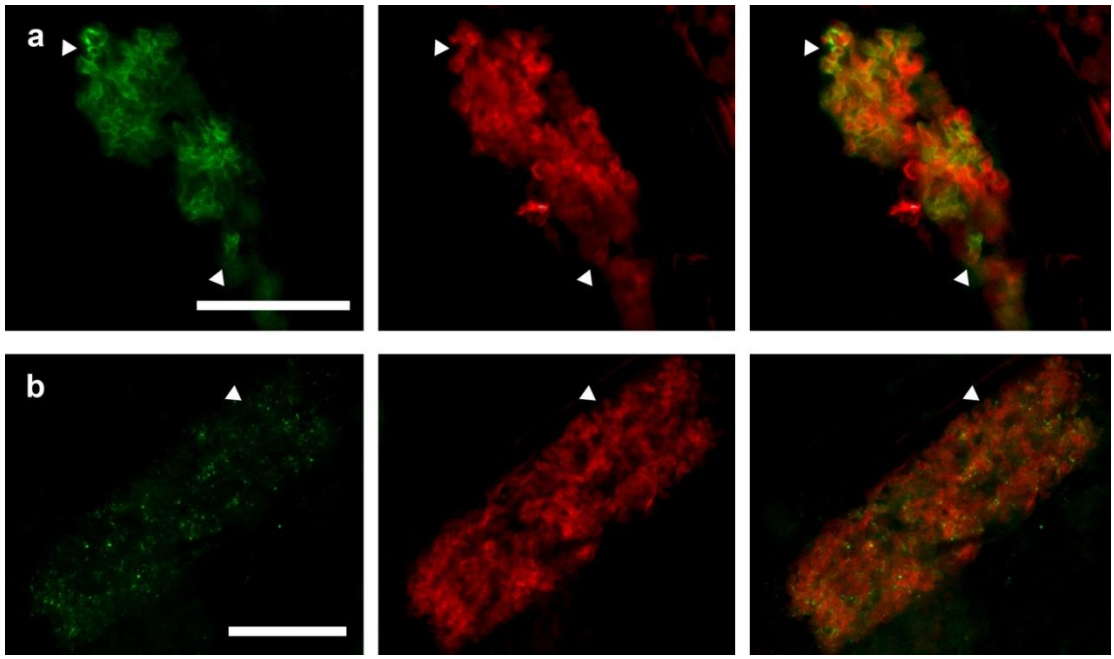

Figure 3-7: Immunolocalization of MtPT4 protein in wild type and *mtpt4-3* roots. MtPT4 protein was detected by native antibody in wild type (a) and *mtpt4-3* mutant roots (b). Left panel, detection of MtPT4 antibody by secondary antibody conjugated to AlexaFluor488. Middle panel, visualization of fungal arbuscule by WGA conjugated to AlexaFluor594. Right panel, overlay. Arrowhead identifies an arbuscule branch. Wild type MtPT4 protein localizes around arbuscule branches while mtpt4-3 (mtpt4^{S115F}) is retained in TGN-like puncta.
Bars = 20 µm.

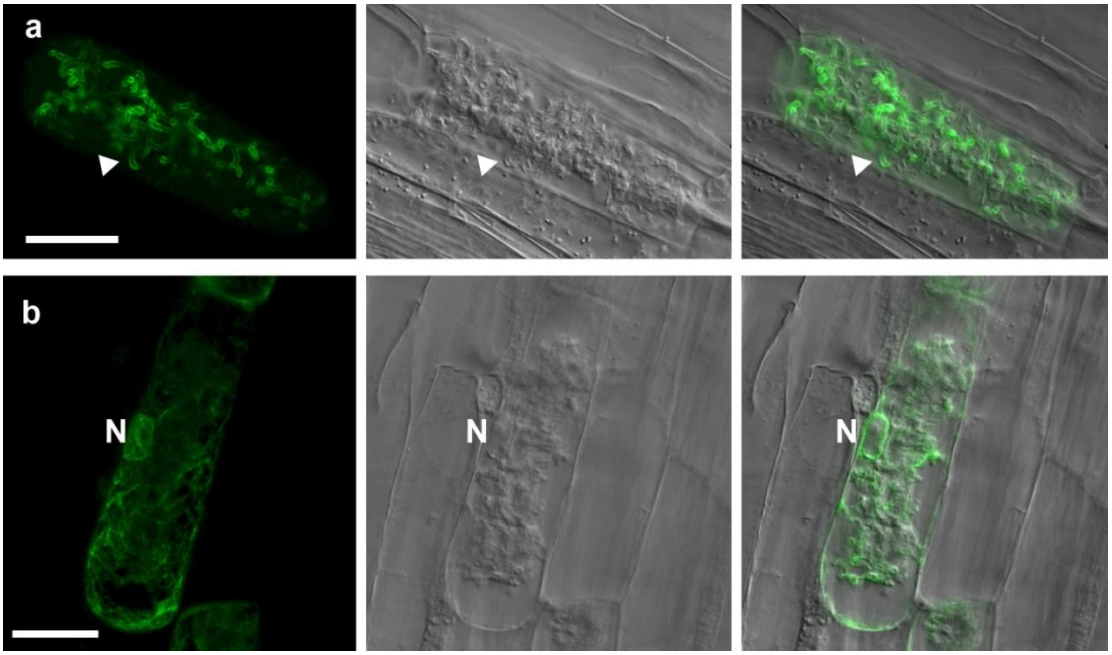

Figure 3-8: Localization of MtPT4^{S115A} (a) and MtPT4^{S115E} (b) mutations. Mutation of serine 115 to alanine does not compromise localization to the periarbuscular membrane (arrowhead). Mutation of serine 115 to the phosphoserine mimic glutamate cause ER retention, as evidenced by strong perinuclear signal surrounding the nucleus (N). Bars = 20 µm.

To determine whether mutation of the conserved serine impaired an MtPT4-specific secretion process or caused a general disruption of phosphate transporter secretion, the equivalent mutation (S117F) was introduced into the *MtPT1-GFP* construct and expressed under the native MtPT1 promoter or the MtPT4 promoter. Both in epidermal cells when expressed under pMtPT1 and cortical cells harboring arbuscules when expressed under pMtPT4, this mutated MtPT1^{S117F} protein failed to localize in the periarbuscular membrane or the plasma membrane and instead was retained in the ER and endosomal bodies that colocalized with the Syp61-mRFP TGN marker (Fig. 3-9a and b). These results suggest that the TGN is an intermediate secretion compartment for PHT1-type phosphate transporters, as recently shown for a polar-localized boron transporter (Takano et al., 2010; Viotti et al., 2010), and that a TGN export mechanism may be disrupted by the mtpt4^{S115F} and MtPT1^{S117F} mutations. In addition, the secretory pathway following ER exit that controls MtPT4 trafficking during arbuscule development likely involves the same mechanism that functions in phosphate transporter secretion in other cells types, while ER exit of MtPT4 appears to require a symbiosis-specific mechanism.

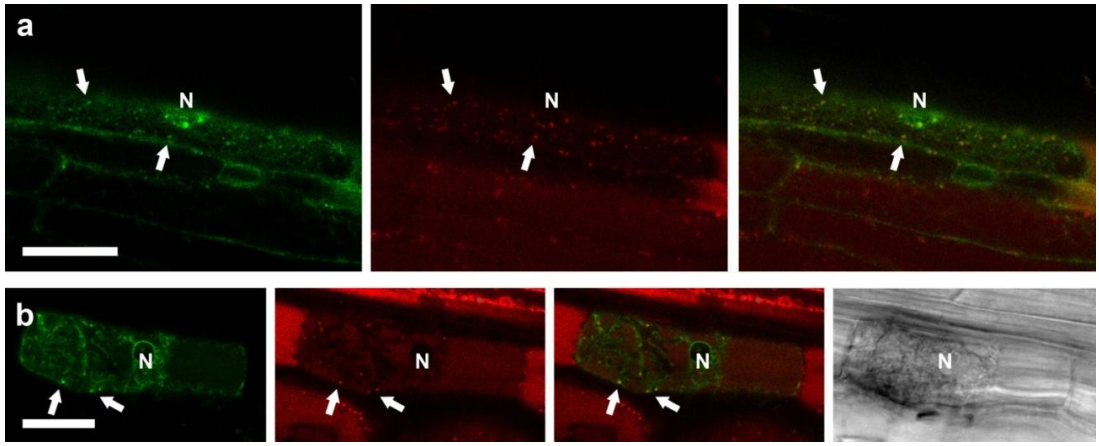

Figure 3-9: Localization of MtPT1^{S117F} in ER and TGN.
AtSyp61-mRFP TGN marker coexpressed with *pMtPT1:MtPT1*^{S117F}*-GFP* (a) and *pMtPT4:MtPT1*^{S117F}*-GFP* (b). Colocalization between markers is observed in epidermal cells (a) and cortical cells harboring arbuscules (b). Retention in the ER is evident by perinuclear signal. Bars = 20 µm.

Discussion

Based on these data we propose that polar targeting of MtPT4 to the periarbuscular membrane is regulated by a polarization of the bulk secretory pathway favoring vesicle fusion with the developing periarbuscular membrane, rather than with the plasma membrane, and a coincident change in the newly synthesized protein cargo entering into the secretion system. This mechanism differs fundamentally from the mechanism elucidated for polar localization of the PIN auxin efflux transporters, which are secreted symmetrically then subsequently endocytosed and recycled in a polar manner (Dhonukshe et al., 2008; Geldner, 2009). The PIN proteins function in relatively mature cells experiencing little growth and polarity is maintained over the life of the cell. In contrast, MtPT4 is synthesized in a cell that must synthesize and secrete the equivalent of three to eight times the amount of its plasma membrane in a short time. The membrane and its resident proteins function for only the few days of active arbuscule lifespan before being degraded. Therefore it seems logical for newly synthesized periarbuscular membrane-specific proteins and membrane material to traffic directly to the location surrounding a developing arbuscule. Transient reorganization of secretion towards the developing membrane at the expense of secretion to the plasma membrane could enable the rapid development of this resource-intensive membrane. A significant change in secreted cargo in cells with developing arbuscules is inferred from studies revealing large transcriptional changes in these cells (Liu et al., 2003; Hohnjec et al., 2005; Gomez et al., 2009; Guether et al., 2009). The surprising result that a native plasma membrane-localized phosphate transporter, MtPT1, localizes in the periarbuscular membrane when expressed during arbuscule development, and that expression prior to arbuscule development is insufficient for localization in this domain, suggests that reorienting secretion is the

driving factor, rather than polar sorting of proteins to the plasma membrane or periarbuscular membrane by specific targeting motifs (Fig. 3-10). The molecular mechanism by which secretion becomes polarized to produce the host-symbiont interface is an intriguing open question. Since our proposed mechanism is based on analysis of a few proteins, we cannot rule out the possibilities of other targeting mechanisms during arbuscule development. Further study will be needed to characterize additional proteins expressed during arbuscule development and test the mechanism underlying their localizations.

Morphologically, development of AM fungal arbuscules in root cells is similar to the development of nutrient-extracting hyphae, called haustoria, formed within plant cells by some pathogenic biotrophic fungi and oomycetes. These haustoria are surrounded by extra-haustorial plant membranes analogous to the periarbuscular membrane (Koh et al., 2005). Recently, Wang et al. (2009) provided the first report of a protein, Arabidopsis RPW8.2, that localizes in the extrahaustorial membrane surrounding haustoria of powdery mildew pathogens. This localization was observed by expressing an RPW8.2-YFP fusion under its native promoter, which is induced coincident with extrahaustorial membrane synthesis. The parallel with our results suggests that extrahaustorial and periarbuscular membrane targeting may share some mechanistic similarities.

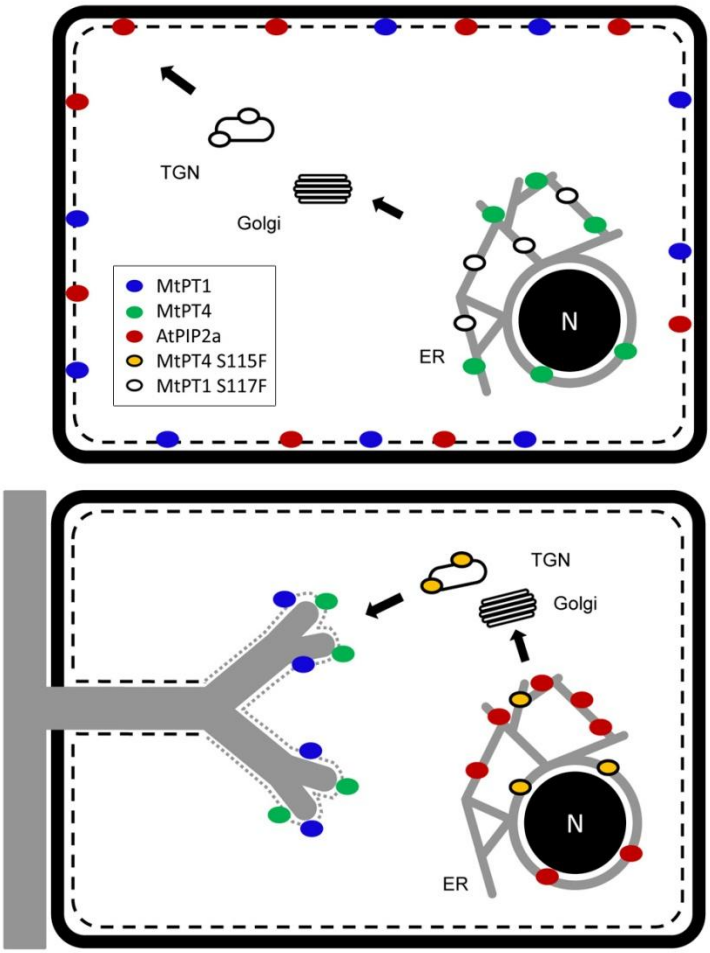

Figure 3-10: Proposed model for protein secretion during arbuscule development.

Two cells are depicted, an uninfected epidermal/cortical cell (upper) and cortical cell harboring a developing arbuscule (lower). In an uninfected cell, MtPT1 and AtPIP2a are secreted to the plasma membrane (black dashed line), while MtPT4 is retained in the ER. The MtPT1^{S117F} mutant protein is retained in the ER and TGN. During arbuscule development (lower cell) in a cortical cell, newly-synthesized MtPT4 and MtPT1 expressed from an arbuscule-specific promoter are secreted to the periarbuscular membrane (gray dotted line), while AtPIP2a is retained in the ER. The mutant protein MtPT4^{S115F} is retained in the ER and TGN.

Some parallels also exist between our proposed targeting mechanism and protein targeting to the cell plate, which is formed *de novo* during cytokinesis. Arabidopsis Knolle, a syntaxin expressed specifically during M phase in dividing cells, localizes in the TGN and developing cell plate, and is required for cytokinesis (Lukowitz et al., 1996). While the *knolle* mutant phenotype is rescued by expressing Knolle under its native promoter, expression under the 35S promoter does not rescue the phenotype due to insufficient protein accumulation during division (Volker et al., 2001). Interestingly, expression of a snapdragon Knolle ortholog from the Arabidopsis Knolle promoter complements the Arabidopsis mutant, and plasma membrane-localized syntaxins, such as AtSyp122, expressed from the Knolle promoter localized to the cell plate (Muller et al., 2003). This suggests that timing of expression, rather than a targeting motif, is the factor that allows Knolle to accumulate in the correct location. Volker et al (2001) suggested that secretion is largely directed to the developing cell plate by a "general redirection of membrane flow", and that Knolle expressed from the 35S promoter before cell plate formation cannot accumulate in the cell plate to sufficient levels for complementation. This is in essence the same property we are describing for MtPT4 localization.

The transient reduction in 35S promoter activity we observed in cells harboring arbuscules was also reported to occur during root nodule symbiosis between *M. truncatula* and rhizobia bacteria. This symbiosis shares a common genetic pathway and related developmental processes with the AM symbiosis, and leads to the formation of nitrogen fixing nodules on the roots of many leguminous plants. Infected nodule cells harbor differentiated rhizobia bacteroids surrounded by the symbiosome membrane, analogous to the periarbuscular membrane. In these cells, the 35S

promoter activity is also strongly reduced (Auriac and Timmers, 2007; Limpens et al., 2009).

One commonality shared by dividing cells and some cells interacting with intracellular microbes including AM fungi, rhizobia bacteria and powdery mildew pathogens, is endoreduplication (Bonfante and Perotto, 1995; Genre et al., 2008; Chandran et al., 2010). One possible explanation for this phenomenon is that DNA duplication increases total transcription by increasing gene dosage, making cells more metabolically active (Chandran et al., 2010). It is tempting to speculate however, that endoreduplication could contribute to specific and rapid transcriptional reprogramming, as occurs during cell division including the downregulation of the 35S promoter, and that this facilitates specialized cellular developmental programs by significantly altering the types of newly synthesized proteins.

In our study of phosphate transporter secretion, we have observed two points at which the proteins can be retained in the endomembrane system: the ER and the TGN (Fig. 3-10). Ectopic expression of MtPT4 leads to ER retention and degradation, as does heterologous expression of OsPT11 (Kobae and Hata, 2010). ER retention of phosphate transporters is also observed in Arabidopsis *phf1* mutant plants. PHF1 encodes a protein with distant homology to SEC12 and appears to function as an ER chaperone specifically for phosphate transporters (Gonzalez et al., 2005). Because MtPT4 is retained in the ER during early arbuscule development events, but appears on the periarbuscular membrane when fine branches begin to form, this suggests that a different ER export chaperone may be expressed coincident with MtPT4 expression and function in the secretion of MtPT4, and possibly other proteins specific to the symbiosis. Another possibility is a symbiosis-specific modification of a *M. truncatula PHF1* ortholog. In yeast, ER exit of an MtPT4-homologous phosphate transporter, PHO84, is dependent on an exit chaperone, PHO86, which is unrelated in sequence to

PHF1 (Lau et al., 2000; Gonzalez et al., 2005). The independent evolution in eukaryotes of two ER export chaperones for phosphate transporters makes the existence of a third specific chaperone plausible, and sequence-based candidate searches would be ineffective if this chaperone arose by convergent evolution.

Accumulation of mtpt4^{S115F} and MtPT1^{S117F} in the TGN suggests this mutation disrupts a process that enables secretion to the destination membrane, such as loss of adaptor protein complex recruitment (Rodriguez-Boulan et al., 2005). It is possible that these proteins become retained in the TGN during initial secretion or following endocytosis from the periarbuscular or plasma membranes. However, distinguishing between these two will require detailed pharmacological analysis. As no mutant protein was observed in the destination membrane, it is more likely that the retention occurs during the initial secretion of MtPT4^{S115F} and MtPT1^{S117F}. The finding that this mutation affects secretion in cells harboring arbuscules and also during native expression of MtPT1 in epidermal cells suggests that a conserved mechanism mediates secretion to the periarbuscular membrane and plasma membrane. This situation would parallel the Arabidopsis response to incompatible powdery mildew pathogens, where focal secretion to the site of haustorium formation is mediated by a SNARE complex that also functions in plant development (Kwon et al., 2008). These mutations may provide a useful tool for dissecting the process that mediates TGN to periarbuscular and plasma membrane trafficking of phosphate transporters

Methods

Growth and transformation

M. truncatula cv. Jemalong line A17 was used for all experiments described, including generation of the *mtpt4-3* mutant line. Transgenic roots were generated by *Agrobacterium rhizogenes*-mediated root transformation as described (Boisson-

Dernier et al., 2001) using the strain ARquaI. Cotransformed composite roots were generated by mixing ARquaI strains harboring appropriate plasmids prior to seedling inoculation. *M. truncatula* seeds were surface-sterilized and germinated by a 24 hour dark treatment at 30 °C, and elongating hypocotyls were excised and inoculated with ARquaI strains. Seedlings were transferred to modified Fahraeus media containing 25 mg/L kanamycin for selection of transgenic roots. After 20 days, plants were transferred to sterilized turface soil and grown for 10 days prior to inoculation with surface-sterilized *Glomus versiforme* spores. Plants were grown in a growth chamber under 16 hr light (25 °C)/8 hr (22 °C) dark cycle and fertilized once per week with half-strength Hoagland's solution modified with full-strength nitrogen and 20 µM potassium phosphate. Mycorrhizal roots were analyzed three to five weeks after inoculation

Plasmid Construction

All constructs created for this report were expressed in the pCAMBIA2301 vector (www.cambia.org) and fused to the S65T variant of green fluorescent protein (GFP) (Chiu et al., 1996), except where indicated.

pMtPT4:MtPT4-GFP was created by amplifying a 2,651 bp genomic fragment corresponding to the MtPT4 coding sequence and 864 bp of upstream sequence with primers that add 5' *XbaI* and 3' *NcoI* restriction sites. This fragment was digested and ligated into the 35S:sGFP (S65T)-Nos modified pUC18 vector (Chiu et al., 1996), creating a 3' fusion of GFP to MtPT4 and removing the 35S promoter. This vector was then digested with *XbaI* and *EcoRI* and the fusion construct was ligated into the similarly-digested pCAMBIA2301 expression vector. *pMtPT4:mtpt4*^{S115F}*-GFP* was created by the same steps using genomic DNA isolated from the *mtpt4-3* mutant. *pMtPT4:MtPT4*$^{\Delta 506}$*-GFP* was created similarly; however, the reverse primer resulted

in a truncated the gene 1,518 bp downstream of the ATG, corresponding to a protein truncation at amino acid 506.

pMtPT1:MtPT1-GFP was created by amplifying a 3,164 bp genomic fragment corresponding to 1,545 bp of promoter and the 1,611 bp CDS with primers that added a 5' *XbaI* and 3' *NcoI* restriction sites. This fragment was digested and ligated into a modified pCAMBIA2301 containing the S65T GFP variant and NOS terminator, resulting in an in-frame 3' fusion to GFP. *pMtPT4:MtPT1-GFP* was created by amplifying the MtPT4 864 bp promoter fragment with primers adding 5'*XbaI* and 3' *KpnI*. This fragment was cloned into the pGEM-T EZ vector. The MtPT1 ORF was amplified with primers adding 5' *KpnI* and 3' *BamHI* sites and cloned into the MtPT4 promoter vector. This fusion was digested with *XbaI* and *BamHI* and ligated into pCAMBIA2301.

pMtPT4:AtPIP2a-GFP was created by amplifying the 861 bp ORF of AtPIP2a from the 35S:AtPIP2a-mCherry vector (Nelson *et al*. 2007) with primers adding 5' *KpnI* and 3' *BamHI* restriction sites. This fragment was digested and ligated into the similarly digested *pMtPT4:MtPT1-GFP* vector, effectively replacing the MtPT1 ORF for AtPIP2a.

p35S:MtPT4-GFP was created by amplifying the 1,581 bp MtPT4 cDNA with primers adding 5' *SalI* and 3' *NcoI* restriction sites. This fragment was digested and ligated into the 35S:sGFP (S65T)-Nos vector, creating an in-frame fusion of GFP to the 3' end of MtPT4. This vector was digested with *HindIII* and *EcoRI*, and ligated into pCAMBIA2301. *p35S:MtPT1-GFP* was created in the same manner, using primers that added 5' *SalI* and 3' *BamHI* restriction sites.

pMtBcp1:MtPT4-GFP and *pMtBcp1:MtPT1-GFP* were created by amplifying the 1179 bp MtBcp1 promoter with primers that added 5' *XbaI* and 3' *SalI* restriction sites. This fragment was digested with *XbaI* and *SalI* and ligated into similarly

digested p35S:MtPT4:sGFP (S65T)-Nos or p35S:MtPT4:sGFP (S65T)-Nos vector, replacing the promoter with pMtBcp1. These plasmids were then digested with *XbaI* and *EcoRI* and ligated into pCAMBIA2301. *pMtBcp1:AtPIP2a-mCherry* was created by amplifying the AtPIP2a-mCherry fusion (Nelson *et al.* 2007) with primers that added 5' *SalI* and 3' *NotI* restriction sites. This fragment was digested with *SalI* and *NotI*, and ligated into the *pMtBcp1:MtPT1-GFP* pUC vector digested similarly. The resulting pMtBcp1:AtPIP2a-mCherry plasmid was digested with *XbaI* and *EcoRI* and ligated into pCAMBIA2301.

p35S:MtPT4 5'UTR-MtPT4-GFP and *p35S:MtPT4 5'UTR-MtPT1-GFP*, UTR swap constructs were created by fusion PCR. A primer was designed to anneal to the 5' end of the 5' UTR of MtPT4, and contain an overhang corresponding to the 35S promoter region at the TATA box. This primer was used together with a reverse primer that amplified either MtPT4 or MtPT1 from the pMtPT4:MtPT1 vector and added a 3' *NcoI* restriction site. A second fragment corresponding to the 35S promoter was amplified using a forward primer that added a 5' *XbaI* site and a reverse primer that corresponded to the 35S TATA box and an overhang corresponding to the 5' end of the MtPT4 5' UTR. These two fragments were then purified and amplified in a combined PCR reaction using the forward primer that added a 5' *XbaI* and the appropriate reverse primer that added a 3' *NcoI* to create the UTR swap. This fused fragment was then digested with *XbaI* and *NcoI* and cloned into the 35S:sGFP (S65T)-Nos vector. This plasmid was subsequently digested with *XbaI* and *EcoRI* and the resulting fragment was ligated into pCAMBIA2301. *pMtPT4:35S 5'UTR-MtPT4-GFP and pMtPT4*:*35S 5'UTR-MtPT1-GFP* were created using the same strategy and restriction sites as described above.

pMtPT4:MtPT4^{TDKGYPTGIG}*–GFP* was also created using a fusion PCR strategy. Two fragments were amplified using the pMtPT4:MtPT4-GFP vector as template.

The 5' fragment was amplified with a forward primer adding the *XbaI* restriction site to the MtPT4 promoter and a reverse primer adding an overhang encoding the TDKGYPTGIG sequence from MtPT1. A 3' fragment was similarly amplified with a forward primer adding a sequence corresponding to the TDKGYPTGIG domain and a reverse primer adding the *NcoI* restriction site for fusing to sGFP. These two fragments were purified, combined and amplified with a forward primer adding an *XbaI* site at the beginning of the promoter and a reverse primer adding an *NcoI* site at the end of the ORF. This fragment was digested with *XbaI* and *NcoI*, cloned into the similarly-digested 35S:sGFP-NOS pUC vector, which was subsequently digested with *XbaI* and *EcoRI* to subclone the fusion construct into pCAMBIA2301.

pMtPT4:MtPT4^{S115A}*-GFP* and *pMtPT4:MtPT4*^{S115E}*-GFP* were created by site-directed mutagenesis using the Quikchange II Mutagenesis kit (Stratagene) starting with pMtPT4:MtPT4-GFP in the pUC vector as template and resulting in a mutated MtPT4 protein with serine 115 substituted for alanine or glutamic acid, respectively. Following mutagenesis, the modified fusion construct was digested with *XbaI* and *EcoRI* and ligated into pCAMBIA2301. *pMtPT4:MtPT4*$^{Y228/239A}$*-GFP* was created in similar manner, using primers that introduced both mutations, changing tyrosine 228 and 239 to alanine. *pMtPT4:MtPT1*^{S117F}*-GFP* and *pMtPT1:MtPT1*^{S117F}*-GFP* were created similarly by the Quikchange II Mutagenesis kit using pMtPT4:MtPT1-GFP and pMtPT1:MtPT1-GFP, respectively, in pUC vector as template. Fusions were also subcloned into pCAMBIA2301 for expression.

p35S:HDEL-mCherry (ER) and *p35S:GmMAN1-mCherry* (Golgi) markers in pBIN vectors are described in (Nelson et al., 2007) and are available from ABRC (http://abrc.osu.edu/). *p35S:AtSyp61-mRFP* TGN marker in pPZP is described in (Sanderfoot et al., 2001; Dettmer et al., 2006).

Immunolocalization

Immunolocalization of MtPT4 was performed according to Harrison (2002), with a modified fixation buffer. Colonized root segments from wild type and *mtpt4-3* plants, stably-transformed with the symbiosis-specific *pMtScp1:GFP* reporter (Liu et al., 2003), were isolated under a dissecting microscope. Samples were fixed for 2 hours on a rotary shaker in a PME buffer (50 mM PIPES, 5 mM MgSO4, and 10 mM ethylene glycol tetraacetic acid, pH 6.9) containing 4% formaldehyde, 1% glutaraldehyde and 5% dimethyl sulfoxide. Roots were then bisected longitudinally placed on a cover slip and overlaid with a thin film of 1% agar according to (Brown and Lemmon, 1995), followed by a 10 minute cell wall digestion in PME buffer containing 0.1% BSA, 1% cellulase (RS) and 0.01% pectolyase (Y23) (Karlan Research Products, Santa Rosa, CA). This was followed by three 5-minute rinses with PME and 10-minute incubation in PBS buffer (135 mM NaCl, 25 mM KCl, and 10 mM Na_2HPO_4, pH 7.4) containing 1% BSA and overnight incubation in a 1/500 dilution of MtPT4 antibody in PBS buffer containing 0.5% BSA (Harrison et al., 2002). The next day, samples were rinsed three times with PBS, and incubated two hours with a 1/100 dilution in PBS of goat anti-rabbit IgG conjugated to AlexaFluor 488 (Molecular Probes) followed by additional rinses and a 30 minute incubation with 0.05 mg/ml wheatgerm agglutinin conjugated to AlexaFluor 594 (Molecular Probes) in PBS. Following four rinses with PBS, samples were rinsed once with PBS pH 8.5 and mounted onto microscope slides in PBS, pH 8.5 containing 13% Mowiol 4-88 (Calbiochem, La Jolla, CA).

Imaging

Imaging of fluorescent protein fusions was performed as described in Pumplin and Harrison (2009). Briefly, transgenic roots expressing appropriate fluorescence

were excised under an Olympus SZX-12 stereo microscope (http://www.olympus.com), bisected longitudinally and sealed under a cover slip with VALAP (Vaseline:lanolin:paraffin, 1:1:1). Samples were then imaged on a Leica TCS-SP5 confocal microscope (Leica Microsystems) using a 63x, NA 1.2 water-immersion objective. GFP was excited with a blue argon ion laser at 488 nm and emitted fluorescence collected from 505 to 545 nm; mCherry and mRFP were excited with a Diode-Pumped Solid State laser, 561 nm, and emitted fluorescence was collected from 590 to 640 nm for mCherry and 570 to 600 nm for mRFP. Bright field differential interference contrast (DIC) images were collected with the transmitted light detector. Image data was processed with the Leica LAS-AF Version 1.7.0 and Adobe Photoshop CS Version 8 (Adobe Systems) software. Only undisrupted cells below the sectioning plane were imaged, and Figures include representative images from multiple independent experiments.

Isolation of mutant

The *mtpt4-3 M. truncatula* line A17 mutant was isolated in a TILLING screen detailed in Javot *et al.* (2007b). The *mtpt4*^{S115F} missense mutation is caused by a C-to-T transition resulting in a substitution of phenylalanine for serine at position 115. Phenotyping of mutant plants was performed by harvesting roots 4-5 weeks after inoculation with the AM fungus *Glomus versiforme*, clearing roots in 20% potassium hydroxide and staining with wheatgerm agglutinin (WGA) conjugated to AlexaFluor 488 (Molecular Probes) to image fungal morphology. *mtpt4-3* roots displayed the same early arbuscule turnover phenotype described in Javot *et al.* (2007b), and this phenotype segregated as a recessive trait in an F2 backcross population.

REFERENCES

Alexander, T., Toth, R., Meier, R., and Weber, H.C. (1989). Dynamics of arbuscule development and degeneration in onion, bean and tomato with reference to vesicular-arbuscular mycorrhizae in grasses. Canadian Journal of Botany **67,** 2505-2513.

Auriac, M.C., and Timmers, A.C. (2007). Nodulation studies in the model legume *Medicago truncatula*: advantages of using the constitutive EF1alpha promoter and limitations in detecting fluorescent reporter proteins in nodule tissues. Mol Plant Microbe Interact **20,** 1040-1047.

Boisson-Dernier, A., Chabaud, M., Garcia, F., Becard, G., Rosenberg, C., and Barker, D.G. (2001). *Agrobacterium rhizogenes*-transformed roots of *Medicago truncatula* for the study of nitrogen-fixing and endomycorrhizal symbiotic associations. Mol Plant Microbe Interact **14,** 695-700.

Bonfante, P., and Perotto, S. (1995). Strategies of arbuscular mycorrhizal fungi when infecting host plants. New Phytologist **130,** 3-21.

Brown, R.C., and Lemmon, B.E. (1995). Methods in plant immunolight microscopy. Methods Cell Biol **49,** 85-107.

Brundrett, M.C., Piché, Y., and Peterson, R.L. (1985). A developmental study of the early stages in vesicular–arbuscular mycorrhiza formation. Can. J. Bot. **63,** 184–194.

Chandran, D., Inada, N., Hather, G., Kleindt, C.K., and Wildermuth, M.C. (2010). Laser microdissection of *Arabidopsis* cells at the powdery mildew infection site reveals site-specific processes and regulators. Proc Natl Acad Sci U S A **107,** 460-465.

Chiou, T.J., Liu, H., and Harrison, M.J. (2001). The spatial expression patterns of a phosphate transporter (MtPT1) from *Medicago truncatula* indicate a role in phosphate transport at the root/soil interface. Plant J **25,** 281-293.

Chiu, W.-l., Niwa, Y., Zeng, W., Hirano, T., Kobayashi, H., and Sheen, J. (1996). Engineered GFP as a vital reporter in plants. Current Biology **6,** 325-330.

Dettmer, J., Hong-Hermesdorf, A., Stierhof, Y.D., and Schumacher, K. (2006). Vacuolar H+-ATPase activity is required for endocytic and secretory trafficking in *Arabidopsis*. Plant Cell **18,** 715-730.

Dhonukshe, P., Aniento, F., Hwang, I., Robinson, D.G., Mravec, J., Stierhof, Y.D., and Friml, J. (2007). Clathrin-mediated constitutive endocytosis of PIN auxin efflux carriers in *Arabidopsis*. Curr Biol **17,** 520-527.

Dhonukshe, P., Tanaka, H., Goh, T., Ebine, K., Mahonen, A.P., Prasad, K., Blilou, I., Geldner, N., Xu, J., Uemura, T., Chory, J., Ueda, T., Nakano, A., Scheres, B., and Friml, J. (2008). Generation of cell polarity in plants links endocytosis, auxin distribution and cell fate decisions. Nature **456,** 962-966.

Geldner, N. (2009). Cell polarity in plants: a PARspective on PINs. Curr Opin Plant Biol **12,** 42-48.

Genre, A., Chabaud, M., Faccio, A., Barker, D.G., and Bonfante, P. (2008). Prepenetration apparatus assembly precedes and predicts the colonization patterns of arbuscular mycorrhizal fungi within the root cortex of both *Medicago truncatula* and *Daucus carota*. Plant Cell **20,** 1407-1420.

Gianinazzi-Pearson, V., Arnould, C., Oufattole, M., Arango, M., and Gianinazzi, S. (2000). Differential activation of H+-ATPase genes by an arbuscular mycorrhizal fungus in root cells of transgenic tobacco. Planta **211,** 609-613.

Gomez, S.K., Javot, H., Deewatthanawong, P., Torres-Jerez, I., Tang, Y.H., Blancaflor, E.B., Udvardi, M.K., and Harrison, M.J. (2009). *Medicago*

truncatula and *Glomus intraradices* gene expression in cortical cells harboring arbuscules in the arbuscular mycorrhizal symbiosis. Bmc Plant Biology **9,** 1-19.

Gonzalez, E., Solano, R., Rubio, V., Leyva, A., and Paz-Ares, J. (2005). PHOSPHATE TRANSPORTER TRAFFIC FACILITATOR1 is a plant-specific SEC12-related protein that enables the endoplasmic reticulum exit of a high-affinity phosphate transporter in *Arabidopsis*. Plant Cell **17,** 3500-3512.

Guether, M., Balestrini, R., Hannah, M., He, J., Udvardi, M.K., and Bonfante, P. (2009). Genome-wide reprogramming of regulatory networks, transport, cell wall and membrane biogenesis during arbuscular mycorrhizal symbiosis in *Lotus japonicus*. New Phytol **182,** 200-212.

Harrison, M.J., Dewbre, G.R., and Liu, J. (2002). A phosphate transporter from *Medicago truncatula* involved in the acquisition of phosphate released by arbuscular mycorrhizal fungi. Plant Cell **14,** 2413-2429.

Hohnjec, N., Vieweg, M.F., Pühler, A., Becker, A., and Küster, H. (2005). Overlaps in the transcriptional profiles of *Medicago truncatula* roots inoculated with two different *Glomus* fungi provide insights into the genetic program activated during arbuscular mycorrhiza. Plant Physiology **137,** 1283-1301.

Huang, F., Kemel Zago, M., Abas, L., van Marion, A., Galvan Ampudia, C.S., and Offringa, R. (2010). Phosphorylation of Conserved PIN Motifs Directs *Arabidopsis* PIN1 Polarity and Auxin Transport. Plant Cell **22,** 1129-1142.

Javot, H., Pumplin, N., and Harrison, M.J. (2007a). Phosphate in the arbuscular mycorrhizal symbiosis: transport properties and regulatory roles. Plant Cell Environ **30,** 310-322.

Javot, H., Penmetsa, R.V., Terzaghi, N., Cook, D.R., and Harrison, M.J. (2007b). A *Medicago truncatula* phosphate transporter indispensable for the arbuscular mycorrhizal symbiosis. Proc Natl Acad Sci U S A **104,** 1720-1725.

Kobae, Y., and Hata, S. (2010). Dynamics of periarbuscular membranes visualized with a fluorescent phosphate transporter in arbuscular mycorrhizal roots of rice. Plant Cell Physiol **51,** 341-353.

Koh, S., Andre, A., Edwards, H., Ehrhardt, D., and Somerville, S. (2005). *Arabidopsis thaliana* subcellular responses to compatible *Erysiphe cichoracearum* infections. Plant Journal **44,** 516-529.

Kwon, C., Neu, C., Pajonk, S., Yun, H.S., Lipka, U., Humphry, M., Bau, S., Straus, M., Kwaaitaal, M., Rampelt, H., El Kasmi, F., Jurgens, G., Parker, J., Panstruga, R., Lipka, V., and Schulze-Lefert, P. (2008). Co-option of a default secretory pathway for plant immune responses. Nature **451,** 835-840.

Lau, W.T., Howson, R.W., Malkus, P., Schekman, R., and O'Shea, E.K. (2000). Pho86p, an endoplasmic reticulum (ER) resident protein in *Saccharomyces cerevisiae*, is required for ER exit of the high-affinity phosphate transporter Pho84p. Proc Natl Acad Sci U S A **97,** 1107-1112.

Limpens, E., Ivanov, S., van Esse, W., Voets, G., Fedorova, E., and Bisseling, T. (2009). *Medicago* N2-fixing symbiosomes acquire the endocytic identity marker Rab7 but delay the acquisition of vacuolar identity. Plant Cell **21,** 2811-2828.

Liu, J.Y., Blaylock, L.A., Endre, G., Cho, J., Town, C.D., VandenBosch, K.A., and Harrison, M.J. (2003). Transcript profiling coupled with spatial expression analyses reveals genes involved in distinct developmental stages of an arbuscular mycorrhizal symbiosis. Plant Cell **15,** 2106-2123.

Lukowitz, W., Mayer, U., and Jurgens, G. (1996). Cytokinesis in the *Arabidopsis* embryo involves the syntaxin-related KNOLLE gene product. Cell **84,** 61-71.

Marx, C., Dexheimer, J., Gianinazzipearson, V., and Gianinazzi, S. (1982). Enzymatic Studies on the Metabolism of Vesicular-Arbuscular Mycorrhizas .4. Ultracytoenzymological Evidence (Atpase) for Active Transfer Processes in the Host-Arbuscule Interface. New Phytologist **90,** 37-43.

Michniewicz, M., Zago, M.K., Abas, L., Weijers, D., Schweighofer, A., Meskiene, I., Heisler, M.G., Ohno, C., Zhang, J., Huang, F., Schwab, R., Weigel, D., Meyerowitz, E.M., Luschnig, C., Offringa, R., and Friml, J. (2007). Antagonistic regulation of PIN phosphorylation by PP2A and PINOID directs auxin flux. Cell **130,** 1044-1056.

Misson, J., Thibaud, M.C., Bechtold, N., Raghothama, K., and Nussaume, L. (2004). Transcriptional regulation and functional properties of *Arabidopsis* Pht1;4, a high affinity transporter contributing greatly to phosphate uptake in phosphate deprived plants. Plant Mol Biol **55,** 727-741.

Muller, I., Wagner, W., Volker, A., Schellmann, S., Nacry, P., Kuttner, F., Schwarz-Sommer, Z., Mayer, U., and Jurgens, G. (2003). Syntaxin specificity of cytokinesis in *Arabidopsis*. Nat Cell Biol **5,** 531-534.

Nelson, B.K., Cai, X., and Nebenfuhr, A. (2007). A multicolored set of in vivo organelle markers for co-localization studies in *Arabidopsis* and other plants. Plant Journal **51,** 1126-1136.

Pumplin, N., and Harrison, M.J. (2009). Live-cell imaging reveals periarbuscular membrane domains and organelle location in *Medicago truncatula* roots during arbuscular mycorrhizal symbiosis. Plant Physiol **151,** 809-819.

Rodriguez-Boulan, E., Kreitzer, G., and Musch, A. (2005). Organization of vesicular trafficking in epithelia. Nat Rev Mol Cell Biol **6,** 233-247.

Sanderfoot, A.A., Kovaleva, V., Bassham, D.C., and Raikhel, N.V. (2001). Interactions between syntaxins identify at least five SNARE complexes within the golgi/prevacuolar system of the *Arabidopsis* cell. Molecular Biology of the Cell **12,** 3733-3743.

Shewan, A.M., Marsh, B.J., Melvin, D.R., Martin, S., Gould, G.W., and James, D.E. (2000). The cytosolic C-terminus of the glucose transporter GLUT4 contains an acidic cluster endosomal targeting motif distal to the dileucine signal. Biochem J **350,** 99-107.

Smith, S.E., and Read, D.J. (2008). Mycorrhizal Symbiosis. (San Diego, CA: Academic Press, Inc.).

Takano, J., Tanaka, M., Toyoda, A., Miwa, K., Kasai, K., Fuji, K., Onouchi, H., Naito, S., and Fujiwara, T. (2010). Polar localization and degradation of *Arabidopsis* boron transporters through distinct trafficking pathways. Proc Natl Acad Sci U S A **107,** 5220-5225.

Vance, C.P., Uhde-Stone, C., and Allan, D.L. (2003). Phosphorus acquisition and use: critical adaptations by plants for securing a nonrenewable resource. New Phytologist **157,** 423-447.

Verhey, K.J., Hausdorff, S.F., and Birnbaum, M.J. (1993). Identification of the carboxy terminus as important for the isoform-specific subcellular targeting of glucose transporter proteins. J Cell Biol **123,** 137-147.

Viotti, C., Bubeck, J., Stierhof, Y.D., Krebs, M., Langhans, M., van den Berg, W., van Dongen, W., Richter, S., Geldner, N., Takano, J., Jurgens, G., de Vries, S.C., Robinson, D.G., and Schumacher, K. (2010). Endocytic and Secretory Traffic in *Arabidopsis* Merge in the Trans-Golgi Network/Early Endosome, an Independent and Highly Dynamic Organelle. Plant Cell **22,** 1344-1357.

Volker, A., Stierhof, Y.D., and Jurgens, G. (2001). Cell cycle-independent expression of the *Arabidopsis* cytokinesis-specific syntaxin KNOLLE results in mistargeting to the plasma membrane and is not sufficient for cytokinesis. J Cell Sci **114,** 3001-3012.

Wang, W., Wen, Y., Berkey, R., and Xiao, S. (2009). Specific targeting of the *Arabidopsis* resistance protein RPW8.2 to the interfacial membrane encasing the fungal Haustorium renders broad-spectrum resistance to powdery mildew. Plant Cell **21,** 2898-2913.

Xiao, K., Liu, J., Dewbre, G., Harrison, M., and Wang, Z.Y. (2006). Isolation and characterization of root-specific phosphate transporter promoters from *Medicago truncatula*. Plant Biol (Stuttg) **8,** 439-449.

Zhang, Q., Blaylock, L.A., and Harrison, M.J. (2010). Two *Medicago truncatula* Half-ABC Transporters Are Essential for Arbuscule Development in Arbuscular Mycorrhizal Symbiosis. Plant Cell **22,** 1483-1497.

.

CHAPTER 4

ANALYSIS OF PHT1 MEMBERS FROM *MEDICAGO TRUNCATULA* REVEALS A SECOND PERIARBUSCULAR MEMBRANE-LOCALIZED PROTEIN, MTPT8[3]

Abstract

To acquire the essential mineral nutrient phosphate (Pi), plants evolved multiple phosphate transporters and symbioses with arbuscular mycorrhizal (AM) fungi. Members of the PHT1 family of phosphate transporters have been shown to mediate Pi uptake into cells from the soil and AM fungi, and distribution between tissues. Six members of this gene family have been previously described in *Medicago truncatula* (*MtPT1-Mtpt6*). Here, *MtPT6* and three additional members of the PHT1 family (*MtPT7-MtPT9*) from *M. truncatula* are described and their expression patterns analyzed by RT-PCR, and transcriptional and translational gene reporter fusions. *MtPT6* and *MtPT9* are expressed predominantly in root vascular tissue and endodermis, and shoots. These results suggest *MtPT6* and *MtPT9* are involved in transporting Pi from the root cortex to the stele for eventual transport to aerial tissues. *MtPT7* transcripts were not detectable. *MtPT8* is expressed specifically during AM symbiosis and MtPT8-GFP localizes to the periarbuscular membrane. *MtPT8* likely acts in Pi uptake from AM fungi; however, analysis of an *mtpt8* knockout mutant did not reveal a requirement for the symbiosis. The presence of putative *MtPT8* orthologs in other plants suggests an early duplication within the dicot lineage.

[3] Generation of *mtpt8-1* populations, including genotyping and transcript analysis, was performed by Roslyn Noar. RN also assisted in preliminary transcript analysis of MtPT6,7,8 and 9. Identification of *mtpt8-1* was performed by Vagner Benedito and Michael Udvardi

Introduction

Phosphate is an essential macronutrient that plays a fundamental role in many structural and metabolic processes. Free inorganic orthophosphate (Pi) is the only form available to plants, and in most soils this form exists in low concentrations. Pi is readily sequestered by cations, such as iron and aluminum and incorporated into organic complexes by microbes, both of which contribute to immobilization of Pi in the soil (Schachtman et al., 1998). This chemical nature is also a major limitation on the efficiency of Pi fertilizer application in agriculture, particularly in acidic soils, as only a fraction of applied Pi will be taken up by crops (Vance et al., 2003). While available Pi concentrations in natural soils can range from 1-10 μM, cellular requirements are roughly 1,000-fold higher, in the millimolar range (Bieleski, 1973). To acquire sufficient levels of Pi, plants have evolved strategies to take up scarce Pi, distribute it throughout tissues, and respond to changes in availability.

Pi can be taken up directly from the soil through epidermal cells and root hairs. Due to the immobility of Pi in soil, uptake results in a depletion zone surrounding roots, and roots must continually explore new areas of soil to acquire Pi. Localized regions of low Pi levels can inhibit root growth (Desnos, 2008), while lateral root growth is stimulated where Pi is more abundant (Ticconi and Abel, 2004). In addition to direct uptake from the soil, plants have evolved an alternative mechanism to access and take up Pi indirectly through symbiosis with arbuscular mycorrhizal (AM) fungi. These fungi, obligate symbionts of the phylum Glomeromycota, require plant partners to provide carbon in order to complete their life cycle (Bucher, 2007; Parniske, 2008). Extensive hyphal networks produced by AM fungi greatly increase the area of soil that can be exploited for Pi uptake (Jakobsen et al., 1992). Once Pi is taken up into hyphae, it is transferred to plants through nutrient-exchanging fungal structures called arbuscules, which form within root cortical cells. Arbuscules are surrounded by the

plant periarbuscular membrane, a distinct membrane domain which is continuous with the plasma membrane and acts as a large area for nutrient exchange between symbionts (Bonfante and Perotto, 1995).

Phosphate is taken up from the soil and mycorrhizal fungi into plant cells primarily by plasma membrane-localized H^+:Pi symporters of the PHT1 family (Bucher et al., 2001). These proteins are conserved in plants and fungi, and represent a subgroup of the major facilitator superfamily, sharing a 12 transmembrane domain structure with two groups of six membrane domains separated by a large hydrophilic loop (Pao et al., 1998). PHT1 is a multi-gene family, with nine members in *Arabidopsis thaliana* and 13 in rice. In angiosperms, PHT1 genes are further divided into four subfamilies based on sequence similarity (Nagy et al., 2005). Subfamily I members, including *M. truncatula MtPT4*, potato *StPT4*, tomato *LePT4*, eggplant *SmPT4*, Nicotiana *NtPT4*, pepper *CfPT4*, maize *ZmPT6* and rice *OsPT11*, show specific or highly induced expression during the AM symbiosis (Harrison et al., 2002; Paszkowski et al., 2002; Glassop et al., 2005; Nagy et al., 2005; Nagy et al., 2006; Chen et al., 2007). MtPT4 and OsPT11 localize in the periarbuscular membrane, suggesting a conserved role for this subfamily in taking up Pi during the AM symbiosis (Harrison et al., 2002; Kobae and Hata, 2010). A duplication of this gene (e.g. *StPT4*) within the Solanaceae is also apparent, represented by subfamily I members *StPT5*, *LePT5*, *NtPT5*, *SmPT5* and *CfPT5*, which are also induced during AM symbiosis (Nagy et al., 2005; Chen et al., 2007).

The remaining subfamilies, III from dicots, IV from monocots, and subfamily II which includes *AtPht1;8* and *1;9* and *OsPht1;9* and *OsPht1;10*, are expressed in a variety of tissues, with the majority expressed in roots under phosphate starvation conditions (Chiou et al., 2001; Mudge et al., 2002; Paszkowski et al., 2002; Liu et al., 2008; Ai et al., 2009). Expression of some phosphate transporters was also observed

in aerial tissues, suggesting a role for PHT1 genes in Pi distribution between tissues (Mudge et al., 2002; Rae et al., 2003; Ai et al., 2009). Interestingly, a few members of subfamily III, including potato *StPT3* and *Lotus japonicus LjPT3*, are highly-induced in cells harboring arbuscules in a pattern similar to that of subfamily I members (Rausch et al., 2001; Maeda et al., 2006).

In roots, the tissue localization of many PHT1 subfamily III and IV genes has been studied by promoter reporter fusions. These experiments have revealed expression patterns ranging from predominantly epidermal and cortical (*AtPht1;1*, *1;2* and *1;4*, *OsPht1;6*) to predominantly vascular (*AtPh1;3*, *OsPT2*, *HORvu;Pht1;6*) (Maeda et al., 2006; Ai et al., 2009). PHT1 genes expressed in the epidermis and outer cortex likely mediate Pi uptake from the soil, while it is hypothesized that members expressed in the vascular tissue play a role in loading Pi into the xylem for transport to shoot tissues (Mudge et al., 2002; Ai et al., 2009).

In *M. truncatula*, six PHT1 genes have been characterized to date including four closely-related phosphate transporters, *MtPT1*, *2*, *3* and *5* (*MEDtr;Pht1;1*, *2*, *3*, and *5*), which likely arose from recent gene duplication, *MtPT6* (*MEDtr;Pht1;6*), and the AM symbiosis-specific *MtPT4* (*MEDtr;Pht1;4*) (Liu et al., 1998; Harrison et al., 2002; Liu et al., 2008; Grunwald et al., 2009). Expression analyses and transcriptional reporter fusions have revealed unique expression patterns for each gene as follows: *MtPT1* and *MtPT2* are expressed only in roots, and *MtPT1* expression was localized to the epidermis and cortex while *MtPT2* is expressed in the epidermis, cortex and vascular tissue (Liu et al., 1998; Chiou et al., 2001; Xiao et al., 2006). *MtPT3* is expressed in root vascular tissue, and *MtPT5* is expressed in the root epidermis and cortex (Liu et al., 2008). *MtPT3* and *MtPT5* transcripts are also found in the shoots, but the tissue specificity of expression is unknown. *MtPT1*, *2*, *3* and *5* are most strongly expressed in Pi limiting conditions and downregulated by high Pi. *MtPT1*, *2*

and *3* are downregulated during the course of AM symbiosis while expression of *MtPT5*, a high-affinity transporter, is unaffected (Chiou et al., 2001; Liu et al., 2008). *MtPT6* expression was described as unaffected by growth in different Pi conditions but repressed during the course of AM symbiosis, while the tissue localization has not been shown (Grunwald et al., 2009). *MtPT4* expression, in contrast, is specific to mycorrhizal roots and restricted to cortical cells harboring arbuscules (Harrison et al., 2002).

Biochemical characterization of PHT1 proteins in heterologous systems has revealed a range of affinities for Pi (Leggewie et al., 1997; Mitsukawa et al., 1997; Daram et al., 1998; Liu et al., 1998; Rae et al., 2003). For *M. truncatula* PHT1 proteins, Pi uptake kinetics determined by analyses in complemented yeast mutants revealed Km values ranging from 13 μM for MtPT5, to 668 μM for MtPT4 (Harrison et al., 2002; Liu et al., 2008). Mutagenesis or RNAi knockdown studies of some AM symbiosis-induced PHT1 transporters has revealed a role for these genes in symbiotic Pi transport and subsequent effects on regulation of the symbiosis. RNAi-inducedsilencing of the AM symbiosis-induced *LjPT3* reduced arbuscule formation and growth benefit due to the symbiosis (Maeda et al., 2006), and mutation of *MtPT4* resulted in a complete loss of growth benefit from the symbiosis and an early death of arbuscules (Javot et al., 2007b). A loss-of-function tomato *LePT4* allele caused only a moderate loss of growth benefit from the symbiosis, a phenotype likely dampened by the existence of *LePT5*, a recent paralogous duplication of this gene (Xu et al., 2007).

Here, we report the expression patterns of additional members of the PHT1 family in *M. truncatula*, including members of subfamily I, II and III. We show that *MtPT8* is specifically expressed during AM symbiosis in cells with arbuscules and that the protein localizes in the periarbuscular membrane. Functional analysis of this gene

in *M. truncatula* suggests it likely plays a minor role in the symbiosis relative to MtPT4.

Results

PHT1 family members in the Medicago truncatula genome

To determine the full extent of PHT1 gene family in *Medicago truncatula*, *in silico* searches were carried out for genes with sequence similarity to known phosphate transporters in the Mt3.0 genome release (www.medicago.org). This search revealed a total of nine genes, which is similar to the size of PHT1 families in Arabidopsis (nine members) and rice (13 members). Six of the genes identified have been described previously as *MtPT1* through *MtPT6* (Liu et al., 1998; Chiou et al., 2001; Harrison et al., 2002; Xiao et al., 2006; Liu et al., 2008; Grunwald et al., 2009). The three additional genes were named MtPT7, MtPT8 and MtPT9 (official nomenclature *MEDtr;Pht1;7*, *MEDtr;Pht1;8*, and *MEDtr;Pht1;9*).

To assign these genes into the correct subfamilies, a phylogenetic tree was constructed using full length deduced amino acid sequences of previously-described PHT1 genes. This analysis included the nine *M. truncatula* phosphate transporters and additional homologous sequences, including all nine Arabidopsis, 13 rice and additional representative sequences from monocots and dicots, and two fungal PHT1 genes for reference (Fig. 4-1). Searches of available databases yielded unpublished gene sequences from additional species with ongoing sequencing efforts, and these were useful as markers for assigning gene subfamilies. This analysis showed these new *M. truncatula* PHT1 members fall into subfamilies I, II, and III.

MtPT6 and *7* are included in subfamily III. This subfamily contains *MtPT1*, *2*, *3*, and *5* and the majority of other dicot PHT1 genes that have been studied in the context of epidermal phosphate transport at the root-soil interface, such as *AtPht1;1*,

AtPht1;4, *StPT1* and *StPT2* (Leggewie et al., 1997; Shin et al., 2004). This group appears to be a monophyletic sister group to the monocot-specific subfamily IV, which includes *OsPht1;2* and *OsPht1;6* (Ai et al., 2009), suggesting that these families may have arisen from a single gene in ancient angiosperms. *MtPT1*, *MtPT2*, and *MtPT3* are closely-related in sequence and located in the same region of chromosome 1, suggesting they likely arose from recent gene duplication (Liu et al., 2008); *MtPT7* is located within 5 kb of *MtPT5* on chromosome 1; however, *MtPT5* is more closely related in sequence to *MtPT1-3* and *LjPT1* than to *MtPT7*. *MtPT6* is located on chromosome 3 and is most closely related to *LjPT3* from *Lotus japonicus*, which is highly induced during AM symbiosis (Maeda et al., 2006). Subfamily III also includes genes from Solanaceous species which are highly induced during symbiosis with AM fungi, such as *StPT3* (Rausch et al., 2001). *MtPT6* differs in gene structure from other subfamily III genes in *M. truncatula*. *MtPT1*, *2*, *3*, and *5* all have introns within the 5' UTR, *MtPT6* has an intron in its coding sequence.

MtPT8 is clustered in subfamily I along with *MtPT4*. All genes analyzed to date from this group are expressed specifically or high-induced during AM symbiosis (Chen et al., 2007; Javot et al., 2007a). While a duplication of these genes has been reported in the Solanaceae (e.g. *StPT4* and *5*, *CfPT4* and *5* (Nagy et al., 2005; Chen et al., 2007), it is apparently a recent duplication within that family (Fig. 4-1). Putative orthologs of *MtPT8* were found in the genomes of poplar, grape, castor bean and soybean, but not in any monocots, suggesting this gene likely arose from a more ancient dicot-specific subfamily I duplication. *MtPT8* lacks introns, in contrast to *MtPT4*, which has an intron in its coding sequence.

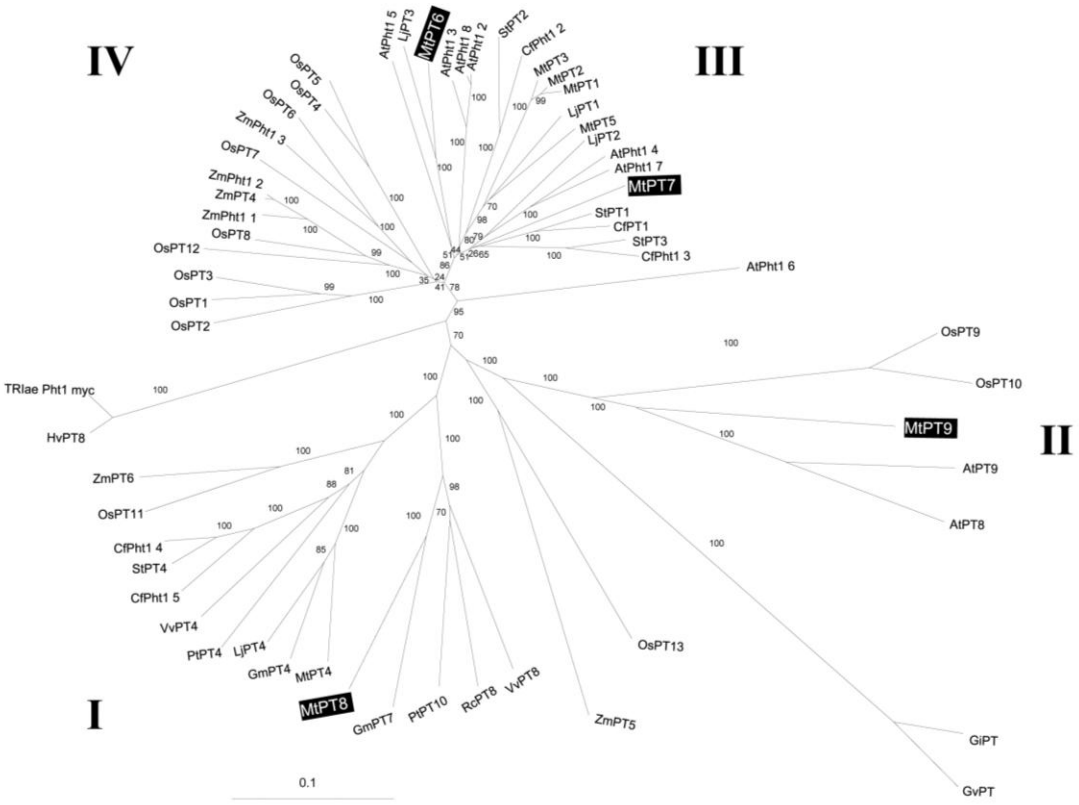

Figure 4-1: Unrooted phylogenetic tree of PHT1 proteins.
Neighbor-joining phylogram was constructed using full-length deduced amino acid sequences of *Medicago truncatula MtPT1-MtPT9*, the full complement of Arabidopsis (At) and rice (Os) PHT1 genes, and representative homologs from additional species for reference: *Populus trichocarpa* (Pt), *Vitis vinifera* (Vv), *Glycine max* (Gm), *Solanum tuberosum* (St), *Ricinus communis* (Rc), *Oryza sativa* (Os), *Zea mays* (Zm), *Capsicum frutescens* (Cf), *Triticum aestivum* (TRIae), *Hordeum vulgare* (Hv), *Lotus japonicus* (Lj), *Glomus versiforme* (Gv), and *Glomus intraradices* (Gi). Subfamily I, II, III and IV are marked. Accession numbers are listed in Table 4-1. The phylogram was constructed in TREEVIEW (http://taxonomy.zoology.gla.ac.uk/rod/treeview.html), and bootstraps reflect values from 100 trials. Scale bar: 0.1 substitutions per site.

MtPT9 is a member of subfamily II that includes Arabidopsis *AtPht1;8* and *1;9*, and *OsPht1;9* and *1;10*. This subfamily displays the highest sequence divergence from the rest of plant PHT1 genes and the role these genes play in Pi transport within plants is not well characterized. *MtPT9* has a large intron in its coding sequence, similar to *AtPht1;8* and *1;9* (Bari et al., 2006).

Expression of MtPT6 and 9 is Pi regulated, while MtPT8 is AM symbiosis specific

Genes in the PHT1 family show alterations in expression in response to changes in available phosphate and colonization by AM fungi. To study the expression patterns of *MtPT6*, *7*, *8* and *9*, we designed primers for each gene suitable for RT-PCR. Specificity of each primer pair was confirmed by the inability to amplify vector template containing non-target PHT1 genes from *M. truncatula*.

MtPT6 and *MtPT9* transcripts were detected in shoots and roots of *M. truncatula* plants grown under phosphate-limiting conditions by RT-PCR (Fig. 4-2a). In an experiment where these Pi-starved plants were resupplied with high levels (1mM) of phosphate for 24 or 54 hours (Liu et al., 2008), *MtPT6* transcript levels decreased in the roots but remained unaltered in the shoots. *MtPT9* transcript levels decreased strongly in roots and shoots in response to Pi resupply; however, transcript in roots remained detectable. *MtPT3* by comparison, showed a similar downregulation in roots to *MtPT6*, while *MtPT5* transcript abundance diminished little over the course of the experiment (Liu et al., 2008). *MtPT7* and *MtPT8* transcripts were not detected in these samples under any conditions.

Similar RT-PCR analysis was performed on *M. truncatula* roots inoculated with AM fungi or a control roots. Roots were harvested one to four weeks after inoculation as described in Liu et al (2008), and MtPT4 transcript detection in these samples confirms progression of the symbiosis (Fig. 4-2b). *MtPT6* and *MtPT9*

expression was mostly constant over the course of the experiment, with a slight downregulation of *MtPT9* evident by the fourth week of colonization. In contrast, *MtPT1*, *MtPT2* and *MtPT3* were downregulated during the course of colonization (Liu et al., 1998; Liu et al., 2008). These results are consistent with an Affymetrix array/gene atlas (Fig. 4-3), which shows a small reduction in *MtPT6* and *9* transcripts in mycorrhizal roots relative to control roots, but a more significant reduction in *MtPT1/2/3* transcript levels (Fig. 4-3). *MtPT8* transcripts were detected in mycorrhizal roots by two weeks post inoculation but not in control samples, and transcript levels were significantly lower than *MtPT4* (Fig. 4-2b). *MtPT7* transcripts were not detected in any of the samples tested, including flowers, suggesting that *MtPT7* may be a pseudogene (Fig. 4-2c).

MtPT6 and MtPT9 are expressed in the root vascular tissue and endodermis

Previously described PHT1 genes display tissue-specific expression patterns, suggestive of their specific roles in Pi uptake and/or homeostasis. To determine the tissue specificity of *MtPT6* and *MtPT9*, 1,937 and 1,928 bp of genomic sequence upstream of *MtPT6* and *MtPT9*, respectively, was fused to the *UidA* gene and transformed into *M. truncatula* roots using *Agrobacterium rhizogenes* according to (Boisson-Dernier et al., 2001). Following three to four weeks of growth in phosphate limiting conditions, β-glucuronidase (GUS) staining revealed expression of *pMtPT6:UidA* and *pMtPT9:UidA* in the vascular tissue and endodermis (Fig. 4-4a and b). Occasional expression of *pMtPT9:UidA* in the epidermis was also observed. Expression was absent from root tips, but became apparent within 200 μm from the tip, revealing these genes are expressed early during vascular tissue differentiation. This result is consistent with the gene atlas (Fig. 4-3), showing higher expression 1 cm

from the root tip than 3 mm from the tip, and suggests a role in transport of phosphate into the stele for distribution to aerial tissues.

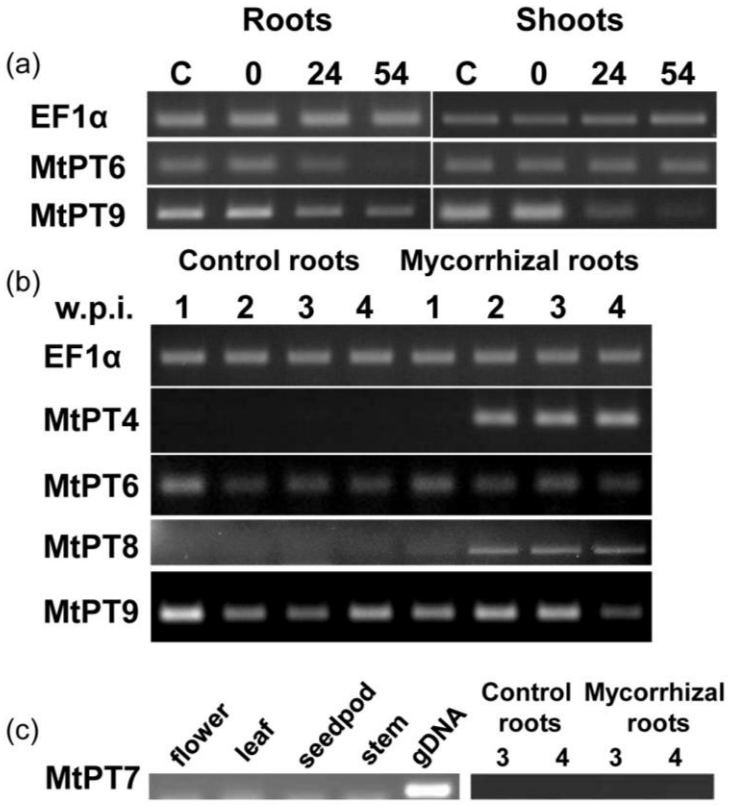

Figure 4-2: Regulation of MtPT6, 8, and 9 by Pi status (a) and AM symbiosis (b). RT-PCR performed on cDNA synthesized from RNA extracted from *M. truncatula* roots and shoots grown under Pi starvation conditions, C, and resupplied with 1mM Pi for 0, 24 or 54 hours (a). RT-PCR performed on cDNA derived from plants inoculated with the AM fungus *Glomus versiforme* or mock-inoculated controls, and harvested 1, 2, 3 and 4 weeks post inoculation (w.p.i.) (b). (c) 45 cycles of RT-PCR using MtPT7 primers performed on cDNA derived from flowers, leaves, seedpods, stems and 3 and 4 w.p.i. with *G. versiforme* or mock-inoculated controls and with genomic DNA (gDNA) included as a positive control. Elongation factor 1α (EF1α) is used as a constitutive marker to assess loading and amplified 30 cycles. MtPT4, MtPT6 and MtPT9 were amplified 35 cycles except MtPT8, which required 40 cycles for detection.

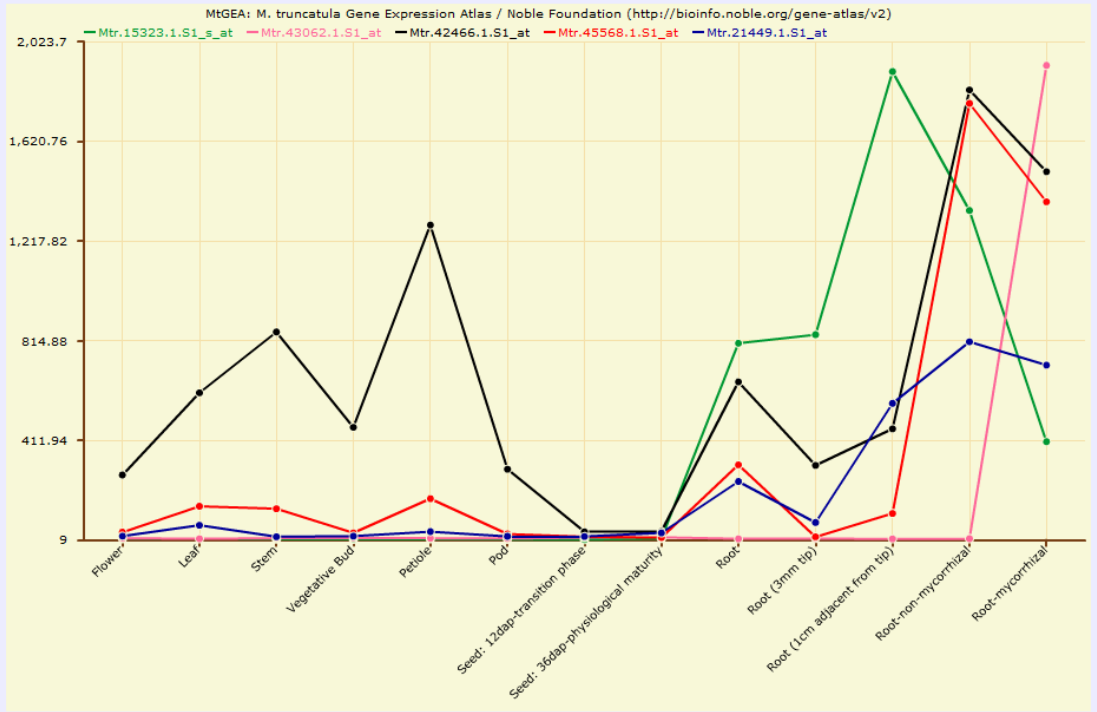

Figure 4-3: Expression of phosphate transporters assessed in the *M. truncatula* gene atlas.

Probesets are available on the *M. truncatula* 16K Affymetrix array for : MtPT1/2/3, Mtr.15323.1.S1_s_at (green); MtPT4, Mtr.43062.1.S1_at (pink); MtPT5, Mtr.42466.1.S1_at (black); MtPT6, Mtr.45568.1.S1_at (red); MtPT9, Mtr.21449.1.S1_at (blue). Expression of phosphate transporters after colonization by the AM fungus *G. intraradices* is shown in the last data point. Gene atlas is available online (http://mtgea.noble.org/v2/) (Benedito et al., 2008).

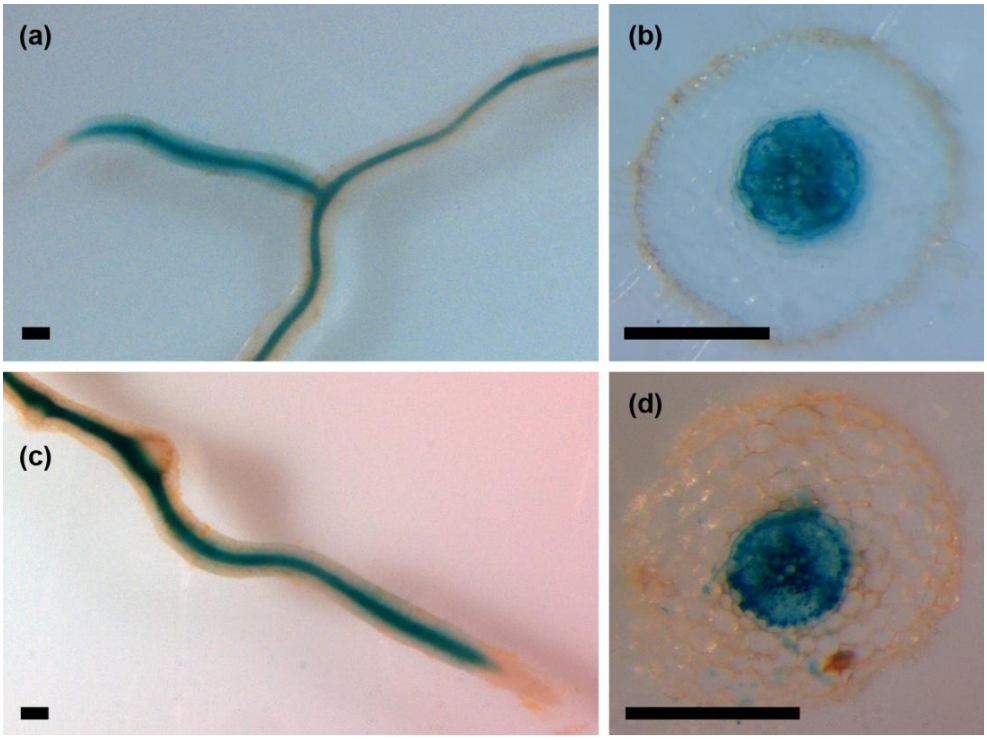

Figure 4-4: Expression of *MtPT6* and *MtPT9* promoter-Gus fusions in the vascular tissue of *M. truncatula* roots.
Histochemical staining for GUS activity in transgenic roots expressing UidA reporter fusions to the promoter of MtPT6 (a, b) and MtPT9 (c, d). Predominant activity of both promoters is in the vascular tissue and endodermis, not in root cap or lateral root primordial. Bar = 100 µm.

MtPT8 is expressed in cortical cells harboring arbuscules and the protein localizes on the periarbuscular membrane

Translational fusions of the AM-specific subfamily I members *MtPT4* and *OsPT11* have been used to reveal expression patterns and subcellular localization of the protein product (Harrison et al., 2002; Pumplin and Harrison, 2009; Kobae and Hata, 2010). To determine whether MtPT8 also exhibits periarbuscular membrane-specific localization, a translational reporter was created by fusing the coding sequence and 1139 bp of genomic sequence upstream of the ATG start codon to the 5' end of green fluorescent protein (GFP) creating *pMtPT8:MtPT8-GFP*. This construct was transformed into *M. truncatula* roots. Following colonization by the AM fungus *Glomus versiforme*, GFP fluorescence was observed only in the root cortex coincident with AM fungal infections, a pattern similar to roots expressing *pMtPT4:MtPT4-GFP* (Pumplin and Harrison, 2009). Root segments expressing *pMtPT8:MtPT8-GFP* were excised, bisected longitudinally and observed by confocal microscopy. This analysis showed MtPT8-GFP accumulation only in cells with arbuscules (Fig. 4-5a) and localization in the periarbuscular membrane and not the plasma membrane (Fig. 4-5b). This suggests that MtPT8 plays a role in Pi acquisition from AM fungi in a similar manner to MtPT4.

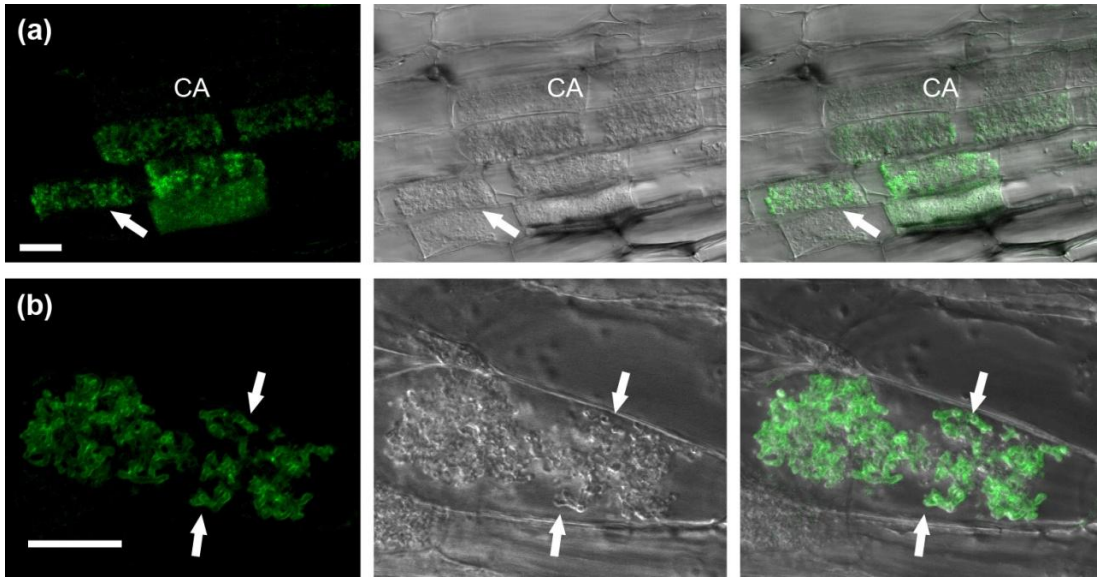

Figure 4-5: *MtPT8* is expressed in cells with arbuscules and MtPT8 localizes to the periarbuscular membrane.
Left panel, GFP fluorescence; middle panel, bright field differential interference contrast; right panel, overlay. (a) GFP signal from *pMtPT8:MtPT8-GFP* is observed only in cells with arbuscules (arrow). Signal is week or absent in cells with collapsed arbuscules (CA). (b) A single cortical cell harboring an arbuscule displays MtPT8-GFP signal in the branch domain of the periarbuscular membrane. (a) 7 1.22 µm optical sections, (b) 7 0.35 µm optical sections. Bars = 20 µm

Loss of MtPT8 function does not disrupt the AM symbiosis

In *MtPT4* loss-of-function mutants the benefit from AM symbiosis in increased accumulation of shoot mass and Pi levels is lost. Inoculated *mtpt4* mutant plants are thus indistinguishable in growth from uninoculated wild type plants. In *mtpt4* mutant plants, the AM fungus displays an early arbuscule death phenotype, which is identified by abundant collapsed arbuscules and a reduction in mature arbuscules (Javot et al., 2007b). To test whether *MtPT8* might serve a required function for the AM symbiosis as is the case for *MtPT4*, a *M. truncatula* line harboring a Tnt1 transposon in the *MtPT8* coding sequence was identified. The 5.3 kb transposon was inserted 657 nucleotides downstream of the ATG (Fig. 4-6a and b) (Tadege et al., 2008). *mtpt8-1* plants homozygous for the MtPT8 insertion showed a similar benefit from the AM symbiosis as wild type R108 plants, with an increase in shoot mass (Fig. 4-6d) and shoot phosphate content (Fig. 4-6e). Arbuscule morphology in mutant roots was similar to that of wild type plants, illustrating that loss of *MtPT8* does not lead to premature arbuscule death, as observed in *mtpt4* mutants (Fig. 4-6f and g). Expression of *MtPT4* was detected in *mtpt8-1* mutant roots (Fig. 4-6c), indicating that this mutation does not impair colonization.

Figure 4-6: A *M. truncatula* line with an insertion in MtPT8 shows a wild type AM symbiosis.

mtpt8-1 harbors a Tnt1 transposon insertion 657 nucleotides downstream of the ATG (a). This is predicted to truncate the protein at the sixth transmembrane domain. Primers used for genotyping and expression analysis are indicated with arrows. Plants from a population segregating for the insertion allele were genotyped with these primers in the transposon sequence and MtPT8 sequence, or spanning the insertion. Line #5 is homozygous for the wild type allele, lines #2 and #8 are homozygous for the *mtpt8-1* allele (b). Lines #2, 5 and 8 and the wild type parent R108 inoculated with the AM fungus *Glomus versiforme* were used for transcript analysis (c). EF1α was used as a constitutive control. MtPT8 primers spanning the insertion only detected transcript from R108 and line #5, while all samples displayed expression of fungal α-tubulin and MtPT4. Shoot mass (d) and shoot phosphate levels (e) from R108 and lines #2, 5 and 8 inoculated with the AM fungus *Glomus intraradices* (black bars) or a mock-inoculated (grey bars) at seven weeks post inoculation. Graphs display the average of three replicate pots each containing four plants. Error bars represent standard error. Arbuscule morphology was similar in the roots of wild type R108 (f) and *mtpt8-1* (g), as visualized by a chitin fungal wall stain, wheatgerm agglutinin conjugated to AlexaFluor488. Bars = 50 μm

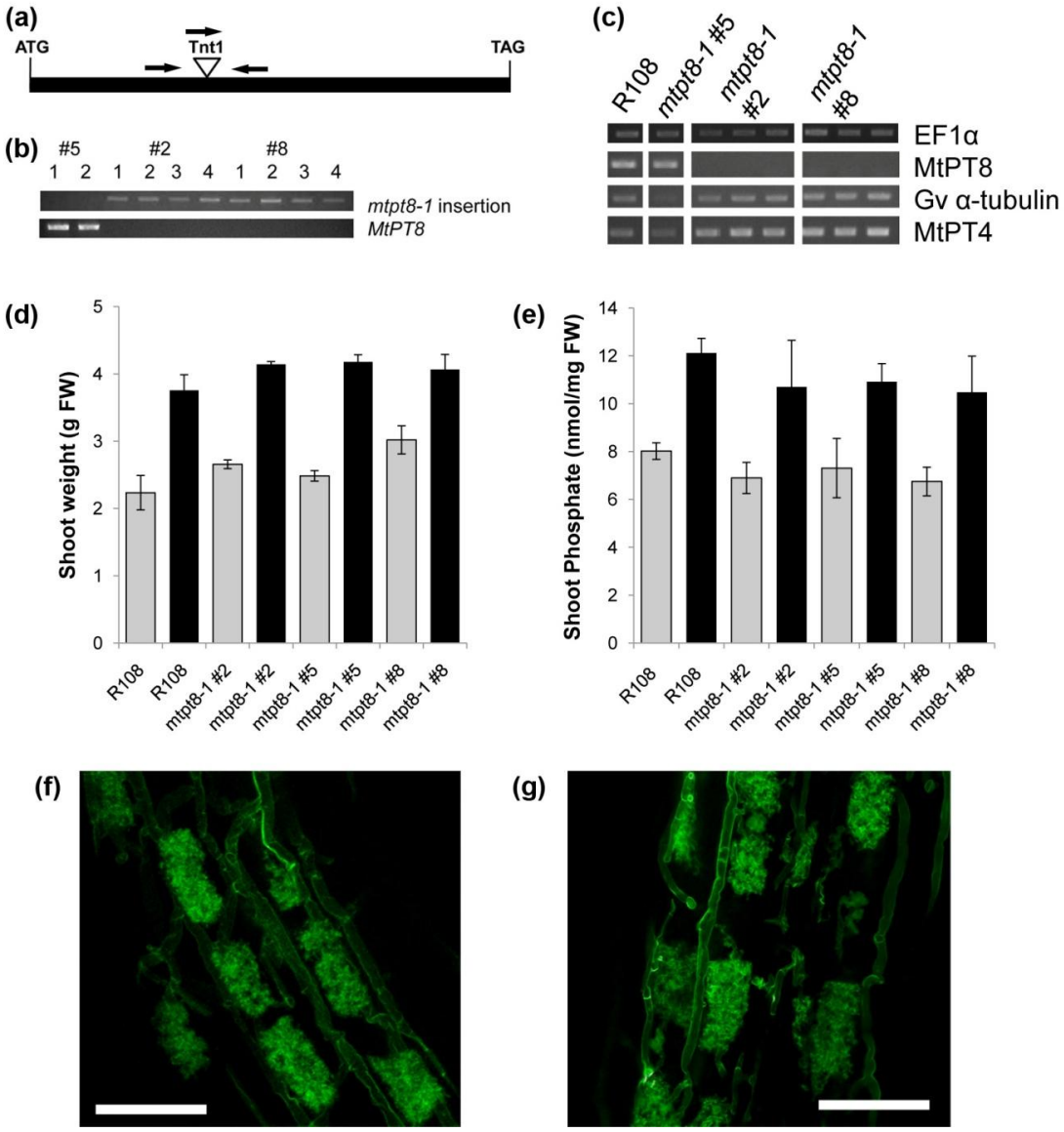
(a)
ATG
Tnt1
TAG
(b)
#5
#2
#8
1 2 1 2 3 4 1 2 3 4
mtpt8-1 insertion
MtPT8
(c)
R108
mtpt8-1 #5
mtpt8-1 #2
mtpt8-1 #8
EF1α
MtPT8
Gv α-tubulin
MtPT4
(d)
Shoot weight (g FW)
0
1
2
3
4
5
R108
R108
mtpt8-1 #2
mtpt8-1 #2
mtpt8-1 #5
mtpt8-1 #5
mtpt8-1 #8
mtpt8-1 #8
(e)
Shoot Phosphate (nmol/mg FW)
0
2
4
6
8
10
12
14
R108
R108
mtpt8-1 #2
mtpt8-1 #2
mtpt8-1 #5
mtpt8-1 #5
mtpt8-1 #8
mtpt8-1 #8
(f)
(g)

Discussion

A complete understanding of the molecular mechanisms by which plants regulate Pi uptake, translocation and homeostasis will require an in-depth understanding of the roles played by many genes, including PHT1 transporters. *M. truncatula* is a useful model system for studying phosphate acquisition and distribution because it acquires Pi from the soil and also indirectly through AM symbiosis. Discovery of PHT1 genes in the nearly-complete *M. truncatula* genome enables more complete studies of Pi uptake and homeostasis during both symbiotic and non-symbiotic growth and enables studies of the contribution of individual genes.

In *M. truncatula*, MtPT4 is specifically involved in Pi acquisition from arbuscules and loss of *MtPT4* function abolishes symbiotic Pi uptake (Javot et al., 2007b). *MtPT8* is also specifically expressed during the AM symbiosis and the protein localizes on the periarbuscular membrane (Fig. 4-2 and 4-5). However, AM symbiosis was not disrupted in *mtpt8* mutant plants, suggesting that *MtPT8* function is not a requirement under our experimental conditions. While these data do not show a significant function for *MtPT8*, homologs of *MtPT8* are present in other dicots (Fig. 4-1), suggesting that this gene serves a function that has been conserved through evolution. It is possible that this gene provides a subtle but significant benefit during the symbiosis, sufficient to be maintained but not observable in our experiments. Alternatively it may serve a more important function during symbiosis with other AM fungi or under different environmental conditions. Based on phylogeny, *MtPT8* probably arose early in dicot evolution. This is in contrast to the duplication of the *PT4* group in the Solanaceae (e.g. *StPT4* and *StPT5*), which appears to be more recent and the duplicated genes are functionally redundant (Nagy et al., 2005; Xu et al., 2007).

Subfamily III genes have also been shown to play important roles in AM symbiosis (Rausch et al., 2001; Maeda et al., 2006). In *L. japonicus*, *LjPT3* is strongly induced in cells with arbuscules and RNAi-induced silencing decreases AM symbiosis (Maeda et al., 2006). *MtPT6* shares the highest sequence similarity with *LjPT3*, however *MtPT6* is expressed in the endodermis and vascular tissue, and not induced by AM symbiosis (Fig. 4-1, 4-2, 4-3). In *M. truncatula*, no subfamily III members showed induction during AM symbiosis. This difference suggests that in some plants, subfamily III genes have acquired promoter elements that lead to induction in cortical cells with arbuscules, and likely add benefit during the symbiosis through increased Pi uptake. The phenotype described for *LjPT3* RNAi roots is milder than the MtPT4 silencing or loss-of-function phenotype in *M. truncatula* (Maeda et al., 2006; Javot et al., 2007b). Based on the sequence conservation of subfamily I genes in angiosperms, it is likely that these genes evolved a unique function in regulating the AM symbiosis.

Expression of *MtPT6* and *MtPT9* in the endodermis and stele suggests that these two transporters may participate in Pi transport into the vascular tissue for eventual transport to aerial tissues, as inferred for other vascular-expressed PHT1 genes (Rae et al., 2003; Ai et al., 2009). *MtPT2* is the only other PHT1 gene in *M. truncatula* expressed in the endodermis, while *MtPT3* expression appears restricted to the stele but not the endodermis (Liu et al., 2008). The mechanisms underlying Pi transport into the vascular tissue are not known; however, RNAi-induced silencing of the vascular-expressed *OsPht1;2* from rice resulted in a decreased accumulation of Pi in shoots (Ai et al., 2009). The exact role that PHT1 genes play in vascular transport has not been defined; however, another unrelated gene family represented by *AtPho1* in Arabidopsis is implicated in xylem loading of Pi (Hamburger et al., 2002). *AtPho1* is expressed in the vascular tissue, and loss-of-function *atpho1* mutant plants show Pi deficiency in shoots, but Pi overaccumulation in roots (Hamburger et al., 2002). In

Arabidopsis, members of this family are expressed throughout the plant, and it is hypothesized they may function in Pi efflux from xylem stelar cells (Hamburger et al., 2002). If these proteins function in Pi efflux, the interaction with *PHT1*-mediated influx may provide insights into Pi distribution in the vascular tissue.

We observed that *MtPT6* and *MtPT9* transcript levels remained constant in mycorrhizal roots, while *MtPT2* and *MtPT3*, the two other phosphate transporters expressed in the vascular tissue, were previously reported as downregulated (Fig. 4-2 and 4-3) (Liu et al., 1998; Liu et al., 2008). It is well documented that during AM symbiosis, phosphate transporters implicated in Pi uptake from the soil are downregulated, as plants shift Pi acquisition to the symbiotic interface in the cortex (Javot et al., 2007a). Transport of Pi in the vascular tissue, in contrast, should be equally important regardless of the original source of Pi uptake. Expression of *MtPT6* and *MtPT9* during the AM symbiosis is further consistent with a role for these genes in Pi loading into cells of the vascular tissue for aerial transport. While *MtPT6* was previously reported to be downregulated in roots colonized by *G. intraradices* (Grunwald et al., 2009), our data disagree with this result (Fig. 4-2 and 4-3). The difference may lie in the conditions used for plant growth, as our plants were fertilized with a solution containing a much lower Pi concentration than those of Grunwald *et al.* (20 μM versus 130 μM).

MtPT9 is a member of subfamily II, which includes *AtPht1;8* and *9* and *OsPT9* and *10*. Interestingly, transcriptional reporter fusions to the promoters of *AtPht1;8* and *9* failed to show expression in Arabidopsis (Mudge et al., 2002), and prior to the current study, the tissue-specific expression pattern had not been shown for any members of this subfamily. Transcript analysis of these *PHT1* genes in Arabidopsis and rice did show expression in roots and repression in high Pi conditions (Mudge et

al., 2002). In contrast to *AtPht1;8* and *9*, which are expressed only in roots, *MtPT9* is also expressed in aerial tissues.

In Arabidopsis, *AtPht1;8* and *9* are repressed in high Pi conditions by the *PHO2* E2 ubiquitin conjugase. Under Pi limiting conditions, *PHO2* is post-transcriptionally repressed by a shoot-generated microRNA *miR399*, leading to transcript accumulation of the subfamily II members. In *pho2* mutant plants or *miR399* overexpressing plants, *AtPht1;8* and *9* are expressed in Pi sufficient conditions, resulting in overaccumulation of Pi in the shoots (Aung et al., 2006; Bari et al., 2006; Liu et al., 2010). If this family plays a conserved role in Pi loading into the xylem, as suggested by vascular expression of *MtPT9*, the induction by *miR399*-mediated de-repression could provide a rapid increase in aerial Pi transport. Recently, overexpression of endogenous *miR399* in *M. truncatula* has revealed a similar Pi overaccumulation phenotype, and *miR399* also directs post-transcriptional cleavage of *M. truncatula Pho2* (Branscheid et al., 2010). Dissection of the miR399 pathway may lead to new insights in the regulation of phosphate homeostasis.

Characterization of the complete suite of PHT1 members from additional plants and dissection of the specific protein function of subfamily I members in regulating the AM symbiosis will help to address how plants regulate direct and indirect Pi uptake and possibly lead to genetic strategies for more efficient utilization of phosphate resources.

Materials and Methods

Plant Growth Conditions and Transformation

All experiments utilized *M. truncatula* cv. Jemalong, line A17, except for analysis of the *mtpt8-1* Tnt1 insertional mutant, which was generated in the R108-1 background (Tadege et al., 2008).

Transgenic composite root systems were created by *Agrobacterium rhizogenes*-mediated root transformation as detailed in Boisson-Dernier *et al*. (2001). Briefly, following surface-sterilization and germination of seeds, root tips were cut and inoculated with *A. rhizogenes* strain ARqua1 containing the construct of interest. Seedlings were grown on modified Fahraeus media containing 25 mg/L kanamycin for selection of transgenic roots for three weeks, then transplanted to sterilized turface, four to five plants per 5 inch diameter pot. Inoculation with surface-sterilized AM fungal spores was performed ten days after transplanting. All plants were grown in growth chambers under 16 hour light (25 °C)/8 hour (22 °C) dark regime and fertilized once a week with ½-strength Hoagland's solution with normal-strength nitrogen and 20 μM potassium phosphate. Analysis of mycorrhizal and non-mycorrhizal plants was made three to five weeks after inoculation or four to six weeks after transplanting. Plant material produced for the Pi resupply experiment and AM fungal colonization time course has been previously reported. Briefly, for Pi resupply, *M. truncatula* A17 plants were grown aeroponically in 0.5x Hoagland's solution containing 1 μM potassium phosphate for 28 days and solution was changed weekly. At 29 days, solution was replaced with original low Pi Hoagland's solution supplemented with 1 mM potassium sulfate (control) or a new 0.5x Hoagland's containing 1 mM potassium phosphate (Pi resupply). Root and shoot tissues were then harvested 0, 24 and 54 hours after replacing nutrient solutions (Liu et al., 2008). AM fungal colonized and control material was grown as described above and inoculated with 5,000 spores or

mock-inoculated with a solution consisting of a final spore rinse. Plants were harvested 8, 15, 22 and 31 days after inoculation, and colonization levels were measured as 8.7, 11, 39, and 55% of root length, respectively (Liu et al., 2003).

The MtPT8 transposon insertion mutant (*mtpt8-1*) was isolated from a population reported by Tadege *et al.* (2008) and available at http://bioinfo4.noble.org/mutant/. Shoot mass and total phosphate was analyzed in F3 progeny from F2 plants homozygous for the MtPT8 insertion allele (#2 and #8) or homozygous for the wild type allele (#5) and the R108 wild type six weeks after inoculation with *Glomus intraradices* or mock inoculation. Phosphate analysis was performed according to Ames (1966).

Isolation of Phosphate Transporter Sequences and Vector Construction

BLAST searches in the *M. truncatula* genome assembly (www.medicago.org/genome) using different PHT1 members as queries uncovered MtPT6-MtPT9 as then previously unreported genes. MtPT6 was found on BAC CT030180 from chromosome 3, MtPT7 is contained in the same BAC as MtPT5, AC152186, on chromosome 1, MtPT8 is on BAC CT571262 on chromosome 5 and MtPT9 is on BAC AC149576 on chromosome 4.

The full mRNA sequence of MtPT8 was determined by sequencing from nested RACE PCR on cDNA created by SMART cDNA synthesis (Clontech) using RNA extracted from *G. versiforme*-colonized *M. truncatula* roots. The MtPT8 transcript includes the predicted open reading frame, 53 nucleotides of 5' UTR and 181 nucleotides of 3' UTR.

UidA reporter fusions were created in a modified version of the pCAMBIA2301 vector. The *UidA* coding sequence was amplified by PCR with a forward primer adding either a 5' *PstI* or 5' *HindIII* restriction site, and a reverse

primer that included an endogenous *BstEII* site. The pCAMBIA2301 vector was digested with *BstEII* and either *PstI* or *HindIII*, releasing 35S:*UidA,* and the amplified fragment containing *UidA*, but no promoter was ligated in its place. An MtPT6 genomic fragment including 1,937 nucleotides upstream of the ATG was amplified from A17 genomic DNA with primers introducing 5' *SalI* and 3' *HindIII* restriction sites and cloned into this modified 5' *HindIII*:*UidA* vector creating *pMtPT6:UidA*. An MtPT9 genomic fragment including 1928 nucleotides upstream of the ATG was amplified with primers adding 5' *XbaI* and 3' *HindIII* sites and cloned into the same vector to create *pMtPT9:UidA*. A genomic fragment encompassing 1139 nucleotides upstream of the MtPT8 ATG was amplified with primers adding 5' *BamHI* and 3' *PstI* restriction sites and cloned into the modified 5' *PstI*:*UidA* vector creating *pMtPT8:UidA*.

The *pMtPT8:MtPT8-GFP* translational fusion vector was constructed in the background of a modified pCAMBIA2301 vector containing the S65T GFP variant (Chiu et al., 1996) in the multiple cloning site under control of the CaMV 35S promoter and NOS terminator. A 2,810 bp genomic fragment was amplified from *M. truncatula* A17 DNA corresponding to 1,139 bp of sequence upstream of the MtPT8 ATG and the predicted ORF, excluding the stop codon, with primers that add flanking *BamHI* restriction enzyme sites. The modified pCAMBIA2301 GFP vector was digested with *BamHI*, which released the 35S promoter. *BamHI* digestion of the amplified MtPT8 genomic fragment and ligation into the prepared vector resulted in an in-frame fusion of the 3' of MtPT8 to the 5' ATG of GFP.

All vectors were sequenced to confirm correct insertions and the absence of introduced mutations.

Phylogram construction

Full length deduced amino acid sequences of representative PHT1 family members from plants, and the fungal GiPT and GvPT, were aligned using Clustal multiple sequence alignment (www.clustal.org). Neighbor-joining alignment produced a phylogram, constructed in TreeView (taxonomy.zoology.gla.ac.uk/rod/treeview.html) with bootstrap support shown for 100 trials.

Expression Analysis

Transcript analysis was performed following RNA extraction by the Trizol method (Invitrogen Corporation, Carlsbad, CA). 2 µg of DNase-treated RNA was used as template for cDNA synthesis using SuperScript III Reverse Transcriptase (Invitrogen), following the protocol outlined in Gomez *et al.* (2009). Transcript abundance was determined by RT-PCR analysis with GoTaq polymerase (Promega Corporation, Madison, WI) in 20 µl reactions with 1 µl of cDNA as template. Due to the sequence similarity of phosphate transporter genes, primer specificity was tested and confirmed by amplifying template DNA consisting of inappropriate phosphate transporter genes. Different cycle numbers appropriate for each gene were used for RT-PCR as follows: Elongation factor 1α (EF1α), 30 cycles; MtPT4, MtPT6 and MtPT9, 35 cycles; MtPT8, 40 cycles; MtPT7, 45 cycles.

Transcript levels of phosphate transporters across Affymetrix GeneChip experiments, including mycorrhizal samples reported in Gomez *et al.* (2009) was analyzed using the *Medicago truncatula* Gene Atlas (http://mtgea.noble.org/v2/) (Benedito et al., 2008). Unique probe sets are available for MtPT4 (Mtr.43062.1.S1_at), MtPT5 (Mtr.42466.1.S1_at), MtPT6 (Mtr.45568.1.S1_at), and

MtPT9 (Mtr.21449.1.S1_at). And additional probe set hybridizes with the highly-similar transcripts of MtPT1, MtPT2 and MtPT3 (Mtr.15323.1.S1_s_at)

Analysis of transcriptional reporter fusions

Activity of MtPT6 and MtPT9 promoter:*UidA* reporter fusions was evaluated in composite root systems grown three to five weeks in low phosphate conditions; MtPT8 promoter:UidA-transformed roots were evaluated three to four weeks after inoculation with the AM fungus *Glomus versiforme*. β-glucuronidase (GUS) activity was determined by histochemical staining with X-gluc (5-bromo-4-chloro-3-indolyl-beta-D-glucuronic acid) at 37 °C as described in (Liu et al., 2003) and imaged on a Leica DM6000B compound microscope.

Imaging of MtPT8-GFP fusion protein

Composite root sections displaying *pMtPT8:MtPT8-GFP* signal following colonization were selected and excised using a dissecting microscope (Olympus SZX-12 stereo microscope). Fluorescing root sections were then bisected longitudinally and imaged on a Leica TCS-SP5 confocal microscope as previously described (Pumplin and Harrison, 2009). Samples were excited with the blue argon ion laser (488 nm), and emitted fluorescence from GFP was collected from 505 to 545 nm; differential interference contrast (DIC) images were collected using the transmitted light detector. Images were analyzed and prepared using Leica LAS-AF Version 1.7.0 and Adobe Photoshop CS Version 8 (Adobe Systems) software.

REFERENCES

Ai, P., Sun, S., Zhao, J., Fan, X., Xin, W., Guo, Q., Yu, L., Shen, Q., Wu, P., Miller, A.J., and Xu, G. (2009). Two rice phosphate transporters, OsPht1;2 and OsPht1;6, have different functions and kinetic properties in uptake and translocation. Plant J **57,** 798-809.

Ames, B.N. (1966). Assay of inorganic phosphate, total phosphate and phosphatases. Methods Enzymol. **8,** 115-118.

Aung, K., Lin, S.I., Wu, C.C., Huang, Y.T., Su, C.L., and Chiou, T.J. (2006). pho2, a phosphate overaccumulator, is caused by a nonsense mutation in a microRNA399 target gene. Plant Physiol **141,** 1000-1011.

Bari, R., Datt Pant, B., Stitt, M., and Scheible, W.R. (2006). PHO2, microRNA399, and PHR1 define a phosphate-signaling pathway in plants. Plant Physiol **141,** 988-999.

Benedito, V.A., Torres-Jerez, I., Murray, J.D., Andriankaja, A., Allen, S., Kakar, K., Wandrey, M., Verdier, J., Zuber, H., Ott, T., Moreau, S., Niebel, A., Frickey, T., Weiller, G., He, J., Dai, X., Zhao, P.X., Tang, Y., and Udvardi, M.K. (2008). A gene expression atlas of the model legume *Medicago truncatula*. Plant J **55,** 504-513.

Bieleski, R.L. (1973). Phosphate pools, phosphate transport and phosphate availability. Ann. Rev. Plant Physiol. **24,** 225-252.

Boisson-Dernier, A., Chabaud, M., Garcia, F., Becard, G., Rosenberg, C., and Barker, D.G. (2001). *Agrobacterium rhizogenes*-transformed roots of *Medicago truncatula* for the study of nitrogen-fixing and endomycorrhizal symbiotic associations. Mol Plant Microbe Interact **14,** 695-700.

Bonfante, P., and Perotto, S. (1995). Strategies of arbuscular mycorrhizal fungi when infecting host plants. New Phytologist **130,** 3-21.

Branscheid, A., Sieh, D., Pant, B.D., May, P., Devers, E.A., Elkrog, A., Schauser, L., Scheible, W.R., and Krajinski, F. (2010). Expression Pattern Suggests a Role of MiR399 in the Regulation of the Cellular Response to Local Pi Increase During Arbuscular Mycorrhizal Symbiosis. Mol Plant Microbe Interact **23,** 915-926.

Bucher, M. (2007). Functional biology of plant phosphate uptake at root and mycorrhiza interfaces. New Phytologist **173,** 11-26.

Bucher, M., Rausch, C., and Daram, P. (2001). Molecular and biochemical mechanisms of phosphorus uptake into plants. Journal of Plant Nutrition and Soil Science-Zeitschrift Fur Pflanzenernahrung Und Bodenkunde **164,** 209-217.

Chen, A., Hu, J., Sun, S., and Xu, G. (2007). Conservation and divergence of both phosphate- and mycorrhiza-regulated physiological responses and expression patterns of phosphate transporters in solanaceous species. New Phytol **173,** 817-831.

Chiou, T.J., Liu, H., and Harrison, M.J. (2001). The spatial expression patterns of a phosphate transporter (MtPT1) from *Medicago truncatula* indicate a role in phosphate transport at the root/soil interface. Plant J **25,** 281-293.

Chiu, W.-l., Niwa, Y., Zeng, W., Hirano, T., Kobayashi, H., and Sheen, J. (1996). Engineered GFP as a vital reporter in plants. Current Biology **6,** 325-330.

Daram, P., Brunner, S., Persson, B.L., Amrhein, N., and Bucher, M. (1998). Functional analysis and cell-specific expression of a phosphate transporter from tomato. Planta **206,** 225-233.

Desnos, T. (2008). Root branching responses to phosphate and nitrate. Curr Opin Plant Biol **11,** 82-87.

Glassop, D., Smith, S.E., and Smith, F.W. (2005). Cereal phosphate transporters associated with the mycorrhizal pathway of phosphate uptake into roots. Planta **222,** 688-698.

Grunwald, U., Guo, W., Fischer, K., Isayenkov, S., Ludwig-Muller, J., Hause, B., Yan, X., Kuster, H., and Franken, P. (2009). Overlapping expression patterns and differential transcript levels of phosphate transporter genes in arbuscular mycorrhizal, Pi-fertilised and phytohormone-treated *Medicago truncatula* roots. Planta **229,** 1023-1034.

Hamburger, D., Rezzonico, E., MacDonald-Comber Petetot, J., Somerville, C., and Poirier, Y. (2002). Identification and characterization of the *Arabidopsis* PHO1 gene involved in phosphate loading to the xylem. Plant Cell **14,** 889-902.

Harrison, M.J., Dewbre, G.R., and Liu, J. (2002). A phosphate transporter from *Medicago truncatula* involved in the acquisition of phosphate released by arbuscular mycorrhizal fungi. Plant Cell **14,** 2413-2429.

Jakobsen, I., Abbott, L.K., and Robson, A.D. (1992). External hyphae of vesicular-arbuscular mycorrhizal fungi associated with *Trifolium subterraneum*L. 2. Hyphal transport of ^{32}P over defined distances. New Phytol. **120,** 509-516.

Javot, H., Pumplin, N., and Harrison, M.J. (2007a). Phosphate in the arbuscular mycorrhizal symbiosis: transport properties and regulatory roles. Plant Cell Environ **30,** 310-322.

Javot, H., Penmetsa, R.V., Terzaghi, N., Cook, D.R., and Harrison, M.J. (2007b). A *Medicago truncatula* phosphate transporter indispensable for the arbuscular mycorrhizal symbiosis. Proc Natl Acad Sci U S A **104,** 1720-1725.

Kobae, Y., and Hata, S. (2010). Dynamics of periarbuscular membranes visualized with a fluorescent phosphate transporter in arbuscular mycorrhizal roots of rice. Plant Cell Physiol **51,** 341-353.

Leggewie, G., Willmitzer, L., and Riesmeier, J.W. (1997). Two cDNAs from potato are able to complement a phosphate uptake-deficient yeast mutant: identification of phosphate transporters from higher plants. Plant Cell **9,** 381-392.

Liu, F., Wang, Z., Ren, H., Shen, C., Li, Y., Ling, H.Q., Wu, C., Lian, X., and Wu, P. (2010). OsSPX1 suppresses the function of OsPHR2 in the regulation of expression of OsPT2 and phosphate homeostasis in shoots of rice. Plant J **62,** 508-517.

Liu, H., Trieu, A.T., Blaylock, L.A., and Harrison, M.J. (1998). Cloning and characterization of two phosphate transporters from *Medicago truncatula* roots: regulation in response to phosphate and to colonization by arbuscular mycorrhizal (AM) fungi. Mol Plant Microbe Interact **11,** 14-22.

Liu, J., Versaw, W.K., Pumplin, N., Gomez, S.K., Blaylock, L.A., and Harrison, M.J. (2008). Closely related members of the *Medicago truncatula* PHT1 phosphate transporter gene family encode phosphate transporters with distinct biochemical activities. J Biol Chem **283,** 24673-24681.

Liu, J.Y., Blaylock, L.A., Endre, G., Cho, J., Town, C.D., VandenBosch, K.A., and Harrison, M.J. (2003). Transcript profiling coupled with spatial expression analyses reveals genes involved in distinct developmental stages of an arbuscular mycorrhizal symbiosis. Plant Cell **15,** 2106-2123.

Maeda, D., Ashida, K., Iguchi, K., Chechetka, S.A., Hijikata, A., Okusako, Y., Deguchi, Y., Izui, K., and Hata, S. (2006). Knockdown of an Arbuscular

Mycorrhiza-inducible Phosphate Transporter Gene of *Lotus japonicus* Suppresses Mutualistic Symbiosis. Plant Cell Physiol. **47,** 807-817.

Mitsukawa, N., Okumura, S., Shirano, Y., Sato, S., Kato, T., Harashima, S., and Shibata, D. (1997). Overexpression of an *Arabidopsis thaliana* high-affinity phosphate transporter gene in tobacco cultured cells enhances cell growth under phosphate-limited conditions. Proc Natl Acad Sci U S A **94,** 7098-7102.

Mudge, S.R., Rae, A.L., Diatloff, E., and Smith, F.W. (2002). Expression analysis suggests novel roles for members of the Pht1 family of phosphate transporters in *Arabidopsis*. Plant J **31,** 341-353.

Nagy, R., Vasconcelos, M.J., Zhao, S., McElver, J., Bruce, W., Amrhein, N., Raghothama, K.G., and Bucher, M. (2006). Differential regulation of five Pht1 phosphate transporters from maize (*Zea mays* L.). Plant Biol (Stuttg) **8,** 186-197.

Nagy, R., Karandashov, V., Chague, W., Kalinkevich, K., Tamasloukht, M., Xu, G.H., Jakobsen, I., Levy, A.A., Amrhein, N., and Bucher, M. (2005). The characterization of novel mycorrhiza-specific phosphate transporters from *Lycopersicon esculentum* and *Solanum tuberosum* uncovers functional redundancy in symbiotic phosphate transport in solanaceous species. Plant Journal **42,** 236-250.

Pao, S.S., Paulsen, I.T., and Saier, M.H., Jr. (1998). Major facilitator superfamily. Microbiol Mol Biol Rev **62,** 1-34.

Parniske, M. (2008). Arbuscular mycorrhiza: the mother of plant root endosymbioses. Nature Reviews Microbiology **6,** 763-775.

Paszkowski, U., Kroken, S., Roux, C., and Briggs, S.P. (2002). Rice phosphate transporters include an evolutionarily divergent gene specifically activated in arbuscular mycorrhizal symbiosis. Proc Natl Acad Sci U S A **99,** 13324-13329.

Pumplin, N., and Harrison, M.J. (2009). Live-cell imaging reveals periarbuscular membrane domains and organelle location in *Medicago truncatula* roots during arbuscular mycorrhizal symbiosis. Plant Physiol **151,** 809-819.

Rae, A.L., Cybinski, D.H., Jarmey, J.M., and Smith, F.W. (2003). Characterization of two phosphate transporters from barley; evidence for diverse function and kinetic properties among members of the Pht1 family. Plant Mol Biol **53,** 27-36.

Rausch, C., Daram, P., Brunner, S., Jansa, J., Laloi, M., Leggewie, G., Amrhein, N., and Bucher, M. (2001). A phosphate transporter expressed in arbuscule-containing cells in potato. Nature **414,** 462-470.

Schachtman, D.P., Reid, R.J., and Ayling, S.M. (1998). Phosphorus Uptake by Plants: From Soil to Cell. Plant Physiol **116,** 447-453.

Shin, H., Shin, H.S., Dewbre, G.R., and Harrison, M.J. (2004). Phosphate transport in *Arabidopsis*: Pht1;1 and Pht1;4 play a major role in phosphate acquisition from both low- and high-phosphate environments. Plant J **39,** 629-642.

Tadege, M., Wen, J., He, J., Tu, H., Kwak, Y., Eschstruth, A., Cayrel, A., Endre, G., Zhao, P.X., Chabaud, M., Ratet, P., and Mysore, K.S. (2008). Large-scale insertional mutagenesis using the Tnt1 retrotransposon in the model legume *Medicago truncatula*. Plant J **54,** 335-347.

Ticconi, C.A., and Abel, S. (2004). Short on phosphate:plant surveillance and countermeasures. Trends Plant Sci. **9,** 548-555.

Vance, C.P., Uhde-Stone, C., and Allan, D.L. (2003). Phosphorus acquisition and use: critical adaptations by plants for securing a nonrenewable resource. New Phytologist **157,** 423-447.

Xiao, K., Liu, J., Dewbre, G., Harrison, M., and Wang, Z.Y. (2006). Isolation and characterization of root-specific phosphate transporter promoters from *Medicago truncatula*. Plant Biol (Stuttg) **8,** 439-449.

Xu, G.H., Chague, V., Melamed-Bessudo, C., Kapulnik, Y., Jain, A., Raghothama, K.G., Levy, A.A., and Silber, A. (2007). Functional characterization of LePT4: a phosphate transporter in tomato with mycorrhiza-enhanced expression. Journal of Experimental Botany **58,** 2491-2501.

.

CHAPTER 5

MEDICAGO TRUNCATULA VAPYRIN IS A NOVEL PROTEIN REQUIRED FOR ARBUSCULAR MYCORRHIZAL SYMBIOSIS[4]

Abstract

The arbuscular mycorrhizal (AM) symbiosis is a widespread mutualism formed between vascular plants and fungi of the Glomeromycota. In this endosymbiosis, fungal hyphae enter the roots, growing through epidermal cells to the cortex where they establish differentiated hyphae called arbuscules in the cortical cells. Reprogramming of the plant epidermal and cortical cells occurs to enable intracellular growth of the fungal symbiont, however plant genes underlying this process are largely unknown. Here, through the use of RNAi, we demonstrate that expression of a *Medicago truncatula* gene named *Vapyrin* is essential for arbuscule formation and also for efficient epidermal penetration by AM fungi. *Vapyrin* is induced transiently in the epidermis coincident with hyphal penetration and then in the cortex during arbuscule formation. The Vapyrin protein is cytoplasmic and in cells containing AM fungal hyphae, the protein accumulates in small puncta that move through the cytoplasm. Vapyrin is a novel protein composed of two domains that mediate protein-protein interactions: an N-terminal VAP/MSP domain and a C-terminal ankyrin repeat domain. Putative Vapyrin orthologs exist widely in the plant kingdom, but not in Arabidopsis, or in non-plant species. The data suggest a role for Vapyrin in cellular remodeling to support intracellular development of fungal hyphae during AM symbiosis.

[4] This paper was published as **Pumplin, N., Mondo, S.J., Topp, S., Starker, C.G., Gantt, J.S. and Harrison, M.J.** (2010) *Medicago truncatula* Vapyrin is a novel protein required for arbuscular mycorrhizal symbiosis. *Plant J*, **61**, 482-494. It is reprinted with permission. CGS and JSG created the original Vapyrin RNAi construct, SM and MJH performed the first screen of Vapyrin RNAi and SJT created the RNAi-2 construct.

Introduction

Plants have evolved various strategies to enhance their access to essential mineral nutrients including the development of symbioses with microorganisms. One of the most widespread examples is the arbuscular mycorrhizal (AM) symbiosis, formed between vascular plants and fungi of the phylum, Glomeromycota. In this association, the AM fungi contribute to plant phosphate and nitrogen nutrition (Smith et al., 2003; Govindarajulu et al., 2005; Javot et al., 2007a) by delivering these mineral nutrients directly to the root cortex. In exchange, they receive carbon from their plant partners (Bago et al., 2000). This association, which arose over 400 million years ago (Remy et al., 1994; Bonfante and Genre, 2008) is estimated to occur in over 80% of the angiosperm species and exists in terrestrial ecosystems throughout the world.

Development of the symbiosis has been clearly described including the existence, and more recently, the identity of some of the early signaling molecules. In response to strigolactones present in plant exudates, AM fungal hyphae branch and their metabolism is activated (Akiyama et al., 2005; Besserer et al., 2006). In turn, AM fungal exudates contain an unidentified 'myc factor' that induces gene expression and calcium spiking in plant roots. (Kosuta et al., 2003; Navazio et al., 2007; Kosuta et al., 2008). Upon contact with a root, AM fungal hyphae develop hyphopodia and subsequently penetrate and pass through the epidermal cells guided by a preformed cellular apparatus, named the prepenetration apparatus (Genre et al., 2005). Within the cortex, hyphae grow both intra- and intercellularly, and finally enter the cortical cells where they branch to form arbuscules, for which the symbiosis is named. Arbuscule development is accompanied by rearrangement of the plant cortical cells, including repositioning of organelles and cytoskeleton, nuclear enlargement, and deposition of the periarbuscular membrane (Gianinazzi-Pearson, 1996; Bonfante and Genre, 2008). The periarbuscular membrane is continuous with the plasma membrane

but is functionally distinct, and in the case of phosphate, is the site of nutrient exchange between symbionts (Javot et al., 2007b).

Plant mutants impaired at different stages of symbiotic development have been identified. Mutants blocked at the earliest phases include the tomato *premycorrhizal infection* (*pmi*) *1* and *pmi2*, which suppress fungal growth and hyphopodium formation (David-Schwartz et al., 2003; Gadkar et al., 2003), and maize *no perception* (*nope1*), which displays a major reduction in the formation of hyphopodia and intraradical colonization (Paszkowski et al., 2006). The most detailed genetic analyses exist for a class of mutants that are blocked in epidermal penetration. These mutants were identified initially in legumes and they are also unable to form root nodule symbiosis with Rhizobia (Parniske, 2008). In *Medicago truncatula* and *Lotus japonicus*, the genes underlying eight of these mutants have been cloned including the receptor-like kinase DMI2 (Endre et al., 2002)/SYMRK (Stracke et al., 2002), cation channels CASTOR (Imaizumi-Anraku et al., 2005) and DMI1 (Ane et al., 2004)/POLLUX (Imaizumi-Anraku et al., 2005), nucleoporins NUP85 (Saito et al., 2007) and NUP133 (Kanamori et al., 2006), the calcium and calmodulin-dependent kinase DMI3 (Levy et al., 2004; Mitra et al., 2004)/CCaMK (Tirichine et al., 2006) and nuclear-localized CYCLOPS (Yano et al., 2008). Mutations in these genes impair fungal passage through the epidermis and entry in to the cortex, resulting in swollen hyphopodia on the root surface. Loss-of-function *cyclops* mutants of *L. japonicus* and rice also permit a low level of cortical colonization by AM fungi, but fail to develop arbuscules (Kistner et al., 2005; Gutjahr et al., 2008; Yano et al., 2008). A petunia mutant, *pam1* (*penetration and arbuscule morphogenesis*) exhibits a similar phenotype with impaired epidermal penetration, a high frequency of aborted and swollen hyphopodia and no formation of arbuscules (Reddy et al., 2007). Additional mutants impaired in cortical development include the maize mutant *taciturn1*,

(Paszkowski et al., 2006), the pea mutant *myc*$^{-2}$, which fails to develop mature arbuscules (Gianinazzi-Pearson et al., 1991; Gianinazzi-Pearson, 1996) and the tomato *rmc* mutant, in which the phenotype varies slightly with the species of AM fungus (Barker et al., 1998; Gao et al., 2001; Poulsen et al., 2005). Additionally, RNA-silencing has been used to knockdown a calcium-dependent protein kinase (Ivashuta et al., 2005) and two plant subtilases (Takeda et al., 2009), both of which lead to a reduction in cortical colonization and arbuscule formation. Finally, mutating phosphate transporters MtPT4 from *M. truncatula* (Javot et al., 2007b) and LjPT3 from *L. japonicus* (Maeda et al., 2006) caused premature arbuscule degeneration and loss of functional symbiosis.

While some details of the pathway and molecular events regulating epidermal penetration by AM fungi have been established (Parniske, 2008), relatively little is known about the genetic and cellular mechanisms that control arbuscule development within cortical cells. Transcriptome studies have identified many hundreds of *M. truncatula* genes induced during the symbiosis (Liu et al., 2003; Guimil et al., 2005; Hohnjec et al., 2005; Gomez et al., 2009; Guether et al., 2009), some of which have specific expression patterns in the cortex coincident with fungal colonization, suggesting that the cortical cells undergo significant transcriptional reprogramming during symbiosis. The transcript profiling and spatial expression data therefore provide a useful guide for the selection of candidate genes that may play a role in arbuscule formation. Here, we report that silencing an AM symbiosis-induced gene, called *Vapyrin*, impairs epidermal penetration by AM fungi and abolishes arbuscule formation. Based on expression and localization studies and the presence of known protein domains, we hypothesize Vapyrin plays a cellular role to enable AM fungal development within plant cells.

Results

Vapyrin knock-down impairs passage across the epidermis by AM fungi and abolishes arbuscule formation

To identify genes that are required for AM symbiosis, we introduced RNAi constructs targeting individual candidate genes into *Medicago truncatula* via *Agrobacterium rhizogenes*-mediated transformation (Boisson-Dernier et al., 2001). The resulting composite plants, which have transgenic root systems and non-transgenic shoots, were then evaluated for their ability to form an AM symbiosis (Ivashuta et al., 2005). Increased expression in mycorrhizal roots was one criterion used for the selection of candidate genes, and included in this category was a candidate gene represented by TC104091 that was induced three-fold in roots colonized by AM fungi (Gomez et al., 2009). Subsequently, we named this gene *Vapyrin*. *M. truncatula* composite plants with transgenic roots expressing an RNAi construct targeting the 5' region of TC104091, referred to as Vapyrin RNAi-1, were compared with those expressing a control RNAi construct targeting the *UidA* gene, referred to as GUS RNAi.

M. truncatula GUS RNAi roots colonized with *G. versiforme* showed a phenotype typical for this combination of plant and fungus (Harrison and Dixon, 1993). *G. versiforme* formed hyphopodia on the root surface from which hyphae penetrated through the epidermis, grew intercellularly through the cortex, forming arbuscules in the inner cortical cells (Figure 5-1a, d). In contrast, in Vapyrin RNAi-1 roots, a significantly higher proportion of the hyphopodia arrested in the epidermis, indicating a partial block in root penetration (Figure 5-5-1b, f). In these arrested infections, the hyphopodia became swollen with multiple aborted projections into the

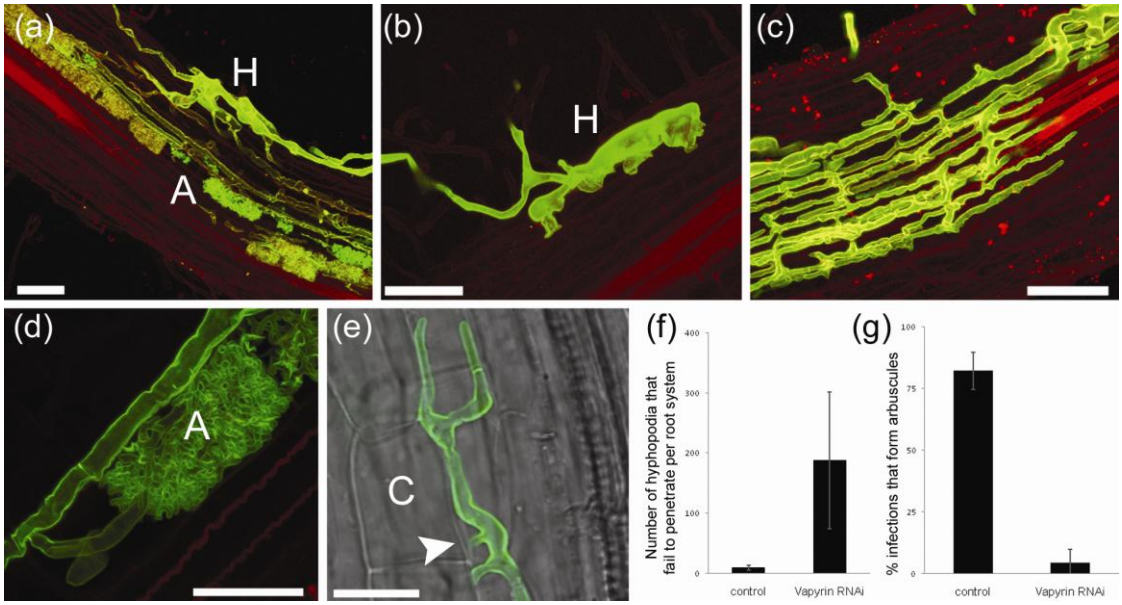

Figure 5-1. Reduced expression of *Vapyrin* impairs AM symbiosis.
Confocal microscope images of *G. versiforme* in *M. truncatula* roots expressing GUS RNAi (a, d) and Vapyrin RNAi-1 constructs (b, c, e) colonized with *G. versiforme*. *G. versiforme* stained with wheatgerm agglutinin (WGA) conjugated to Alexa Fluor 488 is shown in green. Propidium iodide (PI) overlay (a-d) stains plant cell walls red. Brightfield overlay (e) shows outline of cortical cells. A control GUS RNAi root shows a typical mycorrhizal phenotype with a hyphopodium penetrating the root and hyphae growing through the cortex to form arbuscules (a, d). In Vapyrin RNAi roots, *G. versiforme* shows a high instance of aborted hyphopodia and hyphae that successfully penetrate the root do not form arbuscules (b and c). Hyphal branches (arrowhead) arising from the main runner hyphae do not enter cortical cells (e). Scale bar in a-c = 50 µm, d-e = 20 µm. Hyphopodia (H), Arbuscule (A), Cortical cell (C). Roots were harvested four weeks post inoculation. (f) Total number of hyphopodia that fail to penetrate control (GUS RNAi) and Vapyrin RNAi-1 root systems. (g) Percentage of AM infections that produce arbuscules. (f,g) Control n = 5 plants, Vapyrin RNAi-1 n = 6. Error bars depict standard deviation, $p<0.001$ student's t test. Results shown in (f, g) are representative of four independent experiments on more than 45 Vapyrin RNAi-1 transgenic plants.

root epidermis. In the infection events where hyphae successfully penetrated the epidermis, the fungus developed intercellular hyphae and grew through the cortex but failed to form arbuscules (Figure 5-5-1c, e). In some infections, intercellular hyphal development in the cortex included many cross-connections between the individual runner hyphae, which resulted in a lattice-like appearance (Fig. 1c). Short, hyphal projections, possibly attempts to penetrate cortical cells, were also apparent (Fig. 1e). This aberrant mycorrhizal phenotype was observed in more than 45 transgenic plants from four independent experiments and was also observed in Vapyrin RNAi-1 roots colonized by a different species of AM fungus, *Gigaspora gigantea* (Appendix 5-2). For one of these experiments with *G. versiforme*, the cortical phenotype was quantified by scoring the presence or absence of arbuscules in infections that had reached the root cortex. The control GUS RNAi roots had arbuscules in 82% (+/- 8% s.d. n = 5) of cortical infections while Vapyrin RNAi-1 roots had arbuscules in 5% (+/- 5% s.d. n = 6) (Figure 5-5-1g, Appendix 5-1). The *A. rhizogenes* transformation produces composite root systems that can include non-transgenic roots, and the few arbuscules observed in Vapyrin RNAi-1 roots probably occurred in roots not expressing the RNAi construct. *Vapyrin* transcript levels were assayed in RNA from these Vapyrin RNAi-1 and GUS RNAi roots by quantitative RT-PCR (qRT-PCR). Vapyrin RNAi-1 roots showed a significant (20-fold) reduction in *Vapyrin* transcript levels relative to the GUS RNAi control roots (Figure 5-2a). In addition, Vapyrin RNAi-1 roots showed significantly reduced expression of the phosphate transporter *MtPT4*, which serves as an indicator of arbuscule levels (Harrison et al., 2002). *G. versiforme α-tubulin* transcripts confirmed the presence of the AM fungus in all samples (Figure 5-2a).

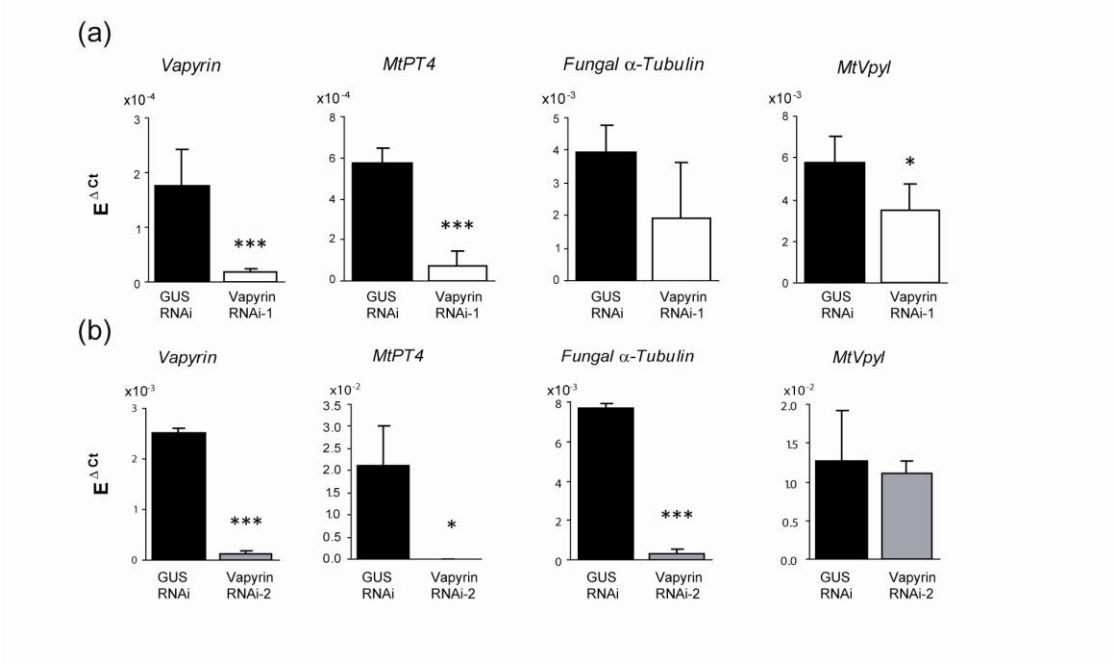

Figure 5-2. Reduction of *Vapyrin* transcript levels by two independent RNAi constructs, *Vapyrin* RNAi-1 and RNAi-2.
(a) Transcript levels in Vapyrin RNAi-1 (n=6) and GUS RNAi control roots (n=4) assayed by quantitative RT-PCR. RNA was extracted from samples of whole root systems used for phenotype quantification shown in Figure 5-1.
(b) Transcript levels in Vapyrin RNAi-2 (n=3) and GUS RNAi (n=2) control roots assayed by qRT-PCR. Single transgenic roots were excised and used for RNA extraction and phenotyping. Vapyrin RNAi-2 roots included here showed aborted hyphopodia and infections that failed to produce arbuscules similar to RNAi-1, while GUS RNAi controls showed wild type infections.
The values represent the transcript levels of *Vapyrin*, *MtPT4*, *G. versiforme* α-*Tubulin* and *Vapyrin-like* (*MtVpyl*) relative to the constitutively-expressed *M. truncatula Elongation Factor 1-α* ($E^{\Delta Ct}$) with order of magnitude indicated above the y-axis. Vapyrin is downregulated 20-fold in RNAi-1 roots and 60-fold in RNAi-2 roots. Error bars indicate standard deviation.
*, $p<0.05$; ***, $p<0.0005$.

To further confirm that down-regulation of Vapyrin gene expression results in this aberrant mycorrhizal phenotype, a second Vapyrin RNAi construct targeting the 3' region of the gene was created. Following colonization with *G. versiforme*, transgenic roots expressing Vapyrin RNAi-2 showed the same aberrant mycorrhizal phenotype observed in the initial Vapyrin RNAi-1 roots, including failed epidermal penetration attempts and cortical infections lacking arbuscules. In this experiment individual transgenic roots from Vapyrin RNAi-2 and GUS RNAi root systems were sampled and in each case, part of the root was stained to visualize the fungus, while the remainder was used for transcript analysis by qRT-PCR. *Vapyrin* transcript levels were reduced significantly (60 fold) in the single Vapyrin RNAi-2 roots relative to the GUS RNAi roots (Figure 5-2b). Vapyrin RNAi-2 single roots showed many aborted hyphopodia and no arbuscules, while GUS RNAi control roots showed wild type infections with arbuscules. Consistent with this, *MtPT4* transcripts were undetectable in the Vapyrin RNAi-2 roots but present in the GUS RNAi controls (Figure 5-2b). *G. versiforme α-tubulin* transcripts were detected in all samples confirming the presence of the AM fungus (Figure 5-2b) but levels were lower in the Vapyrin RNAi-2 roots where the fungus did not proliferate extensively. To test whether the Vapyrin RNAi constructs might target other genes, we monitored the expression of the gene with highest sequence similarity to *Vapyrin*, TC111041. This gene was named *MtVpyl* and is the gene most like to be cross-silenced by the RNAi constructs. *MtVpyl* transcript levels were slightly lower in Vapyrin RNAi-1 roots (<1.5-fold lower relative to GUS RNAi control) but did not change in the Vapyrin RNAi-2 roots relative to the GUS RNAi controls (Figure 5-2). Thus, the aberrant mycorrhizal phenotype observed in the Vapyrin RNAi roots cannot be attributed to MtVpyl. Overall, the data from two independent Vapryin RNAi constructs indicate that downregulation of *Vapyrin*

expression impairs development of AM symbiosis in *M. truncatula* and in particular prevents arbuscule formation.

Vapyrin is a member of a plant-specific gene family

The EST contig TC104091 contained 197 nucleotides of 5' UTR sequence and a predicted open reading frame, but was not full length and lacked the 3' end of the gene. To obtain the missing region, 3' RACE was performed on a cDNA library derived from *M. truncatula*/*G. versiforme* mycorrhizal roots. In addition, a 1761 bp DNA fragment representing the region 5' proximal to the predicted first ATG codon, was amplified from *M. truncatula* genomic DNA. The whole gene was then reconstructed and sequenced. The full-length *Vapyrin* gene has no introns and is predicted to encode a cytosolic protein of 541 amino acids which contains two previously-described protein motifs (Figure 5-3). The amino-terminal (N-terminal) portion of the protein shares high similarity with the N-terminal end of Vamp-Associated Protein (VAP), which is highly conserved in plants, animals and fungi. This region is also similar to the nematode Major Sperm Protein (MSP), an oligomeric protein, which regulates movement of nematode sperm cells (Tarr and Scott, 2005). The N-terminal domain of VAP is a protein interaction domain capable of interaction with a range of other proteins, while the carboxy-terminal (C-terminal) region of VAP includes a transmembrane domain via which the VAPs are localized in endomembranes (Lev et al., 2008; Saravanan et al., 2009). In contrast, the C-terminal portion of Vapyrin does not contain a transmembrane domain, but instead contains eight ankyrin repeats, a widely-distributed protein domain with a helix-turn-helix structure that mediates protein-protein interactions (Rubtsov and Lopina, 2000; Li et al., 2006).

(a)

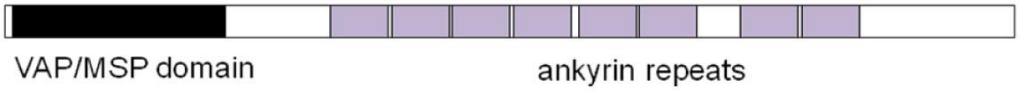

(b)

MDRLIKLDPSNIVLIRVEEGQKCLGKITLNNVMYTMPVAFRIQPLIKTRYTIKPQSGIISPLASLVIEI
TYHPPQQQGSNNLPHSFPFSDDSFLLHSVLAPGAAIKEPSSMFDSVPSDWFTTKKKQVFIDSAIKVMFV
GSQILTQLVEDGNSMDDIREVLEKSDPLWESVNSKDSQGQTLLHLAISKTRPDLVQLILEFKPDIEAIN
SVGSTPLEAASSSGESLIVELLLAHKANTEGSESSVFRPIHHASREGHMEILRLLLLKGARVDSLTKDG
NTSLHLAVEEKRRDCARLLLANGARTDVRNMREGDTPLHIAAANGDENMVKLLLHKGATKYVRNKLGKT
AFDVAAENGHSRLFDALRLGDNLCAAARKGEVRTIQKVLESGGVINGRDQNGWTSLHRAAFKGRMDAVR
FLVEKGIDLDAKDEDGYTALHCAAESGHADVTEFLVKKGADVEARTNKGVSALQIVESLNYVGITRILV
NGGASREGLGEKPPSAPSKIPFGRKVESGSVMTMKKKMSSRTRALRGSFDHSMPLAVL*

Figure 5-3. *Vapyrin* gene structure.
(a) The *Vapyrin* gene does not contain introns and is predicted to encode a protein of 541 amino acids. The N-terminal region contains a VAP/MSP domain and the C-terminal region contains 8 ankyrin repeats. Domains were predicted by SMART protein motif prediction software and highlighted motifs are shown to scale.
(b) Amino acid sequence with VAP domain underlined and ankyrin repeats highlighted in grey.

BLAST searches enabled the identification of putative *Vapyrin* orthologs from monocot and dicot plant species, and the lycopod *Selaginella moellendorffii*, however no putative ortholog was found in the non-mycorrhizal plant Arabidopsis (Figure 5-4 and Appendix 5-3). All of the putative *Vapyrin* genes are predicted to encode proteins with an N-terminal VAP/MSP domain and a C-terminal domain with eight or nine ankyrin repeats. The proteins share high sequence similarity with approximately 70% identity between Vapyrin and other putative dicot orthologs and approximately 40% with Rice. Within the *M. truncatula* genome, the gene with the highest sequence similarity to *Vapyrin* is TC111041, which we subsequently named *MtVpyl* (*Vapyrin-like*). *MtVpyl* also encodes a protein with a VAP domain and an ankyrin repeat domain. *MtVpyl* homologs were identified from dicots and they form a sister group to *Vapyrin*. Again, Arabidopsis does not contain a *MtVpyl* homolog and additionally, no *MtVpyl* homologs were identified in monocot species. As expected, both *M. truncatula* and Arabidopsis have homologs of *VAP* and *MSP* and these genes form independent sister groups to the *Vapyrin* group. Genes encoding proteins with the VAP and ankyrin domain combination were not present in the genomes of any non-plant species. Together the functional data and the phylogenetic distribution of putative *Vapyrin* orthologs suggest that this novel combination of VAP and ankyrin domains was a plant-specific evolution that arose for AM symbiosis.

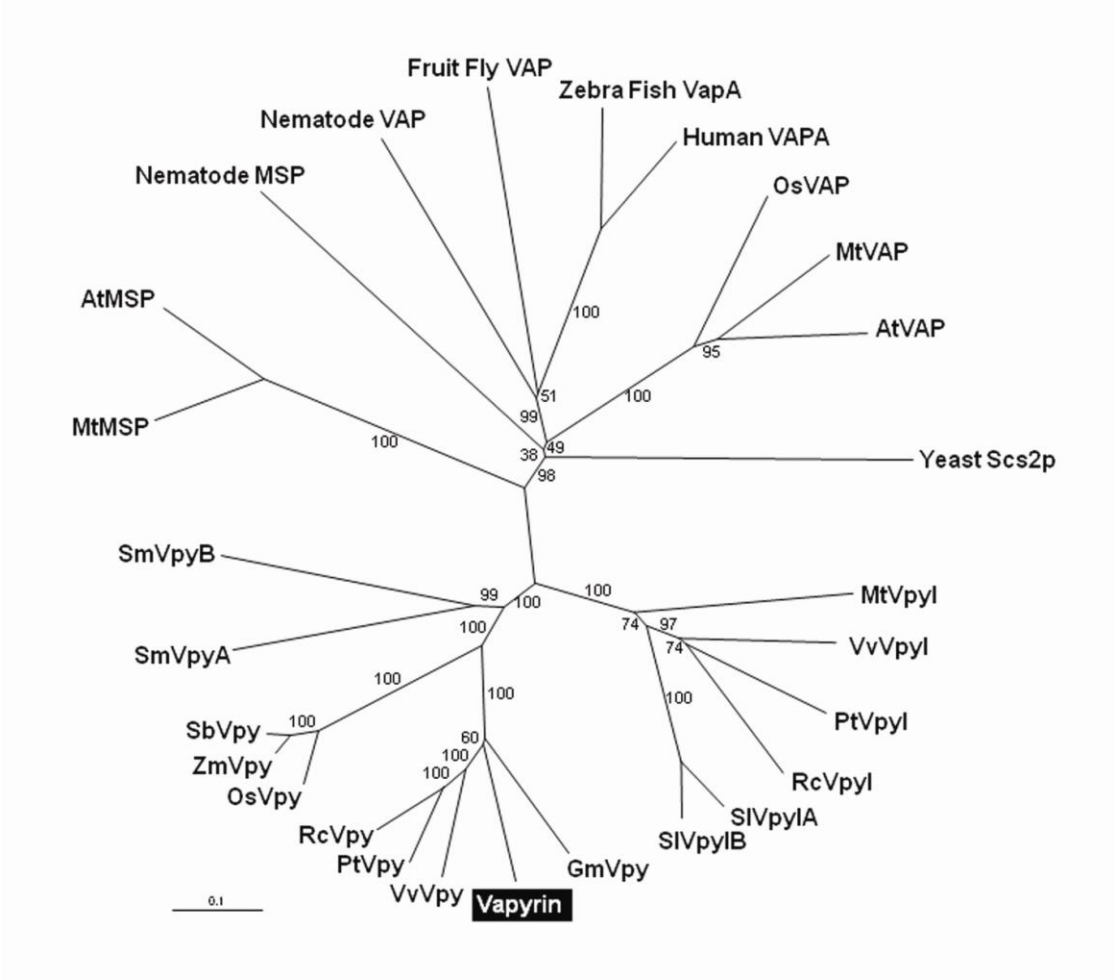

Figure 5-4. Phylogram of Vapyrin and related gene families.
The phylogram was constructed by a neighbor-joining Clustal X alignment of full-length amino acid sequences of *M. truncatula* proteins Vapyrin, MtVpyl, and representative MSP and VAP homologs. Included are putative Vapyrin orthologs from the plants *Populus trichocarpa* (Pt), *Vitis vinifera* (Vv), *Glycine max* (Gm), *Solanum lycopersicum* (Sl), *Ricinus communis* (Rc), *Oryza sativa* (Os), *Sorghum bicolor* (Sb), *Zea mays* (Zm) and the lycopod *Selaginella moellendorffii* (Sm) compared with VAP orthologs in *Arabidopsis thaliana* (At), Human, yeast, zebra fish, fruit fly, nematode and yeast (Scs2) and nematode MSP. Accession numbers are listed in Appendix 5-7. Distances calculated by neighbor joining and bootstraps reflect values from 100 trials. The phylogram was constructed in TreeView (http://taxonomy.zoology.gla.ac.uk/rod/treeview.html)
Scale bar represents 0.1 substitutions per site.

Vapyrin expression is induced coincident with AM fungal colonization of root cells

Our previous GeneChip experiment had indicated that *Vapyrin* was induced in mycorrhizal roots (Gomez et al., 2009). In addition, following identification of the complete *Vapyrin* gene, it was apparent that the GeneChip contains a second distinct probeset (TC112496) that corresponds to the 3' end of the Vapyrin gene. This probeset also indicated a three-fold induction of *Vapryin* in roots colonized by *Glomus intraradices* (Gomez et al., 2009). To extend the GeneChip analysis, *Vapyrin* transcript levels were assessed by qRT-PCR in *M. truncatula* roots during symbiosis with two different AM fungi, *Glomus versiforme* and *Gigaspora gigantea* (Appendix 5-4). This analysis revealed that *Vapyrin* transcripts are present at low levels in roots and increase 5-fold during interaction with the two AM fungal species. The Medicago Gene Atlas (http://bioinfo.noble.org/gene-atlas (Benedito et al., 2008) reports that *Vapyrin* has a basal level of expression in roots but no expression in aerial tissues. Interestingly, gene atlas data show *Vapyrin* transcripts increase in tissue from root nodules that arise from symbiotic associations with nitrogen-fixing *Rhizobia* bacteria. Furthermore, some *Vapyrin* ESTs are derived from root nodule libraries. *MtVpyl* was expressed in roots but did not show consistent differential expression during AM symbiosis as assessed by qRT-PCR analysis (Appendix 5-4) or in the previous GeneChip experiment (Gomez et al., 2009).

To determine the temporal and spatial expression pattern of *Vapyrin*, 1761 bp of genomic sequence upstream of the ATG was fused to the *UidA* reporter and transformed into *M. truncatula* roots using *A. rhizogenes*. In plants grown without AM fungi, expression of *proVapyrin:UidA* was observed primarily in vascular tissue and root caps (Figure 5-5a-c). After colonization by *G. versiforme*, GUS staining was

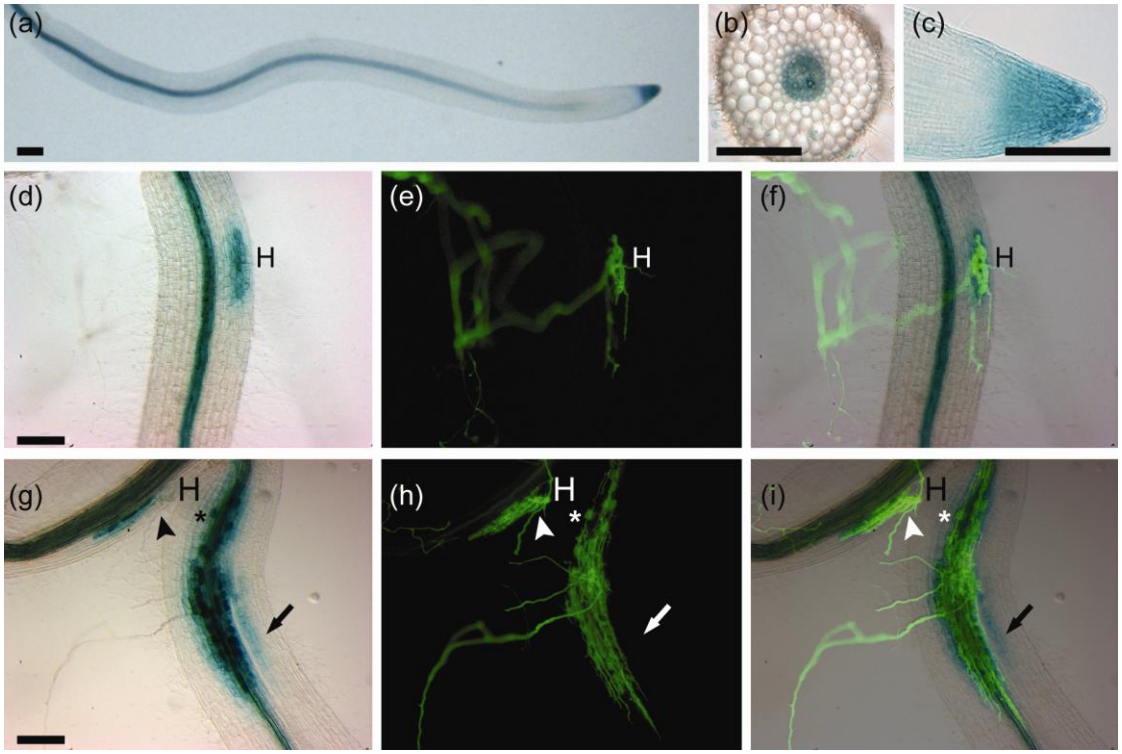

Figure 5-5. *Vapyrin* expression in *M. truncatula* roots.
Vapyrin promoter activity revealed by histochemical staining for GUS activity in transgenic roots expressing the 1761 bp of upstream sequence fused to the UidA reporter (a-d, g). *proVapyrin:UidA* is expressed is the stele and root cap (a-c). Upon colonization by *G. versiforme*, GUS activity is present in epidermal and outer cortical cells beneath fungal hyphopodia, H, (d-f) and in the cortex during arbuscule formation (g-i), both in cells with arbuscules (*) and in cortical cells adjacent to those with arbuscules (arrow). Expression coincident with hyphopodia is transient and turns off after cortical colonization (arrowhead under H in g-i). (e, h) fungal structures are detected by WGA-Alexa Fluor 488, (f, i) overlay of GUS and WGA. Scale bar = 100 µm

observed in the epidermis and outer cortical cells below penetrating hyphopodia (Figure 5-5d-f), and then in the cortex in cells with arbuscules and in cells adjacent to those with arbuscules (Figure 5-5g-i). After fungal development in the inner cortex, GUS expression was no longer visible in the epidermis below hyphopodia, suggesting this expression is transient and attenuated after cortical colonization. This expression pattern is consistent with the Vapyrin RNAi phenotype, in which fungal development during penetration and arbuscule formation is impaired.

Vapyrin protein localizes in cytoplasm and distinct, mobile complexes

To study the subcellular localization of Vapyrin during the AM symbiosis, we constructed translational fusions between GFP and the 5' and 3' ends of the full *Vapyrin* coding sequence. The constructs were expressed from the native *Vapyrin* promoter and were named *proVapyrin:Vapyrin-GFP* and *proVapyrin:GFP-Vapyrin* for C- and N-terminal GFP fusions, respectively. The constructs were introduced into *M. truncatula* roots through *A. rhizogenes* transformation, inoculated with *G. versiforme* and following development of AM symbiosis, the roots were examined by confocal microscopy.

Similar to the transcriptional reporter fusions, expression of the C-terminal GFP fusion was observed in the epidermis and outer cortex underneath the hyphopodia (Figure 5-6a-d). Vapyrin-GFP signal was present in cytoplasmic strands including cytoplasmic accumulations below hyphopodia, and in some cells GFP was detected in the nucleus. Following entry of the hypha into an epidermal cell, in addition to cytoplasmic and nuclear locations, Vapyrin-GFP accumulated in very small puncta (Figure 5-6c,d). After colonization of the root cortex, both Vapyrin-GFP and GFP-Vapyrin were observed in the cytoplasm of cells with arbuscules and

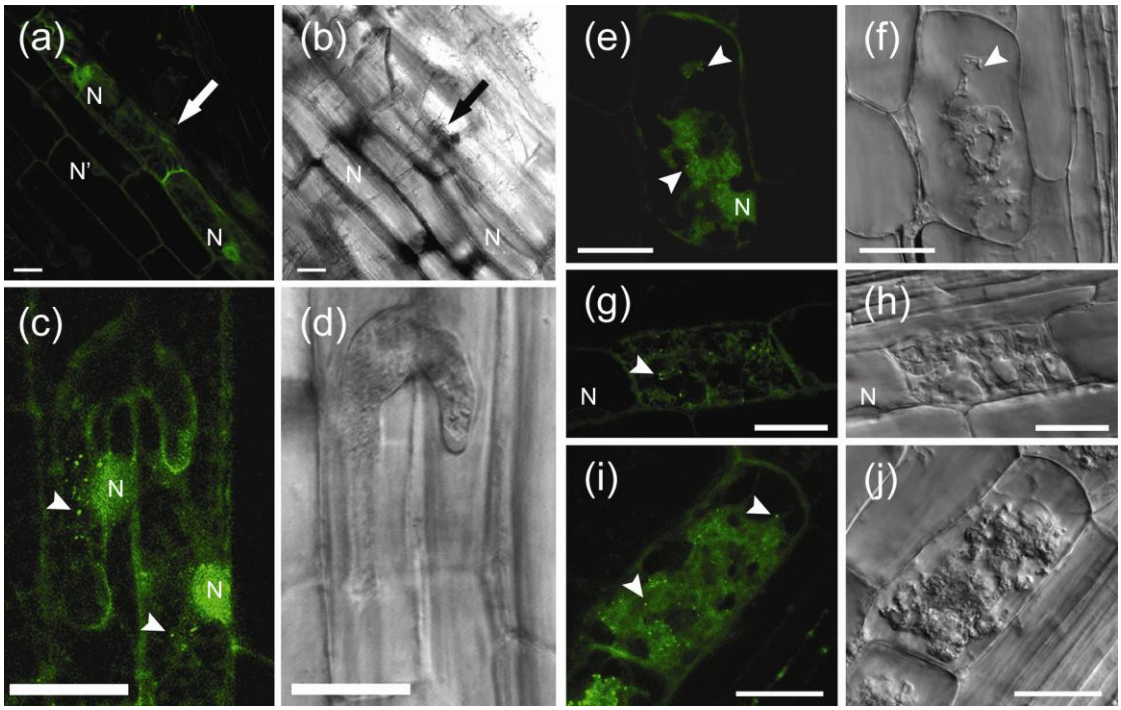

Figure 5-6. Localization of Vapyrin tagged with Green Fluorescent Protein (GFP) GFP signal from *proVapyrin:Vapyrin-GFP* (a,c,e,g) and *proVapyrin:GFP-Vapyrin* (i) and corresponding Nomarski (DIC) brightfield images (b,d,f,h,j).
(a,b) Vapyrin-GFP localizes in cytoplasmic accumulation beneath a hyphopodium (arrow) and in the nuclei of two epidermal cells (N) but not in the nucleus of a nearby cell (N'). (c,d) Vapyrin-GFP expressed in two epidermal cells penetrated by a hypha that has branched and grown into both cells. Signal accumulates in the cytoplasm and nuclei (N) and also in distinct puncta (arrowhead). (c) is a projection of 22 optical sections on the z axis taken at 0.4 μm intervals, (d) is a single DIC section, zoom = 2.5. (e,f) a cortical cell with a young arbuscule exhibits similar Vapyrin-GFP localization in cytoplasm, nucleus (N) and puncta (arrowheads). (e) is a projection of nine optical sections along the z axis at 0.5 μm intervals, (d) corresponding DIC of a single section, zoom = 3.5. (g,h) Vapyrin-GFP in a cell harboring a mature arbuscule. An adjacent cell with no intracellular fungus shows GFP signal in the cytoplasm but excluded from the nucleus (N). Single optical sections, zoom = 3.2. (i,j) N-terminal GFP fusion to Vapyrin (GFP-Vapyrin) localizes in the cytoplasm and discrete puncta (arrowheads) in a cell with an arbuscule. (i) is a projection of six optical sections along the z axis at 0.7 μm intervals, (j) single DIC section, zoom = 4.0.
Scale bars = 20 μm

adjacent cortical cells (Figure 5-6e-j). In cells with arbuscules, GFP signal was present in the cytoplasm and also concentrated in small puncta similar to those observed in the epidermal cells. These discrete, punctate accumulations occurred only in cells that contained arbuscules and were not observed in adjacent cortical cells. Free GFP does not show any punctate accumulation in colonized cells (Appendix 5-5) indicating the Vapyrin GFP patterns reflect an inherent property of the Vapyrin protein. The N-terminal fusion displayed a weaker GFP signal than the C-terminal fusion and we did not observe its expression in epidermal cells during hyphopodia formation likely for that reason. Both N- and C-terminal Vapyrin fusions showed similar localization patterns in the cortical cells, but in some cells, the C-terminal fusion showed a GFP signal in the nucleus, while the N-terminal fusion was visible only in the cytoplasm and not in the nucleus (Appendix 5-6 d, e). Interestingly, the nuclear signal was observed only in cells harboring fungal arbuscules or hyphae, but not in adjacent cells (Figure 5-6 a,g and Appendix 5-6 b). This could be the result of a post-translational modification, such as cleavage, that occurs specifically in cells accommodating fungal hyphae. For either construct, we were unable to detect GFP in the vascular tissue or root caps, regardless of AM colonization, suggesting the Vapyrin protein may be present at low levels, or possibly unstable in these cells.

To further evaluate the discrete GFP complexes that formed in cells with arbuscules, a series of time-lapse images were recorded using confocal microscopy. These revealed that the Vapyrin GFP puncta, both N- and C-terminal fusions, can move through the cytoplasm (Figure 5-5-7), and the style of movement resembles that of membrane-bound vesicles (daSilva et al., 2004). Vapyrin has no transmembrane domains, or predicted acylation sites, but has two protein

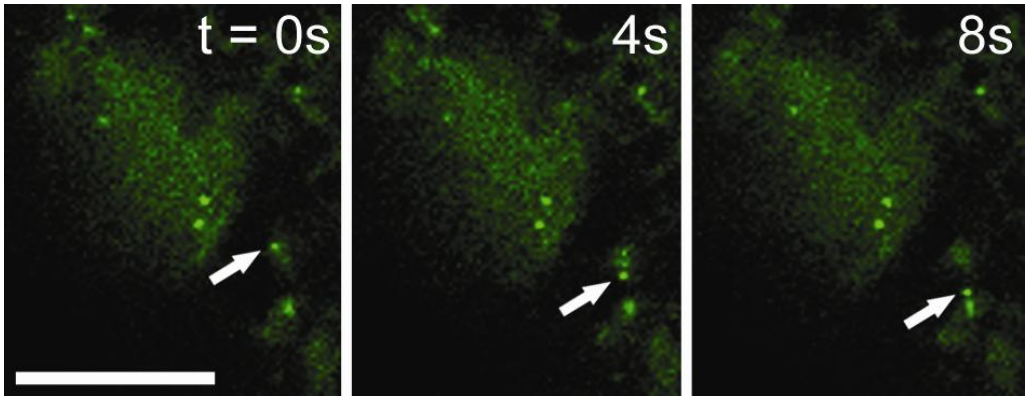

Figure 5-7. Vapyrin-GFP moves in discrete complexes.
Three successive images from a confocal time series of transgenic roots expressing *proVapyrin:Vapyrin-GFP* in a cell with an arbuscule reveal Vapyrin-labeled complexes move through the cytoplasm in discrete, vesicle-like complexes (arrow). Images at four second intervals. Zoom = 3.0. Scale bar = 10 µm.

interaction domains via which it could potentially interact with membrane-bound proteins trafficking through colonized cells.

Discussion

Vapyrin is required for AM symbiosis

There is much evidence to indicate that plant cells undergo substantial cellular alterations to accommodate their AM fungal symbionts, but the nature of the molecular components involved in the cellular reprogramming are largely unknown. While there has been considerable progress with the identification of a signaling pathway that controls fungal entry into the root, almost nothing is known about the molecular events that enable arbuscule formation within the root cortical cells. Here we report the discovery and initial characterization of a gene called *Vapyrin* from *M. truncatula* that is essential for arbuscule formation and required also for efficient epidermal penetration by AM fungi.

Vapyrin shows a basal level of expression in roots and is induced transiently in the epidermis and outer cortical cells as the fungal hyphae traverse these cells. *Vapyrin* is also induced in cortical cells containing arbuscules and in cells adjacent to those with arbuscules. The mycorrhizal phenotype of Vapyrin RNAi roots is consistent with the expression patterns and indicates a requirement for Vapyrin function both in the epidermis and in the cortical cells. In both cases, Vapyrin is needed to enable fungal hyphae to enter the plant cell. Vapyrin RNAi roots show a high frequency of hyphopodia which attempt, but fail, to penetrate the epidermal cells and infection arrests in the epidermis. This aspect of the phenotype is similar, although less severe, than that of the 'Common Sym' mutants (Parniske, 2008), where the fungus forms hyphopodia almost 100% of which are blocked at the epidermis. When the fungus succeeded in entering the cortex of Vapyrin RNAi roots, intercellular hyphae spread

laterally through the root but arbuscules were not formed. This phenotype is similar to that of the *cyclops* mutants of *Lotus japonicus* and rice (Kistner et al., 2005; Gutjahr et al., 2008; Yano et al., 2008) and the petunia mutant *pam1*, (Reddy et al., 2007) where fungal penetration of the epidermis is reduced and arbuscule formation is abolished. Taken together, these mutant phenotypes support the hypothesis that a common cellular mechanism may be required to enable hyphal growth through epidermal cells and arbuscule development in cortical cells. In addition to the mutant phenotypes, the 'pre-penetration apparatus', an intracellular structure composed of ER, cytoplasm and cytoskeletal components, that is assembled in the epidermal cells below the hyphopodia, was also observed in cortical cells prior to arbuscule development, and further supports this hypothesis (Genre et al., 2008). It could be envisaged that a single pathway evolved to enable intracellular passage of AM fungi, with additional tissue-specific or developmental signals to specify hyphal branching and development of the periarbuscular membrane in the cortical cells. The expression patterns and RNAi phenotype of *Vapyrin* suggest that it is a component of the cellular machinery necessary to accommodate intracellular AM fungal growth.

Why would one process, arbuscule formation, be absolutely abolished while another, root penetration, only impaired? For the RNAi phenotype reported here, it is possible that incomplete knockdown of Vapyrin mRNA produced sufficient protein to enable epidermal penetration but not arbuscule formation. This pattern of impaired epidermal penetration together with no arbuscule formation was also described for the *cyclops*, *ccamk* and *pam1* mutants, and may suggest these components can be bypassed for penetration of epidermal cells but not inner cortical cells. Conversely, other common sym mutants, such as *symrk*, do allow arbuscule formation after cortical colonization (Demchenko et al., 2004; Kistner et al., 2005).

Vapyrin may function in cellular rearrangement

Whereas the Common Sym genes, including *CYCLOPS*, encode signaling proteins, we hypothesize that *Vapyrin* may play a role in the cellular remodeling process. In contrast to Common Sym mutants, in Vapyrin RNAi roots, the fungus attempts to penetrate the cells and numerous hyphal projections are visible below the hyphopodia, but these generally fail to penetrate the cell. Similar aspects are observed in the cortex. This phenotype suggests that the signaling necessary to induce the penetration is intact but the cellular processes that support entry, possibly those that facilitate membrane invagination, are impaired.

The location of the Vapyrin protein is also consistent with a role in cellular remodeling. Both Vapyrin GFP fusions were localized primarily in the cytoplasm, and in cells harboring intracellular hyphae or arbuscules, the protein accumulated in distinct, mobile puncta. These puncta were not observed in non-colonized cells, which suggests that they signify a process specific to cells harboring intracellular fungal hyphae. It is possible the puncta represent vesicles or endomembrane compartments of the secretory pathway that might play a role in the deposition of membrane material. Alternatively, if Vapyrin behaves like the MSP proteins (Tarr and Scott, 2005) and has the ability to oligomerize, it is possible that the puncta represent Vapyrin oligomers. Interestingly, the C-terminal GFP fusion displayed some GFP signal in the nucleus, and while the relevance of this remains to be determined, overall, the Vapyrin location stands in sharp contrast to that of CCaMK/DMI3 and Cyclops/IPD3, which localize exclusively in the nucleus, supporting their roles in signal transduction (Smit et al., 2005; Messinese et al., 2007; Yano et al., 2008).

Finally, the Vapyrin protein is a unique combination of two domains that are well-established to mediate protein-protein interactions: An N-terminal VAP/MSP

homology domain and C-terminal ankyrin repeats. This composition could act as a scaffolding bridge between proteins to facilitate structural changes within the cell. The *VAP* family (for Vamp-Associated Protein) of proteins is conserved across eukaryotes and is characterized by an N-terminal MSP (Major Sperm Protein) domain, a central coiled-coil domain and a C-terminal transmembrane domain. The first VAP was discovered as an interactor of VAMP (Vesicle-Associated Membrane Protein) and required the central coiled-coil domain (Lev et al., 2008). Subsequent studies have shown a multitude of interacting proteins that function in various processes from secretion to cytoskeletal to lipid signaling (Lev et al., 2008). Many of these interactions are mediated by conserved residues that bind FFAT motifs (double phenylalanine in an acidic tract) in target proteins. Hetero- and homodimerization has also been reported for VAPs and requires the transmembrane domain (Nishimura et al., 1999). In Arabidopsis, VAP homologs (PVA genes) have been shown to localize in the ER and vacuolar membranes, and to interact with a sterol-binding protein and a motif that mediates transport to protein storage vacuoles (Oufattole et al., 2005; Saravanan et al., 2009). Vapyrin contains the VAP/MSP region at its N-terminus but does not have the coiled-coil or transmembrane domains of the VAP family, nor the conserved residues required for binding FFAT-containing proteins.

Ankyrin repeats are one of the most widely-dispersed eukaryotic protein motifs and function exclusively in mediating protein-protein interactions (Li et al., 2006). The repeated motif consists of a well-conserved 33 amino acid sequence that forms a helix-turn-helix structure. Ankyrin repeat-containing proteins function in diverse processes within cells. Examples of plant proteins containing ankyrin repeats include IGN1 (Ineffective Greenish Nodules), a protein from *Lotus japonicus* required for nodule function (Kumagai et al., 2007) and Arabidopsis Accelerated Cell Death 6 (ACD6) (Lu et al., 2005) involved in mediating defense responses; both of the

proteins also have transmembrane domains. The Arabidopsis genome is predicted to encode over 100 ankyrin repeat-containing proteins that fall into 16 classes based on additional motifs (Becerra et al., 2004). Despite the diversity of proteins containing ankyrin repeats, currently, the Vapyrin family is the only example in nature of a combination with a VAP/MSP domain.

In summary, the phylogenetic distribution of this novel protein suggests that Vapyrin is a unique evolution of the plant kingdom that arose early in the vascular plant lineage. Its absence from non-mycorrhizal species, Arabidopsis, is consistent with its role in symbiosis and is a pattern shared by several other genes required for AM symbiosis (Javot et al., 2007a; Parniske, 2008; Yano et al., 2008). While the molecular function of Vapyrin remains to be determined, the domain structure of the protein along with the localization data support a structural role, mediating interactions between two or more proteins, while the phenotypic data indicate a role in enabling AM fungi to enter plant cells.

EXPERIMENTAL PROCEDURES

Plant Growth and Transformation

M. truncatula cv. Jemalong, line A17 was used for all experiments described. Transgenic plants were produced by *Agrobacterium rhizogenes*-mediated root transformation (Boisson-Dernier et al., 2001). Briefly, seeds were surface-sterilized, germinated and root tips were excised and inoculated with *A. rhizogenes* strain ARqua1 harboring the appropriate vectors. Inoculated seedlings were grown on modified Fahraeus media with 25 mg/L kanamycin to select transformed roots (Liu et al., 2003). After three weeks, seedlings were transferred to sterile turface, four to six plants per 11-inch diameter pot, and grown for ten days and then inoculated with surface-sterilized *G. versiforme* spores or mock-inoculated with the final spore rinse

water as described previously (Liu et al., 2004). Plants were grown in growth rooms under a 16-h light (25 °C)/8-h (22 °C) dark regime and fertilized once a week with a modified ½-strength Hoagland's solution with full-strength nitrogen and 20 µM potassium phosphate (Arnon and Hoagland, 1940). Plants were analyzed 21-35 dpi with *G. versiforme*.

Cloning and Vector Construction

The Vapyrin promoter was amplified from a *M. truncatula* genomic library (Harrison et al., 2002) using the iProof enzyme (BioRad) with a Vapyrin primer, R1, and a standard T3 primer present in the vector. After amplification, the reaction was diluted and used as a template for a second and third PCR reactions using nested primers R2 and R3 resulting in a band of 1761 bp which was cloned and sequenced. To obtain the full-length Vapyrin ORF, first strand cDNA was synthesized from RNA from *M. truncatula/G. versiforme* roots by the SMART cDNA synthesis kit (Clontech). The cDNA was then used as a template for nested PCR with Vapyrin primers F1, F2, F3 (Appendix 5-8) and the provided 3' primer, and sequenced. The Vapyrin RNAi-1 and -2 plasmids were created by Gateway cloning (Invitrogen) in a modified pHellsgate 8 (Helliwell et al., 2002), that includes a Ubiquitin promoter:dsRed reporter cassette (J. Liu and M.J. Harrison, unpublished). The Vapyrin RNAi-1 construct was amplified from the EST clone CF069730 by a gene-specific reverse primer and vector-specific forward primer producing an RNAi hairpin corresponding to a 383 nucleotide region -150 to +233 nucleotides relative to the ATG. The Vapyrin RNAi-2 construct was amplified from genomic DNA with specific forward and reverse primers creating an RNAi hairpin corresponding to a 262 nucleotide region 1375 to 1748 nucleotides downstream of the ATG. This includes 238 nucleotides at the 3' end of the coding sequence and 24 nucleotides of 3' UTR.

This region is downstream of the ankyrin repeats to avoid possible silencing of other genes containing ankyrin repeats. A control RNAi vector was created similarly targeting a 400bp fragment of the GUS (UidA) gene. Primer sequences are shown in Appendix 5-8.

pVapyrin:UidA was created in pCAMBIA2301. A fragment corresponding to1761 bp upstream of the Vapyrin ATG was amplified from *M. truncatula* genomic DNA with primers that add 5' SacI and 3' PstI restriction sites, and ligated into SacI and PstI digested pCAMBIA2301. The UidA coding sequence was amplified from pCAMBIA2301 with primers that add a 5' PstI restriction site directly upstream of the ATG and include an endogenous 3' BstEII site. pCAMBIA2301 containing the *Vapyrin* promoter was digested with PstI and BstEII and the UidA gene inserted between these sites.

pVapyrin:GFP-Vapyrin was assembled beginning with the pCAMBIA2301 vector containing the *Vapyrin* promoter digested with PstI and BstEII. The Vapyrin open reading frame from the ATG to TAG, was amplified by PCR using primers that introduce a 5' PstI site directly upstream of the ATG and a 3' BstEII site directly downstream of the TAG. This fragment was ligated into the pCAMBIA2301 vector containing the *Vapyrin* promoter. The Green Fluorescent Protein, S65T variant (Chiu et al., 1996) was amplified using primers that introduce 5' and 3' PstI restriction sites and ligated into pCAMBIA2301 between the *Vapyrin* promoter and ORF after digestion with PstI restriction enzyme, resulting in an in-frame fusion of GFP to the 5' end of the *Vapyrin* ORF.

pVapyrin:Vapyrin-GFP was created using a pCAMBIA2301 vector with GFP S65T and the NOS terminator cloned into the multiple cloning site between the BamHI and EcoRI restriction sites. The *Vapyrin* promoter and ORF minus the stop codon were amplified with primers that added a 5' SalI site and a 3' BamHI site

(Appendix 5-8). This fragment was inserted between the SalI and BamHI sites of modified pCAMBIA2301 containing GFP. This created an in-frame fusion of GFP to the 3' end of the *Vapyrin* ORF.

All vectors were sequenced to confirm correct insertions and absence of mutations.

Protein predictions, alignments and phylogram construction

Protein domains were predicted by SMART through the ELM server (http://elm.eu.org, (Puntervoll et al., 2003)). The phylogram was constructed by a neighbor-joining ClustalX alignment of full-length amino acid sequences of genes with highest sequence similarity to *M. truncatula* Vapyrin, and included representative members of VAP and MSP gene families from plants, animals and fungi. Accession numbers are listed in Appendix 5-7. Distances were calculated by neighbor joining and bootstraps reflect values from 100 trials. The phylogram was constructed in TreeView (http://taxonomy.zoology.gla.ac.uk/rod/treeview.html).

Expression analysis

Induction of Vapyrin on an Affymetrix GeneChip array was reported in Gomez et al. (2009) as probesets Mtr.39050.1.S1, corresponding to the 5' end of *Vapyrin* (TC104091) and Mtr.42828.1.S1, representing the 3' end of *Vapyrin* (TC112496). *MtVpyl* is represented by Mtr.11779.1.S1 (TC111041) and is not significantly differentially-regulated on this array. These probesets were queried in the Medicago Gene Atlas (http://bioinfo.noble.org/gene-atlas). Gene expression in AM roots was analyzed using RNA extracted from *M. truncatula/G. versiforme* mycorrhizal roots and corresponding mock-inoculated controls, and *M. truncatula*/*Gigaspora gigantea* mycorrhizal roots and corresponding mock-inoculated control. In both cases, roots were harvested 28 days post inoculation and colonization levels were 76% and 44%

root length colonized (RLC) respectively. RNA was extracted from these samples, and also Vapyrin RNAi and GUS RNAi roots, using the Trizol method (Invitrogen Corporation, Carlsbad, CA) and 1 µg was used as template for cDNA synthesis with SuperScript III Reverse Transcriptase (Invitrogen) according to the protocol outlined in Gomez et al (2009).

To analyze transcript levels in RNAi plants, RNA was extracted with Trizol (Invitrogen Corporation, Carlsbad, CA) and 1 µg was used as template for cDNA synthesis with SuperScript III Reverse Transcriptase (Invitrogen) according to the protocol outlined in Gomez et al (2009). Quantitative RT-PCR was performed using an ABI PRISM 7900 HT sequence detection system in optical 384-well plates with SYBR Green PCR Master Mix (Applied Biosystems, http://www.appliedbiosystems.com). Three technical replicates were performed for each primer/cDNA combination in a 10 ul reaction including 40 ng cDNA and 200 nmoles of each primer. PCR cycle conditions were: 50°C for 2 min, 95°C for 10 min, 43 cycles of 95°C for 30 sec and 60°C for 30 sec, except *G. versiforme α-tubulin* which annealed at 57°C. Following amplification, a dissociation cycle of 95°C for 15 sec, 60°C for 15 sec and 95°C for 15 sec was performed and primers used in this study were confirmed to amplify one specific PCR product. Cycle threshold (Ct) values were calculated with SDS2.3 software (Applied Biosystems) using manual baseline and threshold values. Primer efficiency was calculated independently for each plate by LinRegPCR software (Ramakers et al., 2003) and used in calculating relative transcript abundance ($E^{\Delta Ct}$) after normalizing to *M. truncatula elongation factor 1α.*

The relative transcript levels in *G. versiforme* or *Gi. gigantea* mycorrhizal roots versus non-colonized roots was determined by the $E^{\Delta\Delta Ct}$ method. Primers are listed in Appendix 5-8.

Analysis of RNAi plants

Vapyrin RNAi and control plants were harvested 21 to 28 dpi with *G. versiforme*. For Vapyrin RNAi-1 and its GUS RNAi control, a representative sample of root tissue was excised from each whole root system and frozen in liquid nitrogen for RNA extraction. The remaining root samples were stained with wheat germ agglutinin (WGA) conjugated to Alexa Fluor 488 (Molecular Probes) to visualize fungal structures (Javot et al., 2007b). For Vapyrin RNAi-2 and corresponding GUS RNAi controls, individual transgenic roots were excised and part of the root was samples for RNA extraction, while the remainder was stained as described above and the mycorrhizal phenotype evaluated. Some samples were counter-stained with propidium iodide (PI, 10 µg/ml) to visualize plant cell walls (De Smet et al., 2008). Roots were examined microscopically and Vapyrin RNAi-1 and GUS RNAi control phenotypes were quantified by counting. For each individual root system, the number of hyphopodia that did not penetrate into the inner cortex, infections that penetrated the cortex and spread laterally but did not form arbuscule structures, and infections that penetrated and did form arbuscules were counted.

Conclusions were drawn from four independent experiments, which all showed similar phenotypes and included more than 45 individual Vapyrin RNAi-1 plants. Individual root sections from Vapyrin RNAi-2 and GUS root systems used for qRT-PCR showed similar phenotypes as those shown for Vapyrin RNAi-1 and GUS RNAi controls respectively, and the phenotype was observed in more than 10 individual Vapyrin RNAi-2 transgenic root systems. Representative infections from control and Vapyrin RNAi roots were imaged on a Leica TCS-SP5 confocal microscope (Leica Microsystems, Exton, PA USA) with a 63 x or 20 x water immersion objective, numerical apertures 1.2 and 0.7, respectively. WGA was excited with blue argon ion laser (488 nm), and emitted fluorescence was collected from 510 nm to 540 nm, PI

was excited with Diode-Pumped Solid State (DPSS) laser at 561 nm and fluorescence was collected from 640 to 710 nm.

Analysis of GUS reporter fusions

Expression of *pVapyrin:UidA* was evaluated in transgenic plants grown alone or 21 to 28 dpi with *G. versiforme*. Histochemical staining for β-glucuronidase (GUS) activity was performed as previously (Liu et al., 2008).

Analysis of GFP fusion proteins

Roots expressing Vapyrin GFP fusions were identified using a dissecting microscope (Olympus SZX-12 Stereo Microscope). To study protein localization during hyphopodia formation, roots expressing epidermal GFP were excised and imaged on a Leica TCS-SP5 confocal microscope. To analyze GFP expression in the inner cortex, roots were bisected longitudinally through the stele and imaged as described previously (Pumplin and Harrison, 2009). Only undisrupted cells in layers below the cut surface were imaged. GFP was excited with the blue argon ion laser (488 nm), and emitted fluorescence was collected from 505 nm to 545 nm; DIC (differential interference contrast) images were collected together with fluorescence images using the transmitted light detector. GmMan1-mCherry was excited with a Diode-Pumped Solid State (DPSS) laser at 561 nm and emitted fluorescence was collected from 590 to 640 nm. Controls were performed to assure no cross over between channels. Images were processed using Leica LAS-AF software (version 1.6.3 and 1.7.0), Adobe Photoshop CS2 version 7 (Adobe systems).

Vapyrin and *Vapyrin-like (MtVpyl)* gene sequences were deposited in Genbank™ under accession numbers GQ423209 (*Vapyrin*) and GQ423210 (*Vapyrin-like*).

Appendix 5-1 Vapyrin RNAi inhibits arbuscule formation

G. versiforme infections with arbuscules (left) and without arbuscules (right) were counted in *M. truncatula* GUS RNAi control (white bars) and Vapyrin RNAi roots (black bars). Control n = 5 plants, Vapyrin RNAi n = 6. Error bars depict standard deviation, $p<0.001$ student's t test.

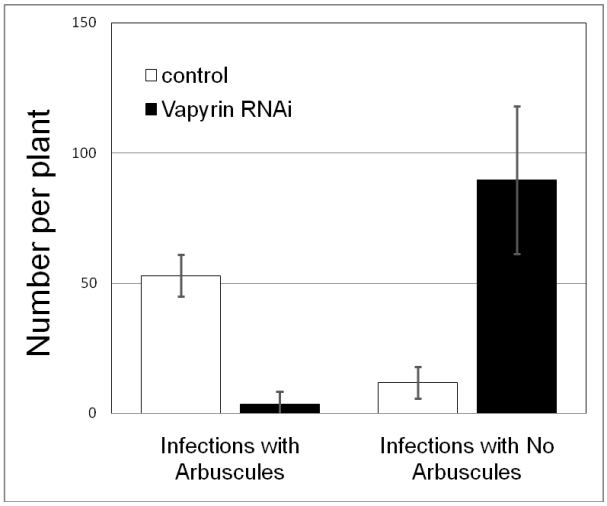

Appendix 5-2 Vapyrin knockdown impairs arbuscule formation by Gigaspora gigantea

Colonization morphology of the AM fungus *Gigaspora gigantea* (*Gg*) in (a) control and (b) Vapyrin RNAi roots visualized by wheatgerm agglutinin (WGA) conjugated to Alexa Fluor 488. *Gg* fails to form arbuscules in Vapyrin RNAi roots and instead displays short hyphal protrusions and septate hyphae. (a) is a projection of 26 optical sections on the z axis taken at 0.5 µm intervals. (b) is a projection of 7 sections at 0.31 µm intervals. Scale bar = 25 µm.

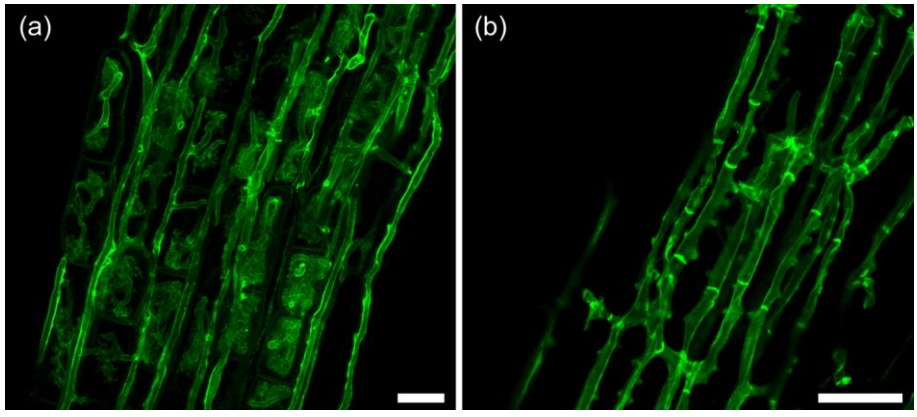

Appendix 5-3 Vapyrin conservation in angiosperms.
ClustalW alignment performed with putative orthologs of *M. truncatula* Vapyrin found in *Poplar* (Pt) and Rice (Os). These genes exist as single-copy in sequence databases. N-terminal VAP/MSP domain and C-terminal ankyrin repeats are underlined. While Vapyrin is predicted to have eight ankyrin repeats, the Poplar homolog has a ninth predicted ankyrin repeat (highlighted in gray) with high similarity to *M. truncatula* Vapyrin, suggesting a possible ninth functional ankyrin repeat. Rice Vapyrin is predicted to have eight ankyrin repeats. Vapyrin shares ~70% identity with PtVpy and ~40% with OsVpy

```
Vapyrin       MDRLIKLDPSNIVLIRVEEGQKCLGKITLNNVMYTMPVAFRIQPLIKTRYTIKPQSGIIS
PtVpy         MDRLIGLEPSNLVSIRIEPGQKCYGELTLRNVMYTMPVAFRIQALNKTRYTIKPQSGIIS
OsVpy         MDRLVIPEPTNEVVVRVEPGRPARGELTLRNAMHTMPVAFRLQPAVRSRFAVRPHTGILA
              ****:  :*:* * :*:* *: . *::**.*.*:*******:*.  ::*::::*::**::

Vapyrin       PLASLVIEITYHPPQQQGSNNLPHSFPFSDDSFLLHSVLAPGAAIKEPSSMFDSVPSDWF
PtVpy         PLATLTIEITYHLSP--GS-LLPETFPHCEDSFLLHSVVVPGAAIKDATSSMDAVPIDWF
OsVpy         PLAAVTVEVVYLASAAPEGPGGGGGAGRGEDAFLLHSVVAPGAAVREPVTALDSVNPEWF
              ***::.:*:.*  .    .          :*:******:.****:::. : :*:*  :**

Vapyrin       TTKKKQVFIDSAIKVMFVGSQILTQLVEDGNSMDDIREVLEKSDPLWESVNSKDSQGQTL
PtVpy         TTRKKQVFIDSGIKVMFVGSPILAQLVMDG-LMDEIREVLEHSDPAWNPADAVDFHGKTL
OsVpy         SARRKQVFVDSGIRACFVGAAVAARLVEAG-AVEALREVLDRSEPEWRAADAVDESGRTL
              ::::****:**.*:. ***: : ::**  *  :: :****::*:* *...:: *  *:**

Vapyrin       LHLAISKTRPDLVQLILEFKPDIEAINSVGSTPLEAASSSGESLIVELLLAHKANTEGSE
PtVpy         LHLAISQSRADIVQLLLEFEPDVEFQSRSGYSPLEAAARSGEALIVELLLARRASTERSQ
OsVpy         LDLAVGLGRADIVQVLLEYGADADKPSR-GRTPLETAAASGECLIAELLLANGATPAGSD
              *.**:.  *.*:**::**: .* :  .  * :***:*: ***.**.*****. *..  *:

Vapyrin       SSVFRPIHHASREGHMEILRLLLLKGAR-----------------VDSLTKDGNTSLHLA
PtVpy         SSTWGPIHLAAGGGHLEVLRLLLLKGAN-----------------VNALTKDGNTALHLA
OsVpy         -----ALHVAAAAGHNDVLKLLLGKPASASPSSASSASFSCSFTSIDAAGRDGKTPLRLA
                   .:* *:  ** ::*:*** * *                   :::  :**:*.*:**

Vapyrin       VEEKRRDCARLLLANGARTDVRNMREGDTPLHIAAANGDENMVKLLLHKGAT--KYVRNK
PtVpy         VEERRRDCARLLLASGAKADIRNNGDGDTPLHIAAGLGDENMVKLLLHKGAN--KDIRNK
OsVpy         AEAGRRDAVKALLAAGARADARCGADGGTALHAAARRGDEVIARLILANGAAGTAAVRDA
              .*  ***..: *** **::* *   :*.*.** **  *** :.:*:* :**     :*:

Vapyrin       LGKTAFDVAAENGHS-RLFDALRLGDNLCAAARKGEVRTIQKVLESGGVINGRDQNGWTS
PtVpy         NGKIAYDIAAEHGHA-RLFDALKLGDSLCIAARKGEVRTINRLIENGAAINGRDQHGWTA
OsVpy         AGKTAFEIAAEECHGGRIMDFLGLGEAILAAARKGEARAVRRAADGGASVEGRDAHGWTP
               ** *:::***. *. *::* * **: :  ******.*::.:  :.*. ::*** :***.

Vapyrin       LHRAAFKGRMDAVRFLVEKGIDLDAKDEDGYTALHCAAESGHADVTEFLVKKGADVEART
PtVpy         LHRAAFKGKTDAVRVLIEKGIDVDAKDEDGYTALHCAVESGHADVIELLVKKGADVEART
OsVpy         LMRAAFKGRADTVRDLVDRGADMDATDAEGYTALHCAAEAGRADVVDLLLKSGANAKTTT
              * ******: *:** *:::* *:**.* :********.*:*:*** ::*:*.**:.:: *

Vapyrin       NKGVSALQIVESLNYVGITRILVNGGASREGLGE-KPPSAPSKIPFGRKVESGSVMTMKK
PtVpy         NKGVTALQIAESLHYVGITRVLIHGGAAKDGVTQLVVPALHSPFRNGMAGKEVETKPMKK
OsVpy         VKGRSAAEVAAAAGKSKVVRLLEKAG----GVGRKEVAEKTSPAAVVGKAGSLDRRRRGR
               ** :* ::. :     :.*:* :.*    *: .   .   *         . .     :

Vapyrin       KMSSRTRALRGSFDHSMPLAVL-----
PtVpy         RP-LRARTLRGSFDRAMPLAVV-----
OsVpy         KGSSGAIRFGGGKDGFETAAVAVGWSH
              :    :  : *. *   . **
```

Appendix 5-4 Vapyrin gene expression in M. truncatula roots during interaction with Glomus versiforme and Gigaspora gigantea.

cDNA generated from RNA extracted from *M. truncatula* roots colonized by *Glomus versiforme* (*Gv*) and *Gigaspora gigantea* (*Gigi*) and non-mycorrhizal control plants grown under the same conditions was used for transcript analysis by Quantitative RT-PCR. Transcripts were normalized to the constitutive *Elongation Factor 1-α* (*EF*) and relative transcript levels in colonized and non-colonized samples were determined by the $E^{\Delta\Delta Ct}$ method and graphed on a log scale. *MtVpyl* is not induced by colonization, while *Vapyrin* is induced 5-fold in each sample relative to non-colonized controls. Transcripts of *MtPT4*, a marker for arbuscules, and fungal *α-tubulin* are specific to colonized samples and show strong induction over 1000-fold. Data are derived from three technical replicates.

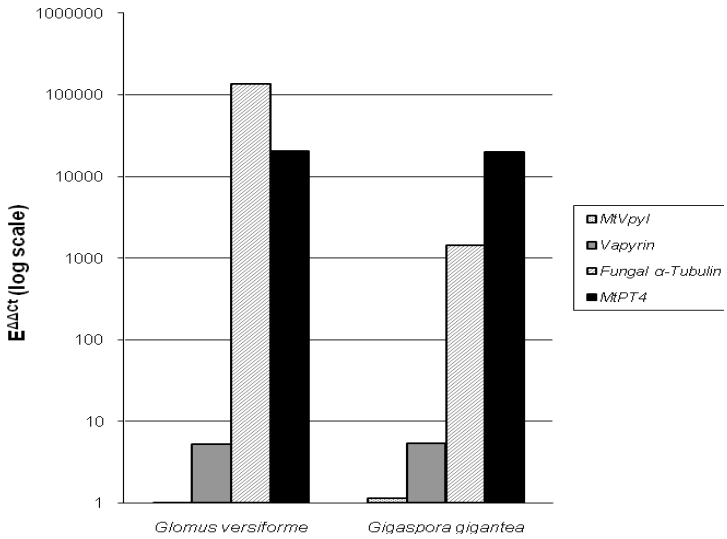

Appendix 5-5 Localization of free GFP in cells with arbuscules

Free GFP expressed from the MtSCP1 promoter localizes in the cytoplasm and nucleus of cortical cells in *M. truncatula /G. versiforme* mycorrhizal roots as described by Liu *et al.* (2003) and does not present any punctate staining patterns. Scale bar = 20 μm.

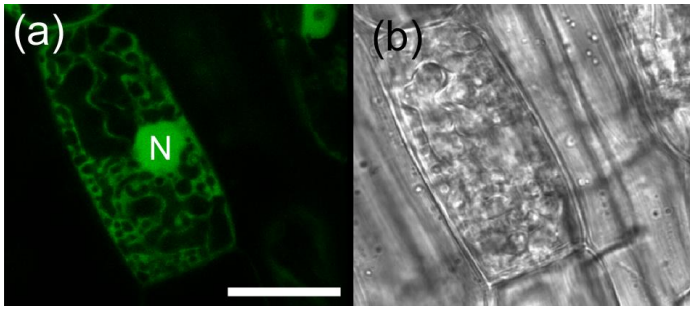

Appendix 5-6 Comparison of N- and C-terminal Vapyrin GFP fusions
(a-c) GFP and DIC images of colonized roots expressing *proVapyrin:Vapyrin-GFP*, (d) *proVapyrin:GFP-Vapyrin*. (a) Multiple Vapyrin-GFP puncta in a cell harboring an arbuscule. (b) Vapyrin-GFP is excluded from nuclei in cells adjacent to a cell with an arbuscule, A. (c) Vapyrin-GFP in the nucleus of a cell harboring an arbuscule.
(d) GFP-Vapyrin does not show signal in the nucleus in cells with arbuscules.
Scale bar = 20 μm

(a)

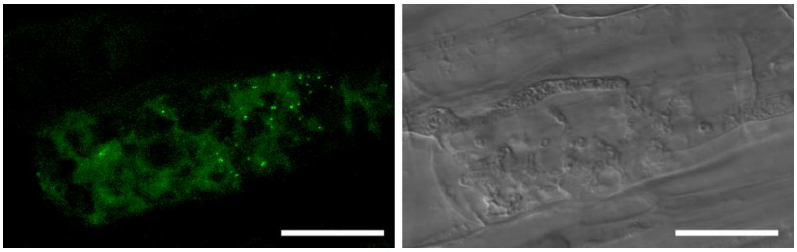

(b)

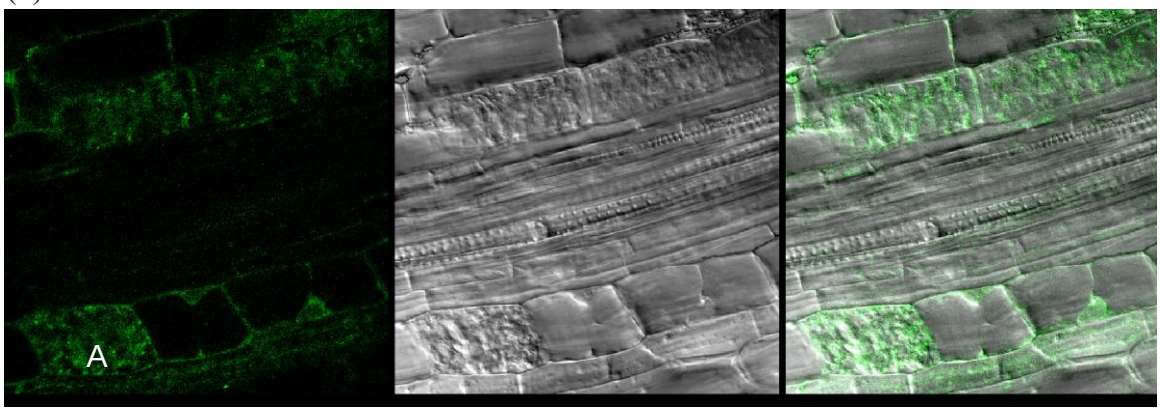

(c)

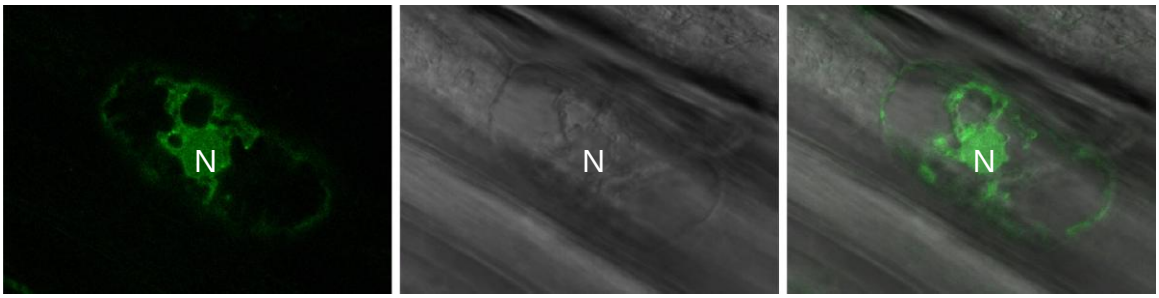

(d)

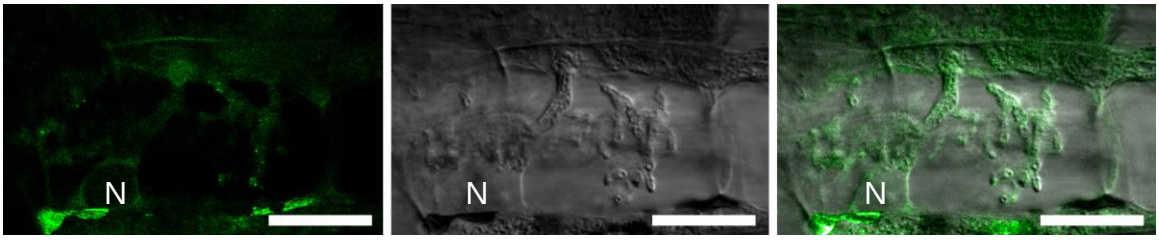

Appendix 5-7 Accession Numbers used in phylogram construction

Medicago Vapyrin	GQ423209	*Medicago truncatula*
Medicago Vpyl	GQ423210	*Medicago truncatula*
Poplar Vpy	EEE95634	*Populus trichocarpa*
Grape Vpy	CAN63755	*Vitis vinifera*
Castor Vpy	EEF36691	*Ricinus communis*
Soybean Vpy	AC235255	*Glycine max*
Rice Vpy	AAT78832	*Oryza sativa*
Maize Vpy	ACG29376	*Zea mays*
Sorghum Vpy	EER93727	*Sorghum bicolor*
Selaginella VpyA	Scaffold 113	*Selaginella moellendorffii*
Selaginella VpyB	Scaffold 8	*Selaginella moellendorffii*
Poplar Vpyl	EEE80831	*Populus trichocarpa*
Grape Vpyl	CAN75193	*Vitis vinifera*
Tomato VpylA	AC214463 13500-12000	*Solanum lycopersicum*
Tomato VpylB	AC214463 10300-11700	*Solanum lycopersicum*
Castor Vpyl	EEF41675	*Ricinus communis*
Zebra fish VapA	AAI54768	*Danio rerio*
Drosophila VAP	EDW72210	*Drosophila willistoni*
Human VAP	AF154847	*Homo sapiens*
Nematode VAP	AAB96705	*Caenorhabditis elegans*
Yeast Scs2p	AAC03218	*Saccharomyces cerevisiae*
Medicago VAP	ABW70158	*Medicago truncatula*
Arabidopsis VAP	AAP13405	*Arabidopsis thaliana*
Medicago MSP	ABD32337	*Medicago truncatula*
Arabidopsis MSP	AAL49912	*Arabidopsis thaliana*
Rice MSP	EAZ05645	*Oryza sativa*
Nematode MSP	AAA28116	*Caenorhabditis elegans*

Appendix 5-8 List of primers used in these studies.

Quantitative RT-PCR	
Vapyrin F	TCATCCTCCACAACAACAAGGT
Vapyrin R	TCAAGCACTTCTCTTATGTCATCCATTG
MtVpyl F	TAGTAGGTCCCACCGTCGC
MtVpyl R	CCAGCGGTGATTAGATCGGTAAC
EF-1 alpha F	TGACAGGCGATCTGGTAAGG
EF-1 alpha R	TCAGCGAAGGTCTCAACCAC
TC105406 F Gv/Gi a-Tub	TGTCCAACCGGTTTTAAAGT
TC105406 R Gv/Gi a-Tub	AAAGCACGTTTGGCGTACAT
AJ717314 F Gigi a-Tub	TTCCCATTGGTTACCTACGC
AJ717314 R Gigi a-Tub	ACAAATTGGATGGTGCGTTT
MtPT4 F	gacacgaggcgctttcatagcagc
MtPT4 R	gtcatcgcagctggaacagcaccg
RACE primers	
Vapyrin F1	ACCAAAAGTGTTGTGAAACATCA
Vapyrin F2	GTCATGTACACTATGCCAGTTGCA
Vapyrin F3	TAGGCTTTTGTTAGCGAACGGG
Vapyrin R1	CCAAAGACATCAGACAACCACA
Vapyrin R2	TCCATTGGCTGCTGCTATGT
Vapyrin R3	CAAGGATCAATTGACCAAGATCA
cloning	
Vapyrin Promoter 5' SacI	gagagagctcCGGTAAGGGTTACATAAAAGATCGA
Vapyrin Promoter 3' PstI	GTGTCTGCAGGTTTTTGGTTTAGGGTTTGTATTGA
UidA 5′ PstI	GagactgcagtAtggtagatctgagggtaaatttc
UidA 3' BstEII	GGTCACCTGTAATTCACACG
Vapyrin CDS 5′ PstI	gagactgcagATGGATAGACTCATAAAGTTAGATCCA
Vapyrin CDS 3′ BstEII	cacaggtgaccctaAAGAACAGCCAAAGGCATTGA
GFP 5′ PstI	gagactgcagatggtgagcaagggcga
GFP 3' PstI	gagaCTGCAGCTTGTACAGCTCGTCCATGC
Vapyrin Promoter 5' SalI	gagagtcgacCGGTAAGGGTTACATAAAAGATCGA
Vapyrin CDS 3′ BamHI	cacaggatccAAGAACAGCCAAAGGCATTGA
GUS RNAi F	GGGGACAAGTTTGTACAAAAAAGCAGGCTcccttacgctgaagagatgc
GUS RNAi R	GGGGACCACTTTGTACAAGAAAGCTGGGTggcacagcacatcaaagaga
Vapyrin RNAi-1 R	Ccttgttgttgtggaggatg
Vapyrin RNAi-2 F	GGGGACAAGTTTGTACAAAAAAGCAGGCTAGGTGTTAGTGCTTTGCAAATTGT
Vapyrin RNAi-2 R	GGGGACCACTTTGTACAAGAAAGCTGGGTCCCTCCAACTAACTCGATTGCT

REFERENCES

Akiyama, K., Matsuzaki, K., and Hayashi, H. (2005). Plant sesquiterpenes induce hyphal branching in arbuscular mycorrhizal fungi. Nature **435,** 824-827.

Ane, J.M., Kiss, G.B., Riely, B.K., Penmetsa, R.V., Oldroyd, G.E., Ayax, C., Levy, J., Debelle, F., Baek, J.M., Kalo, P., Rosenberg, C., Roe, B.A., Long, S.R., Denarie, J., and Cook, D.R. (2004). *Medicago truncatula* DMI1 required for bacterial and fungal symbioses in legumes. Science **303,** 1364-1367.

Arnon, D.I., and Hoagland, D.R. (1940). Crop production in artificial culture solutions and in soils with special reference to factors influencing yields and absorption of inorganic nutrients. Soil Sci. **50,** 463-483.

Bago, B., Pfeffer, P.E., and Shachar-Hill, Y. (2000). Carbon metabolism and transport in arbuscular mycorrhizas. Plant Physiology **124,** 949-957.

Barker, S.J., Stummer, B., Gao, L., Dispain, I., O'Connor, P.J., and Smith, S.E. (1998). A mutant in *Lycopersicon esculentum* Mill. with highly reduced VA mycorrhizal colonization: isolation and preliminary characterisation. Plant Journal **15,** 791-797.

Becerra, C., Jahrmann, T., Puigdomènech, P., and Vicient, C.M. (2004). Ankyrin repeat-containing proteins in *Arabidopsis*: characterization of a novel and abundant group of genes coding ankyrin-transmembrane proteins. Gene **340,** 111-121.

Benedito, V.A., Torres-Jerez, I., Murray, J.D., Andriankaja, A., Allen, S., Kakar, K., Wandrey, M., Verdier, J., Zuber, H., Ott, T., Moreau, S., Niebel, A., Frickey, T., Weiller, G., He, J., Dai, X., Zhao, P.X., Tang, Y., and Udvardi, M.K. (2008). A gene expression atlas of the model legume *Medicago truncatula*. Plant J **55,** 504-513.

Besserer, A., Puech-Pages, V., Kiefer, P., Gomez-Roldan, V., Jauneau, A., Roy, S., Portais, J.C., Roux, C., Becard, G., and Sejalon-Delmas, N. (2006). Strigolactones stimulate arbuscular mycorrhizal fungi by activating mitochondria. PLoS Biol **4,** e226.

Boisson-Dernier, A., Chabaud, M., Garcia, F., Becard, G., Rosenberg, C., and Barker, D.G. (2001). *Agrobacterium rhizogenes*-transformed roots of *Medicago truncatula* for the study of nitrogen-fixing and endomycorrhizal symbiotic associations. Mol Plant Microbe Interact **14,** 695-700.

Bonfante, P., and Genre, A. (2008). Plants and arbuscular mycorrhizal fungi: an evolutionary-developmental perspective. Trends Plant Sci **13,** 492-498.

Chiu, W.-l., Niwa, Y., Zeng, W., Hirano, T., Kobayashi, H., and Sheen, J. (1996). Engineered GFP as a vital reporter in plants. Curr. Biol. **6,** 325-330.

daSilva, L.L., Snapp, E.L., Denecke, J., Lippincott-Schwartz, J., Hawes, C., and Brandizzi, F. (2004). Endoplasmic reticulum export sites and Golgi bodies behave as single mobile secretory units in plant cells. Plant Cell **16,** 1753-1771.

David-Schwartz, R., Gadkar, V., Wininger, S., Bendov, R., Galili, G., Levy, A.A., and Kapulnik, Y. (2003). Isolation of a premycorrhizal infection (pmi2) mutant of tomato, resistant to arbuscular mycorrhizal fungal colonization. Mol Plant Microbe Interact **16,** 382-388.

De Smet, I., Vassileva, V., De Rybel, B., Levesque, M.P., Grunewald, W., Van Damme, D., Van Noorden, G., Naudts, M., Van Isterdael, G., De Clercq, R., Wang, J.Y., Meuli, N., Vanneste, S., Friml, J., Hilson, P., Jurgens, G., Ingram, G.C., Inze, D., Benfey, P.N., and Beeckman, T. (2008). Receptor-like kinase ACR4 restricts formative cell divisions in the *Arabidopsis* root. Science **322,** 594-597.

Demchenko, K., Winzer, T., Stougaard, J., Parniske, M., and Pawlowski, K. (2004). Distinct roles of *Lotus japonicus* SYMRK and SYM15 in root colonization and arbuscule formation. New Phytologist **163,** 381-392.

Endre, G., Kereszt, A., Kevei, Z., Mihacea, S., Kalo, P., and Kiss, G.B. (2002). A receptor kinase gene regulating symbiotic nodule development. Nature **417,** 962-966.

Gadkar, V., David-Schwartz, R., Nagahashi, G., Douds, D.D., Wininger, S., and Kapulnik, Y. (2003). Root exudate of pmi tomato mutant M161 reduces AM fungal proliferation in vitro. Fems Microbiology Letters **223,** 193-198.

Gao, L.L., Delp, G., and Smith, S.E. (2001). Colonization patterns in a mycorrhiza-defective mutant tomato vary with different arbuscular-mycorrhizal fungi. New Phytologist **151,** 477-491.

Genre, A., Chabaud, M., Timmers, T., Bonfante, P., and Barker, D.G. (2005). Arbuscular mycorrhizal fungi elicit a novel intracellular apparatus in *Medicago truncatula* root epidermal cells before infection. Plant Cell **17,** 3489-3499.

Genre, A., Chabaud, M., Faccio, A., Barker, D.G., and Bonfante, P. (2008). Prepenetration apparatus assembly precedes and predicts the colonization patterns of arbuscular mycorrhizal fungi within the root cortex of both *Medicago truncatula* and *Daucus carota*. Plant Cell **20,** 1407-1420.

Gianinazzi-Pearson, V. (1996). Plant cell responses to arbuscular myorrhiza fungi: Getting to the roots of the symbiosis. Plant Cell **8,** 1871-1883.

Gianinazzi-Pearson, V., Gianinazzi, S., Guillemin, J., Trouvelot, A., and Duc, G. (1991). Genetic and cellular analysis of resistance to vesicular arbuscular (VA) mycorrhizal fungi in pea mutants. In Advances in Molecular Genetics of Plant-Microbe Interactions, Vol. 1, H. Hennecke and D.P.S. Verma, eds (Netherlands: Kluwer Academic Publishers), pp. 336-342.

Gomez, S.K., Javot, H., Deewatthanawong, P., Torres-Jerez, I., Tang, Y.H., Blancaflor, E.B., Udvardi, M.K., and Harrison, M.J. (2009). *Medicago truncatula* and *Glomus intraradices* gene expression in cortical cells harboring arbuscules in the arbuscular mycorrhizal symbiosis. Bmc Plant Biology **9,** 1-19.

Govindarajulu, M., Pfeffer, P.E., Jin, H., Abubaker, J., Douds, D.D., Allen, J.W., Bucking, H., Lammers, P.J., and Shachar-Hill, Y. (2005). Nitrogen transfer in the arbuscular mycorrhizal symbiosis. Nature **435,** 819-823.

Guether, M., Balestrini, R., Hannah, M., He, J., Udvardi, M.K., and Bonfante, P. (2009). Genome-wide reprogramming of regulatory networks, transport, cell wall and membrane biogenesis during arbuscular mycorrhizal symbiosis in *Lotus japonicus*. New Phytol **182,** 200-212.

Guimil, S., Chang, H.S., Zhu, T., Sesma, A., Osbourn, A., Roux, C., Ioannidis, V., Oakeley, E.J., Docquier, M., Descombes, P., Briggs, S.P., and Paszkowski, U. (2005). Comparative transcriptomics of rice reveals an ancient pattern of response to microbial colonization. Proc Natl Acad Sci U S A **102,** 8066-8070.

Gutjahr, C., Banba, M., Croset, V., An, K., Miyao, A., An, G., Hirochika, H., Imaizumi-Anraku, H., and Paszkowski, U. (2008). Arbuscular mycorrhiza-specific signaling in rice transcends the common symbiosis signaling pathway. Plant Cell **20,** 2989-3005.

Harrison, M.J., and Dixon, R.A. (1993). Isoflavonoid Accumulation and Expression of Defense Gene Transcripts During the Establishment of Vesicular-Arbuscular Mycorrhizal Associations in Roots of *Medicago truncatula*. Mol. Plant-Microbe Interactions **6,** 643-654.

Harrison, M.J., Dewbre, G.R., and Liu, J. (2002). A phosphate transporter from *Medicago truncatula* involved in the acquisition of phosphate released by arbuscular mycorrhizal fungi. Plant Cell **14,** 2413-2429.

Helliwell, C.A., Wesley, S.V., Wielopolska, A.J., and Waterhouse, P.M. (2002). High-throughput vectors for efficient gene silencing in plants. Funct. Plant Biol. **29,** 1217-1225.

Hohnjec, N., Vieweg, M.F., Pühler, A., Becker, A., and Küster, H. (2005). Overlaps in the transcriptional profiles of *Medicago truncatula* roots inoculated with two different *Glomus* fungi provide insights into the genetic program activated during arbuscular mycorrhiza. Plant Physiology **137,** 1283-1301.

Imaizumi-Anraku, H., Takeda, N., Charpentier, M., Perry, J., Miwa, H., Umehara, Y., Kouchi, H., Murakami, Y., Mulder, L., Vickers, K., Pike, J., Downie, J.A., Wang, T., Sato, S., Asamizu, E., Tabata, S., Yoshikawa, M., Murooka, Y., Wu, G.J., Kawaguchi, M., Kawasaki, S., Parniske, M., and Hayashi, M. (2005). Plastid proteins crucial for symbiotic fungal and bacterial entry into plant roots. Nature **433,** 527-531.

Ivashuta, S., Liu, J., Lohar, D.P., Haridas, S., Bucciarelli, B., VandenBosch, K.A., Vance, C.P., Harrison, M.J., and Gantt, J.S. (2005). RNA interference identifies a calcium-dependent protein kinase involved in *Medicago truncatula* root development. Plant Cell **17,** 2911-2921.

Javot, H., Pumplin, N., and Harrison, M.J. (2007a). Phosphate in the arbuscular mycorrhizal symbiosis: transport properties and regulatory roles. Plant Cell Environ **30,** 310-322.

Javot, H., Penmetsa, R.V., Terzaghi, N., Cook, D.R., and Harrison, M.J. (2007b). A *Medicago truncatula* phosphate transporter indispensable for the arbuscular mycorrhizal symbiosis. Proc Natl Acad Sci U S A **104,** 1720-1725.

Kanamori, N., Madsen, L.H., Radutoiu, S., Frantescu, M., Quistgaard, E.M., Miwa, H., Downie, J.A., James, E.K., Felle, H.H., Haaning, L.L., Jensen, T.H., Sato, S., Nakamura, Y., Tabata, S., Sandal, N., and Stougaard, J. (2006). A nucleoporin is required for induction of Ca2+ spiking in legume nodule development and essential for rhizobial and fungal symbiosis. Proc Natl Acad Sci U S A **103,** 359-364.

Kistner, C., Winzer, T., Pitzschke, A., Mulder, L., Sato, S., Kaneko, T., Tabata, S., Sandal, N., Stougaard, J., Webb, K.J., Szczyglowski, K., and Parniske, M. (2005). Seven *Lotus japonicus* genes required for transcriptional reprogramming of the root during fungal and bacterial symbiosis. Plant Cell **17,** 2217-2229.

Kosuta, S., Chabaud, M., Lougnon, G., Gough, C., Denarie, J., Barker, D.G., and Becard, G. (2003). A diffusible factor from arbuscular mycorrhizal fungi induces symbiosis-specific MtENOD11 expression in roots of *Medicago truncatula*. Plant Physiol **131,** 952-962.

Kosuta, S., Hazledine, S., Sun, J., Miwa, H., Morris, R.J., Downie, J.A., and Oldroyd, G.E. (2008). Differential and chaotic calcium signatures in the symbiosis signaling pathway of legumes. Proc Natl Acad Sci U S A **105,** 9823-9828.

Kumagai, H., Hakoyama, T., Umehara, Y., Sato, S., Kaneko, T., Tabata, S., and Kouchi, H. (2007). A novel ankyrin-repeat membrane protein, IGN1, is required for persistence of nitrogen-fixing symbiosis in root nodules of *Lotus japonicus*. Plant Physiol **143,** 1293-1305.

Lev, S., Ben Halevy, D., Peretti, D., and Dahan, N. (2008). The VAP protein family: from cellular functions to motor neuron disease. Trends Cell Biol **18,** 282-290.

Levy, J., Bres, C., Geurts, R., Chalhoub, B., Kulikova, O., Duc, G., Journet, E.P., Ane, J.M., Lauber, E., Bisseling, T., Denarie, J., Rosenberg, C., and Debelle, F. (2004). A putative Ca2+ and calmodulin-dependent protein kinase required for bacterial and fungal symbioses. Science **303,** 1361-1364.

Li, J.N., Mahajan, A., and Tsai, M.D. (2006). Ankyrin repeat: A unique motif mediating protein-protein interactions. Biochemistry **45,** 15168-15178.

Liu, J., Blaylock, L., and Harrison, M.J. (2004). cDNA arrays as tools to identify mycorrhiza-regulated genes: identification of mycorrhiza-induced genes that encode or generate signaling molecules implicated in the control of root growth. Can. J. Bot. **82,** 1177-1185.

Liu, J., Versaw, W.K., Pumplin, N., Gomez, S.K., Blaylock, L.A., and Harrison, M.J. (2008). Closely related members of the *Medicago truncatula* PHT1 phosphate transporter gene family encode phosphate transporters with distinct biochemical activities. J Biol Chem **283,** 24673-24681.

Liu, J., Blaylock, L., Endre, G., Cho, J., Town, C.D., VandenBosch, K., and Harrison, M.J. (2003). Transcript profiling coupled with spatial expression analyses reveals genes involved in distinct developmental stages of the arbuscular mycorrhizal symbiosis. Plant Cell **15,** 2106-2123.

Lu, H., Liu, Y., and Greenberg, J.T. (2005). Structure-function analysis of the plasma membrane- localized Arabidopsis defense component ACD6. Plant J **44,** 798-809.

Maeda, D., Ashida, K., Iguchi, K., Chechetka, S.A., Hijikata, A., Okusako, Y., Deguchi, Y., Izui, K., and Hata, S. (2006). Knockdown of an Arbuscular

Mycorrhiza-inducible Phosphate Transporter Gene of *Lotus japonicus* Suppresses Mutualistic Symbiosis. Plant Cell Physiol. **47,** 807-817.

Messinese, E., Mun, J.H., Yeun, L.H., Jayaraman, D., Rouge, P., Barre, A., Lougnon, G., Schornack, S., Bono, J.J., Cook, D.R., and Ane, J.M. (2007). A novel nuclear protein interacts with the symbiotic DMI3 calcium- and calmodulin-dependent protein kinase of *Medicago truncatula*. Mol Plant Microbe Interact **20,** 912-921.

Mitra, R.M., Gleason, C.A., Edwards, A., Hadfield, J., Downie, J.A., Oldroyd, G.E., and Long, S.R. (2004). A Ca2+/calmodulin-dependent protein kinase required for symbiotic nodule development: Gene identification by transcript-based cloning. Proc Natl Acad Sci U S A **101,** 4701-4705.

Navazio, L., Moscatiello, R., Genre, A., Novero, M., Baldan, B., Bonfante, P., and Mariani, P. (2007). A diffusible signal from arbuscular mycorrhizal fungi elicits a transient cytosolic calcium elevation in host plant cells. Plant Physiol **144,** 673-681.

Nishimura, Y., Hayashi, M., Inada, H., and Tanaka, T. (1999). Molecular cloning and characterization of mammalian homologues of vesicle-associated membrane protein-associated (VAMP-associated) proteins. Biochem Biophys Res Commun **254,** 21-26.

Oufattole, M., Park, J.H., Poxleitner, M., Jiang, L., and Rogers, J.C. (2005). Selective membrane protein internalization accompanies movement from the endoplasmic reticulum to the protein storage vacuole pathway in Arabidopsis. Plant Cell **17,** 3066-3080.

Parniske, M. (2008). Arbuscular mycorrhiza: the mother of plant root endosymbioses. Nature Reviews Microbiology **6,** 763-775.

Paszkowski, U., Jakovleva, L., and Boller, T. (2006). Maize mutants affected at distinct stages of the arbuscular mycorrhizal symbiosis. Plant J **47,** 165-173.

Poulsen, K.H., Nagy, R., Gao, L.L., Smith, S.E., Bucher, M., Smith, F.A., and Jakobsen, I. (2005). Physiological and molecular evidence for Pi uptake via the symbiotic pathway in a reduced mycorrhizal colonization mutant in tomato associated with a compatible fungus. New Phytologist **168,** 445-453.

Pumplin, N., and Harrison, M.J. (2009). Live-cell imaging reveals periarbuscular membrane domains and organelle location in *Medicago truncatula* roots during arbuscular mycorrhizal symbiosis. Plant Physiol **151,** 809-819.

Puntervoll, P., Linding, R., Gemund, C., Chabanis-Davidson, S., Mattingsdal, M., Cameron, S., Martin, D.M.A., Ausiello, G., Brannetti, B., Costantini, A., Ferre, F., Maselli, V., Via, A., Cesareni, G., Diella, F., Superti-Furga, G., Wyrwicz, L., Ramu, C., McGuigan, C., Gudavalli, R., Letunic, I., Bork, P., Rychlewski, L., Kuster, B., Helmer-Citterich, M., Hunter, W.N., Aasland, R., and Gibson, T.J. (2003). ELM server: a new resource for investigating short functional sites in modular eukaryotic proteins. Nucleic Acids Research **31,** 3625-3630.

Ramakers, C., Ruijter, J.M., Deprez, R.H., and Moorman, A.F. (2003). Assumption-free analysis of quantitative real-time polymerase chain reaction (PCR) data. Neurosci Lett **339,** 62-66.

Reddy, D.M.R.S., Schorderet, M., Feller, U., and Reinhardt, D. (2007). A petunia mutant affected in intracellular accommodation and morphogenesis of arbuscular mycorrhizal fungi. Plant J **51,** 739-750.

Remy, W., Taylor, T., Hass, H., and Kerp, H. (1994). Four Hundred-Million-Year-Old Vesicular Arbuscular Mycorrhizae. PNAS **91,** 11841-11843.

Rubtsov, A.M., and Lopina, O.D. (2000). Ankyrins. Febs Letters **482,** 1-5.

Saito, K., Yoshikawa, M., Yano, K., Miwa, H., Uchida, H., Asamizu, E., Sato, S., Tabata, S., Imaizumi-Anraku, H., Umehara, Y., Kouchi, H., Murooka, Y., Szczyglowski, K., Downie, J.A., Parniske, M., Hayashi, M., and Kawaguchi, M. (2007). NUCLEOPORIN85 is required for calcium spiking, fungal and bacterial symbioses, and seed production in *Lotus japonicus*. Plant Cell **19,** 610-624.

Saravanan, R.S., Slabaugh, E., Singh, V.R., Lapidus, L.J., Haas, T., and Brandizzi, F. (2009). The targeting of the oxysterol-binding protein ORP3a to the endoplasmic reticulum relies on the plant VAP33 homolog PVA12. Plant J **58,** 817-830.

Smit, P., Raedts, J., Portyanko, V., Debelle, F., Gough, C., Bisseling, T., and Geurts, R. (2005). NSP1 of the GRAS protein family is essential for rhizobial Nod factor-induced transcription. Science **308,** 1789-1791.

Smith, S.E., Smith, F.A., and Jakobsen, I. (2003). Mycorrhizal fungi can dominate phosphate supply to plants irrespective of growth responses. Plant Physiology **133,** 16-20.

Stracke, S., Kistner, C., Yoshida, S., Mulder, L., Sato, S., Kaneko, T., Tabata, S., Sandal, N., Stougaard, J., Szczyglowski, K., and Parniske, M. (2002). A plant receptor-like kinase required for both bacterial and fungal symbiosis. Nature **417,** 959-962.

Takeda, N., Sato, S., Asamizu, E., Tabata, S., and Parniske, M. (2009). Apoplastic plant subtilases support arbuscular mycorrhiza development in *Lotus japonicus*. Plant J **58,** 766-777.

Tarr, D.E., and Scott, A.L. (2005). MSP domain proteins. Trends Parasitol **21,** 224-231.

Tirichine, L., Imaizumi-Anraku, H., Yoshida, S., Murakami, Y., Madsen, L.H., Miwa, H., Nakagawa, T., Sandal, N., Albrektsen, A.S., Kawaguchi, M., Downie, A., Sato, S., Tabata, S., Kouchi, H., Parniske, M., Kawasaki, S., and Stougaard, J. (2006). Deregulation of a Ca2+/calmodulin-dependent kinase leads to spontaneous nodule development. Nature **441,** 1153-1156.

Yano, K., Yoshida, S., Muller, J., Singh, S., Banba, M., Vickers, K., Markmann, K., White, C., Schuller, B., Sato, S., Asamizu, E., Tabata, S., Murooka, Y., Perry, J., Wang, T.L., Kawaguchi, M., Imaizumi-Anraku, H., Hayashi, M., and Parniske, M. (2008). CYCLOPS, a mediator of symbiotic intracellular accommodation. Proc Natl Acad Sci U S A **105,** 20540-20545.

CHAPTER 6

CONCLUSION

The fascinating complexity of cellular organization and response is elegantly demonstrated during arbuscular mycorrhizal symbioses, as the genetic programs of two organisms interact to form a mutually beneficial and efficient means of growth. Experiments on *Medicago truncatula* conducted for this dissertation derive from questioning the fundamental changes that occur in order to form this interaction. Particular attention has focused on the plant genetic and cellular mechanisms that enable formation of the intriguing fungal structure central to this symbiosis: the arbuscule.

We are currently in a golden age for molecular biology and functional genomics, where large amounts of data and the ability to manipulate organisms genetically has already led to a deeper understanding of some molecular pathways guiding plant development and interactions with microbes. Due to biological and technical limitations and the resources of a limited community, the molecular genetic events regulating the AM symbiosis are relatively poorly understood. This area of study is therefore an exciting and rewarding focus for scientific inquiry. In addition to satisfying basic questions, the promise of exciting practical applications employing AM symbiosis propels the research forward. Feeding the world's growing population is the major focal point for applied plant research. While huge yield improvements have been achieved for many crops, they derive in a large part from increased global use of fertilizers. Drawbacks of this development include higher crop production costs and nutrient runoff from fields into waterways, which can lead to eutrophication and ecosystem disruption. There is now strong momentum in agricultural research to seek

sustainable means of producing high-yielding crops while reducing fertilizer application. Most major crop plants can derive benefit in increased nutrient uptake through the AM symbiosis, and the potential to exploit this symbiosis in a sophisticated genetic manner may provide a substantial means for achieving sustainability goals. One clear strategy towards this goal is to manipulate symbioses such that plants acquire more nutrients from AM fungi, while providing relatively less carbon resources in exchange. Executing these types of deliberate engineering approaches will require a thorough understanding of the mechanisms regulating the symbiosis, particularly the plant genetic and cellular regulation.

The research presented in this dissertation represents fundamental new discoveries in the cellular and genetic regulation of the AM symbiosis by the legume *Medicago truncatula*. In Chapter 2, the periarbuscular membrane was revealed for the first time to contain two distinct domains of protein composition, providing evidence that developmental transition toward synthesis of the specialized periarbuscular membrane is initiated following hyphal penetration of the cell and subsequent branching, rather than at the point of cellular penetration. Chapter 3 presents an analysis of the mechanism that facilitates polar localization of the phosphate transporter MtPT4 in the periarbuscular membrane, revealing that correct targeting is likely coupled with new periarbuscular membrane secretion and that discrete steps of ER and TGN exit are required for the secretion of phosphate transporters. These discoveries may enable exciting future studies of necessary trafficking components for transporters and their subsequent environmental regulation. Chapter 4 provides a description of the complete, or near-complete, PHT1 family of phosphate transporters in *M. truncatula* and includes more detailed analysis of *MtPT8*, showing for the first time a dicot-wide duplication of the AM- specific phosphate transporter family (subfamily I). Chapter 5 presents the discovery and characterization of *Vapyrin*, a

gene required for arbuscule formation that may function to regulate secretion during fungal penetration of plant cells.

These discoveries lead directly into future experiments that could delve deeper into the mechanisms regulating arbuscule development. Initially, a series of experiments testing the proposed model of protein secretion during arbuscule development will be prudent. A first priority is to show, through immunolabeling and transmission electron microscopy, the localization of MtPT4 and the mtpt4^{S115F} mutant in the periarbuscular and TGN membranes, respectively. The analysis of additional transporters and membrane proteins specifically induced during AM symbiosis will allow rigorous testing of the mechanism underlying secretion in these cells. In addition, uncovering the molecular basis of MtPT4 ER exit will be an exciting discovery. While a candidate gene approach for the putative exit chaperone may not be feasible, analysis of genes induced during symbiosis and mutants displaying *mtpt4*-like phenotypes may uncover the gene(s) that regulate this process and enable functional characterization. Targeted biochemical/proteomics experiments may also allow characterization of membrane proteins and interacting proteins associated with MtPT4, potentially revealing many players in the regulation of this protein. Moreover, we hypothesize that additional proteins are responsible for phosphate transporter secretion from the TGN to target periarbuscular and plasma membranes, and possibly for recycling. Cargo-binding proteins of adaptor protein complexes are good first candidates and could be tested by reverse genetics approaches; however, an unbiased screen is likely to yield the most useful and comprehensive information. The discovery (Chapter 3) that the S115F mutation affects MtPT1 trafficking in the epidermis in a similar manner suggests the potential to carry out secretion studies in seedlings without fungal colonization, which is a more tractable system for high-throughput genetic screening and biochemical approaches.

Establishing a functional role for MtPT8 should contribute to a better understanding of phosphate transport during the AM symbiosis. Its conservation in dicots suggests this gene confers an evolutionary advantage; however, our experiments did not reveal a requirement for this gene in establishing and maintaining the AM symbiosis. This result may be explained by a requirement for *MtPT8* primarily during symbiosis in an environment, or with a fungal partner, not tested in our conditions; alternatively *MtPT8* may play a more significant role in other species and be vestigial in *M. truncatula*. Future experiments will consider whether MtPT8 interacts with additional genetic or regulatory elements. The report and initial characterization of *MtPT6* and *MtPT9* may also contribute to our understanding of the complex regulation of phosphate signaling and transport in plants.

The discovery of *Vapyrin* (Chapter 5) should enable exciting discoveries in the regulation of fungal penetration into plant cells. This protein has predicted protein-protein interaction domains and we hypothesize that this mediates recruitment to an endosomal compartment, where it facilitates a unique secretion process to allow fungal penetration. While our initial RNA interference experiments uncovered a requirement for this gene in the symbiosis, future studies will focus on stable *Vapyrin* loss-of-function alleles, which will enable more detailed phenotypic characterization and functional analysis of the protein. As Vapyrin likely acts through protein interactions, discovery of those interacting partners will contribute greatly to understanding its function and offer a unique strategy for identifying additional genes required for the symbiosis. While the role for Vapyrin in secretion is speculative and based on circumstantial evidence of its knockdown phenotype and localization, it is tempting to propose a hypothesis that it specifically mediates secretion to the periarbuscular membrane or point of entry into a cell by AM fungi. This hypothesis will be tested through molecular analysis of Vapyrin function.

Throughout the experiments reported here, one emergent theme is the extreme specialization displayed by plant cells interacting with AM fungi. Previous studies revealed specific gene expression changes in roots and cells during this interaction, as well as cellular rearrangements. Through live-cell imaging techniques applied to translational reporter fusions expressed under native promoters, we saw with great detail the activities of individual cells in the process of accommodating their symbionts. Chapter 3, in particular, highlighted the drastic commitment to specialized function made by these cells, likely at the expense of "normal" metabolism. These cells displayed specific changes in secretion and downregulation of an allegedly constitutive exogenous promoter. Our ability to dissect changes in gene expression, protein function and metabolism at the cell-specific and subcellular level will certainly continue to improve in resolution through technological development. Through such new approaches, we might expect to uncover an astounding and important level of cellular distinctiveness, both shared by similar cell types responding to similar stimuli, as well as differing between individuals of similar type due to slight homeostatic differences eliciting unique responses.

Beyond revealing mechanistic details about the AM symbiosis, it is hoped that the scientific discoveries and approaches reported in this dissertation will contribute to the greater body of biological knowledge. Due to the conserved laws of evolution that appear to guide all of life, the knowledge generated in one field can be extremely informative to seemingly diverse fields. Mechanisms of gene evolution and cellular function are good examples of this. While details and specifics may vary, paradigms of biological function are often broadly applicable. These studies of the AM symbiosis therefore represent one step towards the ultimate goal: An integrated understanding that explains how every biological molecule contributes to the diversity of living organisms.